

---

# **THE USE OF ALGAL AND YEAST BIOMASS TO ACCUMULATE TOXIC AND VALUABLE HEAVY METALS FROM WASTEWATER**

Final Report to the  
Water Research Commission

by

JR Duncan, A Stoll, B Wilhelmi, M Zhao and R van Hille

Department of Biochemistry and Microbiology  
Rhodes University  
Grahamstown, 6140, South Africa

WRC Report No 616/1/03  
ISBN 1-77005-123-6

DECEMBER 2003

#### **Disclaimer**

This report emanates from a project financed by the Water Research Commission (WRC) and is approved for publication. Approval does not signify that the contents necessarily reflect the views and policies of the WRC or the members of the project steering committee, nor does mention of trade names or commercial products constitute endorsement or recommendation for use.

## Background and Motivation

Water is an important though often under-rated resource. Water availability and quality are of paramount importance in socio-economic growth in South Africa. It has been calculated on present rates of growth of population and industry that the supply and demand curves for potable water available in R.S.A. will cross in the year 2020, beyond which demand will exceed supply. Metal ions can be toxic and contribute to the pollution of water, moreover they may be concentrated in certain organisms and passed on in high concentrations to humans. The importance of this problem is highlighted by the fact that humans are now the largest agent in the biogeochemical cycles of trace metals on a global scale and the toxicity of these metals now exceeds that of all radioactive and organic wastes released into the environment.

Many industrial processes produce heavy metal containing wastewaters. This represents not only a highly toxic effluent but, in the case of the mining industry, a loss of valuable metals. Removal of these metal ions is consequently vital if the wastewater is to be recycled without significant contamination of the streams/dumps into which they are discharged or loss of a potential resource.

Traditional methods of metal removal from solutions, such as ion exchange and precipitation, have not proved cost-effective especially in the lower concentration ranges. Biotechnology based processes can, however, play a significant role in metal recovery. Microorganisms are known to play an active role in the solubilisation, accumulation, transport and deposition of metals in the environment. Microorganisms are known to accumulate metals from dilute metal ion solutions and thereby concentrate them. This would facilitate the restoration of metal contaminated wastewater and recovery of valuable metals.

The two organisms of interest in this study, yeast and algae, have been found to be effective accumulators of metal ions. Since *S. cerevisiae* is a readily available by-product of alcohol based fermentation industries in South Africa, it represents a relatively cheap source of biomass which requires little pretreatment before it can be utilised for metal binding. Algae may be considered to be non-pathogenic, which gives these organisms a certain advantage over many other forms of microbial biomass when used for bioaccumulation purposes. One of the other advantages of algae is that they may be grown in ponds with little nutritional input or maintenance as they are autotrophs, whereas many other organisms capable of metal accumulation, including yeasts, are heterotrophs.

An initial study in our laboratory indicated that yeast cells and a modified, non-viable yeast cell mass provide an efficient means of removing a wide range of metal ions from solution. The modified, non-viable biomass had a slightly reduced capacity for metal accumulation but appeared to be a useful source of biomass for biosorption purposes as it can be readily used on a large scale and is easily stored. The ability of a number of species of algae to accumulate heavy metal ions has also been investigated in our department as part of a project carried out in collaboration with Professor Rose.

This study is essentially a continuation of these earlier investigations and was aimed at obtaining further information on the full potential of yeast and algal biosorption as a cost-effective means of treating metal laden effluents. In addition, the application of this

technology to actual effluents and the scale-up of a process to pilot scale were further objectives of the study.

### Objectives

- (1) To determine the efficiency and capacity of different types and forms of microbial biomass in removal of heavy metals from wastewaters generated by mining, electroplating, battery, tannery and other industries.
- (2) To evaluate cross-flow hollow fibre membranes and other systems of biomass retention and immobilisation for purposes of large scale and continuous use of yeast and algal cells for heavy metal removal from effluents.
- (3) To further define the general mechanism of heavy metal accumulation and the more metal specific mechanisms of biosorption using x-ray micro-analysis electron microscopy. This information will also be used to determine the most effective systems for use in treatment of particular heavy metal containing wastewaters.
- (4) To investigate methods of heavy metal desorption from biomass as a means of concentrating the metal and also for possible reuse of the biomass.
- (5) To transfer the technology developed as a result of these studies to the relevant industries and to develop a pilot scale system for effluent treatment.

### Summary of Results and Conclusions

The aim of the first section of this study was twofold. The initial part of this work attempted to define the mechanisms of metal accumulation by the yeast cells and cellular components. The information obtained from these initial studies provided a data base required for the development of a bioremediation system.

Initial contact with the metal ions occurs at the wall interface of the yeast cell. Metal accumulation appears to be a function of all the cell wall components. The isolated cell wall components are better metal chelators than the intact cell walls. An apparent affinity series of mannan > chitin > glucan > intact cell walls exists. However, these components differ in their affinities for different metal ions.

Storage of metal ions within the cell occurs predominantly in the vacuole. The present study concluded that metal accumulation by the vacuole could be related to ionic size. Metal accumulation occurred in the order of  $\text{Cu}^{2+} > \text{Co}^{2+} > \text{Cd}^{2+}$  with a corresponding decrease in atomic radii of  $\text{Cd}^{2+} > \text{Co}^{2+} > \text{Cu}^{2+}$ . Vacuolar ion deposition occurs at an early stage during the internalization of metal ions within the yeast cells. At the onset of vacuolar saturation, depositions of metal ions as granules occurs within the cytosol. In the presence of heavy metal cations viable yeast cell can be shown to elicit two types of cellular responses. Uptake of  $\text{Cu}^{2+}$  and  $\text{Cd}^{2+}$  cause the loss of intracellular physiological cations from within the yeast cell. In comparison, uptake of  $\text{Co}^{2+}$  into the cell does not have this effect. Since all three heavy metal cations increase plasma cell membrane permeability, the  $\text{Cu}^{2+}$  and  $\text{Cd}^{2+}$ -induced loss of the intracellular cations, occurs as a result of ion-exchange

mechanisms and not due to cation leakage brought about by membrane permeabilization.

Uptake of heavy metals by viable yeasts appears to be generally non-selective though the amount of metals accumulated is largely affected by the ratio of ambient metal concentration to biomass quantity. In addition, the energy dependent nature of internalization necessitates the availability of an external energy source for metal uptake by viable yeast cells. For these reasons metal removal from industrial wastewater was investigated using non-viable biomass.

By immobilising the yeast cells additional mechanical integrity and stability was conferred upon the biomass. The three types of biomass preparations developed in this study, viz. PVA Na-alginate, PVA Na-orthophosphate and alkali treated PEI:GA biomass pellets, all fulfilled the necessary physical requirements. However, the superior metal accumulating properties of the PEI:GA biomass determined its selection as a biosorbent for bioremediation purposes. Biosorption of heavy metals by PEI:GA biomass is of a competitive nature, with the amount of metal accumulated influenced by the availability of the metal ions. This availability is largely determined by the solution pH. At low pH values the affinity of the biomass for metals decreases, whilst enhanced metal biosorption occurs at higher pHs, e.g. pH 4.5 - 6.0.

PEI:GA biomass pellets can be utilised as a biosorbent for the bioremediation of high-concentration, low-volume metal containing industrial waste. Several options regarding the bioremediation system are available. Depending on the concentration of the metals in the effluent, the bioremediation process can either be used independently or as part of a biphasic remediation system for the treatment of wastewater. Initial phase chemical modification may be required, whilst two types of biological systems can be implemented as part of the second phase. The PEI:GA biomass can either be contained within continuous-flow fixed bed bioreactors or continuous-flow stirred bioreactor tanks. Due to the simplicity of the process and the ease with which scale-up is facilitated, the second type of system shows greater application potential for the treatment of this type of industrial wastewater than the fixed-bed systems. Using continuous-flow reactors, implemented as three tanks linked together in series, complete removal of Cu, Cr and Ni from electroplating wastewater was attained, whilst on average 82% and 83% of the initial Zn and Cd was removed from the waste.

The second section of the study presents a novel method in immobilising *S. cerevisiae* as a biosorbent for treatment of metal-laden waste effluent, in which the immobilising cost can be reduced to an affordable extent on industrial scale. The non-viable yeast cross-linked by 13# FA/1N HNO<sub>3</sub> exhibits good mechanical strength and rigidity in continuous-flow operation. No apparent disruption of the biomass after repeated use has been observed. Cu, Zn and Cd were effectively removed from aqueous solutions by the yeast biomass at natural pHs of their solutions. Complete recovery of the bound metals were achieved by washing the column biomass with 0.1M HCl. The recovered metals were concentrated in such small volumes that recycling or precipitation of them can be carried out. The metal uptake capacity of the regenerated biomass remained constant in comparison with cycle 1 thereby reuse of the yeast would be possible.

In the case of Cr<sup>6+</sup>, a gradual breakthrough curve of Cr in the column profile was noted, with reduction of Cr<sup>6+</sup> to Cr<sup>3+</sup> occurring. However, Cr<sup>6+</sup> in EPE can be significantly minimised either by accumulation onto the biomass or reduced to its trivalent form so that detoxification of Cr<sup>6+</sup>-laden wastewater can be accomplished. Desorption of bound Cr<sup>6+</sup>

with either alkaline or salt could not facilitate the regeneration. A combination of reduction and desorption with FA/HNO<sub>3</sub> appeared promising in regeneration of the saturated biomass at 4°C, while applying the same procedure at room temperature did not show satisfactory results, reflecting the thermochemical effect on binding of the metal to yeast biomass.

In the third section of the study, a more detailed investigation was made of the kinetics of metal removal from solution by *S. cerevisiae* using metals present in a mine effluent obtained from Gold Fields Ltd.

Immobilised *S. cerevisiae* removed metals from aqueous solutions. The removal was relatively rapid with adsorption equilibriums being reached for all metals within 30 minutes of incubation. The process was pH dependant, with the removal of cations most effective at solution pH's above 3. Gold removal by the biosorbent was both high and rapid at pH 2. The isotherms followed typical Michaelis-Menten binding kinetics. The metal removal capabilities of *S. cerevisiae* in this study indicated a biosorbent suitable for relatively low metal concentration, high volume effluents.

In studies on the reusability of the biomass and the recovery of bound metal, copper accumulation by immobilised *S. cerevisiae* biomass was found to be reversible and was most successfully recovered using HCl, H<sub>2</sub>SO<sub>4</sub> and HNO<sub>3</sub>. Removal and recovery efficiencies of the immobilised biosorbent improved with up to 8 repeated adsorption-desorption cycles in batch reactors. Electron micrographs showed no damage to the cells and supported the mechanism of metal binding to the cell surface. The biosorbent showed the potential for reuse in continuous bioremediation systems.

The immobilised *S. cerevisiae* packed-bed biosorption columns removed metals from aqueous solutions. The bioaccumulated metals were recovered by 0.1 M HCl elution. The desorption protocol utilised a minimum quantity of dilute acid and yielded a concentrated, low volume metal eluant. The ease of metal elution and recovery from the columns implied passive binding to the cell wall. The biomass was reusable. The adsorption-desorption process did not adversely affect the uptake capacity of the biosorbent and the uptake of certain metals was enhanced with continuous use. A copper solution was run on a single column through 8 cycles with no apparent decrease in biosorbent performance. The potential for selective recovery by the biosorbent and elution protocol was demonstrated. The success of selective binding and recovery of metals from mixed metal solutions was dependant on affinity of the metals and their initial concentration in solution. The reusability of the biosorbent and the selective recovery of target metals could lead to the development of a viable, cost-effective metal bioremediation technology.

*S. cerevisiae* biomass was applied to the treatment of a copper-zinc mine effluent which contained high levels of copper, zinc, lead and iron. At its natural pH (2.0) very little metal could be removed from the effluent but at a pH of 4 effective metal removal was achieved through a combination of pH precipitation of the metal and bioremediation. The complexity of the effluent and its interaction with the biomaterial requires substantial fundamental and applied research before its full potential can be attained. At present, the immobilised *Saccharomyces cerevisiae* biomass has limited application to the effluent investigated and at best may be used to complement a chemical remediation operation.

The final section of the report deals with the use of algae (*Spirulina*) for the treatment of zinc-copper mine (Black Mountain) effluent. The system utilised was one of metal removal by both pH control induced by the algae and bioremediation. The data indicated that metals in the effluent could be effectively removed from solution using this system and that there is potential for the development of a viable, biologically based system for the treatment of the effluent at the Black Mountain Mine. A pH mediated precipitation of the majority of the metals has been achieved using an algal based system. Micro algae have been very successfully cultivated on a large scale in pond systems and the climatic conditions prevalent in the area surrounding the mine are ideal for the large scale cultivation of algae in ponds. The one potential problem with a *Spirulina* based system is the lack of availability of a large volume of high saline medium. Using a defined medium such as Zarrouk's medium used in this study on a large scale will most likely be prohibitively expensive.

### **Achievement of Contractual Objectives**

In terms of the objectives as outlined earlier in this summary the following was achieved:

- (1) This has been achieved with yeast and algal biomass treatment of mining and electroplating effluent. Further effluents and forms of biomass will be investigated in follow-up studies.
- (2) A number of immobilised and bioreactor systems have been evaluated. Membrane studies were not conducted as they were considered impractical for the effluents under investigation. They may be reconsidered in follow-up studies.
- (3) This has been achieved particularly for yeast. More in-depth studies on uptake mechanisms will be investigated in future studies.
- (4) This has been achieved and will continue to be evaluated for other forms of biomass.
- (5) The technology developed to date has been passed-on to the relevant industries. Pilot plant studies have not commenced as these were considered to be premature at this stage. However, a pilot plant is currently being designed for an electroplating factory and will hopefully be in operation during 1997.

### **Contribution and Action**

This is one of the few biosorption studies worldwide to investigate the application of this technology to actual effluents rather than laboratory prepared solutions. It is also one of the few studies which has investigated in-depth, the mechanism of metal uptake and binding by biomass.

Further novel applications have been the use of the waste product of one industry, the brewing industry, to treat the effluent from other industries, and the potential use of algal ponding systems to treat metal contaminated wastewater.

The technology that has been developed and which will be scaled-up in the near future offers the potential of a low-cost means of treating toxic effluents in a manner which could facilitate

the reuse of the water in the plant and the recycling of the metal which would reduce the nett costs of the effluent treatment while also reducing the volume of water used by the industry. In order to evaluate the feasibility of this, a pilot scale and eventually a full scale treatment plant will need to be constructed and tested. It is suggested that this be done initially in a system which generates relatively low volumes of effluent such as that produced by electroplating or battery industries.

### **Future Research**

A number of areas for future study have been indicated in earlier sections. In essence these studies will investigate other forms of biomass which have potential for metal biosorption, the treatment of other metal containing effluents, studies on the mechanisms of metal uptake by different forms of biomass, the possible exploitation of exopolysaccharides produced by certain microorganisms as metal binding agents, and ultimately the development of a pilot-scale and then full scale treatment plant probably treating a low volume effluent produced by an industry in the Eastern Cape.

In addition, the technology developed to date will be used in conjunction with algal integrated ponding processes (AIPS) developed by Professor Rose's group to treat mine water problems in the Blesbokspruit catchment area. This project has already been initiated by our group and that of Professor Rose at LIRI and is at present being sponsored by the Water Research Commission and Hanni Leathers.



## Acknowledgements

The financing of the project by the Water Research Commission and the contribution of the members of the Steering Committee is gratefully acknowledged.

The Steering Committee consisted of the following persons:

Mr G N Steenveld	(Chairman)
Dr H M Saayman	(Chairman)
Mr F P Marais	(Secretary)
Dr S A Mitchell	
Prof T E Cloete	
Dr A de Kok	
Prof J R Duncan	
Prof H R Hepburn	
Prof P D Rose	
Mr R A Rowsell	
Prof P D Swart	

Additional financial support for the project relating to the mine effluents and technical assistance is gratefully acknowledged from Gold Fields Ltd and Mr R Beck in particular.

This project was also only possible with the assistance and co-operation of a number of individuals and institutions. The authors wish to express their sincere thanks to the following:

The Rhodes Electron Microscopy Unit and Mr Robin Cross in particular for their assistance with all the E M studies.

The Physics Department at the University of Port Elizabeth for the use and technical assistance with the x-ray diffraction analysis.

P E Plating for the supply of electroplating effluent.

Black Mountain and Deelkraal mines for the supply of mining effluents.

LIRI workshops for assistance with bioreactor design and construction.

Prof Peter Rose for constant support and discussion.

Honours students Mr T C Makhale and Miss L Wallace for their contribution to aspects of the experimental work.

Mrs Joan Miles for typing numerous reports, papers, etc arising from this project.

# TABLE OF CONTENTS

CONTENTS	PAGE
Executive Summary	i
Table of Contents	ix
List of Figures	xvi
List of Tables	xxv
1. General Introduction	1
Part 1.	2
1.1. Historical overview	2
1.2. Microbial bioaccumulation of metal cations	3
1.2.1. Extracellular adsorption	3
1.2.2. Internalization of metal cations by <i>S. cerevisiae</i>	4
1.2.2.1. Transport of monovalent cations	4
1.2.2.2. Divalent metal cation uptake	5
1.3. Localization of accumulated heavy metal cations	7
1.3.1. Cell wall	7
1.3.1.1. Metal binding by microbial cell walls	7
1.3.1.2. Composition of yeast cell wall	8
1.3.1.2.1. Glucans	9
1.3.1.2.2. Chitin and chitosan	9
1.3.1.2.3. Mannans	10
1.3.1.2.4. Proteins	10
1.3.1.3. Yeast cell wall-metal interactions	10
1.3.2. Yeast vacuoles	11
1.3.3. Yeast mitochondria	13
Part 2.	13
2.1. Water availability and drinking water criteria in South Africa	13
2.2. Metals as pollutants in water	14
2.3. Bioremediation of metal containing water	15
2.4. Industrial applications	17
2.4.1. Industrial effluents	17
2.4.1.1. Electroplating effluent	18
2.4.2. Biomass systems for industrial bioremediation	18
2.5. Research aims	20

<b>CONTENTS</b>	<b>PAGE</b>
<b>2. Interaction with, and accumulation of metal ions by yeast cell walls and cell wall components</b>	<b>21</b>
2.1. Introduction	21
2.2. Materials and methods	24
2.2.1. Preparation of isolated cell walls	24
2.2.2. Cell wall component extraction	24
2.2.2.1. Chitin and chitosan extraction	24
2.2.2.2. Mannan isolation	25
2.2.2.3. Glucan isolation	25
2.2.3. Protein and carbohydrate determination	25
2.2.4. Quantitative metal binding studies	26
2.2.5. Qualitative assessment of metal bound to cell wall and cell wall components	27
2.3. Results	27
2.3.1. Quantitative analysis	27
2.3.2. Qualitative analysis	30
2.4. Discussion	36
2.5. Conclusions	37
<b>3. Uptake of heavy metals by vacuoles isolated from <i>S. cerevisiae</i></b>	<b>38</b>
3.2. Materials and methods	38
3.2.1. Pretreatment of yeast	38
3.2.2. Spheroplast formation	38
3.2.3. Vacuole isolation	39
3.2.4. Determination of vacuole integrity	39
3.2.5. Metal uptake	39
3.2.6. ATPase inhibition	40
3.3. Results	40
3.3.1. Spheroplast and vacuole integrity	40
3.3.2. Heavy metal uptake	41
3.4. Discussion	45
3.5. Conclusions	46
<b>4. Accumulation and internalization of heavy metals by viable yeast cells</b>	<b>47</b>
4.1. Introduction	47
4.2. Methods and materials	49
4.2.1. Scanning electron microscopy (SEM) of Cu-loaded cells	49
4.2.1.1. Metal accumulation	49
4.2.1.2. Cryo-SEM preparation	50

CONTENTS	PAGE
4.2.2. Distribution studies of accumulated heavy metal cations by transmission electron microscopy (TEM)	50
4.2.2.1. Metal accumulation	50
4.2.2.2. Embedding protocol for microscopic analysis	50
4.2.2.3. Sectioning for transmission electron microscope (TEM) and X-ray diffraction analysis	51
4.2.2.3.1. Ultrathin sectioning and staining of samples for TEM	51
4.2.2.3.2. X-ray diffraction preparation and analysis	51
4.2.3. Influence of metals on membrane integrity	52
4.3. Results	53
4.3.1. Heavy metal induced morphological changes	53
4.3.2. Cellular distribution of metal ions	59
4.3.3. The effect of metals on membrane integrity	65
4.4. Discussion	66
4.5. Conclusions	69
 5. Bioaccumulation of heavy metals from waste water by viable <i>S. cerevisiae</i> cells	 70
5.1. Introduction	70
5.2. Methods and materials	73
5.2.1. Metal equilibration	73
5.2.2. Optimization studies	73
5.2.2.1. Biomass ratio determination	73
5.2.2.2. Glucose supplementation	74
5.2.3. Bioaccumulation from waste water using batch reactions	74
5.3. Results	75
5.4. Discussion	82
5.4.1. Effect of pH and glucose treatment on metal bioaccumulation	82
5.4.2. The relationship between bioaccumulation and ambient metal concentration in a multi-ion environment	83
5.5. Conclusions	84
 6. Biosorption of heavy metal cations by immobilized non-viable yeast biomass	 85
6.1. Introduction	85
6.2. Materials and methods	88
6.2.1. Biomass preparation	88
6.2.1.1. Polyvinylalcohol (PVA) Na-orthophosphate immobilization	88
6.2.1.2. PVA Na-alginate immobilization	89
6.2.1.3. PEI:GA immobilization	90
6.2.1.3.1. Immobilization	90
6.2.1.3.2. Hot alkali treatment	90

<b>CONTENTS</b>	<b>PAGE</b>
6.2.2.	Determination of structural properties 90
6.2.3.	Determination of the biomass biosorptive properties 91
6.2.3.1.	Metal accumulation in packed-bed columns 91
6.2.3.2.	Biomass regeneration and metal reaccumulation 91
6.2.4.	Metal biosorption tests 92
6.2.5.	Fixed-bed biosorption using PEI:GA biomass 92
6.2.5.1.	Breakthrough determination of individual cation species 92
6.2.5.2.	Multi-element competition and effect of solution pH on breakthrough determination 93
6.3.	Results 93
6.3.1.	Immobilization and structural properties of the biomass 93
6.3.2.	Metal accumulation 98
6.3.3.	Column biosorption 102
6.3.4.	PEI:GA biomass sorption capacity 107
6.4.	Discussion 108
6.5.	Conclusions 110
<b>7.</b>	<b>Application of metal biosorption by non-viable yeast biomass to an electroplating effluent 111</b>
7.1.	Introduction 111
7.2.	Materials and methods 113
7.2.1.	Electroplating effluent 113
7.2.2.	Continuous-flow fixed bed bioreactors 114
7.2.2.1.	Processing of raw effluent 114
7.2.2.2.	Dual columns in series 116
7.2.2.3.	Single and dual reactor treatment of PST effluent 116
7.2.2.4.	Process scale up: experimental parameters 116
7.2.3.	Continuous-flow stirred bioreactors 117
7.2.3.1.	Bioreactor design 117
7.2.3.2.	Single bioreactor system 117
7.2.3.3.	Dual bioreactors linked in series 118
7.2.3.4.	Determination of maximum loading capacity 118
7.3.	Results 120
7.3.1.	Continuous-flow fixed bed reactors 120
7.3.1.1.	Single and multi-phased raw and PST effluent treatment 120
7.3.1.1.1.	Raw effluent 120
7.3.1.1.2.	PST effluent 123
7.3.1.2.	Process scale up 125
7.3.2.	Continuous-flow stirred bioreactors 125
7.3.2.1.	Bioreactor efficiency 126
7.3.2.2.	Dual bioreactors in series 126
7.3.2.3.	Breakthrough determination 128
7.3.2.3.	Process scale up 129
7.4.	Discussion 133
7.5.	Conclusions 136

CONTENTS	PAGE
<b>8. General discussions and conclusions on metal bioaccumulation by yeast biomass</b>	<b>138</b>
8.1. Bioaccumulation	138
8.2. Biosorption and effluent treatment	140
8.3. General comments	141
<b>9. The use of formaldehyde cross-linked <i>S. cerevisiae</i> for column removal of metals from aqueous solution and electroplating effluent</b>	<b>142</b>
9.1. Introduction	142
9.2. Materials and methods	142
9.2.1. Materials	142
9.2.2. Immobilization	143
9.2.3. Metal determination	143
9.2.4. Column operation	143
9.2.5. Desorption of $\text{Cr}^{6+}$ with various desorbents	144
9.3. Results and discussion	144
9.3.1. Stability of the cross-linked biomass	144
9.3.2. Column adsorption of Cu, Zn and Cd from aqueous solutions	145
9.3.3. Desorption and recovery of cation metals	147
9.3.4. Column adsorption of $\text{Cr}^{6+}$ from electroplating effluent	149
9.3.5. Desorption of $\text{Cr}^{6+}$	151
9.3.6. Reduction and desorption of $\text{Cr}^{6+}$	152
9.4. Conclusions	153
<b>10. The removal of metals from aqueous solutions by immobilised <i>Saccharomyces cerevisiae</i></b>	<b>155</b>
10.1. Introduction	155
10.2. Materials	155
10.3. Method	155
10.3.1. <i>S. cerevisiae</i> immobilisation	155
10.3.2. Adsorption kinetic profiles	156
10.3.3. pH profiles	156
10.3.4. Equilibrium profiles	156
10.4. Results	157
10.4.1. Metal removal over time	157
10.4.2. Effect of pH on bioaccumulation	158
10.4.3. Sorption isotherms	161
10.5. Discussion	163
10.6. Conclusion	165

CONTENTS	PAGE
<b>11. Recovery of metal bioaccumulated by immobilised <i>Saccharomyces cerevisiae</i></b>	<b>166</b>
11.1. Introduction	166
11.2. Materials	166
11.3. Method	166
11.3.1. <i>S. cerevisiae</i> immobilisation	166
11.3.2. Metal adsorption-desorption profiles	167
11.3.3. Repeated use of the biosorbent	167
11.3.4. Metal analysis	167
11.3.5. Transmission electron microscopy of <i>Saccharomyces cerevisiae</i>	167
11.4. Results	168
11.4.1. Copper recovery from the biosorbent	168
11.4.2. Adsorption-desorption cycles	168
11.4.3. Transmission electron microscopy of <i>S. cerevisiae</i>	170
11.5. Discussion	172
11.6. Conclusion	173
<b>12. Metal removal and recovery from <i>Saccharomyces cerevisiae</i> biosorption columns</b>	<b>174</b>
12.1. Introduction	174
12.2. Materials	174
12.3. Method	174
12.3.1. <i>S. cerevisiae</i> immobilisation	174
12.3.2. Biosorption columns preparation	174
12.3.3. Selective recovery of metals from a mixed metal solution	175
12.3.4. Reusability of the biosorbent columns	175
12.4. Results	175
12.4.1. Metal uptake on immobilised <i>S. cerevisiae</i> biosorption columns	175
12.4.2. Selective recovery of metals from mixed metal solutions	178
12.4.3. Repeated adsorption-desorption cycles of a biosorption column	178
12.5. Discussion	180
12.6. Conclusion	182
<b>13. The removal of metals from mining effluent by immobilised <i>Saccharomyces cerevisiae</i></b>	<b>183</b>
13.1. Introduction	183
13.2. Materials	183
13.2.1. Mine effluent	183
13.3. Method	183
13.3.1. pH profile	183
13.3.2. Batch remediation	184
13.4. Results	184
13.4.1. Effluent composition and pH profile	184
13.4.2. Bioremediation of heavy metals iron, lead, copper and zinc by immobilised <i>S. cerevisiae</i>	184

<b>CONTENTS</b>	<b>PAGE</b>
13.5. Discussion	187
13.6. Conclusion	187
<b>14. The use of <i>Spirulina sp</i> for the treatment of a mine effluent</b>	<b>188</b>
14.1. Introduction	188
14.2. Materials and methods	190
14.3. Results	191
14.3.1. Effluent treatment in a volume controlled system	196
14.3.2. Autoclaved control experiment (volume controlled)	201
14.3.3. Distilled water control	204
14.4. Discussion	205
<b>15. General discussion and conclusions</b>	<b>206</b>
<b>16. References</b>	<b>208</b>



## LIST OF FIGURES

	PAGE
<b>Figure 2.1:</b> Comparison of heavy metal cation binding by <i>S. cerevisiae</i> isolated cell walls and extracted cell wall macromolecular components.	28
<b>Figure 2.2:</b> Infrared analysis (1800 - 800 cm <sup>-1</sup> ) of <i>S. cerevisiae</i> cell walls and extracted components: (a) isolated cell walls, (b) chitin, (c) mannan, and (d) glucan preparations.	31
<b>Figure 2.3:</b> Infrared spectra (1800 - 800 cm <sup>-1</sup> ) of isolated <i>S. cerevisiae</i> cell walls before and after metal biosorption. (a) Untreated cell walls, (b) Cd <sup>2+</sup> , (c) Co <sup>2+</sup> and (d) Cu <sup>2+</sup> exposed cell walls.	32
<b>Figure 2.4:</b> Infrared spectra (1800 - 800 cm <sup>-1</sup> ) of mannan extracted from <i>S. cerevisiae</i> cell walls before and after metal biosorption. (a) Untreated mannan, (b) Cd <sup>2+</sup> , (c) Co <sup>2+</sup> and (d) Cu <sup>2+</sup> interaction with mannan.	33
<b>Figure 2.5:</b> Infrared spectra (1800 - 800 cm <sup>-1</sup> ) of glucan extracted from <i>S. cerevisiae</i> cell walls before and after metal biosorption. (a) Untreated glucan, (b) Cd <sup>2+</sup> , (c) Co <sup>2+</sup> and (d) Cu <sup>2+</sup> interaction with glucan.	34
<b>Figure 2.6:</b> Infrared spectra (1800 - 800 cm <sup>-1</sup> ) of chitin isolated from <i>S. cerevisiae</i> cell walls before and after metal biosorption. (a) Untreated chitin, (b) Cd <sup>2+</sup> , (c) Co <sup>2+</sup> and (d) Cu <sup>2+</sup> interaction with chitin.	35
<b>Figure 3.1:</b> Accumulation of Cu <sup>2+</sup> by isolated yeast vacuoles over time from Cu <sup>2+</sup> -containing solutions.	42
<b>Figure 3.2:</b> Accumulation of Co <sup>2+</sup> by isolated yeast vacuole over time from Co <sup>2+</sup> -containing solutions.	42
<b>Figure 3.3:</b> Accumulation of Cd <sup>2+</sup> by isolated yeast vacuoles over time from Cd <sup>2+</sup> -containing solutions.	43
<b>Figure 3.4:</b> Effect of DNP-pretreatment on vacuolar uptake of Cu <sup>2+</sup> .	43
<b>Figure 3.5:</b> Effect of DNP-pretreatment on vacuolar uptake of Co <sup>2+</sup> .	44
<b>Figure 3.6:</b> Effect of DNP-pretreatment on vacuolar uptake of Cd <sup>2+</sup> .	44
<b>Figure 4.1:</b> Electron micrographs of native <i>S. cerevisiae</i> cells. (a) SEM (3500x) and (b) TEM micrographs (10 000x).	54 - 55
<b>Figure 4.2:</b> SEM micrographs of Cu <sup>2+</sup> exposed <i>S. cerevisiae</i> cells (8 000x).	55

	<b>PAGE</b>
<b>Figure 4.3:</b> TEM micrographs (10 000x) of <i>S. cerevisiae</i> cells after (a) 5, (b) 12 and (c) 24 h exposure to $\text{Cu}^{2+}$ ions.	56
<b>Figure 4.4:</b> TEM micrographs of yeast cells (14 000x) after (a) 5 and (b) 12 h of exposure to $\text{Co}^{2+}$ ions.	57
<b>Figure 4.5:</b> TEM micrographs (14 000x) of <i>S. cerevisiae</i> cells after (a) 5, (b) 12 and (c) 24 h exposure to $\text{Cd}^{2+}$ ions.	58
<b>Figure 4.6:</b> A typical EDAX ion profile spectra of native <i>S. cerevisiae</i> biomass.	59
<b>Figure 4.7:</b> EDAX spectra of the electron dense inclusions in (a) $\text{Cu}^{2+}$ , (b) $\text{Cd}^{2+}$ and (c) $\text{Co}^{2+}$ loaded cells.	61
<b>Figure 4.8:</b> Intracellular ion composition of yeast cells exposed to a $\text{Cu}^{2+}$ containing solution (a) 1, (b) 12 and (c) 24 h of metal exposure.	62
<b>Figure 4.9:</b> Intracellular ion composition of yeast cell exposed to a $\text{Cd}^{2+}$ containing solution after (a) 1, (b) 12 and (c) 24 h.	63
<b>Figure 4.10:</b> Intracellular ion composition of yeast cells exposed to a $\text{Co}^{2+}$ containing solution after (a) 1, (b) 12 and (c) 24 h.	64
<b>Figure 4.11:</b> Fluorescence determination of the supernatant of $\text{Cu}^{2+}$ , $\text{Cd}^{2+}$ and $\text{Co}^{2+}$ exposed cells as an indicator of the effect of metals on plasma membrane integrity of yeast cells.	66
<b>Figure 5.1:</b> The rate of bioaccumulation of metal ions from effluent A over time ( $\mu\text{g/g}$ biomass/h) by viable yeast cells.	77
<b>Figure 5.2:</b> The rate of bioaccumulation of metal ions from effluent B over time ( $\mu\text{g/g}$ biomass/h) by viable yeast cells.	77
<b>Figure 5.3:</b> The rate of bioaccumulation of metal ions from effluent C over time ( $\mu\text{g/g}$ biomass/h) by viable yeast cells.	78
<b>Figure 5.4:</b> The effect of a metabolizable energy source on the uptake of $\text{Zn}^{2+}$ and $\text{Cd}^{2+}$ from effluent A by viable yeast cells.	78
<b>Figure 5.5:</b> Percentage metal removal from effluent A by treated and untreated viable yeast cells in batch systems.	79
<b>Figure 5.6:</b> Percentage metal removal from effluent B by treated and untreated viable yeast cells in batch systems.	79
<b>Figure 5.7:</b> Percentage metal removal from effluent C by treated and untreated viable yeast cells in batch systems.	80

	<b>PAGE</b>
<b>Figure 6.1:</b> Scanning electron micrographs (SEM) of the surface of yeast containing PVA Na-alginate pellets (500x).	95
<b>Figure 6.2:</b> Scanning electron micrographs (SEM) of the surface of yeast containing PVA Na-alginate pellets (5 000x).	95
<b>Figure 6.3:</b> Scanning electron micrographs (SEM) of the surface of the yeast containing PVA Na-orthophosphate pellets (500x).	96
<b>Figure 6.4:</b> Scanning electron micrographs (SEM) of the surface of yeast containing PVA Na-orthophosphate pellets (5 000x).	96
<b>Figure 6.5:</b> Scanning electron micrographs (SEM) of KOH treated PEI:GA biomass pellets (500x).	97
<b>Figure 6.6:</b> Scanning electron micrographs (SEM) of KOH treated PEI:GA biomass pellets (5 000x).	97
<b>Figure 6.7:</b> The effect of pH of the influent solution on Cu-accumulation and breakthrough volume of KOH PEI:GA biomass in a fixed-bed reactor.	98
<b>Figure 6.8:</b> The effect of pH of the influent metal solution on Cu-accumulation and breakthrough volume of PVA Na-alginate pellets in a fixed-bed reactor.	99
<b>Figure 6.9:</b> The effect of pH of the influent metal solution on Cu-accumulation and breakthrough volume of PVA Na-orthophosphate pellets in a fixed-bed reactor.	99
<b>Figure 6.10:</b> A comparison between Cu-biosorption by fresh and regenerated KOH treated PEI:GA biomass pellets.	101
<b>Figure 6.11:</b> A comparison between Cu-biosorption by fresh and regenerated PVA Na-alginate pellets.	101
<b>Figure 6.12:</b> A comparison between Cu-biosorption by fresh and regenerated PVA Na-orthophosphate pellets.	102
<b>Figure 6.13:</b> Comparison of metal biosorption by KOH treated PEI:GA biomass in fixed-bed reactors from respective single element solutions.	103
<b>Figure 6.14:</b> Effect of pH on the percentage metal accumulated by PEI:GA biomass in columns and the respective breakthrough volumes of multi-element equimolar solutions, (a) Zn, (b) Cu, (c) Cr, (d) Ni and (e) Cd.	104 - 106

	<b>PAGE</b>
<b>Figure 6.15:</b> Adsorption isotherms indicating the relationship between initial ambient metal concentration and metal biosorption by PEI:GA biomass in batch reaction studies.	107
<b>Figure 7.1:</b> The waste water treatment tanks operated in the electroplating factory. Two sets of tanks (a) - (b) were linked together in series allowing precipitation of the metals to occur.	115
<b>Figure 7.2:</b> The continuous-flow stirred tank bioreactor system.	119
<b>Figure 7.3:</b> Comparison between alkali (KOH) treatment and settling tanks as a means of precipitating out excess metal from raw effluent.	122
<b>Figure 7.4:</b> Metal removal from raw effluent (pH 5.0) using dual columns linked in series.	123
<b>Figure 7.5:</b> Metal removal from PST effluent (pH 4.5) using a single column system.	124
<b>Figure 7.6:</b> Metal removal from PST effluent (pH 4.5) using dual bioreactor columns in series.	124
<b>Figure 7.7:</b> Biomass saturation and resultant breakthrough volume of tank 1 in a dual tank system.	128
<b>Figure 7.8:</b> Metal accumulation from PST effluent by tank 1 (in a set of three tanks linked in series).	130
<b>Figure 7.9:</b> Metal removal from PST effluent in tank 2 (from a set of three tanks linked in series).	131
<b>Figure 7.10:</b> Metal removal from PST effluent in tank 3 (from a set of three tanks linked in series).	131
<b>Figure 7.11:</b> Comparison of the efficiency of Cd removal from the initial influent PST solution by each of the bioreactor tanks.	132
<b>Figure 7.12:</b> Comparison of the efficiency of Zn removal from the initial influent PST solution by each of the bioreactor tanks.	132
<b>Figure 7.13:</b> Comparative metal accumulation from PST effluent in tank 2 (triple tanks linked in series). The biomass in tank 2 was replaced by that from tank 3 after 22.0 l.	133
<b>Figure 9.1:</b> Breakthrough curves for column removal of cation metals by yeast biomass from aqueous solutions at respective pHs. Biomass, 10 g; Flow rate, 50 ml/h; Infl. metal conc.: Cu, 127 mg/l; Zn, 130.7 mg/l; Cd, 112.4 mg/l.	146

	PAGE
<b>Figure 9.2:</b> Breakthrough curves for removal of Zn by yeast biomass for 2 cycles. Biomass, 10 g; Flow rate, 50 ml/h; Infl. Zn conc., Zn, 130.7 mg/l; Infl. pH, 6.1	146
<b>Figure 9.3:</b> Desorption of cation metals with 0.1M HCl. Flow rate, 50 ml/h.	148
<b>Figure 9.4:</b> Recovery of cation metals from saturated biomass with 0.1M NaCl.	148
<b>Figure 9.5:</b> Breakthrough curves for column removal of Cr <sup>6+</sup> by yeast biomass from EPE at varying influent pHs. Biomass, 10 g; Flow rate, 50 ml/h; Infl. Cr <sup>6+</sup> conc., 30 mg/l.	149
<b>Figure 9.6:</b> Breakthrough curves in scale-up for column removal of Cr <sup>6+</sup> by yeast biomass from EPE at influent pHs of 2.5 and 3. Biomass, 150 g; Flow rate, 11/h; Infl. Cr <sup>6+</sup> conc., 30 mg/l.	149
<b>Figure 9.7:</b> Desorption of Cr <sup>6+</sup> with varying desorbents. Flow rate, 50 ml/h.	151
<b>Figure 9.8:</b> Recovery of Cr <sup>6+</sup> from saturated biomass with 0.1% FA/1N HNO <sub>3</sub> .	152
<b>Figure 10.1:</b> Percentage copper accumulated in batch reactors by immobilised <i>Saccharomyces cerevisiae</i> as a function of time (n = 5, ± SD). Initial copper concentration was 200 µmol/l.	157
<b>Figure 10.2:</b> Percentage cobalt accumulated in batch reactors by immobilised <i>Saccharomyces cerevisiae</i> as a function of time (n = 5, ± SD). Initial copper concentration was 200 µmol/l.	158
<b>Figure 10.3:</b> Removal of copper from aqueous solutions over a pH range in batch reactors by immobilised <i>Saccharomyces cerevisiae</i> (n = 5, ± SD). The pH of the copper solutions was adjusted using HCl and NaOH and the initial concentration was 200 µmol/l.	159
<b>Figure 10.4:</b> Removal of zinc from aqueous solutions of varied pH by immobilised <i>Saccharomyces cerevisiae</i> (n = 5, ± SD). The pH of the zinc solutions was adjusted using HCl and NaOH and the initial concentration was 200 µmol/l.	159
<b>Figure 10.5:</b> Removal of cobalt from aqueous solutions over a pH range in batch reactors by immobilised <i>Saccharomyces cerevisiae</i> (n = 5, ± SD). The pH of the cobalt solutions was adjusted using HCl and NaOH and the initial concentration was 200 µmol/l.	160
<b>Figure 10.6:</b> Removal of gold from aqueous solutions over a pH range in batch reactors by immobilised <i>Saccharomyces cerevisiae</i> (n = 5, ± SD). The pH of the gold solutions was adjusted using HCl and NaOH and the initial concentration was 200 µmol/l.	160

	PAGE
<b>Figure 10.7:</b> Removal of chromium from an aqueous solution by immobilised <i>Saccharomyces cerevisiae</i> in batch reactors ( $n = 5, \pm \text{SD}$ ). $K_d$ and $B_{\text{max}}$ were calculated as $144 \mu\text{mol/l}$ and $20.2 \mu\text{mol/g}$ respectively.	161
<b>Figure 10.8:</b> Removal of cadmium from an aqueous solution by immobilised <i>Saccharomyces cerevisiae</i> in batch reactors ( $n = 5, \pm \text{SD}$ ). $K_d$ and $B_{\text{max}}$ were calculated as $457 \mu\text{mol/l}$ and $52.5 \mu\text{mol/g}$ respectively.	162
<b>Figure 10.9:</b> Removal of gold from an aqueous solution by immobilised <i>Saccharomyces cerevisiae</i> in batch reactors ( $n = 5, \pm \text{SD}$ ). $K_d$ and $B_{\text{max}}$ were calculated as $1513 \mu\text{mol/l}$ and $155 \mu\text{mol/g}$ respectively.	162
<b>Figure 11.1:</b> A flow-diagram of the batch reactor adsorption-desorption protocol.	167
<b>Figure 11.2:</b> Desorption of copper accumulated to immobilised <i>Saccharomyces cerevisiae</i> ( $n = 4, \pm \text{SD}$ ). The desorption profile was generated by sequential reduction of the pH using dilute HCl.	169
<b>Figure 11.3:</b> Eight repeated asorption-desorption cycles in batch reactors determined the reusability of the immobilised <i>Saccharomyces cerevisiae</i> biosorbent ( $n = 5, \pm \text{SD}$ ). The initial copper concentration was $200 \mu\text{mol/l}$ and desorption was achieved using HCl.	169
<b>Figure 11.4:</b> A transmission electron micrograph of a yeast cell. <i>Saccharomyces cerevisiae</i> cells were washed in d.d. milli-Q water and prepared as controls. A single cell is shown at a magnification of 14 000.	170
<b>Figure 11.5:</b> A transmission electron micrograph showing a cross-sectional view of a <i>Saccharomyces cerevisiae</i> cell (magnification 14 000). The cells were prepared for TEM after 30 minutes exposure to copper chloride.	171
<b>Figure 11.6:</b> A transmission electron micrograph of a cross-sectional view of a <i>Saccharomyces cerevisiae</i> cell. The yeast cells were prepared for TEM after a 30 minute exposure to copper chloride and acid treatment to release bound metal. A single cell is shown at a magnification of 19 000.	171
<b>Figure 12.1:</b> Bioaccumulation of copper ona 20 ml immobilised <i>Saccharomyces cerevisiae</i> column. The copper was desorbed using 0.1M HCl, the column was reconditioned and the copper reapplied to determine reusability of the biosorbent.	176
<b>Figure 12.2:</b> Bioaccumulation of cadmium on a 20 ml immobilised <i>Saccharomyces cerevisiae</i> column. The cadmium was desorbed by 0.1M HCl, the column was reconditioned and cadmium reapplied determined reusability.	176

	PAGE
<b>Figure 12.3:</b> Bioaccumulation of zinc on a 20 ml immobilised <i>Saccharomyces cerevisiae</i> column. The zinc was desorbed by 0.1M HCl, the column was reconditioned and zinc reapplied to determine reusability of the biosorbent.	177
<b>Figure 12.4:</b> Bioaccumulation of gold on a 20 ml immobilised <i>Saccharomyces cerevisiae</i> column.	177
<b>Figure 12.5:</b> Desorption of copper and cobalt from a 20 ml immobilised <i>Saccharomyces cerevisiae</i> column (column 1 of 2 in series). Desorption was achieved using 0.1M HCl. The results are expressed as $\mu$ moles metal recovered per 2 ml eluent. The predominant metal eluted from this first column was copper.	179
<b>Figure 12.6:</b> Desorption of copper and cobalt from a 20 ml immobilised <i>Saccharomyces cerevisiae</i> column (column 2 of 2 in series). Desorption was achieved using 0.1M HCl. The results are expressed as $\mu$ moles metal recovered per 2 ml eluent. The predominant metal eluted from this second column was cobalt.	179
<b>Figure 13.1:</b> Removal of copper from the Black Mountain mine effluent by immobilised <i>Saccharomyces cerevisiae</i> in batch reactors. The initial copper concentration was 21.3 $\mu$ mol/l. By increasing the effluent pH using NaOH the copper was removed from solution by <input type="checkbox"/> precipitation and <input checked="" type="checkbox"/> bioaccumulation.	185
<b>Figure 13.2:</b> Removal of lead from the Black Mountain mine effluent by immobilised <i>Saccharomyces cerevisiae</i> in batch reactors. The initial concentration was 6.2 $\mu$ mol/l. The effluent pH was increased using NaOH and the lead was removed from solution by <input type="checkbox"/> precipitation and <input checked="" type="checkbox"/> bioaccumulation.	185
<b>Figure 13.3:</b> Removal of zinc from the Black Mountain mine effluent by immobilised <i>Saccharomyces cerevisiae</i> in batch reactors. The initial zinc concentration was 6.2 $\mu$ mol/l. The effluent pH was increased using NaOH and the lead was removed from solution by <input type="checkbox"/> precipitation and <input checked="" type="checkbox"/> bioaccumulation.	186
<b>Figure 13.4:</b> Removal of iron from the Black Mountain mine effluent by immobilised <i>Saccharomyces cerevisiae</i> in batch reactors. The initial iron concentration was 1078 $\mu$ mol/l. The effluent pH was increased using NaOH and the iron was removed from solution by <input type="checkbox"/> precipitation and <input checked="" type="checkbox"/> bioaccumulation.	186
<b>Figure 14.1:</b> Standard curve for the estimation of algal dry mass from chlorophyll $\alpha$ concentrations.	189
<b>Figure 14.2:</b> Graph of pH vs time.	191

	<b>PAGE</b>
<b>Figure 14.3:</b> Graph of algal concentration vs time. Algal concentration (mg dry mass/ml).	191
<b>Figure 14.4:</b> Graph of salinity vs time. NaCl salinity determined using a salinity refractometer.	192
<b>Figure 14.5:</b> Cumulative copper addition ( $\mu$ moles vs time for experimental groups.	193
<b>Figure 14.6:</b> Amount of copper ( $\mu$ moles) remaining in solution.	193
<b>Figure 14.7:</b> Cumulative iron addition ( $\mu$ moles) vs time in experimental groups.	194
<b>Figure 14.8:</b> Amount of iron ( $\mu$ moles) remaining in solution.	194
<b>Figure 14.9:</b> Efficiency (cumulative %) of algal system at removing copper from added effluent.	195
<b>Figure 14.10:</b> Efficiency (cumulative %) of algal system at removing iron from added effluent.	195
<b>Figure 14.11:</b> Efficiency (cumulative %) of algal system at removing lead from added effluent.	195
<b>Figure 14.12:</b> Efficiency (cumulative %) of algal system at removing zinc from added effluent.	195
<b>Figure 14.13:</b> Change in pH over time for flasks in volume controlled system.	196
<b>Figure 14.14:</b> Change in algal concentration over time. Algal concentration as mg dry mass per ml.	196
<b>Figure 14.15:</b> Light micrograph showing the presence of a mixed culture of <i>Spirulina</i> , <i>Oscillatoria</i> and diatoms - day 37. (Magnification x 40).	197
<b>Figure 14.16:</b> Copper concentration ( $\mu$ M) in solution over time in volume controlled (400 ml) algal system.	198
<b>Figure 14.17:</b> Copper removal (cumulative %) from solution in a volume controlled algal system.	198
<b>Figure 14.18:</b> Lead removal (cumulative %) vs time.	199
<b>Figure 14.19:</b> Zinc removal (cumulative %) vs time.	199
<b>Figure 14.20:</b> Iron removal (cumulative %) vs time.	199
<b>Figure 14.21:</b> pH profile of Plaatjiesvlei effluent.	200



	<b>PAGE</b>
<b>Figure 14.22:</b> Graph of pH vs time for autoclaved control experiment.	201
<b>Figure 14.23:</b> Cumulative removal (%) of copper added to Zarrouk's medium.	202
<b>Figure 14.24:</b> Cumulative removal (%) of iron added to Zarrouk's medium.	202
<b>Figure 14.25:</b> Cumulative removal (%) of lead added to Zarrouk's medium.	202
<b>Figure 14.26:</b> Cumulative removal (%) of zinc added to Zarrouk's medium.	203

## LIST OF TABLES

	PAGE
<b>Table 1.1:</b> Chemical composition of the cell wall of <i>S. cerevisiae</i> .	9
<b>Table 2.1:</b> Parameters of metal binding by isolated cell wall and cell wall components of yeasts.	29
<b>Table 2.2:</b> Affinity constant ( $K_A$ ) (mol/l) of the intact and extracted cell wall components for $Cu^{2+}$ , $Co^{2+}$ and $Cd^{2+}$ .	30
<b>Table 4.1:</b> Ion profile of yeast cells exposed to respective 1M $Cu^{2+}$ , $Co^{2+}$ and $Cd^{2+}$ solutions for 1 h.	60
<b>Table 5.1:</b> Heavy metal profiles for effluents A, B and C. Metal levels of the effluents are compared to suggested median levels for drinking and dam/river water.	75
<b>Table 5.2:</b> Metal accumulation ( $\mu g$ metal/g (wet mass)) by yeast from electroplating effluents A, B and C.	81
<b>Table 5.3:</b> Metal accumulation ( $\mu g$ metal/g (wet mass)) from a spiked solution containing $Cu^{2+}$ , $Cd^{2+}$ , $Cr^{3+}$ , $Zn^{2+}$ and $Ni^{2+}$ in 50 mg/l concentrations.	81
<b>Table 7.1:</b> Levels of metal (mg/l) present in raw and PST electroplating effluent compared to stipulated national drinking water and aquatic ecosystems criteria (median levels).	114
<b>Table 7.2:</b> The effect of pH on the metal concentration of the influent raw effluent and the resultant breakthrough volumes in each of the small-scale single columns.	120
<b>Table 7.3:</b> The effect of process scale-up on the breakthrough volumes and final concentrations of the Cd in solution.	125
<b>Table 7.4:</b> Comparison between the efficiency of metal removal by 2.5 l and 5.0 l tanks.	126
<b>Table 7.5:</b> Comparison of efficiency of metal removal from PST effluents between two dual bioreactor systems, viz 2.5 l and 5.0 l or 2 x 5.0 l tanks.	127
<b>Table 9.1:</b> Levels of metals present in electroplating effluent (PE Plating), compared to stipulated criteria (mg/l).	143
<b>Table 9.2:</b> Granule stabilities of the yeast biomass cross-linked with differing FA/0.1M HCl ratios.	145
<b>Table 9.3:</b> Column removal of cation metals from aqueous solutions.	147

	<b>PAGE</b>
<b>Table 9.4:</b> Cation metal recovery with 0.1M HCl.	147
<b>Table 9.5:</b> Column removal of Cr <sup>6+</sup> from electroplating effluent.	150
<b>Table 9.6:</b> Chromium recovery with various desorbents.	153
<b>Table 10.1:</b> Biosorption capacities of metals by <i>S. cerevisiae</i> as generated from Hanes-Woolf transformation plots.	163
<b>Table 11.1:</b> Percentage desorption of copper from immobilised <i>S. cerevisiae</i> in batch reactors.	168
<b>Table 12.1:</b> Metal uptake on a <i>S. cerevisiae</i> column and metal recovery.	178
<b>Table 12.2:</b> Adsorption-desorption reusability investigation. Adsorption of copper to an immobilised <i>S. cerevisiae</i> column over 8 cycles.	180
<b>Table 13.1:</b> Composition of the mine effluent.	184
<b>Table 14.1:</b> Results from day 34 to 42 showing zinc removal per day in group 4 of the control experiment. Zinc added and removed values expressed as $\mu$ moles.	203
<b>Table 14.2:</b> Progression of pH over time for duration of distilled water control.	204

## **1. GENERAL INTRODUCTION**

Water is an important, though often underrated resource, with the availability and quality thereof being of paramount importance. This fact was recognized by the United Nations during the 1980's, resulting in the designation of that decade to maintaining the quality of international drinking water. With such a high demand for potable water, it is essential to prevent, or at least to limit the pollution of this resource. A commonly encountered group of pollutants in water are the toxic heavy metals. The concentration of these metals in natural waters varies greatly with locality and time. Since the onset of the industrial revolution, anthropogenic sources have contributed to such variations, though natural fluctuations often predominate depending on the underlying geology of the area (1).

If not processed correctly, these metals can be extremely toxic and therefore become a health hazard to both humans and the environment. In addition, metals are a non-renewable resource and expensive to locate, mine and refine. Reclaiming heavy metals downstream of their source will minimize the hazard that they pose to the environment and depending on the species of metal being recovered, the financial rewards of such an operation could be vast.

Biological based metal-recovery may provide a possible solution to metal removal from waste or natural waters. Microorganisms in metal-contaminated environments have been forced to cope and utilize the inorganic world around them to ensure their survival (2, 3). These microorganisms play an important role in the solubilization, accumulation, transport and deposition of metals in the environment. To achieve this they participate in a number of metal-interactions, eg. bioleaching, biotransformations and bioaccumulation (2, 4, 5).

The incorporation of these natural phenomenon into biological metal removal processes in polluted or waste water will result in the development of a potential bioremediation tool. Such a process would offer an alternative to the existing conventional metal removal technologies (6).

## **PART 1: METAL BIOACCUMULATION**

### **1.1. HISTORICAL OVERVIEW**

Microorganisms and plants have been depositing and decomposing minerals in the earth's crust and oceans since geologically ancient times. Because microbes serve as the basis of all ecosystems this will influence the concentration of metal elements in the environment which will have a significant impact on the food chains and food webs. For example, cells of algae, bacteria, plants, yeasts and other fungi can all accumulate metal ions, often at levels up to 25% of cell dry weight. Ingestion of these microbes and plants result in the cumulative effect of metals at the higher levels of the food chain.

Metal-microbial interactions can, however, be beneficial and have been used throughout human history to the benefit of mankind. As early as 1000 BC mine workers in the Mediterranean basin recovered the copper that was leached into mine drainage waters by bacteria. Metal recovery using bacterial leaching was also practiced by the Romans in the first century, the Welsh in the sixteenth century and the Spanish who worked the Rio Tinto mine during the eighteenth century (7).

The ability of a specialized species of the nettle family to grow on toxic soil and subsequently accumulate the copper from the soil enabled archaeologists to unearth the ancient Kabambian culture which flourished in Central Africa. The soil at the sites of the Kabambian copper smelters remained extremely toxic, preventing all plant growth bar the small nettle plant. By following the trail of these plants, the culture of these ancient people could be elucidated (8).

During the 200 years following the beginning of industrialization, changes in the distribution of elements at the surface of the earth have occurred and due to elevations in the levels of many toxic metals in the environment, microbes and other living organisms have had to adapt. This has necessitated enhanced metal accumulation by the microbes and subsequently these microbes have had to develop metal tolerance and metal resistance for their to survival.

## 1.2. MICROBIAL BIOACCUMULATION OF METAL CATIONS

The bioaccumulation mechanism of heavy metal cations such as  $\text{Co}^{2+}$  and  $\text{Cd}^{2+}$  by the yeast *Saccharomyces cerevisiae* was first reported by Norris and Kelly (4). The accumulation occurs as a biphasic process. The initial phase involves a rapid, metabolism and temperature independent stage, which is followed by slower, progressive metabolism dependent uptake (4). The uptake system which allows for the accumulation of  $\text{Cd}^{2+}$  and  $\text{Co}^{2+}$  appears to be a general one with only limited specificity, since competition for the uptake of cations occurs. Further investigations (5) proved that yeasts are capable of accumulating other cations, eg.  $\text{Mg}^{2+}$ ,  $\text{Zn}^{2+}$ ,  $\text{Ni}^{2+}$ ,  $\text{Ca}^{2+}$ ,  $\text{Cu}^{2+}$  and  $\text{Mn}^{2+}$ . In addition, this process is not limited to yeasts, with similar uptake mechanisms being exhibited by bacteria (5) and fungi (9).

### 1.2.1. EXTRACELLULAR ADSORPTION

The first stage of the biphasic metal uptake process involves cation binding to the cell surface, eg. to the extracellular microbial polysaccharide layers of slime produced by the alga *Zoogloea*, or to the cell wall matrix of *S. cerevisiae* or *Rhizopus arrhizus*. Biosorption of metal ions to microbial cell walls is a rapid, reversible process. The overall nett negative charge of microbial cell walls facilitates physico-chemical reactions between the cell wall and the positively charged metal cations. This process has been compared to an ion exchange phenomenon, with the reaction chemistry of both the receptors sites and metal species subject to environmental conditions (2, 10 - 12).

Microorganisms are able to accumulate metal ions from solution up to 25% of their dry weight. However, the number of binding sites available on the cell wall for biosorptive complexations are insufficient to account for the amount of metal accumulated. This suggests that associated binding phenomenon occur whereby the deposition of insoluble metal cations at the microbial cell surfaces can proceed. In some cases microbial transformation of the metals is necessitated. Beveridge (cited by 13), noted the formation of gold deposits on the cell walls of *Bacillus subtilis*. He proposed that the metal ions reacted initially with the carboxyl groups of the cell walls, then subsequently acted as nucleation sites for the crystallization of additional gold molecules. A similar phenomenon was observed by Strandberg (cited by 13), regarding the crystalline deposits of uranium on the surface of *S. cerevisiae* cells. Large quantities of insoluble lead (490 mg/g dry weight) have also been observed on the surface of *Micrococcus luteus* (2).

## 1. GENERAL INTRODUCTION

Precipitation of metal residues in the microbial wall may also explain the elevated levels of cell wall associated metal ions, eg. uranium is precipitated as uranyl hydroxide within the wall of *R. arrhizus* (11).

### 1.2.2. INTERNALIZATION OF METAL CATIONS BY *S. cerevisiae*

Secondary uptake of metal ions is responsible for the accumulation of large quantities of metal ions. The process is usually metabolism-dependent (4), although intracellular metal deposition can also occur via non-metabolically mediated processes (13). Internalization involves the movement of the metal cations from the external surface, across the cell membrane or envelope into the cell interior. Diverse transport mechanisms can be associated with these actions: diffusion through pores, carrier mediated diffusion, uphill thermodynamically active transport, group translocation and pinocytosis (14). A distinction is usually drawn between the uptake of monovalent and divalent cations (2, 15, 16).

#### 1.2.2.1. TRANSPORT OF MONOVALENT CATIONS

The transport of monovalent cations in *S. cerevisiae* is regulated by the action of the plasma membrane-bound  $H^+$ -ATPase (15, 17 - 24). The  $H^+$ -ATPase enzyme system is based on a  $K^+/H^+$  antiport action, whereby protons are expelled from the cell. In doing so a transmembrane electrochemical proton gradient, which has both a chemical component (pH) and electrical component (membrane potential), is created. It is the electrical component, *ie.* the membrane potential, which is predominantly responsible for monovalent cation transport into the cell.

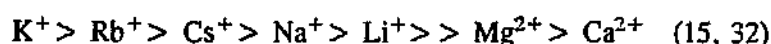
The mechanism of uptake of monovalent metal cation into the cell is governed by complex kinetic interactions. Initial kinetics (25) suggested that uptake of monovalent cations adhered to Michaelis-Menton principles. However, these kinetics are influenced by the number of binding sites involved in the translocation process. The kinetics are further influenced by indirect effects of the surface potential (pH) and in addition the membrane potential of the yeast cell across the plasmalemma may also alter the transport kinetics (14, 16, 19, 26).

Sustained transport of cations into the cell requires a metabolizable energy source to maintain ATPase activity and to sustain  $H^+$  efflux from the cell. Addition of glucose (27) and other sugar

## 1. GENERAL INTRODUCTION

monosaccharides (28) to the yeast cell stimulate  $H^+$ -ATPase activity, through two processes: glucose can act as an energy source for the biosynthesis of both cytoplasmic and membrane transport proteins, or alternatively the  $H^+$  efflux pump is activated, thereby stimulating accumulation (15).

The majority of information on the monovalent cation system focusses on  $K^+$  accumulation, since the affinity of the transport system for this ion is high. Other cations which can be translocated via this process, include  $Ca^{2+}$  (29, 30) and  $Mg^{2+}$  (31). The relative order of affinities of cations for the monovalent cation transport system is:



Heavy metal cations and organometallic compounds inhibit the ATPase antiport system. This results in the reduced ability to maintain the electrochemical gradients, though the  $H^+$  efflux is affected to a lesser extent than the  $K^+$  influx.  $H^+$  efflux is inhibited by a toxicity sequence of divalent cations of  $Cd^{2+} > Cu^{2+} > Ni^{2+} > Zn^{2+} > Co^{2+} > Mn^{2+}$  whilst inhibition of  $K^+$  uptake occurs in order of  $Cd^{2+} > Cu^{2+} > Ni^{2+} > Co^{2+} > Mn^{2+} > Zn^{2+}$  (15).

The variation in  $K^+$  and  $H^+$  inhibition suggests that  $K^+$  uptake is not limited to  $H^+$ -ATPase activity, but that  $K^+$  accumulation can occur via alternative routes, eg. membrane permeability (14, 15).

### 1.2.2.2. DIVALENT METAL CATION UPTAKE

Although certain divalent metal cations, eg.  $Mg^{2+}$ ,  $Ca^{2+}$ ,  $Zn^{2+}$ ,  $Mn^{2+}$  and  $Cu^{2+}$ , are essential for yeast cell growth and metabolism, and therefore need to be accumulated from the external environment, many metal divalent cations are toxic to yeast cells above certain concentrations. The most toxic include the group of heavy metal cations, many of which do not fulfill any essential functions in the yeast cell, yet are still sequestered within the cell.

The uptake of divalent cations into the yeast cell is complex. Kelly *et al.* (2), reviewed numerous transport systems and intracellular accumulation patterns of divalent and heavy metal cations, but hesitated to identify any accumulation mechanisms.

Divalent cation uptake in yeast is an energy dependent mechanism (25), which exhibits apparent



## 1. GENERAL INTRODUCTION

saturation kinetics (16, 33). The involvement of either a dual mechanism consisting of two simultaneously operating single-site transport processes, or that of a single site transport mechanism (16, 33), results in deviations occurring from Michaelis-Menton kinetics. Addition of glucose, especially in the presence of inorganic phosphate, enhances the uptake of divalent metal cations (25).

Early work by Fuhrmann and Rothstein (25) demonstrated an apparent affinity series of accumulation of  $Mg^{2+} > Co^{2+} > Zn^{2+} > Mn^{2+} > Ni^{2+} > Ca^{2+} > Sr^{2+}$  by yeasts. Subsequent work (34 - 37) has demonstrated uptake of  $Cd^{2+}$  and  $Fe^{2+}$ .  $Co^{2+}$ ,  $Zn^{2+}$  and  $Ni^{2+}$  appear to be transported into the cell by the same mechanism responsible for the uptake of  $Mn^{2+}$  and  $Mg^{2+}$  (25), which are accumulated to a greater extent than  $Ca^{2+}$  and  $Sr^{2+}$ . The difference in accumulation is not due to differences in the affinity for the transport system, but can be ascribed to the leakage and efflux of  $Ca^{2+}$  and  $Sr^{2+}$  from the cells due to increased cell membrane permeabilization (15, 16, 25).

Active divalent cation transport is dependent on plasma membrane  $H^+$ -ATPase activity, although non-competitive inhibition of  $Co^{2+}$  and  $Ni^{2+}$  by  $K^+$  implicates that they are not translocated by the monovalent cation carrier (25). Similarly  $Ca^{2+}$  and  $Sr^{2+}$  uptake is inhibited in a non-competitive way by  $Rb^+$  (38). The major role of the plasma membrane  $H^+$ -ATPase in the uptake of divalent cations is one of energizing the cell membrane thereby sustaining an electrochemical gradient. Enhancement of the membrane potential, eg. increased  $K^+$  efflux, results in increased divalent cation accumulation.

Mutual interaction between divalent cations can also occur. In the presence of specific metal cations, uptake of other divalent cations may be enhanced. For example the uptake of  $Zn^{2+}$  is increased specifically by  $Cu^{2+}$ , whereas the uptake of  $Mn^{2+}$  remains unaffected (16). Similarly  $Co^{2+}$  enhances  $Zn^{2+}$  uptake, with the reciprocal also being true (25). In comparison  $Ca^{2+}$  inhibits  $Zn^{2+}$ ,  $Co^{2+}$  (25) and  $Cd^{2+}$  (4) uptake. The presence of  $Mg^{2+}$  results in a minimal reduction in  $Cd^{2+}$  accumulation (4).

Active divalent metal cation uptake into the cell is inhibited by metabolic inhibitors. Inhibitors of the plasma membrane  $H^+$ -ATPase, eg. DES (diethylstilbestrol) and DNP (2,4 dinitrophenol) block the uptake of divalent cations whilst monovalent cation uptake remains unaffected.

Intracellular divalent cation deposition can also occur via non-metabolically mediated processes. In the presence of  $Cu^{2+}$  the permeability barrier of the yeast cell plasma membrane is lost within 2

## **1. GENERAL INTRODUCTION**

min. The addition of copper ions to the yeast cells causes increased permeability of the plasma membrane, with massive and rapid release of 70% of the cellular  $K^+$ . The  $Cu^{2+}$  causes lesions in the plasma membrane but does not appear to alter the permeability of the vacuole membrane (39). The ability to permeabilize the yeast cell membrane is limited to specific cations, Addition of  $Zn^{2+}$  does not result in  $K^+$  efflux, while  $Cd^{2+}$  does. For every  $Cd^{2+}$  ion accumulated within the cell, approximately 4  $K^+$  ions are released. Though responsible for  $K^+$  efflux from yeast cells,  $Cd^{2+}$  treatment stimulates  $Ca^{2+}$  uptake in yeast by increasing the cation permeability of the cell membrane (36).

Internalized heavy metal cations are distributed between the soluble (cytosol) and insoluble (vacuole and mitochondrial) fractions of the cell. Those divalent cations which have not been sequestered within the cell remained complexed to the yeast cell walls.

## **1.3. LOCALIZATION OF ACCUMULATED HEAVY METAL CATIONS**

### **1.3.1. CELL WALL**

Rapid, yet reversible binding of metal ions occurs at the cell surface. The interaction between the cell surface and metal ions has been observed in several fungal, bacterial and algal species and has been directly observed in transmission electron micrographs.

#### **1.3.1.1. METAL BINDING BY MICROBIAL CELL WALLS**

Sequestration of metal cations by microbial cell walls has been documented for yeast cells (40 - 44), bacteria (45 - 49) and algae (50, 51). Microbial cell walls tend to have an overall nett negative charge enabling interaction with counter ions in the environment (46). Metal-microbial wall interaction can be accounted for by cation exchange with negatively charged groups (41, 52), whilst other microbial wall ligands allow coordination of metal ions (52).

The cell envelopes of *Escherichia coli* K-12 are capable of binding large amounts of Hf and Os, intermediate levels of the group IV and transition elements, but only low amounts of the alkali and alkali-earth metals (47). In comparison *B. subtilis* accumulates substantial amounts of the alkali and alkali-earth metals, viz.  $Mg^{2+}$ ,  $K^+$ , and  $Na^+$ , and intermediate amounts of the higher atomic

## 1. GENERAL INTRODUCTION

numbered elements ( $\text{Mn}^{2+}$ ,  $\text{Zn}^{2+}$ ,  $\text{Ca}^{2+}$ ,  $\text{Au}^{3+}$  and  $\text{Ni}^{2+}$ ). Only small quantities of  $\text{Hg}^{2+}$ ,  $\text{Sr}^{2+}$ ,  $\text{Pb}^{2+}$  and  $\text{Ag}^{+}$  are complexed by the cell walls (48). Yeast cell surfaces are also capable of binding a wide range of metal ions (40, 41, 43).

The ranging affinities of microbial cell walls for specific metal ions can be ascribed to differences in cell wall composition and chemistry, eg. the cell walls of *B. subtilis*, a gram-positive bacterium consists primarily of techoic acid and peptidoglycan. A galactosamine polymer and bound protein may also be present in this structure (49). The chemical and structural composition of gram-positive bacteria differ completely to their gram-negative counterparts. *E. coli*, a gram-negative bacterium contains a minimal amount of peptidoglycan in the cell wall, whilst the outer membrane possesses a lipopolysaccharide (46, 47). In comparison, the rigid cell wall of *S. cerevisiae* consists predominantly of polysaccharides and a lesser amount of protein. Due to the nature of this study, the composition of bakers yeast cell walls and their metal binding properties are discussed in greater detail.

### 1.3.1.2. COMPOSITION OF THE YEAST CELL WALL

Due to its abundance, *S. cerevisiae* has been used intensively to study cell wall morphology. The yeast cell wall which is approximately 70 +/- 10 nm thick (53), has been described as one of the most tough and rigid of all microbial cell walls, imparting mechanical strength to the cells. The portion of the dry cell weight represented by the extracellular wall is large and can account for between 25 - 30% of the dry weight of the cell (54).

The wall fraction of the yeast cell has a layered structure. This bilayered structure consists mainly of intermeshed polysaccharide microfibrils separated into an inner amorphous net of microfibrils (7.5 - 10.0 nm thick) (55) and an interwoven fibrillar outer layer (54). In addition to the polysaccharide components, proteins and lipids occur within the wall (56 - 58) (Table 1.1). A small percentage of the cell wall may be comprised of inorganic ions such as  $\text{Ca}^{2+}$  and  $\text{Mg}^{2+}$  (59).

Table 1.1. Chemical composition of the cell wall of *S. cerevisiae* (from 57, 58)

Component	% Total dry mass
Glucan	28.8
Mannan	31.0
Protein	13.0
Chitin	1.0
Chitosan	1.0
Lipid	8.5
Ash	3.0
Unknown	13.7

The predominant structural component of the cell wall is glucan, whilst the outer layer is represented mainly by mannoproteins. Chitin which occurs in small amounts, constitutes the primary septum, acting as an indicator of bud scars.

#### 1.3.1.2.1. GLUCANS

Yeast cell wall glucan is a homopolymer of glucose linked through either  $\beta(1-3)$  or  $\beta(1-6)$ -D-glycosidic bonds. It forms part of the inner layer of the bilayered cell wall and is responsible for cell rigidity and subsequent maintenance of cell integrity. Two species of glucans, either alkali-soluble or alkali-insoluble fractions occur. The alkali-soluble fractions constitute the minor component, whilst the major glucan component (a  $\beta(1-3)$  linked backbone containing 3%  $\beta(1-6)$  linkages) is insoluble in alkali (54, 55, 57, 58, 60, 61).

#### 1.3.1.2.2. CHITIN AND CHITOSAN

Closely associated with glucans are the chitin polymers. Recent evidence has stated that chitin, a linear polymer of  $\beta(1-4)$  linked N-acetylglucosamine, may be covalently linked to glucan. The glucan chains appear to be directly linked to chitin through a glycosidic linkage between position one of the first residue of the glucan chain and position six of the intra-chain N-acetylglucosamine residue (54,62).

### 1.3.1.2.3. MANNANS

Mannan is a polymer of mannose monomers forming a main chain linked by  $\alpha(1-6)$  bonds and  $\alpha(1-2)$  and  $\alpha(1-3)$  linked mannose sidechains (53). In yeast, mannans are not found as a separate entity within the wall but are covalently linked via serine, threonine or asparagine residues to form a mannoprotein complex of 25 - 500 kDa. The complex has a mannan : protein ratio of 12 : 1, forming a molecule with a slightly larger dimension than pure mannan.

The mannan contains approximately 1% phosphate which appears to be linked to the 6 position of the non-reducing mannose residue of the main chain (57). The phosphate moiety is diesterified, and therefore capable of bonding with another C-mannose residue, thereby fulfilling a cross linking function (53).

### 1.3.1.2.4. PROTEINS

The exact number of cell wall proteins is unknown (54), although different types of proteins varying in molecular mass between 30 - 410 kDa have been extracted from the wall. Though these proteins are found throughout the cell wall they occur more prominently in the outer mannoprotein layer (58).

### 1.3.1.3. YEAST CELL WALL - METAL INTERACTIONS

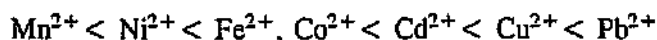
Cell walls of yeast have been proven to bind  $\text{Ca}^{2+}$  (44) and  $\text{UO}_2^{+}$  (40) forming stable, yet reversible complexes. Subsequent work has established an affinity of metal ions for cell wall components, eg.  $\text{Cu}^{2+}$  and  $\text{Ca}^{2+}$  for chitosan (63, 64),  $\text{Cd}^{2+}$  for mannoproteins (65) and  $\text{Co}^{2+}$  interaction with the protein component of both the upper and lower layers of the cell wall (41).

Present in the cell wall is an abundance of ligands capable of complexing with heavy metal and other cations. Each of the major cell wall components contributes specific binding ligands. Depending on the nature of these ligands they can selectively bind certain metals.

Metal ions can be separated into three categories: class A, class B and borderline metal ions (66). Class A metal ions are referred to as hard ligands, whilst class B metal ions are called soft acids. The former are found at the left hand side of the periodic table and include ions of the alkali metals

## 1. GENERAL INTRODUCTION

and alkaline earths. In contrast class B metal ions form a small block of roughly triangular shape with  $\text{Cu}^{2+}$  at its apex ( $\text{Cu}^{2+}$  is a borderline metal) and  $\text{Ir}^{3+}$  and  $\text{Bi}^{3+}$  at its base. The heavy metals are categorized under borderline metal ions (66). When plotted graphically according to their class A or ionic index ( $Z^2/r$ ) vs their class B or covalent index ( $X^2_{\text{m}}r$ ), the borderline ions show a greater affinity towards class B characteristics, with the class B character increasing in the order:



An exception is  $\text{Zn}^{2+}$  which exhibits considerable class A character (66).

A marked difference occurs between the types of binding sites preferred by class A and class B metal ions (52, 66). Class A ions favour oxygen binding sites viz. carboxylate, carbonyl, alcohol, phosphate or phosphodiester groups, whilst class B ions prefer nitrogen and or sulphur centres, eg. sulphydryl (-SH), disulphide (-S-S-), thioester (-SR), amino ( $-\text{NH}_2$ ), or heterocyclic nitrogen (imidazole of histidine or nucleotide bases) (52, 66). Variations of binding affinity within the heavy metal group occurs. For example  $\text{Cu}^{2+}$  prefers the nitrogens of histidine, whilst  $\text{Zn}^{2+}$  binds in preference to the sulphydryl groups of cysteine.

Yeast biomass contains several of these binding ligands on its cell walls, eg. the carboxylate, hydroxyl, phosphate and amino groups of the carbohydrate and protein components (43, 67). The outer layer plays a more significant role in metal binding than the inner layer, suggesting the importance of the mannoprotein fraction in comparison to the glucan and chitin components (67).

### 1.3.2. YEAST VACUOLES

Vacuoles in plants and fungi occupy between 25 - 95% of the cell and have essential and dynamic physiological roles (68). Several hydrolytic enzymes are contained therein and in addition, this organelle is involved in pH homeostasis and the compartmentalization of metabolites and ions.

Many different cellular constituents including amino acids (69 - 71), polysaccharides and polyphosphates (72, 73) are stored within the fungal vacuole. The storage and homeostasis of cellular metal ions are also controlled by this organelle. Cells are obligated to regulate their cytosolic ion concentration for several reasons. Some of the ions are potentially harmful, eg.  $\text{Co}^{2+}$ ,  $\text{Cd}^{2+}$ ,  $\text{Pb}^{2+}$ ,

## 1. GENERAL INTRODUCTION

$\text{Hg}^{2+}$  and  $\text{Fe}^{3+}$  cannot be allowed to accumulate within the cytosol but must be transferred elsewhere. Even the physiological cations may become toxic in excessive concentrations. Their levels must be precisely controlled if they are to play a role in the regulation of cellular processes (73, 74). Vacuole stored metal ions include such physiologically useful cations as  $\text{Zn}^{2+}$ ,  $\text{K}^+$ ,  $\text{Ca}^{2+}$ ,  $\text{Mn}^{2+}$  (74 - 77) as well as the non-physiological cations eg.  $\text{Co}^{2+}$ ,  $\text{Pb}^{2+}$ ,  $\text{Au}^{3+}$ ,  $\text{Cd}^{2+}$  and  $\text{Fe}^{3+}$  (78 - 81) (for review 73).

Studies on the internal distribution of metal ions in yeast cells after accumulation indicate a selective accumulation of metal ions by the vacuole. Whilst the proportion of  $\text{Na}^+$  and  $\text{K}^+$  in the cytosol exceeds that of the vacuole, 21.2% of accumulated  $\text{Cd}^{2+}$  is found in the vacuole compared to 0.8% in the cytosol. Likewise, 31.1% of  $\text{Ag}^+$  is compartmentalized within the vacuole compared to 7.8% which remains soluble in the cytosol (82). Intracellular ferritin, zinc and other heavy metals are also found concentrated within the vacuole. Mutants with defective vacuoles are more sensitive to heavy metal poisoning and antibiotics. Even  $\text{Ca}^{2+}$ , a physiological ion, may be inhibitory to the growth of strains with defective vacuoles (75).

Like the storage of nutrients and metabolites, the accumulation of metal cations within the vacuoles requires a transport system. Vacuolar uptake of several cellular constituents is carried out by  $\text{H}^+$ /ion transport systems, *ie.* ion uptake into the vacuole is driven by a proton efflux from the organelle. *In vitro* studies with purified vacuole vesicles have shown that  $\text{H}^+$ /ion antiports are the principle mechanism of vacuolar uptake of the divalent cations  $\text{Ca}^{2+}$ ,  $\text{Mg}^{2+}$ ,  $\text{Mn}^{2+}$ ,  $\text{Zn}^{2+}$ , arginine and several other amino acids (15, 22, 78, 80, 83, 84).

The proton gradient is generated by an  $\text{H}^+$ -ATPase, the V-ATPase enzyme, comprised of eight subunits (85). Similar to the plasma membrane system, the energy capacity of the vacuolar  $\text{H}^+$  gradient can be increased by the corresponding  $\text{K}^+$  gradient. The efflux of vacuolar  $\text{K}^+$  initiates the accumulation of  $\text{Mn}^{2+}$ ,  $\text{Mg}^{2+}$ ,  $\text{Cu}^{2+}$  and  $\text{Cd}^{2+}$  within the vacuole (38, 39, 79, 86).

Substantial evidence (73) indicates that once the accumulated metal ions and amino acids have entered the vacuole they interact with polyphosphate ions. Polyphosphates are macromolecular anions and are unique to the vacuole. Within the vacuole they serve a dual function. Due to their anionic nature they coordinate with basic amino acids and inorganic cations, thereby acting as storage macromolecules. Secondly, because they lower the concentration of free inorganic phosphate, amino

acid and inorganic cations, they reduce the osmotic pressure within the cell. Hence both the cytosol and vacuole remain isotonic (73).

### **1.3.3. YEAST MITOCHONDRIA**

Although the mitochondria do not appear to be a major site of metal ion accumulation,  $\text{Ca}^{2+}$ ,  $\text{Mg}^{2+}$ ,  $\text{K}^+$  and other monovalent ions have been reported to interact with the mitochondrial enzymatic system, whilst  $\text{Ca}^{2+}$  uptake and release has been documented in yeast mitochondria (87 - 89).

Yeast mitochondria have diverse  $\text{Na}^+$  and  $\text{K}^+$  transport systems. A  $\text{K}^+/\text{H}^+$  ATPase antiport system, similar to that of the plasma membrane and tonoplast has been identified in the mitochondrial membrane. Ion transport is non-specific,  $\text{K}^+$ ,  $\text{Na}^+$ ,  $\text{Rb}^+$ ,  $\text{NH}_4^+$  and  $\text{Li}^+$  all enhance ion transport (87). Mitochondrial ATPases also have an absolute requirement for monovalent cations (89). Should the same non-specificity apply to divalent cations this would imply that the mitochondria could participate in intercellular metal cation sequestration.

## **PART 2: BIOREMEDIATION**

### **2.1. WATER AVAILABILITY AND DRINKING WATER CRITERIA IN SOUTH AFRICA**

The need to take precautions with drinking water to protect public health was recognized as many as 4000 years ago. Today the quality of drinking water is still of primary concern (90). South Africa is not only faced with the problem of maintaining the quality of its drinking water, but also has to protect its dwindling supplies. It has been calculated that the supply and demand curves for potable water available in South Africa will cross in the year 2020 and beyond that, demand will exceed supply (90).

How is drinking water described? Criteria have been established, not as regulatory requirements, but merely to serve as guidelines. No legally enforceable drinking water standards exist in South Africa (90). In short, the drinking water quality criteria represents the maximum level of contaminants present therein that the water can be consumed with adequate safety (90).



## ***I. GENERAL INTRODUCTION***

The task of establishing criteria is not an easy one. The criteria can only be as reliable as the body of knowledge existing for a given constituent (91). Due to technological advances more information has become available which has prompted the need to focus on a new range of determinants, previously regarded as insignificant. Important determinants include microbiological factors, aesthetic considerations, organic chemical material, radionuclide and physical and inorganic determinants. Included within the latter group of determinants are the natural elements which were long regarded as having primarily aesthetic or industrial significance and therefore being of only marginal health importance. However, there are inorganic constituents of more obvious public health significance, eg. the toxic metals. Industrial and mining activities provide numerous opportunities for toxic metal release into the environment and although the waters produced as by-products from these activities have been subject to pollution control guidelines, the water quality continues to deteriorate.

## **2.2. METALS AS POLLUTANTS IN WATER**

The toxicity of metals in natural waters is widely assumed to result from a combination of their solubility, bioavailability and mode and kinetics of uptake in the target organism (1, 66). Microbes in aquatic systems are key components in biochemical cycling of elements and serve as the basis for all food chains and food webs. Micro- and macrobiota sensitive to metal pollutants will be affected at various physiological levels thereby disturbing the equilibrium of the food chains.

Elements exhibiting the most toxic effects on micro- and macrobiota in aqueous systems include in particular the heavy metals. The heavy metals are comprised of 40 elements with a density greater than 5. Many of these metals are essential for growth of both prokaryotic and eukaryotic organisms, but also have a comprehensively toxic effect on cells. Others do not fulfill any physiological functions, but cause metal toxicity within the cell. The mechanisms of metal ion toxicity can be divided into 3 categories: 1) inhibition of the essential biological functional groups of biomolecules, 2) displacement of the essential metal ions in biomolecules and 3) modification of the active conformation of biomolecules (66, 92, 93, 94). Heavy metal contamination of the lowest strata of the food web will have a cumulative effect throughout the food chain. Microbes and fish are more sensitive to the effect of metal interaction than man, and hence the suggested criteria for river and dam water differs from the levels stated for drinking water.

The metal ions can originate from a variety of sources including the nuclear power, defense and fuel

## **1. GENERAL INTRODUCTION**

reprocessing industries, surface finishing and electroplating processes, mining operations, smelting in the metal processing industry and textile industries (95). In addition to contaminating streams, the ground water at many of the sites is affected. By limiting the loss of metal ions during processing, or by removing and concentrating the ions, not only would the impact on the environment be vastly reduced, but the industrial processes would become economically more viable.

The three categories of heavy metal cations: class A, class B and borderline ions have the toxicity sequence:

Class B > Borderline > Class A (66)

In aquatic systems class B and borderline ions are able to form water-soluble organometallic cations capable of crossing biological membranes. Toxicity of the metal ions is largely influenced by speciation, pH, temperature, inorganic ionic concentration, organics and hydrous metal oxides (66, 94, 96).

### **2.3. BIOREMEDIATION OF METAL-CONTAINING WATER**

Bioremediation of polluted water is not a new concept (6), yet it offers an alternative to the existing, conventional metal removal technologies of metal ion exchange, evaporative recovery, electrochemical treatment and chemical reduction. Both approaches have their respective advantages and disadvantages. The disadvantages of bioremediation are compensated for by the high metal binding capacity and selectivity of microorganisms for certain metals and most importantly the low operational costs.

Bioremediation of waste water involves biotechnology-based processes whereby metal ions are removed from the waste water. Microorganisms play an active role in the solubilization, accumulation, transport and deposition of metals in the environment (3).

The mode of action whereby microorganisms remove metal ions from water includes absorption, adsorption and bioaccumulation. Collectively absorption and adsorption constitute biosorption. Due to the physico-chemical nature of biosorption, waste ions are removed from aqueous solutions rapidly and efficiently, thereby enhancing the biomass potential in waste water bioremediation. In addition non-viable biomass can be used, thereby avoiding such problems as the provision of nutrients,

## 1. GENERAL INTRODUCTION

contaminations and toxicity to the biomass (97, 98).

The metal accumulative properties of microbial biomass have prompted research into the removal of radionuclides from industrial wastes. Radionuclides, eg. Tc, Zr, U are formed during fission and activation reactions in nuclear reactors and are released as part of the fission products or enter the waste water due to technical breakdowns, eg corrosion (99 - 103). Due to the longevity of radionuclides, eg.  $^{93}\text{Zr}$  :  $1.5 \times 10^6$  (100) and Tc-99 :  $2.1 \times 10^5$  years (99), the waste will remain active in the natural environment for long periods of time.

Biotechnological processes, for removal of toxic metals and radionuclides from waste has gained impetus and credibility over the years and include a number of microbial interactions: bioleaching (3, 104, 105), biotransformation (104, 106) and bioaccumulation (4, 5, 104, 105).

The use of microbes in leaching metals from ores has been intensively studied. The leaching may involve direct enzymatic oxidation of the substrate, or indirect leaching and biotransformation, eg. *Thiobacillus ferrooxidans* (7). Related to bioleaching are microbial transformations based on the mobilization and immobilization of the toxic metals. Aerobic, anaerobic, mesophilic, autotrophic and heterotrophic groups are involved in the microbial activities, which include solubilization and leaching of the metals, oxidation, reduction and precipitation of metal ions (106). Although bioleaching and biotransformation can mobilize metals from deposits, thereby reducing their environmental impact, subsequent accumulation and removal of the metals ions is necessary.

Bioaccumulation systems can employ a single or a mixture of microorganisms or higher plants. Algal and cyanobacterial blooms have reduced the levels of  $\text{Cd}^{2+}$ ,  $\text{Pb}^{2+}$ ,  $\text{Cu}^{2+}$ ,  $\text{Zn}^{2+}$ ,  $\text{Mn}^{2+}$ ,  $\text{Ni}^{2+}$ ,  $\text{Hg}^{2+}$ ,  $\text{Cr}^{3+}$ ,  $\text{Fe}^{2+}$  and  $\text{Co}^{2+}$  in laboratory solutions (107 - 116),  $\text{Cd}^{2+}$  in water leached from rice paddies (117),  $\text{Cr}^{3+}$  from tannery effluent (118) and  $\text{Zn}^{2+}$  from river water (112). In addition microalgae (100, 99) and cyanobacteria (100) are capable of accumulating Zr and Tc from nuclear reactor waste.

Removal and subsequent sequestration of metal ions by bacteria has also been successful. Yttrium (107) and  $\text{Cr}^{6+}$  (93) have been removed from nuclear waste, whilst  $\text{Cu}^{2+}$ ,  $\text{Cr}^{3+}$ ,  $\text{Zn}^{2+}$ ,  $\text{Ni}^{2+}$ ,  $\text{Fe}^{2+}$ ,  $\text{Pb}^{2+}$ ,  $\text{Se}^{2+}$ ,  $\text{Ag}^{3+}$ ,  $\text{As}^{2+}$  and  $\text{Hg}^{2+}$  have been sequestered from spiked aqueous solutions (119 - 125) and industrial waste (95, 126 - 132).

## 1. GENERAL INTRODUCTION

Plants, although not as frequently used as a bioremediation tool for the removal of metal ions from aqueous solutions, play an important role in metal ecology. A relationship exists between the soil and the vegetation covering it. Plant species colonizing metal contaminated soil or areas containing a high metal content are often stunted with unusual growth features (8, 133, 134). Metal ions removed from the soil are most commonly concentrated in the storage tissue, eg. roots (133, 134).

Fungi and yeasts can accumulate significant amounts of heavy metals and radionuclides. Although this feature is common to other microbial and plant cells, fungi may be better suited for this purpose than other microbial groups because of their high tolerance towards metals and other adverse conditions, eg. high cell wall binding capacity and high intracellular uptake by viable cells, low pH or osmotically unstable conditions (102, 135). Additional advantageous attributes of fungal biomass include the range of morphological types available, which include unicellular and filamentous forms. Large amounts of fungal biomass are derived as waste products from industrial processes and fermentations, eg. *R. arrhizus*, a filamentous fungus, which appears to be a highly successful biosorbent for metal and radionuclide removal (10 - 12, 49, 102, 135, 136). Similarly *S. cerevisiae*, a byproduct from industrial fermentation industries has been employed to monitor and treat aquatic pollutants. *S. cerevisiae* can accumulate numerous metal, eg.  $\text{Cu}^{2+}$ ,  $\text{Cd}^{2+}$ ,  $\text{Co}^{2+}$ ,  $\text{Au}^{3+}$ ,  $\text{Ag}^{3+}$  and  $\text{Pb}^{2+}$  from both synthetic solutions and polluted waste water (4, 86, 102, 105, 108).

## 2.4. INDUSTRIAL APPLICATIONS

### 2.4.1. INDUSTRIAL EFFLUENTS

Since the onset of industrialization, the deposition of heavy metals into the natural water streams has altered the cyclic fluctuations of metal and trace elements previously found therein. The toxicity of these metals in natural waters results from a combination of their solubility, bioavailability and the effect on the organism at a cellular level.

The major sources of metal pollution into aquatic ecosystems include domestic waste water effluents, coal burning power plants, non-ferrous metal smelters, iron and steel plants, mine and metal finishing industries and the dumping of sewage sludge. In 1988 it was estimated that 25% of industrial effluents in Europe were discharged into lakes and rivers (137). However, due to the rapid onset of industrialization and poor control of the water quality guidelines this can be considered a conservative

estimate.

#### **2.4.1.1. ELECTROPLATING EFFLUENT**

The industrial waste effluents of interest in this study were those generated by electroplating processes. With the exception of a few large concerns, the majority of electroplating industries operate as small entities, discharging their waste into the municipal sewage disposal system. In comparison to several other types of industries, eg. the mining industry, the volumes of waste discharge are relatively low. The annual water consumption by the electroplating industry in South Africa is approximately 9 million m<sup>3</sup> of which 80% is discharged as effluent. The primary cause for concern regarding this effluent remains the extremely high levels of metals present.

Depending on the type of electroplating industry, the species of metal present in the discharge varies. Predominant sources of contamination during the finishing operations include the discharge of untreated solutions obtained from: 1) alkali cleaning to remove oil and grease, 2) acid descaling and pickling of various basis metals, 3) metal plating solutions from cyanide complexes of Zn, Cd, Cu, Ag and Au, 4) metal plating solutions based on the acid complexes of Ni, Cu and Cr, 5) tin plating based on acid or alkaline complexes, 6) sulfuric acid anodizing of aluminum, 7) chromium compound based conversion coating on Al, Cd, Zn and Cu alloys, 8) accidental overflows of solutions or possible leaks as well as the periodic discharge of exhausted process solutions.

#### **2.4.2. BIOMASS SYSTEMS FOR INDUSTRIAL BIOREMEDIATION**

In view of the low toxicity, cost effectiveness and comparable results to those of activated charcoal (10) and ion exchange resins, microbial biomass systems appear to be an attractive alternative for the remediation of industrial waste water.

The choice of biomass varies, ranging from easily obtained biomass types, to specially isolated or even genetically engineered strains. Raw biomass which has been processed or modified to improve its metal sorption characteristics may also be utilized. Although the biosorbent biomass can be selected from algal, fungal and bacterial strains, the most convenient source of raw material is that obtained as by-products from large scale fermentations or pharmaceutical processes (138). The biomass can either be applied as viable or non-viable biomass. Advantages of non-viable biomass

## 1. GENERAL INTRODUCTION

include low maintenance costs, enhanced metal sorption levels and absence of maintaining the cultures. Moreover, living cells are prone to the toxic effects of effluents which may result in cell death, thereby nullifying any of the advantages of using live cells (139).

*Bacillus spp.* either immobilized (140) or contained within a packed-bed reactor (141) was exposed to spiked metal solutions. The immobilized cells exhibited good metal loading characteristics, viz. 70 mg  $\text{Cr}^{3+}$ /g cell weight and 64 mg  $\text{Cu}^{2+}$ /g cell weight. Alkali treatment of the immobilized pellets improved the metal retention capabilities, viz. 118 mg  $\text{Cr}^{3+}$ /g cell weight and 116 mg  $\text{Cu}^{2+}$ /g cell weight respectively (140). Uranium removal by *Bacillus subtilis* cells in a packed-bed reactor has exhibited the potential to become an effective, yet simple system whereby metal removal could commence (141).

Numerous applications exist for microbial biomass in the treatment of industrial and mining waste. Pelleted and immobilized yeast, fungal and waste bacterial and algal biomass have been used in the removal and recovery of heavy metals and radionuclides. Waste biomass of *Streptomyces noursei* exhibited the following affinity series for metals:  $\text{Ag}^{3+} > \text{Pb}^{2+} > \text{Cr}^{3+} > \text{Cu}^{2+} > \text{Zn}^{2+} > \text{Cd}^{2+} > \text{Co}^{2+} > \text{Ni}^{2+}$ . The affinity sequence and amount of metal removed differed depending on the biomass, a fact which facilitates specific removal and subsequent sequestration by the microbial biomass. Application of this characteristic to mining effluent containing economically viable metals would provide a cheap alternative to gold and silver recovery.

Two systems incorporating microbial biomass as bioremediation agents which have been particularly successful are firstly a granular metal-accumulating, non-viable biomass product developed by an American company. The biomass, referred to as metal recovery agent (MRA), is capable of accumulating large quantities of metal cations and is more than 99% efficient in cation removal from dilute metal solutions. Its accumulative capacity extends to a wide range of metal cations, inclusive of gold, silver, palladium, platinum, lead, copper, cadmium and zinc (142).

MRA is prepared by exposure of the microbial biomass to caustic conditions and functions in a pH range 2 - 11, with optimum metal accumulation between pH 4 - 8. Although regarded as a good metal removal agent which has been successfully employed in pilot scale trials, limitations with respect to its metal accumulating abilities do occur. Similar to other metal-microbial interactions, metal speciation does influence MRA binding capacities. For example, MRA is only capable of

## 1. GENERAL INTRODUCTION

accumulating reduced levels of gold from gold-cyanide complexes, compared to other salts of gold (142).

The second system which has been successfully employed in industrial bioremediation is one developed by the U.S. Bureau of Mines (143, 144). The Bureau developed BIO-FIX beads (an acronym for biomass-foam immobilized extractant) from a variety of raw materials, eg. blue-green algae (*Spirulina sp.*), marine algae (*Ulva sp.*), yeast (*S. cerevisiae*) and sphagnum peat moss. These systems were subsequently utilized in hydrometallurgical processing.

The BIO-FIX beads displayed superior physical and chemical stability, withstanding several adsorption-desorption cycles. Sphagnum-containing BIO-FIX beads demonstrated the greatest metal sorption capacity. The beads were tested on acid mine drainage metals using stirred tanks, fixed bed columns, fluidized bed columns and a low maintenance passive system. Metal sorption was rapid, with > 50% of equilibrium sorption occurring within 5 minutes, and in excess of 90% sorption achieved after 20 minutes (143, 144).

A number of other systems for heavy metal removal from industrial solutions have been reported, but these have been performed on a smaller scale.

## 2.5. RESEARCH AIMS

The aims of the present study were twofold, to identify and utilize a biological system of metal removal from waste water. Commercially produced bakers yeast, *S. cerevisiae* was used as a source of biomass due to the low cost factor and abundant supply. In order to implement a successful bioremediation system for the treatment of metal contaminated waste water, the mechanisms of metal biosorption and uptake by the yeast cells need to be understood.

The accumulative capacity of yeast for a wide range of metals has been known for a considerable time (see section 1.2.2). The initial aims of this research were thus to elucidate the mechanisms of metal accumulation by *S. cerevisiae*. The uptake and localization patterns of metals in intact yeast cells were studied and following on from this work, a more detailed analysis was focussed on metal accumulation by isolated yeast cell walls and cell wall components as well as isolated vacuoles. The three metals used throughout the biochemical studies, viz.  $\text{Cu}^{2+}$ ,  $\text{Co}^{2+}$  and  $\text{Cd}^{2+}$  differ in many

## **1. GENERAL INTRODUCTION**

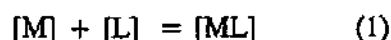
respects, but are representative of the heavy metal group.  $\text{Cu}^{2+}$ , a physiological cation and the least toxic of the metals, is often required by cells as a metalloenzyme. The other two cations  $\text{Co}^{2+}$  and  $\text{Cd}^{2+}$  have a greater toxicity, eg.  $\text{Cd}^{2+}$  serves no function within the cell, and causes cell damage and ultimately cell death. The interaction of the cells and cellular components with these metals of varying toxicities was monitored.

A detailed knowledge of the mechanistic and biochemical aspects of heavy metal processing by viable and non-viable yeast cells enabled the development of subsequent biotechnological processes. Bioaccumulation of metals from electroplating effluent by viable yeast cells were studied and since the biosorptive properties of non-viable yeast cells exhibit similar or greater affinities for heavy metals, additional metal uptake studies were conducted with non-viable yeast biomass preparations. Three immobilization techniques (viz. embedding and crosslinking) were employed to produce potentially viable industrial yeast products, viz PVA Na-alginate, PVA Na-orthophosphate and PEI:GA pellets, which could be implemented in bioremediation processes. These preparations were tested for their metal biosorptive and mechanical properties, with the biomass most suited as a biosorbent being selected for further studies. The analytical results and performance of the biomass as a biosorbent were compared using batch reactors, continuous-flow fixed bed biomass columns and continuous-flow stirred bioreactors. All of the later experimental work was conducted using industrial waste obtained from electroplating plants. This waste contains a wide range of metals in levels exceeding the stipulated criteria. The environmental threat brought about by the direct discharge of this untreated waste into the underground sewage system initiated the above-mentioned research.

## **2. INTERACTION WITH, AND ACCUMULATION OF METAL IONS BY YEAST CELL WALLS AND CELL WALL COMPONENTS**

### **2.1. INTRODUCTION**

The binding of metals to cell walls is an equilibrium reaction, with the interaction between the divalent metal cations and the anionic ligands of the cell wall expressed as:



Where M represents the free metal cations in solution, L the ligands and ML the metal-ligand



## 2. CELL WALLS AND CELL WALL COMPONENTS

interaction. The square brackets denote the concentration in appropriate units for aqueous solutions (40).

Rothstein and Hayes (40) subsequently developed a mass law equation whereby  $K$ , the dissociation constant could be determined. Their determination of  $K$  was dependent on the three activity coefficients:  $f_M$ ,  $f_L$  and  $f_{ML}$ . The value for  $f_M$  can be determined from the ionic strength, but the activity coefficient for the two solid phases are unknown:

$$K = [M][L]/[ML] \times f_M f_L / f_{ML} \quad (2)$$

Others (66, 145) chose to express the formation of a metal-ligand complex differently, and express  $K$  as the equilibrium constant  $K_{ML}$ :

$$K_{ML} = [ML]/[M][L] \quad (3)$$

As an equilibrium (145) or dissociation (40) constant,  $K$  represents the ratio between the forward and reverse reaction rates of metal-ligand complexation. The larger the magnitude of the equilibrium constant  $K_{ML}$ , the more stable the complex  $ML$  is in solution (66). Both of the groups (40, 145) assumed the independent nature of  $K$ , whereby the formation of a complex at one site does not alter the affinity of other sites for metal cations. Although the value of  $K_{ML}$  is almost independent of the nature of the ligand, it depends strongly on the particular metal cation involved. Cations with a high  $K_{ML}$  value will occur mostly as a complex, eg.  $Cu^{2+}$ , whilst those with low equilibrium values eg.  $Na^+$ ,  $K^+$ , will remain as free cations. Metal cations can be classified with the following decreasing values for the equilibrium constant:

$Fe^{3+} > Pb^{2+} > Cu^{2+} > Ni^{2+} > Co^{3+} > Zn^{2+} > Co^{2+} > Cd^{2+} > Fe^{2+} > Mn^{2+} > Mg^{2+}, Ca^{2+} > Sr^{2+} > Ba^{2+} > Na^+, K^+$  (145).

Metal-ligand formations are, however, not always simplistic. The afore-mentioned classification is based on thermodynamic factors independent of kinetic considerations. In a few cases, the ligand preference may be controlled kinetically, one such example being the interaction of  $Pt^{2+}$  with simple ligands, proteins and nucleotides (52, 66). In addition, ligands may be mono-, bi- or multidentate, enabling them to attach to the metal ions using one, two or more donor atoms. If a bidentate ligand co-ordinates with a metal ion through both donor atoms a ring structure is formed. pH is also an important factor in regulating the access of metal ions to binding sites in biological molecules (52, 66, 145). Protons will directly compete with metal ions for binding sites, with metal ions frequently having to displace protons in biological systems (66). Thus equation (1) can be rewritten as a proton displacement reaction:

## 2. CELL WALLS AND CELL WALL COMPONENTS



For example, when an amino acid is the ligand, a heavy metal cation will bind to the carboxylate group in a mildly acidic solution. Binding to the amino nitrogen will not occur until the pH is raised to deprotonate this group.

Initial research work (40) confirmed the presence of multiple binding sites on the cell surface of yeast, although only a small fraction of the cellular structure is involved in the binding of exogenous cations. Due to the composition of the yeast cell wall (section 1.3.1.2.) and the three dimensional arrangement of the ligands, a range of binding sites is available for metal complexation (43, 50, 52, 66, 67, 146).

The amorphous orientation and cross linkages between the cell wall polymers may limit the availability of the ligands for metal binding, through masking. For example, selective removal of mannan causes an increase in copper binding, possibly by exposing metal binding sites on the protein fraction (67). However, enzymatic degradation of the yeast cell wall indicates that the relationship between wall proteins and metal ions, although important, is not the sole metal binding interaction of the wall. The outer mannoprotein layer appears to dominate metal binding. Removal of this layer with its phosphodiester links decreases the cation binding capacity of isolated cell walls by 50% (44).

Each of the respective cell wall components contributes metal ligands for metal binding. The ligands contributed by the carbohydrate moieties are inclusive of a range of groups viz. hydroxyl, carboxyl, amino or phosphate groups, which can either interact with class A or B metals thereby facilitating ionic or covalent interactions. In comparison, protein-metal interactions favour covalent interactions, due to the presence of amino, carbonyl groups and the nitrogen/sulphur centres. Chemical modification of the ligands of isolated cell walls confirmed the importance of amino, carboxyl and hydroxyl groups for metal binding. Brady *et al.* (43), tested the ability of cell walls to bind  $Cu^{2+}$ ,  $Cd^{2+}$  and  $Co^{2+}$  by chemically modifying the respective cell wall components. From this work it was concluded that most, if not all, of the cell wall components play a role in heavy metal accumulation.

The aim of this experimental section was to establish the importance of the carbohydrate fractions of isolated yeast cell walls and cell wall components in metal binding. The metal binding affinities of the polysaccharide fractions for three cations, viz.  $Cu^{2+}$ ,  $Co^{2+}$  and  $Cd^{2+}$  were compared.

## 2. CELL WALLS AND CELL WALL COMPONENTS

Qualitative analysis using infrared spectroscopy was undertaken to determine any change in configuration of carbohydrate groups due to metal interaction.

### 2.2. MATERIALS AND METHODS

#### 2.2.1 PREPARATION OF ISOLATED CELL WALLS

Commercial preparations of *S. cerevisiae* (production strain, approximately 90% cell viability) were obtained from Anchor Yeast Inc. The cells had been grown aerobically in molasses wort, adjusted with phosphoric acid and harvested in the stationary phase. Wet, pressed bakers yeast was stored at 4°C prior to use. Before being used, the yeast was washed three times (3000 g x 10 min) using ultra-pure water (Milli-Q water) and harvested. Preparations of the isolated cell walls were provided courtesy of B. Prior and P. van Zyl (Dept Microbiology and Biochemistry, University of Free State, South Africa). Yeast cells were disrupted using a Braun homogenizer in the presence of glass beads (0.5 mm diameter). To prevent heat build-up and the effects of autolytic enzymes, the disruptions were completed discontinuously at 4 - 10°C using ice and liquid nitrogen to maintain the temperature. This technique achieved cell disruption of 95%. Lysed cells could be seen as dark "ghosts" when viewed under phase contrast microscopy.

Removal of the cell debris was achieved through centrifugation. Yeast cell walls were freeze-dried and this fraction was then suspended in 5 mM 1,4 piperazinediethanesulphonic acid (PIPES) (PIPES, Sigma Co) buffer and centrifuged at 4°C (3000 g x 10 min). PIPES buffer (pH 6.5) was used throughout the biochemical studies due to its negligible metal accumulating properties. The supernatant was discarded and the pellet freeze-dried and stored in a desiccator at room temperature until required.

#### 2.2.2. CELL WALL COMPONENT EXTRACTION

##### 2.2.2.1. CHITIN AND CHITOSAN EXTRACTION

Chitin and chitosan were successfully extracted from a 100 mg sample of yeast cell wall material following the method of Muzarelli (63). The cell walls were demineralized with 5% HCl for 5 h, using 11.8:1 (w/w) ratio of HCl to dry weight of yeast cell walls. After washing the walls to

## **2. CELL WALLS AND CELL WALL COMPONENTS**

neutrality using Milli-Q water, the solution was centrifuged (3000 g x 10 min) and the pellet subsequently deproteinated with 2% NaOH (65°C for 2 hrs under nitrogen) using 30:1 (w/w) ratio of NaOH solution: dry weight yeast cell walls. The material was once again washed to neutrality using ultra-pure water, centrifuged and the pellet dialyzed twice against Milli-Q water (4°C, 4 hrs) before being freeze-dried.

### **2.2.2.2. MANNAN ISOLATION**

Mannan was extracted according to the method of Northcote and Horne (57). Cell wall material (150 mg) was digested with 3% NaOH (w/w) for 6 hrs at 100°C. The digested material was centrifuged (3000 g x 10 min) and the supernatant retained and acidified to pH 6.0 using 2 M acetic acid. The mannan in this solution was precipitated using 4 volumes of ethanol. The supernatant was discarded, the precipitate redissolved in water and reprecipitated using ethanol. The white solid obtained was washed using diethylether to remove lipids, dialyzed twice against Milli-Q water and freeze-dried.

### **2.2.2.3. GLUCAN ISOLATION**

The alkali-insoluble pellet from the mannan extraction was digested using 3% NaOH (w/w) (100°C, 6 hrs) and subsequently by 0.5 M acetic acid (75°C, 6 hrs) before being washed in 2 ml of ethanol and ether, respectively (54). The remaining white precipitate was dialyzed twice against Milli-Q water (4°C, 4 hrs) prior to being dried in the normal fashion.

### **2.2.3. PROTEIN AND CARBOHYDRATE DETERMINATION**

Prior to analysis, cell wall components were hydrolyzed using HCl: 1) chitin was dissolved in 4 M HCl at 1 mg/ml concentration. Digestion proceeded for 4 hrs at 100°C (147), 2) mannan and glucan (1 mg/ml) fractions were hydrolyzed for 6 hrs at 100°C with 2 M HCl.

The Folin-Coicalteau assay was used for protein determination (Appendix 1). Cell wall components were analysed in triplicate using 0.1 ml aliquots of the prepared samples. All absorbance readings were made at 500 nm against a blank. The Nelsons test for reducing sugars was utilized to determine the amount of carbohydrate present in each of the cell wall acid digest samples. All determinations

## 2. CELL WALLS AND CELL WALL COMPONENTS

were done in triplicate against a blank at 540 nm (Appendix 2).

### 2.2.4. QUANTITATIVE METAL BINDING STUDIES

The dialysis apparatus used was similar to that used by Marrack and Smith (148). Two identical "Perspex" units, each containing five separate 1.2 ml chambers were clamped together to form five 2.4 ml chambers bisected by a semi-permeable dialysis membrane (Spectrapor dialysis tubing, 6-8 kDa cut off). Two small "Perspex" balls were placed in each of the chambers to agitate the solution during shaking.

Comparative metal binding studies of the isolated yeast cell walls and cell wall components, using  $\text{Cu}^{2+}$ ,  $\text{Co}^{2+}$  and  $\text{Cd}^{2+}$  cations were conducted in the dialysis chamber at room temperature ( $22^{\circ}\text{C}$ ) in a shaking water bath. Initial range finding experiments were conducted to determine the required metal concentration and duration of contact for optimal metal accumulation.

One milliliter of the metal solution (4 mM  $\text{CuCl}_2$  and  $\text{CdCl}_2$  and 2 mM  $\text{CoCl}_2$ ) was pipetted into one side of the chamber, whilst 1 mg of yeast cell wall material, suspended in 5 mM PIPES/TMAH (Tetramethylammonium hydroxide, Sigma Chemical Co) (pH 6.5) was pipetted into the other side. After three hours of gentle shaking in a water bath, equilibrium was reached for  $\text{Cd}^{2+}$  and  $\text{Co}^{2+}$ , whilst 4 h were required to achieve equilibrium for  $\text{Cu}^{2+}$ . 0.1 ml aliquots were removed from the respective metal ion compartments, diluted to 1 ml and the amount of free metal determined using atomic absorption spectroscopy. On conclusion of the experiment, the empty chambers were filled with Milli-Q water and the apparatus shaken in the water bath for a period equivalent to that of the experiment. The amount of bound metal could be expressed as:  $\text{Bound}_{[\text{M}]} = \text{Total}_{[\text{M}]} - \text{Free}_{[\text{M}]}$ , where  $\text{Free}_{[\text{M}]}$  constitutes both the amount of metal left in solution as well as that associated with the chamber walls and dialysis membranes after incubation with water as described above. In addition, the affinities ( $K_A$ ) of the cell wall and cell wall components for the respective metals could be determined from the slopes of the plots representing the ratio of free/bound metal versus the amount of complexed metal.

### 2.2.5. QUALITATIVE ASSESSMENT OF METAL BOUND TO CELL WALL AND CELL WALL COMPONENTS

In understanding the function of biomolecules, the most critical step is often the determination of its structure. Using infrared spectroscopy, the wall structure can be quantitatively determined and the fingerprints unique to each of the biomolecules obtained. In the case of cell wall biomolecules, exposure of native cell wall material to metal cations will result in ligand-metal complexation occurring, thereby modifying this infrared fingerprint region.

The infrared spectra of yeast cell wall material were recorded prior to, and after metal biosorption, in an attempt to acquire information on the nature of the interactions between the metals and cell wall material. Using a Perkin-Elmer model 180 infrared spectrophotometer, infrared analysis of the native and metal-complexed cell walls and cell wall components were undertaken. The spectra of the respective samples were determined as alkali pellets. One milligram of an oven-dried sample and 100 mg of anhydrous KBr were mixed, ground to fine powder and pressed into solid state disks (96). To obtain information regarding the nature of the chemical interactions between the divalent cations and yeast cell wall material, the shift in the spectra in the  $1800 - 800 \text{ cm}^{-1}$  region (fingerprint region) was measured (11, 12, 149, 150).

## 2.3. RESULTS

### 2.3.1. QUANTITATIVE ANALYSIS

The accumulation of  $\text{Cu}^{2+}$ ,  $\text{Co}^{2+}$  and  $\text{Cd}^{2+}$  by intact cell wall and cell wall isolates can be seen in Figure 2.1. The cell wall isolates accumulated greater quantities of each of the three cations than the intact cell wall. This suggests that each of the wall components possess numerous binding sites, but due to their orientation within the intact cell wall, these ligands are masked or involved in cross-linkages between wall polymers and thus unavailable as binding sites. The general order of binding of the three metals was  $\text{Cu}^{2+} > \text{Cd}^{2+} > \text{Co}^{2+}$ , the exception being mannan, which accumulated slightly more  $\text{Co}^{2+}$  than  $\text{Cd}^{2+}$ .

## 2. CELL WALLS AND CELL WALL COMPONENTS

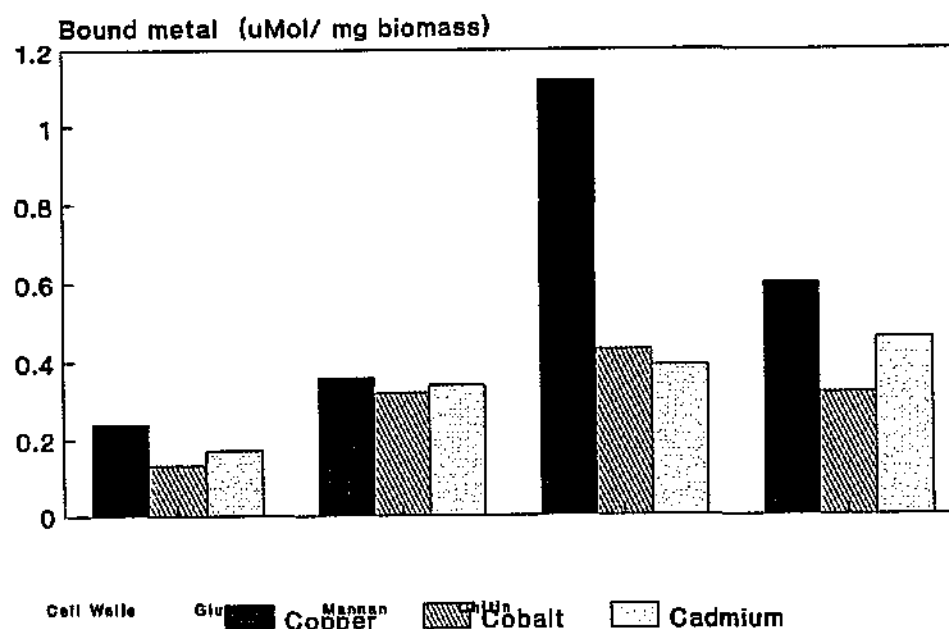


Figure 2.1. Comparison of heavy metal cation binding by *S. cerevisiae* isolated cell walls and extracted cell wall macromolecular components.

No direct relationship appears to exist between the protein content of the extract and the ability to bind metal ions (Table 2.1).

## 2. CELL WALLS AND CELL WALL COMPONENTS

Table 2.1. Parameters of metal binding by isolated cell wall and cell wall components of yeasts. The mean values are obtained from five replicates.

Sample	Prot/CHO ratio	Cu <sup>2+</sup> binding $\mu\text{mol.mg}^{-1}$ dry wt extract	Co <sup>2+</sup> binding $\mu\text{mol.mg}^{-1}$ dry wt extract	Cd <sup>2+</sup> binding $\mu\text{mol.mg}^{-1}$ dry wt extract
Yeast Cell Walls	0.21 <sup>a</sup>	0.2 +/- 0.17	0.13 +/- 0.05	0.17 +/- 0.12
Mannan	0.32	1.12 +/- 0.11	0.43 +/- 0.10	0.39 +/- 0.09
Glucan	0.02	0.36 +/- 0.17	0.32 +/- 0.21	0.34 +/- 0.11
Chitin	0.27	0.60 +/- 0.20	0.32 +/- 0.27	0.46 +/- 0.04

a: Theoretical ratio calculated from Northcote and Horne (57)

A high protein content within the extracted cell wall component fractions signified contamination of the sample with protein. In comparison to the intact cell wall, the protein : carbohydrate ratios of the mannan and chitin fractions were high. During the isolation of these compounds, the amount of carbohydrate present was decreased whilst the amount of residual protein remained relatively high, and is subsequently reflected by these ratios. Mannans are closely linked to the protein moiety, thus the high protein : carbohydrate ratio may be indicative of incomplete extraction. Although metal accumulation is not proportional to the protein content, the latter influenced the amount of metal bound by the extracted fractions. For example, the accumulation of copper by the extracted cell wall fractions decreased with a decline in the protein concentration, suggesting some relationship between protein content and Cu<sup>2+</sup> binding capacity of the cell wall. This phenomenon was limited to Cu<sup>2+</sup> accumulation, while Co<sup>2+</sup> and Cd<sup>2+</sup> binding, although influenced by the presence of protein, appeared to be independent of protein concentration.

The order of metal accumulation capacity of mannan > chitin > glucan > intact cell walls as seen in Figure 2.1, is also reflected by the affinity constants (Table 2.2.) obtained from inverted Scatchard plots. Once again metal ions appear to show a greater affinity for isolated cell wall components than for the intact cell wall.



## 2. CELL WALLS AND CELL WALL COMPONENTS

Table 2.2. Affinity constants ( $K_A$ ) (mol/l) of the intact and extracted cell wall components for  $\text{Cu}^{2+}$ ,  $\text{Co}^{2+}$  and  $\text{Cd}^{2+}$ .

Sample	$\text{Cu}^{2+}$ ( $K_A$ )	$\text{Co}^{2+}$ ( $K_A$ )	$\text{Cd}^{2+}$ ( $K_A$ )
Yeast Cell Walls	0.04	0.03	0.04
Mannan	0.55	0.16	0.07
Glucan	0.06	0.13	0.06
Chitin	0.11	0.08	0.09

### 2.3.2. QUALITATIVE ANALYSIS

Infrared analysis of the cell walls and components yielded distinct patterns in the fingerprint region ( $1800 - 800 \text{ cm}^{-1}$ ) (Figure 2.2.). The characteristic bonds of the isolated virgin *S. cerevisiae* cell walls included: 1) the secondary amide peak between  $1680 - 1630 \text{ cm}^{-1}$  (amide I:  $\text{C}=\text{O}$  stretching) and that between  $1570 - 1515 \text{ cm}^{-1}$  (amide II:  $\text{N-H}$  bending), which are considered to represent the protein fraction of the cell wall, 2) the sharp peak which dominates the  $1385 - 1365 \text{ cm}^{-1}$  region ( $\text{C-H}$  saturation) and 3) the region between  $1200 - 1000 \text{ cm}^{-1}$  which represents the carbohydrate fraction of the cell wall ( $\text{C-O}$  stretching, viz.  $1150 - 1040 \text{ cm}^{-1}$ ;  $\text{C-OH}$  stretching,  $1150 - 1070 \text{ cm}^{-1}$ ;  $\text{C=O}$  stretching).

The reduction in the intensity of the peaks between  $1680 - 1630 \text{ cm}^{-1}$  and  $1580 - 1490 \text{ cm}^{-1}$  wavelength bands of the isolated cell wall components is indicative of deproteination which should occur during component isolation. Whilst the intensity of the carbohydrate peak of the isolated components did not change, the shape of the peak assumed the characteristics of the specific component. Traces of similarity between the native wall structure and isolated mannan fraction could be distinguished. Due to the dominance of mannan and its peripheral location within the wall, this is to be expected.

## 2. CELL WALLS AND CELL WALL COMPONENTS

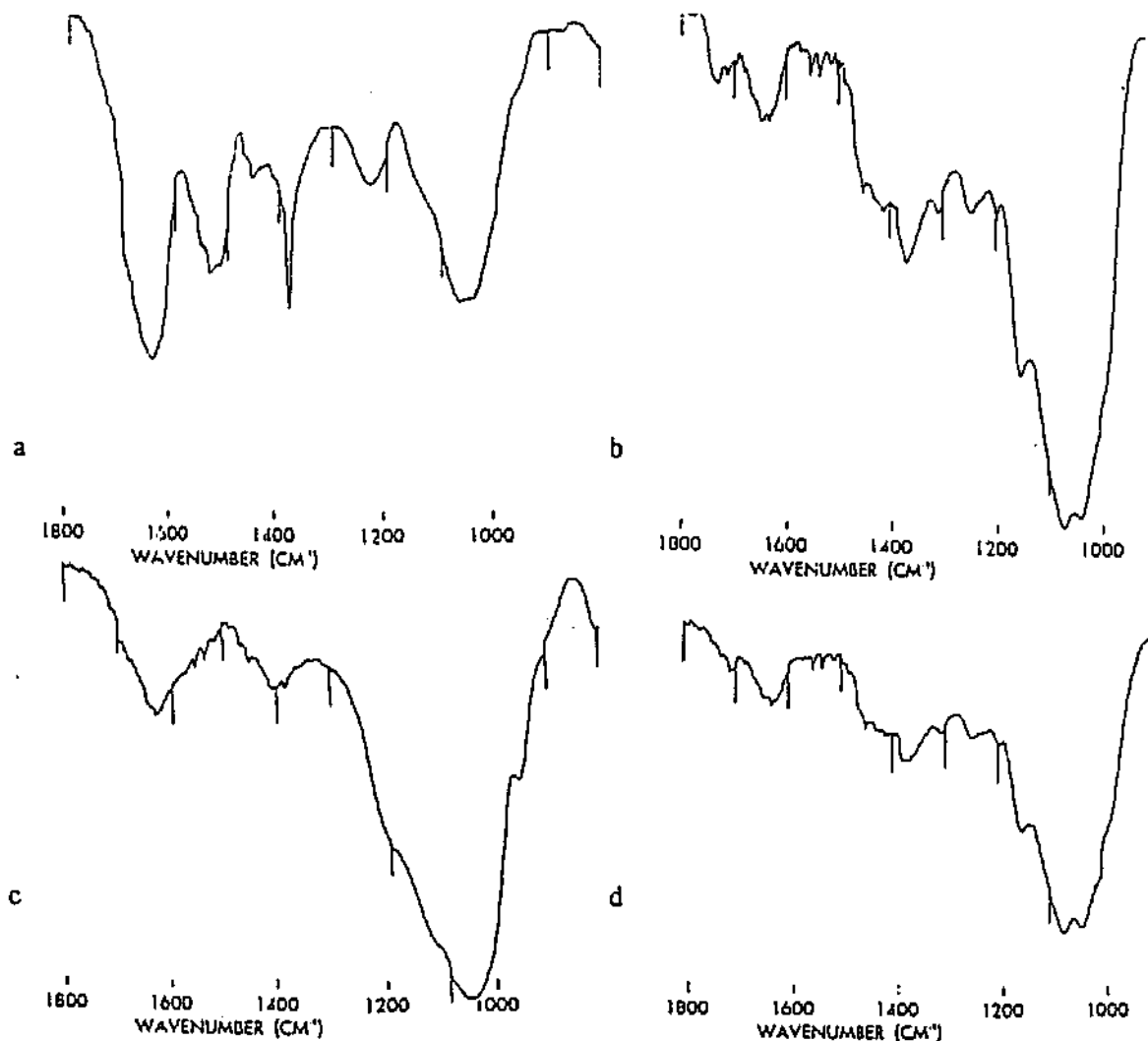


Figure 2.2. Infrared analysis ( $1800 - 800 \text{ cm}^{-1}$ ) of *S. cerevisiae* cell walls and extracted components: (a) isolated yeast cell walls, (b) chitin/chitosan, (c) mannan and (d) glucan preparations.

Metal exposure to isolated, intact cell walls (Figure 2.3.) primarily affected the secondary amide band between  $1570 - 1575 \text{ cm}^{-1}$ . The three heavy metal cations appeared to bind to the amide region of the wall in a similar manner, and metal interaction with the cell wall resulted in a change of the peak frequencies of the spectra. Following metal biosorption, the shape of the amide peak changes from a single to multiple peaked band. However, no discernable shifts could be observed in the carbohydrate region of the spectra of the intact cell walls, suggesting a lack of metal binding or alternatively inadequate sensitivity of the technique to monitor metal complexation by this component.

## 2. CELL WALLS AND CELL WALL COMPONENTS

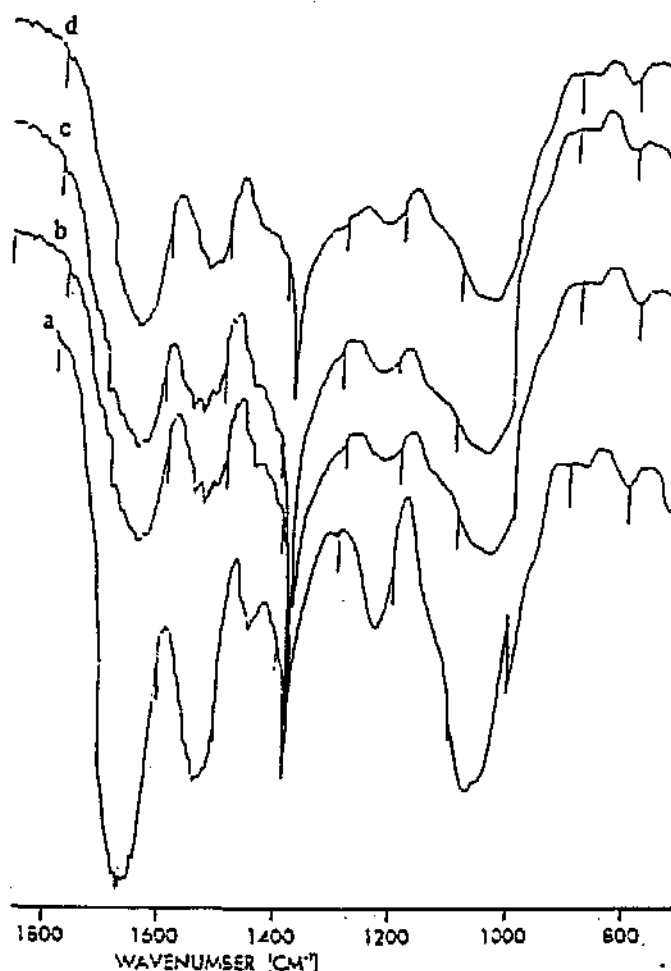


Figure 2.3. Infrared spectra (1800 - 800  $\text{cm}^{-1}$ ) of isolated *S. cerevisiae* cell walls before and after metal biosorption. (a) Untreated cell walls, (b)  $\text{Cd}^{2+}$ , (c)  $\text{Co}^{2+}$  and (d)  $\text{Cu}^{2+}$  exposed cell walls.

The involvement of mannan, glucan and chitin polymers in metal biosorption was confirmed by the infrared spectra of the isolated components (Figures 2.4 - 2.6). Once again the respective metal ions appeared to interact with each of the components in a similar fashion.  $\text{Cu}^{2+}$ ,  $\text{Co}^{2+}$  and  $\text{Cd}^{2+}$  interacted with the C-OH and C=O groups of mannans (Fig 2.4). Although these may only be low affinity interactions, they were sufficient to alter the shape of the 1200 - 1000  $\text{cm}^{-1}$  band. In addition a separate peak was formed at 950  $\text{cm}^{-1}$  in the metal equilibrated spectra. This peak may have resulted from the interaction with residual phosphate groups of the mannoprotein fraction, as

## 2. CELL WALLS AND CELL WALL COMPONENTS

phosphate groups have been identified in the  $970 - 910 \text{ cm}^{-1}$  wavebands. A similar peak was identified in the spectra of thorium-equilibrated *R. arrhizus* cell walls (12), but was ascribed to thorium-chitin interactions. A second peak due to metal interaction was formed at  $1500 \text{ cm}^{-1}$  which is characteristic of  $-\text{NH}_3^+$  groups or may be due to a shift in the amide II groups.

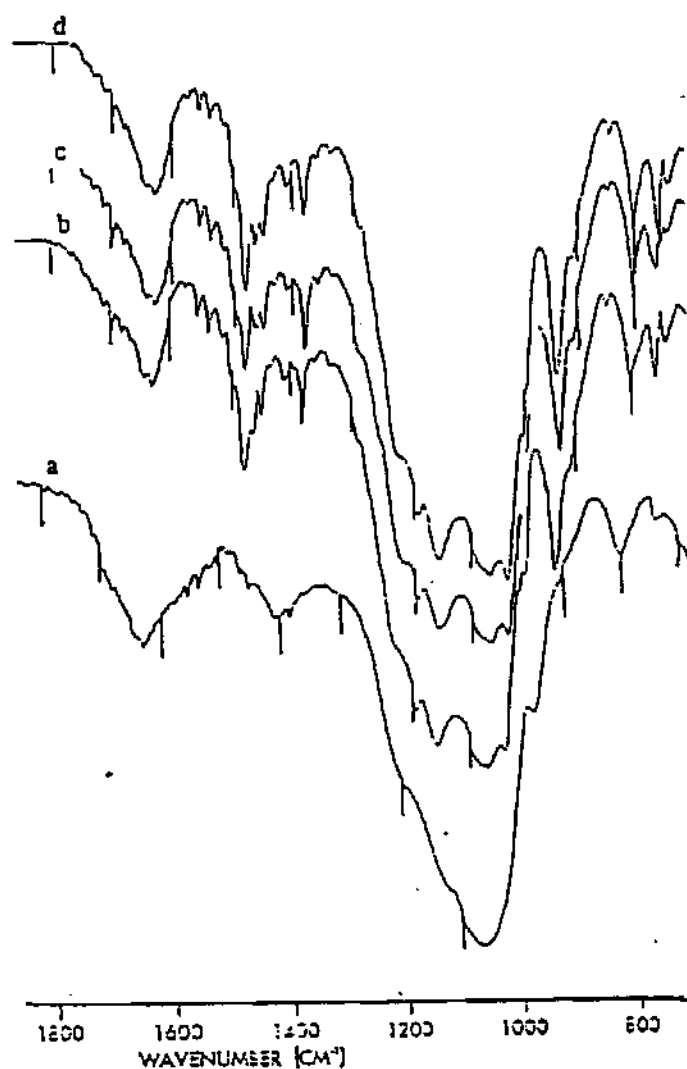


Figure 2.4. Infrared spectra ( $1800 - 800 \text{ cm}^{-1}$ ) of mannan extracted from *S. cerevisiae* cell walls before and after metal biosorption (a) Untreated mannan, (b)  $\text{Cd}^{2+}$ , (c)  $\text{Co}^{2+}$  and (d)  $\text{Cu}^{2+}$  interaction with mannan.

## 2. CELL WALLS AND CELL WALL COMPONENTS

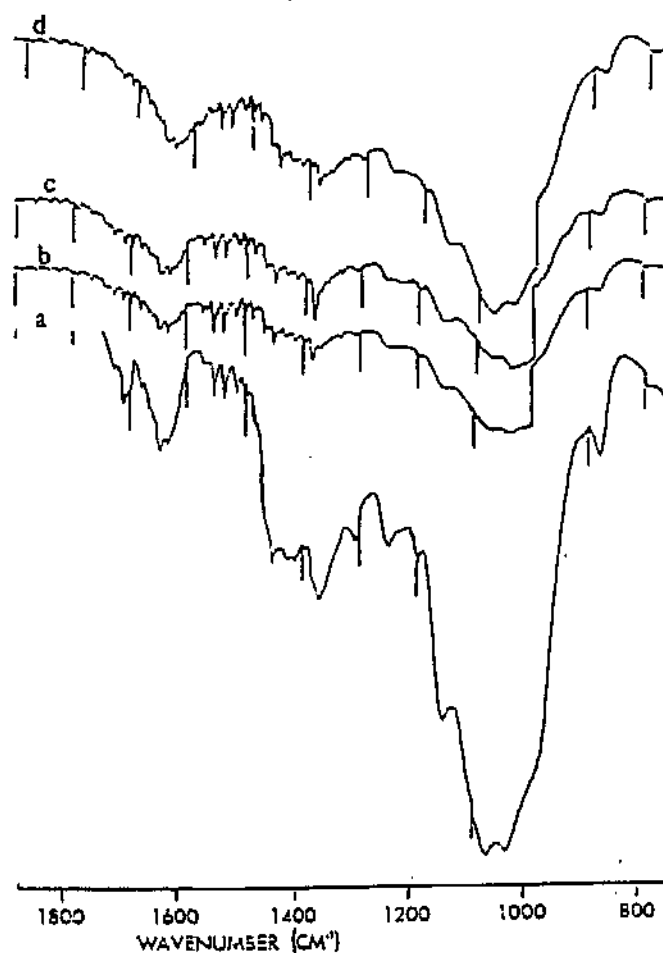


Figure 2.5. Infrared spectra (1800 - 800 cm<sup>-1</sup>) of glucan extracted from *S. cerevisiae* cell walls before and after metal exposure: (a) Untreated glucan, (b) Cd<sup>2+</sup>, (c) Co<sup>2+</sup> and (d) Cu<sup>2+</sup> interaction with glucan.

## 2. CELL WALLS AND CELL WALL COMPONENTS

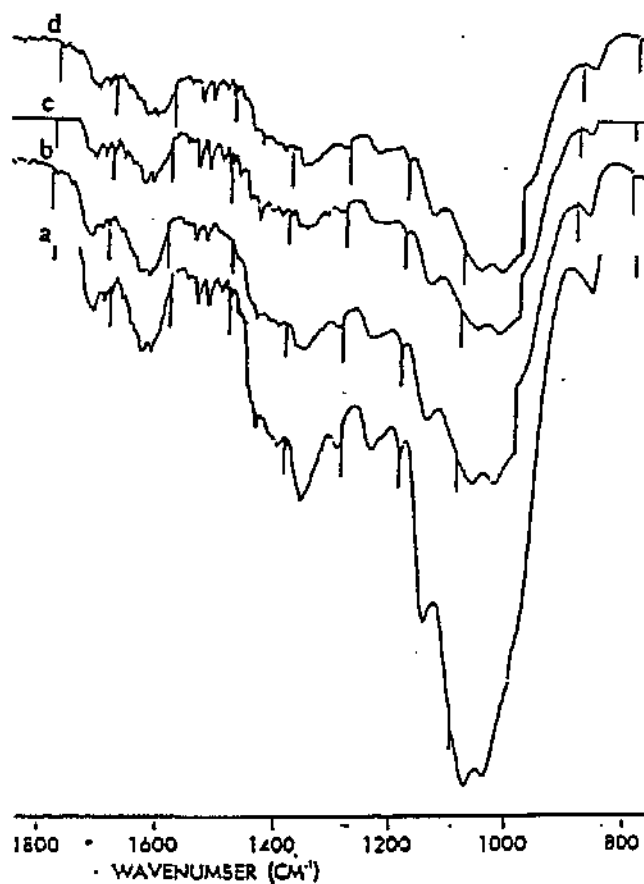


Figure 2.6. Infrared spectra (1800 - 800 cm<sup>-1</sup>) of chitin isolated from *S. cerevisiae* cell walls before and after metal biosorption, (a) Untreated, (b) Cd<sup>2+</sup>, (c) Co<sup>2+</sup> and (c) Cu<sup>2+</sup> interaction with chitin.

## 2.4. DISCUSSION

Alkali and acid treatment to intact cell walls of *S. cerevisiae* resulted in the liberation of the primary carbohydrate components. The purity of the isolated fractions was established through determining their protein : carbohydrate ratios. A high protein : carbohydrate ratio reflected incomplete extraction, whilst a pure extract was characterized by a low protein content. In addition the characteristic fingerprint spectra of each of the components was provided by infrared spectroscopy.

The primary metal-chelating component of the cell walls appeared to be represented by the mannan fraction. Though a more efficient metal-binding component than glucan and chitin, the affinity of mannan for metals depends strongly on the metal involved. The affinity of the three test metals for mannan decreased in the order  $\text{Cu}^{2+} \gg \text{Co}^{2+} > \text{Cd}^{2+}$ . The high  $K_A$  of the mannan for  $\text{Cu}^{2+}$  reflects a number of ligands or species of ligands available on the mannan component for metal interaction. Expressed in terms of the equation  $\text{M} + \text{L} = \text{ML}$ , this implies that the formation of ML is favoured with the metal-ligand forming a stable complex, whilst minimal  $\text{Cu}^{2+}$  dissociation occurs. This has been supported by other studies which have shown that  $\text{Cu}^{2+}$  binding displaces protons associated with the mannans, resulting in the subsequent acidification of the external environment (145). The affinities of the other cell wall isolates used in this study for the respective metal ions varied, depending on both the isolate and the metal species in question. However, the intact cell wall exhibited similar overall affinities for the three metal species, thereby confirming the participation of the glucan and chitin components in metal binding.

Due to the association of mannan with a protein fraction in the intact cell wall, and the presence of phosphate containing side chains, the ligands available on this component for metal biosorption include the hydroxyl and phosphate groups of the carbohydrate moiety, together with the wide range of groups provided by the protein fraction. In other studies bioaccumulation of uranium has been related to the phosphate groups of mannan, whilst experimental evidence has linked cadmium binding predominantly to the protein and not the carbohydrate moiety of mannoproteins (65). Hydroxyl-heavy metal interaction, although of a low affinity (66) have been confirmed by the present study.

The accumulation of heavy metal cations by the isolated cell wall components reflected their spatial arrangement in the cell walls. In comparison to mannoprotein which forms the outer layer of the cell wall, the primary constituents of the inner layer of the wall, glucan and chitin though capable

## 2. CELL WALLS AND CELL WALL COMPONENTS

of forming metal complexes were less involved with metal binding. The affinity of glucan for heavy metals was low, yet due to its dominance in the cell wall (approximately a third), it contributes towards the metal binding characteristics of the wall. Chitin has, however, been documented as a chelating agent for copper (63), thorium (12) and uranium (11, 149) in the cell walls of *R. arrhizus*. The mechanism hypothesized for chitin metal binding suggests that the amino groups of the cell wall chitin act initially as metal concentration sites. Subsequent nucleation of the metal occurs, eg. uranium which is complexed as uranyl hydroxide (149). A similar phenomenon has been reported regarding the complexation of gold with carboxyl groups (151). This characteristic enables the cell wall to bind metal in excess of the number of available binding sites.

While important, the carbohydrate moiety is not the sole metal accumulator in the cell wall. Infra-red spectra characterized the predominant cell wall-metal interactions to occur between the secondary amide groups of the cell wall and the metal ions. Other studies (43) have also implicated the protein component as an important heavy metal chelator. Protease digestion of mannoproteins greatly decreases the mannan accumulation by mannan (65). This does not exclude the carbohydrate components of the cell wall from complexing with metal ions and the involvement of mannan, glucan and chitin in metal binding was also confirmed in this study by infra-red spectra. The respective heavy metal ions appeared to interact with each of the cell wall isolates in a similar fashion, viz. predominantly through the C-OH and C=O groups, though the residual phosphate groups of the mannan component also played a role in metal binding.

## 2.5. CONCLUSIONS

The experimental results presented in this chapter suggest the trend of cell wall components binding to heavy metals in the order: mannan > chitin > glucan. Binding of heavy metals does not appear to be a function of the polysaccharide backbone alone, but rather due to the complexity of the nature of each polymer. Attached amine and phosphate groups in addition to the protein fractions increase the binding capacity of these polysaccharide components. The affinity of the cell wall components for different metals depends on the species of the metal and the nature of the ligands available for metal complexation. The binding of  $\text{Cu}^{2+}$ ,  $\text{Co}^{2+}$  and  $\text{Cd}^{2+}$  to the cell walls of yeast appear to be properties of all the major cell wall components.



### 3. ISOLATED VACUOLES

Divalent cation accumulation by the vacuole of *S. cerevisiae* has been predominantly studied using  $Mg^{2+}$ ,  $Ca^{2+}$  and  $Zn^{2+}$ . The aim of this study was therefore to determine whether or not the same accumulation criteria applied to the uptake of  $Cu^{2+}$ ,  $Co^{2+}$  and  $Cd^{2+}$  by isolated yeast vacuoles. Through the addition of an ATPase uncoupling agent 2,4 dinotrophenol (DNP), the role of the vacuolar  $H^+$  - ATPase antiport system in the uptake of these cations could be determined.

## 3.2. MATERIALS AND METHODS

### 3.2.1. PRETREATMENT OF YEAST

The washing procedure of yeast cells adhered to the protocol described previously (section 2.2.1.). Washed cells were pretreated according to an adapted methodology of Rose *et al.* (156), and Wiemken (157). In order to predispose the yeast cells to the action of the lytic enzyme, they were exposed to a thiol component, 2-mercaptoethanol (Fluka Chemie, AG). The thiol component acts on the disulphide bonds of the cell wall proteins.

Washed yeast cells were suspended in 10 mM sodium citrate buffer containing 0.6 M sorbitol (SOB, pH 6.8) in the ratio 1 g cells (wet wt) : 5 ml buffer. The solution was supplemented with 0.05 ml mercaptoethanol for every gram of the washed yeast cells. The suspension was incubated for 20 min at 28°C, prior to centrifugation (3000 g x 10 min). The centrifuged cells were washed in buffer to remove any residual mercaptoethanol.

### 3.2.2. SPHEROPLAST FORMATION

Enzymatically treated yeast cells are referred to as spheroplasts in preference to protoplasts, due to the residual material which remains adhered to the plasma membrane. Throughout spheroplast formation the yeast cells remained suspended in the SOB buffer to maintain their osmotic stability. Lysing enzyme from *Cytophagia sp.* (Sigma Chemical Co) containing yeast glucanase, protease and cell lytic components was used for spheroplast formation.

The washed, pretreated cells were resuspended in SOB buffer and incubated with the enzyme (1.0 mg enzyme : 1.5 g wet wt yeast cells) at 30°C for 2 h with shaking. Spheroplast formation was monitored using phase contrast microscopy and spectroscopy. A few drops of the spheroplast solution

### **3. ISOLATED VACUOLES**

were heavily diluted in respective buffer (SOB, pH 6.8) and water solutions. These suspensions were allowed to stand with occasional shaking for 5 min. The optical density of the solutions were read at 600 nm, and a comparison was made between the initial and final absorption readings at this wavelength. Spheroplast lysis occurs in water, causing the optical density (OD) to drop, whilst the buffered sorbitol prevents lysis and the OD remains virtually unchanged.

#### **3.2.3. VACUOLE ISOLATION**

Vacuoles were obtained through metabolic lysis of the spheroplasts following the method of Indge (158). One volume of the SOB solution was added to 50 volumes of 10 mM Imidazole - HCl buffer containing mannitol (10% w/v) and 5 mM EDTA (ethylenediaminetetraacetic acid) (pH 6.5). After equilibration at room temperature for 10 min a 10% (w/v) glucose solution (2.5 ml glucose/ml spheroplasts) was added to initiate the reaction. The reaction mixture was incubated at 30°C for 30 min with gentle shaking.

The released vacuoles were contained in a pellet collected after centrifugation (2000 g x 4 min). To obtain the vacuolar fraction the pellet was suspended in Imidazole - HCl buffer containing only 10 mM mannitol (0.1 ml vacuole suspension/ ml buffer). The gelatinous material containing the cell debris readily sedimented out through gravitational forces, leaving a vacuole-rich supernatant which could easily be removed.

#### **3.2.4. DETERMINATION OF VACUOLE INTEGRITY**

Vacuole integrity was determined using neutral red dye (159). Vacuoles were placed in freshly prepared neutral red dye (made up to 0.01% in 0.8 M phosphate buffer, pH 7.2) for one hour, rinsed and viewed under the microscope. Due to the ion trap mechanism of accumulation by the vacuoles (73, 159) intact vacuoles stain red to brick red in colour. Their integrity in suspension could thus be determined using phase contrast microscopy.

#### **3.2.5. METAL UPTAKE**

Metal uptake by vacuoles was determined by incubating the vacuolar fraction with metal salts in a 1:1 ratio (v/v). 1 ml of respective vacuole solutions (25 mg wet weight/ ml buffer) was suspended

### **3. ISOLATED VACUOLES**

in buffered solutions of the chloride salts of  $\text{Cu}^{2+}$ ,  $\text{Cd}^{2+}$  and  $\text{Co}^{2+}$  (Merck Chemical Co) to yield final concentrations of the metals ranging from 2.5 - 30  $\mu\text{M}$ . Metal uptake was determined over time, with sampling occurring at 0, 5, 10, 20, 30, 60, 90 and 120 minutes, respectively. Throughout the experiment the vacuolar fractions were kept on ice.

Sample fractions were subsequently filtered through membrane filters (Millipore filters, 25 mm diameter, 0.45  $\mu\text{m}$  pore size) according to the method of Norris and Kelly (4). The filters containing the vacuolar fraction were washed using 1 ml Imidazole - HCl buffer containing 5 mM EDTA to remove metal ions bound to the surface of the vacuole. (To determine the integrity of the filtered vacuoles, the results from the EDTA washed filters were compared to those washed with Imidazole - HCl buffer not containing EDTA, and unwashed filters.) The filters containing the vacuole-metal fraction were placed in 10 ml of 2 M HCl and digested ( $100^{\circ}\text{C}$ , 2 h) to release the accumulated metal ions. Control samples, excluding vacuoles were run to determine the amount of metal bound by the filter.

Levels of accumulated and free metal ions were detected using atomic absorption spectroscopy (Varian AA 1275 Spectrophotometer) at the relevant wavelengths for each of the respective metals.

#### **3.2.6. ATPase INHIBITION**

Prior to addition of the metal solutions to the vacuole fraction, 0.2 ml of a 2 mM solution of the ATPase uncoupling agent, 2,4 dinitrophenol (DNP, Sigma Chemical Co) was added. Incubation of the vacuole-DNP fraction on ice for 10 min enabled the DNP to interact with the vacuolar ATPase. One ml of the appropriate metal solution was added resulting in the final concentration of the DNP in solution being 0.182 mM. The remainder of the protocol was as outlined in section 3.2.5.

### **3.3. RESULTS**

#### **3.3.1. SPHEROPLAST AND VACUOLE INTEGRITY**

Microscope analysis indicated successful spheroplast formation. These observations were substantiated by those obtained from optical density studies. A substantial change in optical density of cells suspended in water reflected the instability of the spheroplasts, while spheroplasts suspended

### 3. ISOLATED VACUOLES

in SOB (pH 6.8) buffer showed a minimal change in optical density. Spheroplasts suspended in Milli-Q water underwent lysis due to the lack of a buffering agent. In comparison, the SOB (pH 6.8) buffer maintained the osmotic environment, minimizing lysis.

Due to the permeability of the tonoplast to the molecular (carbonium) form of the neutral red dye, the latter was chosen in preference to others in establishing vacuole integrity. The dye is taken up by the vacuole where in the presence of an acidic environment between 88 - 99% of the neutral red molecules are converted to a monovalent cation (159). The tonoplast is impermeable to these cations and the latter are trapped within the vacuoles, resulting in a deep red colour (152, 159). The interior of the vacuoles stained with neutral red dye appeared to contain darkly stained granular material. Very little, or no other cellular material was observed, indicating vacuolar integrity.

#### 3.3.2. HEAVY METAL UPTAKE

Isolated yeast vacuoles accumulated heavy metal cations from solutions of differing concentrations of metal ions. The vacuoles had, however, a limited accumulation capacity, with their maximum uptake depending on the species of metal present. Vacuole suspensions accumulated relative amounts of metal in the order of  $\text{Cu}^{2+} > \text{Co}^{2+} > \text{Cd}^{2+}$  (Figure 3.1 - 3.3).

Vacuolar sequestration of the three heavy metal species exhibited similar trends. The heavy metal cations were removed from the external environment and concentrated within the vacuole. The majority of the metal ions were taken up within the first 30 min of exposure to the test solutions (Figure 3.1 - 3.3). Sequestration of the metal ions within the vacuole appeared to be independent of the external metal ion concentration. A minimal difference was observed between the amounts of metal accumulated by the vacuole from 5, 10 and 30  $\mu\text{M}$  solutions. The initial rapid phase was followed by a secondary phase during which the rate of metal sequestration was slower, resulting in the levels of the metals in the vacuole only increasing slightly, eg.  $\text{Cu}^{2+}$  and  $\text{Co}^{2+}$ , or alternatively levelling off, eg.  $\text{Cd}^{2+}$ .

### 3. ISOLATED VACUOLES

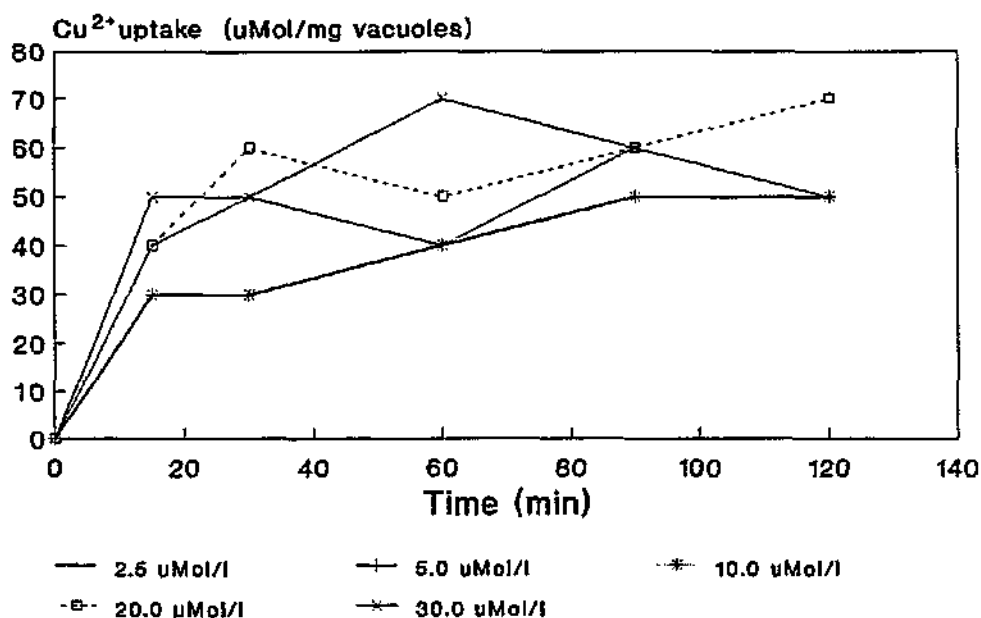


Figure 3.1. Accumulation of  $\text{Cu}^{2+}$  by isolated yeast vacuoles over time from  $\text{Cu}^{2+}$ -containing solutions. The amount of metal accumulated is ascertained through digestion of the metal-treated vacuoles.

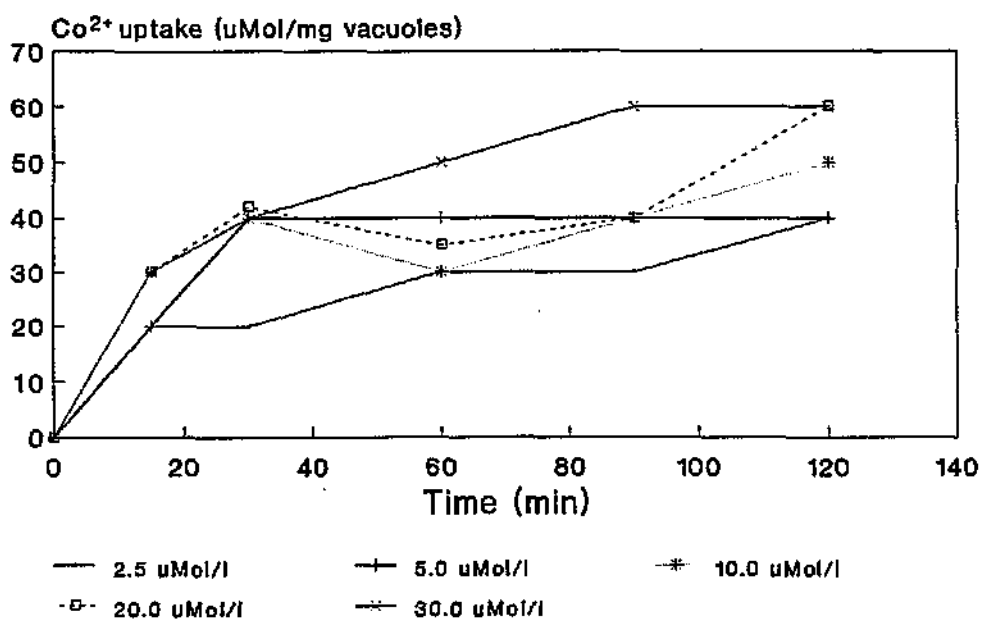


Figure 3.2. Accumulation of  $\text{Co}^{2+}$  by isolated yeast vacuoles over time from  $\text{Co}^{2+}$ -containing solutions.

### 3. ISOLATED VACUOLES

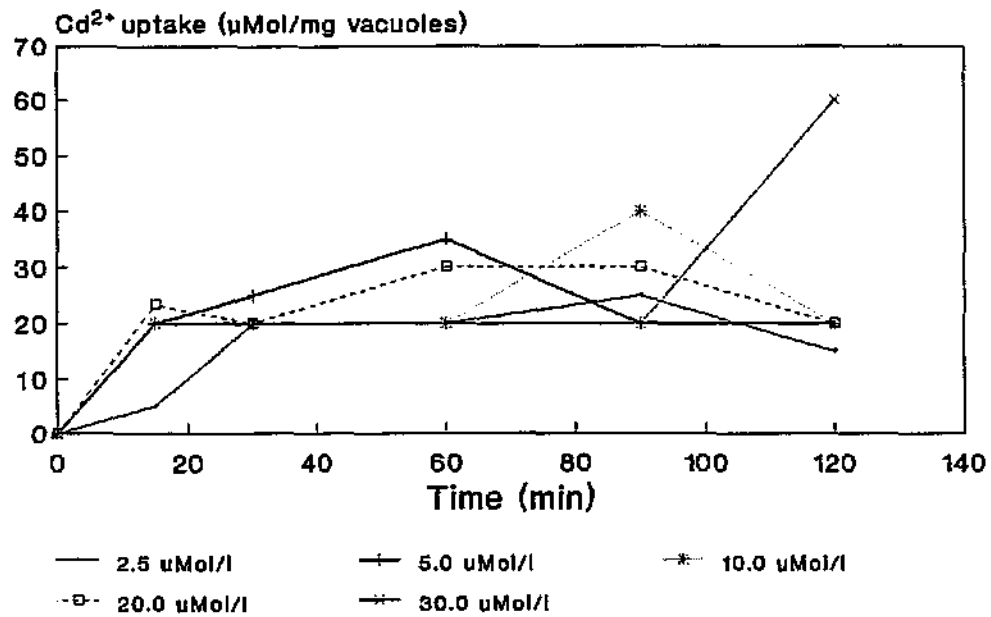


Figure 3.3. Accumulation of  $\text{Cd}^{2+}$  by isolated yeast vacuoles over time from  $\text{Cd}^{2+}$ -containing solutions.

The ATPase uncoupler, DNP, did not exhibit a strong inhibitory effect on the uptake of  $\text{Cu}^{2+}$ ,  $\text{Co}^{2+}$  and  $\text{Cd}^{2+}$  into the vacuoles (Figures 3.4 - 3.6).

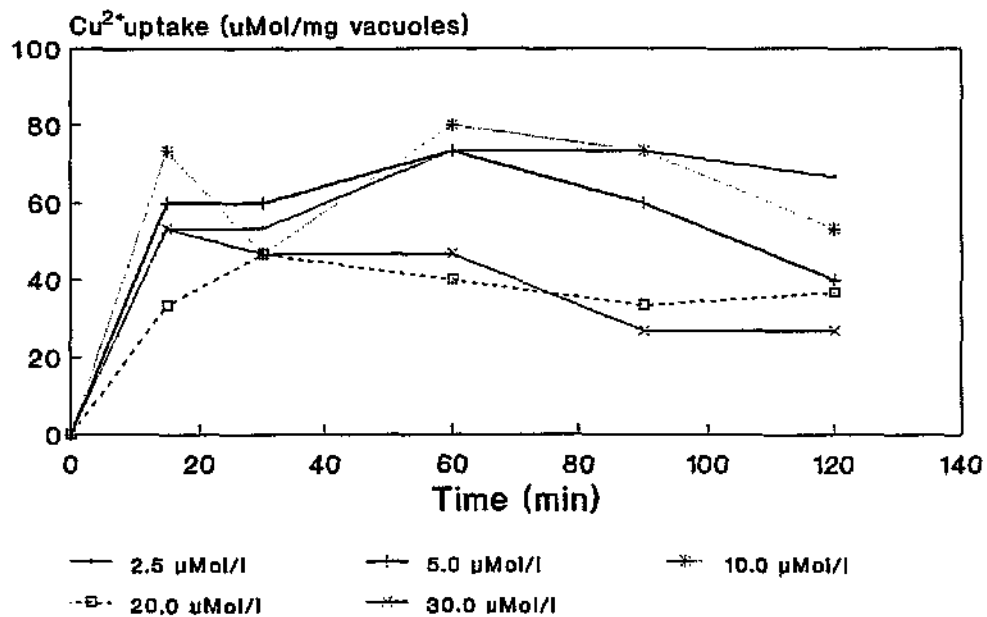


Figure 3.4. Effect of DNP-pretreatment on vacuolar uptake of  $\text{Cu}^{2+}$ . Experimental conditions remained identical to those during uptake by untreated vacuoles.

### 3. ISOLATED VACUOLES

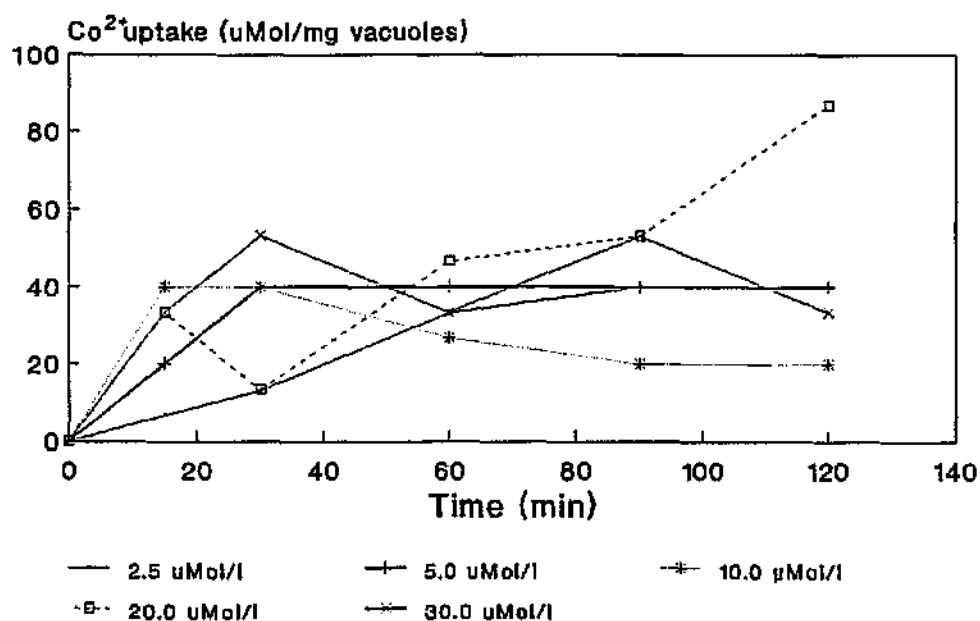


Figure 3.5. Effect of DNP-pretreatment on vacuolar uptake of  $\text{Co}^{2+}$ . Experimental conditions remained identical to those during uptake by untreated vacuoles.

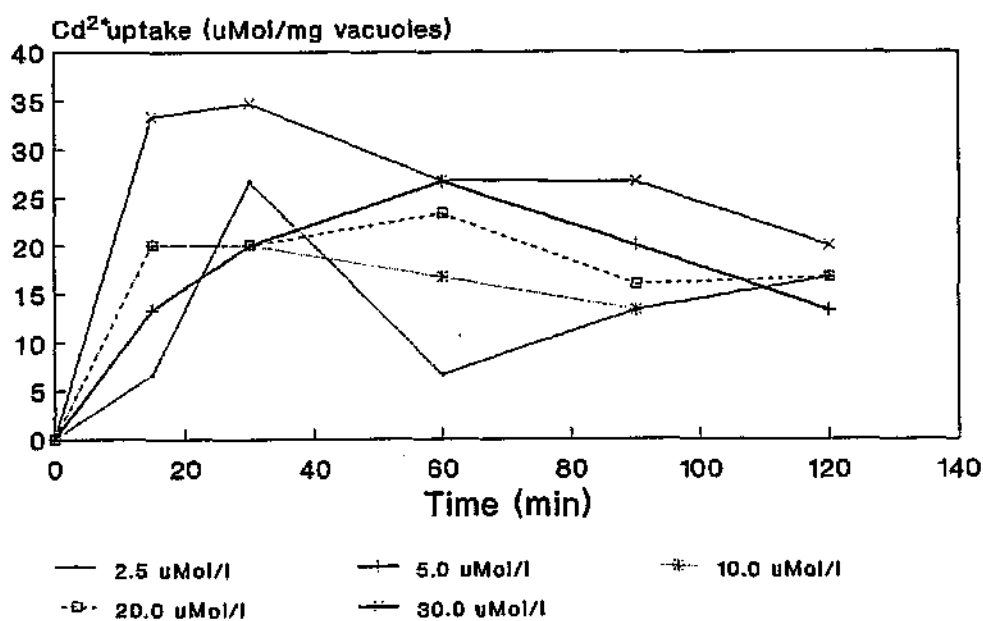


Figure 3.6. Effect of DNP-treatment on vacuolar uptake of  $\text{Cd}^{2+}$ . Experimental conditions remained identical to those during the uptake by untreated vacuoles.

The accumulation of heavy metal cations during the first 30 min (the initial rapid phase) was comparable to that of untreated vacuoles, irrespective of the metal species or their ambient concentrations. With time the effectiveness of the DNP as an ATPase uncoupler was slightly enhanced. After 120 min the levels of the respective metal cations accumulated within the DNP-pretreated vacuoles were less than those of their untreated counterparts.

### 3.4. DISCUSSION

Vacuolar uptake of heavy metal cations (Fig 3.1 - 3.3) exhibit characteristics similar to those of cellular uptake. Both accumulation mechanisms have an initial, rapid phase of uptake. Whereas this phase is followed by a defined, slower secondary uptake phase into intact yeast cells, the amount of metal accumulated by the vacuole levels off, or increases only slightly. Although the vacuole has been reported to possess remarkable elasticity (160), its saturation of metal accumulation may in fact be due to spatial limitations. The sequestration of metal cations by the vacuole in the order of  $\text{Cu}^{2+} > \text{Co}^{2+} > \text{Cd}^{2+}$  may be related to size, with a corresponding decrease in atomic radii of  $\text{Cd}^{2+} > \text{Co}^{2+} > \text{Cu}^{2+}$ .

The mechanisms whereby metals are transported across the tonoplast are complex, with the regulation of these transport systems not being well understood. Both metabolic and non-metabolic transfer systems remain feasible options. Based on data obtained from the present study, the uptake of the three metals by untreated vacuoles could be metabolism dependent. The initial, rapid metal uptake, followed by the decline in accumulation suggests the utilization of a metabolizable energy source during the first phase of uptake. Depletion of this energy source, or alternatively the inhibition of ATPase system would result in the subsequent decline in the amount of metal accumulated.

Several independent transport and translocation systems have been located and identified in the vacuolar membrane. The existence of two  $\text{H}^+$ -translocase systems for chloride (161) and seven for  $\text{H}^+$ /amino acid antiport mechanisms have been identified (154). The transport systems of the vacuolar membranes differ from those of the plasma membranes by having lower substrate affinities (154, 160). Due to the low substrate affinity it is proposed that substitution of the amino acids by heavy metal ions occurs in the ATPase antiport transport system, enabling the uptake of these metals into the vacuolar lumen. Evidence for this transport mechanism was provided by Okorokov (162) who suggested that  $\text{K}^+$ ,  $\text{Ca}^{2+}$ ,  $\text{Zn}^{2+}$ ,  $\text{Mg}^{2+}$  and  $\text{Mn}^{2+}$  activate the ATPase system, thereby initiating



their uptake into the vacuolar interior.

A feasible hypothesis for metal accumulation by vacuoles, would be for metal uptake via an energy dependent  $H^+$ /antiport system. The initial rapid accumulation of the metal ions could be ascribed to ATPase activity in the presence of an energy source. Several reasons could account for the subsequent decline in the rate of metal accumulation: 1) in the absence of a renewable energy source, utilization of the available ATP during the initial uptake would place limitations on the amount of metal accumulated, 2) the presence of high levels of heavy metal cations could act as ATPase inhibitors preventing further accumulation and 3) the spatial limitations of the vacuole may also prevent further metal accumulation.

Researchers have also implicated alternative routes of metal accumulation in yeast. Ohsumi *et al.* (71, 84), reported the permeabilization of the plasma membrane by relatively low amounts of  $Cu^{2+}$ , whilst  $Cd^{2+}$  has also been known to permeabilize membranes. Using fluorescing agents, results were obtained during this study (data presented in chapter 4) which implicate the permeabilization of yeast membranes by certain heavy metal ions. Based on this evidence the possibility of tonoplast permeabilization by heavy metals cannot be excluded. This permeabilization would enable the slow movement of metal ions into the vacuole lumen, thus explaining the gradual increase in the vacuolar metal content after the initial rapid uptake phase.

The results obtained from DNP-treated vacuoles suggest the inability of the metabolic uncoupler DNP to inhibit the accumulation of heavy metal ions by the yeast vacuole. DNP, inhibits the uptake of citrate into vacuoles isolated from the plant *Hevea latex* (152), with the transport of citrate across the vacuolar tonoplast postulated to be similar to that of metals. However, the inability of the DNP to inhibit metal accumulation by yeast vacuoles suggests a different mechanism of metal uptake across the yeast tonoplast, or alternatively the ineffectiveness of DNP as an ATPase uncoupler in yeast vacuolar membranes.

### 3.5 CONCLUSIONS

From this study, and evidence provided in the literature (160), it appears that more than one mechanism exists for solute uptake into the vacuole. It is proposed that the primary route of heavy metal uptake into the vacuole is via the ATPase-dependent  $H^+$ /antiport system. Dependent on ATP

### 3. ISOLATED VACUOLES

as an energy source, this system transfers both essential and non-essential components into the vacuole. A possible secondary accumulation system for heavy metals is based on membrane permeabilization by the cations. The contribution towards the total vacuolar metal accumulation by the latter system is thought to be minor. The possibility exists that membrane permeabilization is triggered by very high levels of heavy metals in the cytosol, or in the absence of a functioning antiport system. Inhibition of the ATPase antiport mechanism can be effected in the presence of metabolic or ATPase-inhibitors and uncouplers, though vacuolar ATPase inhibition appears to be limited to selective agents, eg. DCCD. It can be concluded that DNP, a metabolic uncoupler, is ineffective as an uncoupling agent for vacuolar ATPase, and subsequently unable to prevent metal accumulation by the vacuole.

Having examined metal accumulation by components of yeast cells (cell walls and vacuoles) further studies were conducted on metal accumulation by whole cells.

## 4. ACCUMULATION AND INTERNALIZATION OF HEAVY METALS BY VIABLE YEAST CELLS

### 4.1. INTRODUCTION

A unique attribute of yeast and other viable microbial cells is their ability to maintain an electrochemical balance between the intra- and extracellular environment. To accomplish this, physiological elements are internalized via facilitated transport. In addition to the uptake of essential ions, non-essential and toxic metal cations, eg. heavy metals, can also be accumulated by the cells. Heavy metals are well recognized for their negative effect on the environment and microbial life forms. The severity of the effect on the microorganisms depends largely on the species of heavy metal. The metals used in the present study,  $\text{Cu}^{2+}$ ,  $\text{Co}^{2+}$  and  $\text{Cd}^{2+}$  represent a broad spectrum of heavy metals in terms of their chemical and physical properties, toxicity and behaviour.  $\text{Cu}^{2+}$ , the smallest of the three cations is a physiological cation and in low doses is the least toxic, whilst  $\text{Cd}^{2+}$  is regarded as one of the "big three" toxic metals together with  $\text{Hg}^{2+}$  and  $\text{Pb}^{2+}$  (138).

The affinity displayed by microbial cells for heavy metals is not equimolar. An affinity series of accumulation of  $\text{Mg}^{2+} > \text{Cu}^{2+} > \text{Zn}^{2+} > \text{Mn}^{2+} > \text{Ni}^{2+} > \text{Ca}^{2+} > \text{Sr}^{2+}$  has been demonstrated by

#### 4. ACCUMULATION BY VIABLE CELLS

*Saccharomyces carlsbergensis* cells (22). Regardless of the affinity for heavy metals in the presence of high extracellular concentrations of these ions, metal uptake into yeast cells will occur. As previously noted (chapter 1), metal accumulation by viable yeast cells involves a biphasic uptake mechanism. The initial rapid phase is metabolism-independent, consisting of metal-cell wall interactions. A slower, metabolism-dependent second stage is responsible for the uptake and internalization of the heavy metal cations within the yeast cell interior (4).

The cellular response to metals varies. A relationship between heavy metal transport into yeast cells and toxicity is often observed, with sensitive strains accumulating more metal than resistant strains (163). Regardless of the sensitivity of the yeast strain, the initial response to internalized metal ions is compartmentalization (163, 164). Internalized cations are distributed between the soluble cytosol and the insoluble fractions (organelles) of the cell. Deposition primarily occurs in the vacuole (69 - 71, 73), whilst the majority of heavy metal cations show a lower affinity for cytosolic deposition (82).

Exposure of yeast cells to high levels of toxic heavy metals can confer metal tolerance and resistance upon these cells (163 - 166). Resistance and tolerance mechanisms include: 1) a reduction in metal uptake and the impermeability of the cell plasma membrane. Alternatively the implementation of energy-driven efflux pumps occurs, which keep toxic metal levels low in the interior of the cell. Such mechanisms have been described for  $\text{As}^{2+}$  and  $\text{Cd}^{2+}$  (167). 2) Sequestration of metals in or around the cell. Metal ions can either bind to cell surfaces or precipitate as insoluble complexes, eg. as metal sulfides or oxides at the cell surfaces (92, 164, 167). 3) Chemical modification or biotransformations to less toxic forms of the elements. Oxidation, eg.  $\text{AsO}_3^{2-}$  to  $\text{AsO}_4^{3-}$  or reduction, viz.  $\text{Hg}^{2+}$  to  $\text{Hg}^0$  which occurs intracellularly via enzymatic processes converting these metals to less toxic forms. Methylation and demethylation also constitute mechanisms of resistance (163, 164, 167). 4) One of the most common metal-induced responses in many microorganisms, inclusive of yeast, is the synthesis of intracellular metal binding proteins which not only play a role in detoxification, but also regulate the storage and cytosolic metal ion concentrations (163). A class of proteins which is capable of chelating relatively large quantities of metal are the metallothioneins (MT). These proteins which are rich in cysteine residues bind a wide range of metal cations eg.  $\text{Co}^{2+}$ ,  $\text{Ag}^{3+}$ ,  $\text{Cd}^{2+}$ ,  $\text{Cu}^{2+}$  and  $\text{Zn}^{2+}$  (165). Up to 60% of cellular copper has been associated with MT (168), and a percentage of  $\text{Cd}^{2+}$  in Cd-resistant strains has been found bound to soluble MT fractions (35, 169). 5) In addition to forming complexes with chelating agents such as phosphoglycoproteins (170), ferritin (81), siderophores (81) and ferridoxins,  $\text{Mg}^{2+}$ ,  $\text{Sr}^{2+}$  and  $\text{Ca}^{2+}$  are sequestered in cytoplasmic

#### **4. ACCUMULATION BY VIABLE CELLS**

granules in phosphate-rich cells (16). Polyphosphates, similar to those found in vacuoles have been detected in these granules.

The alternative to metal resistance and tolerance in heavy metal exposed yeast cells, is the loss of cell viability. Although a certain degree of metal resistance can be induced in yeast cells when grown in the presence of elevated levels of extracellular metals (165, 167), eg.  $\text{Cu}^{2+}$  (171),  $\text{Cd}^{2+}$  (169) and  $\text{Co}^{2+}$  (169), most yeast cells are sensitive to such levels of toxic metals. The loss of cell viability can manifest itself in several ways. High levels of intracellular  $\text{Cd}^{2+}$  inhibit nucleic acid and protein synthesis (92) and have also been reported in the permeabilization of the cell plasma membrane as has  $\text{Cu}^{2+}$  (4, 56).

The aim of this section of the study was to monitor the effect of heavy metals on viable yeast cells over time with respect to the sites of deposition of the internalized metal cations and the subsequent cellular response they elicited. In addition, the effect of heavy metals on the integrity of the cell plasma membrane was determined.

### **4.2. METHODS AND MATERIALS**

#### **4.2.1. SCANNING ELECTRON MICROSCOPY (SEM) OF Cu-LOADED CELLS**

##### **4.2.1.1. METAL ACCUMULATION**

Bakers yeast was suspended in ultra-pure Milli-Q water, washed three times (3000 g x 10 min) and subsequently suspended in 5 mM PIPES/TMAH buffer (pH 6.5) in a 1 : 2 wet weight (g) : volume ratio (ml).

Duplicate 20 ml volumes were removed as test and control fractions. To the test fractions a 0.5 mM  $\text{CuCl}_2 \cdot 2\text{H}_2\text{O}$  stock solution was added to obtain a final concentration of 0.357 mM. The yeast was exposed to the metal for 90 minutes at 25°C with shaking. The control fractions were not exposed to any metals ions. On completion of incubation, the yeast was spun down (3000 g x 10 min) and the pellet air-dried for 5 min prior to being mixed with warm 6% (w/v) agar and allowed to set.

#### **4. ACCUMULATION BY VIABLE CELLS**

##### **4.2.1.2. CRYO-SEM PREPARATION**

Small rectangular blocks (2mm<sup>3</sup>) were cut from the agar. These were cooled to -200°C in liquid nitrogen before being transferred to the cryo-chamber of the SEM (JOEL JSM 840 Scanning electron microscope). At no stage of the transferral was the sample allowed to come into contact with air.

The sample was sectioned to expose the cell morphology. To enhance the image obtained the sections were gold coated and subsequently viewed at an acceleration voltage of 20kV. Both backscattered (BED) and secondary (SED) electron images of the sliced cells were examined.

##### **4.2.2. DISTRIBUTION STUDIES OF ACCUMULATED HEAVY METAL CATIONS BY TRANSMISSION ELECTRON MICROSCOPY (TEM)**

###### **4.2.2.1. METAL ACCUMULATION**

Washed yeast cells were suspended in 5 mM PIPES/TMAH buffer (pH 6.5) in a 1:2.5 g:ml ratio. 20 ml volumes of yeast suspensions were exposed to respective Cu, Co or Cd-solutions to yield a final metal concentration in solution of 1M. As for section 4.2.1.1, the control fraction was not exposed to the heavy metal solutions. Metal incubation took place for 1, 2, 5, 12 and 24 h respectively with shaking at 25°C. Air-dried cells were mixed with warm 6% (w/v) agar and allowed to set.

###### **4.2.2.2. EMBEDDING PROTOCOL FOR MICROSCOPIC ANALYSIS**

Blocks (2mm<sup>3</sup>) were cut from the yeast-agar molds and placed into labelled specimen tubes containing cold 2.5% glutaraldehyde in 0.1 M phosphate buffer. Primary fixation of the sample proceeded overnight, after which the glutaraldehyde was decanted and the blocks washed with 0.1 M phosphate buffer. The washing procedure was repeated.

No secondary fixation protocol was observed due to the elemental conflicts caused by the secondary fixative (OsO<sub>4</sub>) in the energy dispersive X-ray spectra of Cu and other ions. Dehydration of the samples was achieved using an alcohol gradient of 30 - 100%. The samples were exposed to each concentration of alcohol for 5 min, with two final washes using absolute ethanol. After dehydration,

#### **4. ACCUMULATION BY VIABLE CELLS**

infiltration and embedding of the samples using resin could commence. The first stage of infiltration required two 15 min washes using propylene oxide.

The embedding process was gradual. On decanting off the second propylene-oxide wash, the tubes were refilled with a 75 : 25 propylene oxide : resin (Araldite) mixture. This was replaced by a 50 : 50 mixture after 60 min, and the process repeated until the samples were transferred into tubes containing 100% pure resin for 12 h to enable embedding to proceed overnight. On completion of infiltration and embedding the samples were polymerized at 60°C for 36 h.

#### **4.2.2.3 SECTIONING FOR TRANSMISSION ELECTRON MICROSCOPY (TEM) AND X-RAY DIFFRACTION ANALYSIS**

Prior to sectioning, the polymerized blocks were trimmed to the correct shape; a trapezium. All sectioning and trimming was conducted on a RMC MT-7 Ultramicrotome, using glass knives.

##### **4.2.2.3.1. ULTRATHIN SECTIONING AND STAINING OF SAMPLES FOR TEM**

Ultrathin sections (100 nm) were cut from the trimmed block. On cutting, the 100 nm sections formed silver-grey ribbons which were collected by floating them onto 300 mesh copper grids. The sections were air-dried prior to staining.

TEM sections were stained in aqueous uranyl acetate for 30 min, and subsequently in lead citrate for 5 min. The grids containing the stained sections were examined under a JOEL JSM 100 CK TEM at an acceleration voltage of 80kV.

##### **4.2.2.3.2. X-RAY DIFFRACTION PREPARATION AND ANALYSIS**

Due to the higher acceleration voltage used for X-ray analysis, thicker sections were required. Thick sections (250 nm) which formed blue-green ribbons when floated on water, were cut. Due to various elemental conflicts not all the samples could be collected onto identical grids. The Cu-containing samples were floated onto gold grids, Co-samples onto formvar coated wide slot copper grids and Cd-samples onto either wide slot formvar coated copper grids or alternatively nickel grids.

#### **4. ACCUMULATION BY VIABLE CELLS**

Once again interference in heavy metal detection prevented the staining of the samples. The presence of intracellular elements was confirmed through examining the carbon coated sections using a Phillips EM 420 TEM at an acceleration voltage of 120kV. The sites of metal ion deposition, localization and evidence of ion exchange were confirmed from EDAX spectra obtained from an EDAX PV 9100 probe attached to the TEM. The limits of the probe were set between 1 - 20 KeV thereby excluding the detection of the essential elements: H, C, N, O and foreign ions. Analysis of the cells or specific cellular components (eg. cell walls, vacuoles and cytosolic inclusions) were accomplished by focussing the electron beam on the area of interest.

#### **4.2.3. INFLUENCE OF METALS ON MEMBRANE INTEGRITY**

Based on the method of Slavik (172), the membrane permeability of yeast cells was determined using fluorescence techniques. Non-fluorescent fluorescein diacetate (FDA, Sigma Chemical Co) when incubated with viable yeast cells, is internalized and deacetylated to yield fluorescent fluorescein. An advantage of this conversion is the fact that fluorescein shows very small permeability across the cell plasma membrane, thus in experiments with intact yeast cell plasma membranes, very little fluorescent dye is lost back to the medium. The amount of fluorescein in the media is an indication of the loss of plasma membrane integrity.

Yeast cells were washed twice (3000 g x 10 min), aerated and suspended in buffer (50 mM PIPES/TMAH, pH 6.5). Prior to the addition of metals, 5 ml of suspended cells were added to each tube and incubated with 0.1 ml fluorescein diacetate (FDA, Sigma Chemical Co) and 4.9 ml Milli-Q water at 25°C for 30 min. Incubated cells were centrifuged, washed and the pellet resuspended in 9.5 ml of PIPES/TMAH buffer (pH 6.5). 0.5 ml of the appropriate metal solution ( $\text{CuCl}_2 \cdot 2\text{H}_2\text{O}$ ,  $\text{CoCl}_2 \cdot 6\text{H}_2\text{O}$  or  $\text{CdCl}_2 \cdot \text{H}_2\text{O}$ ) was added to the respective tubes (the blank contained 0.5 ml Milli-Q water). This suspension was incubated for a further 30 min at 25°C, spun down (3000 g x 10 min) and the supernatant measured for fluorescence. Fluorescence determinations were accomplished using a Perkin-Elmer Fluorescence Spectrophotometer 203. Fluorescence intensity was recorded at 520 nm after excitation at 435 and 490 nm, respectively.

### 4.3. RESULTS

#### 4.3.1. HEAVY METAL INDUCED MORPHOLOGICAL CHANGES

The morphological consequences of  $\text{Cu}^{2+}$  accumulation on yeast intracellular structure are shown in Fig. 4.1. and 4.2. The normal ultrastructure of *S. cerevisiae* in the absence of  $\text{Cu}^{2+}$  contains well defined vacuoles. On uptake of  $\text{Cu}^{2+}$  the cytosol appeared to become dehydrated (Fig 4.2) whilst vacuolar enlargement occurred (Fig 4.3 - 4.5). Also apparent from this study was the effect of heavy metal ion accumulation on the integrity of the cellular tissue. Extensive exposure of yeast cells to metal ions increased the extent of disruption of cellular tissue during sectioning.

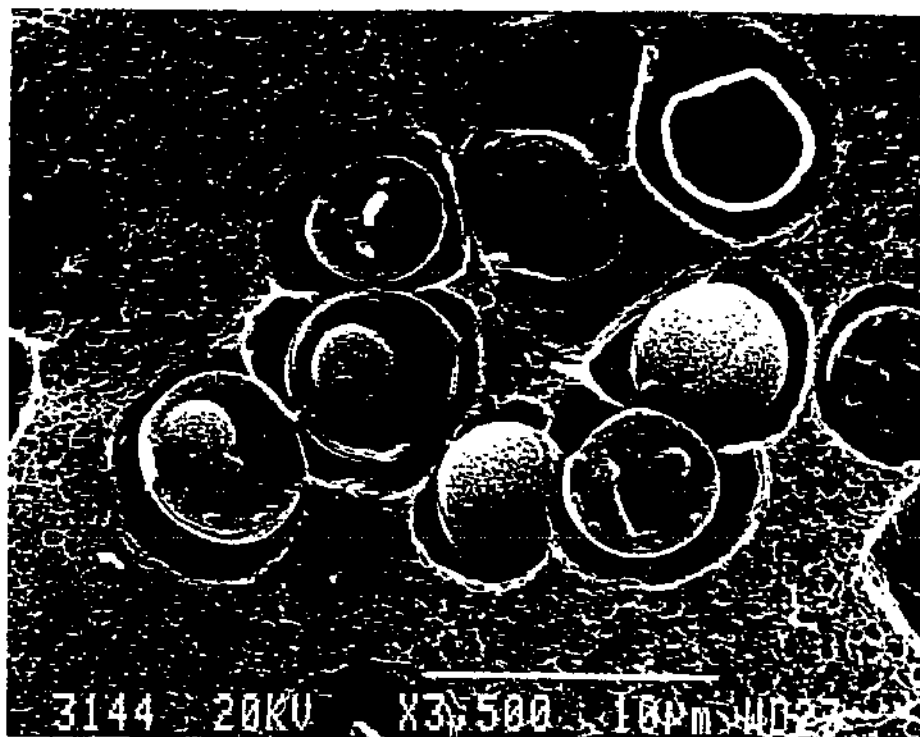
Further consequences of  $\text{Cu}^{2+}$  exposure on the morphology of yeast cells are apparent in Fig 4.3.  $\text{Cu}^{2+}$  accumulation and precipitation after 5, 12 and 24 hrs are represented as dark granules or inclusions throughout the cytosol and in the vacuole. Little evidence of bound or precipitated  $\text{Cu}^{2+}$  was observed on the cell wall, though due to the nature of metal sorption and the reversible association between metal ions and the yeast cell walls, the absence of cell surface metal binding may have been an artifact of the embedding procedure.  $\text{Co}^{2+}$  and  $\text{Cd}^{2+}$  exhibited similar patterns of cellular deposition (Fig 4.4 - 4.5) with  $\text{Co}^{2+}$  and  $\text{Cd}^{2+}$ -rich inclusions located throughout the cytoplasm. However, vacuolar enlargement was not as pronounced as for the  $\text{Cu}^{2+}$  exposed cells.

Sequestered metal ions were either associated with the insoluble fraction (cell wall or vacuole) or the soluble (cytosolic) fractions of yeast cells. The presence of electron dense metal depositions within the cytosol suggested saturation of the soluble fraction, with the subsequent precipitation of metal ions. In addition to these granular depositions, metal association with smaller vacuoles within the cytoplasm was observed.



#### 4. ACCUMULATION BY VIABLE CELLS

a)



#### 4. ACCUMULATION BY VIABLE CELLS

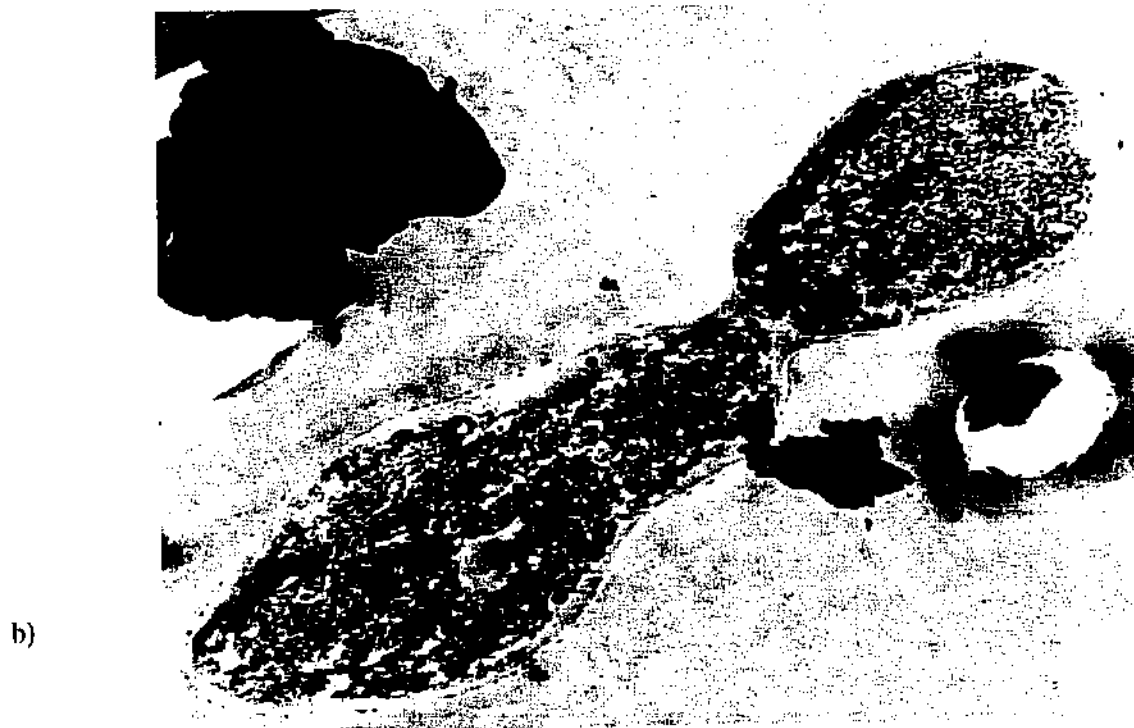


Figure 4.1. Electron micrographs of native *S. cerevisiae* cells. a) scanning electron microscopy micrograph (SEM) (magnification 3 500x) and b) transmission electron micrograph (TEM) (10 000x).



Figure 4.2 SEM micrographs (BEI and SEI images) of  $\text{Cu}^{2+}$  exposed *S. cerevisiae* cells (8 000x).

#### 4. ACCUMULATION BY VIABLE CELLS



Figure 4.3. TEM micrographs (10 000x) of *S. cerevisiae* cells after a) 5, b) 12 and c) 24 hrs exposure to  $\text{Cu}^{2+}$  ions. The granulated electron dense areas in both the cytosol and the enlarged vacuole are  $\text{Cu}^{2+}$  rich areas.

#### 4. ACCUMULATION BY VIABLE CELLS

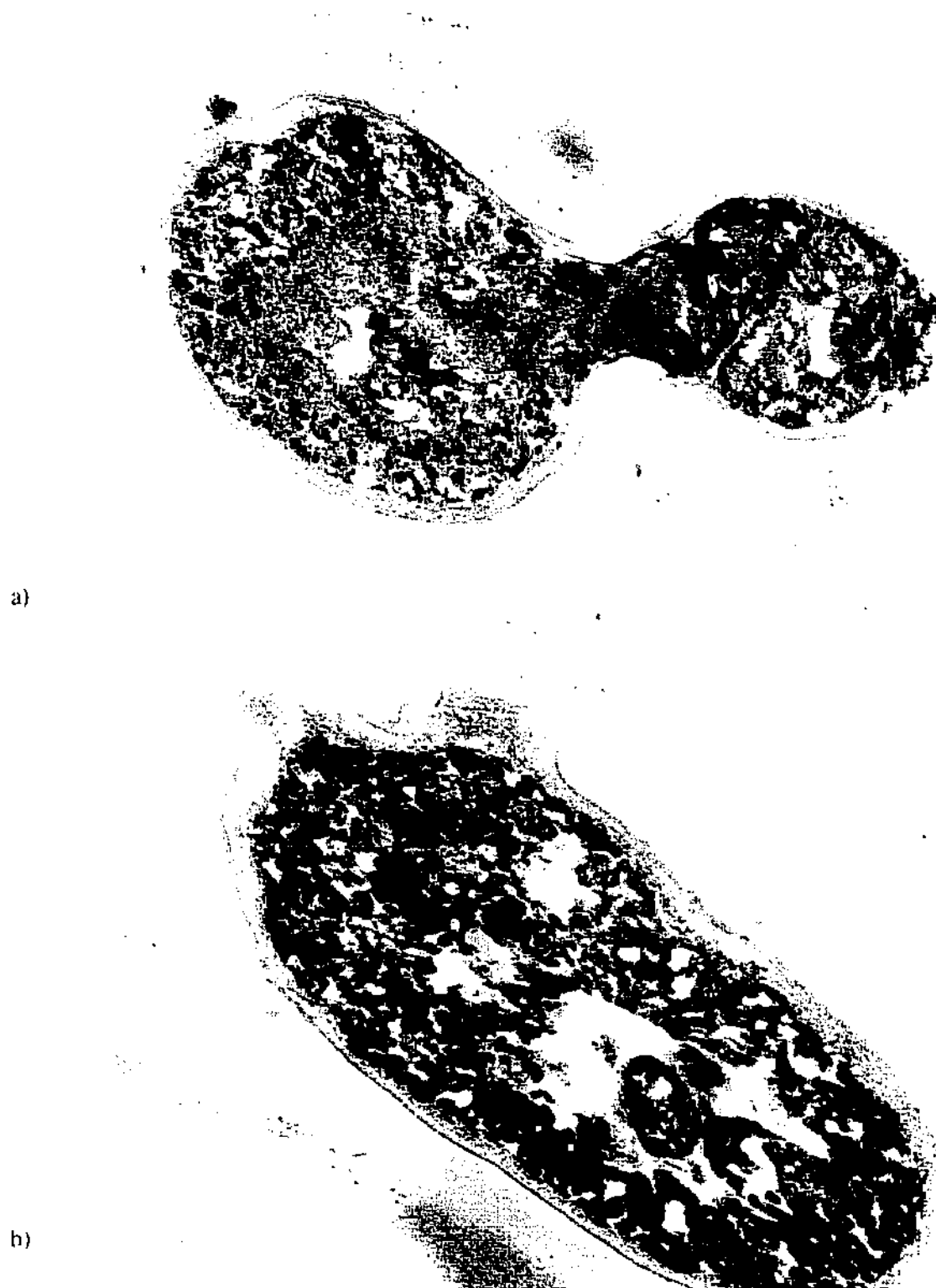


Figure 4.4. TEM micrographs (14 000x) of yeast cells after a) 5 and b) 12 hrs exposure to  $\text{Co}^{2+}$  ions. Vacuolar enlargement is apparent in the presence of  $\text{Co}^{2+}$

#### 4. ACCUMULATION BY VIABLE CELLS



Figure 4.5. TEM micrographs (14 000x) of *S. cerevisiae* after: a) 5, b) 12 and c) 24 hrs exposure to Cd<sup>2+</sup> ions. Deposition of Cd<sup>2+</sup> rich inclusions in the cytosol and vacuole occur.

## 4.3.2. CELLULAR DISTRIBUTION OF METAL IONS

A prerequisite for the detection of elements on the EDAX spectra was a minimum composition of 1% of the area under analysis. Restrictive criteria, eg. biological variables, prevented quantitative analysis of the metal ion concentration within yeast cells, resulting in qualitative interpretation of the results. Elements present in native yeast cells, viz. Na, Mg, Si, P, S, K, Cl and Ca (Figure 4.6) are not all inherent to the yeast cells, but some originate from the external sources, eg. Si, Cl, P and S, which are provided by metal solutions, buffers and embedding resin. The physiological ions: Na, K, Cl and Ca, maintain the ionic equilibrium within the cell, whilst the presence of P, often as a conspicuous phosphorous peak in vacuolar bodies can be ascribed to polyphosphate molecules (173).

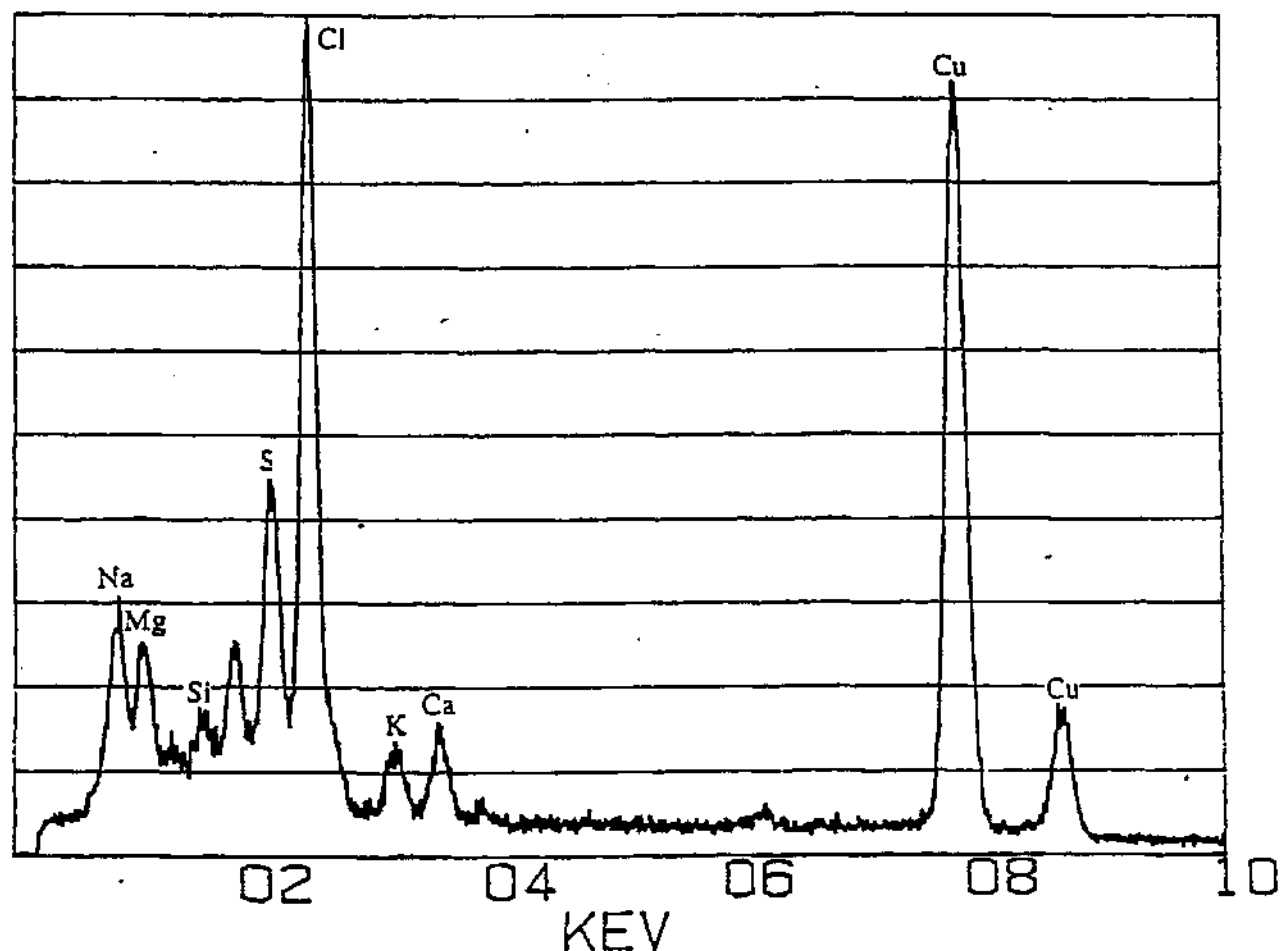


Figure 4.6. A typical EDAX ion profile spectra of native *S. cerevisiae* biomass. The Cu peaks originate from the 300 mesh grids used.

#### 4. ACCUMULATION BY VIABLE CELLS

Not all cells accumulated heavy metal cations, even though high external concentrations of metals were maintained to encourage internalization. Internalization of heavy metal cations occurred as a function of time. After 1 h of metal exposure (Table 4.1) not all intact cells presented a positive identification spectra of the respective heavy metals, regardless of the presence of cytosolic electron dense inclusions, eg. the  $\text{Co}^{2+}$  and  $\text{Cd}^{2+}$  exposed cells. An increase in the number of inclusions over time (or those located in different cells) resulted in positive metal identification in the respective cells. Exposure to 1M solutions containing  $\text{Cu}^{2+}$ ,  $\text{Co}^{2+}$  and  $\text{Cd}^{2+}$  in excess of 5 h resulted in the majority of cells having accumulated heavy metals. Metal ion assessment of the intact cells, cytosol, cell walls and vacuoles were undertaken. The electron dense cytosolic inclusions noted in TEM micrographs (Fig 4.3 - 4.5) were analysed and proven to contain heavy metal ions (Figure 4.7). Though little visual evidence existed to implicate metal interaction with cell walls, positive spectral M-lines of the respective metal ions were noted in spectra of treated cells.

Table 4.1 Ion profiles of yeast cells exposed to respective 1M  $\text{Cu}^{2+}$ ,  $\text{Co}^{2+}$  and  $\text{Cd}^{2+}$  solutions for 1 h. This data, obtained from EDAX spectra represents typical results.

CONTROL			$\text{Cu}^{2+}$ -CELLS			$\text{Co}^{2+}$ -CELLS			$\text{Cd}^{2+}$ -CELLS		
IC <sup>a</sup>	Cyt <sup>b</sup>	Vac <sup>c</sup>	IC	Cyt	Vac	IC	Cyt	Vac	IC	Cyt	Vac
Na	P	Na	Si	Si	Si	Na	P	Na	P	Na	Na
Mg	S	Mg	P	P	P	Mg	S	Mg	S	P	Mg
Si	Cl	Si	Cl	S	S	P	Cl	P	Cl	S	Si
P	K	P	Cu	Cl	Cl	S	Ca	S	K	Cl	P
S	Ca	S		Cu	Cu	Cl		Cl	Ca	Cd	S
Cl		Cl				K		K			Cl
K						Ca		Ca			Cd
Ca								Co			

a: Intact cell

b: Cytosol

c: Vacuole

#### 4. ACCUMULATION BY VIABLE CELLS

The amount and rate of  $\text{Cu}^{2+}$  accumulation exceeded that of  $\text{Co}^{2+}$  and  $\text{Cd}^{2+}$ . Sufficient  $\text{Cu}^{2+}$  was taken into the yeast cells to provide positive detection after 1 h. Whilst  $\text{Cd}^{2+}$  and  $\text{Co}^{2+}$  depositions within the cells could be located after 1 h, this accumulation represented less than 1% of the total cell deposition thereby failing to provide positive cellular detection. Based on random analysis of sites within yeast cells, it appeared that the vacuoles were the initial sites for intracellular metal ion deposition. These deposits became enlarged with increasing time of exposure to the metal containing solutions. Subsequent accumulation and deposition of metal ions in the cytosol may arise as a result of vacuolar saturation.

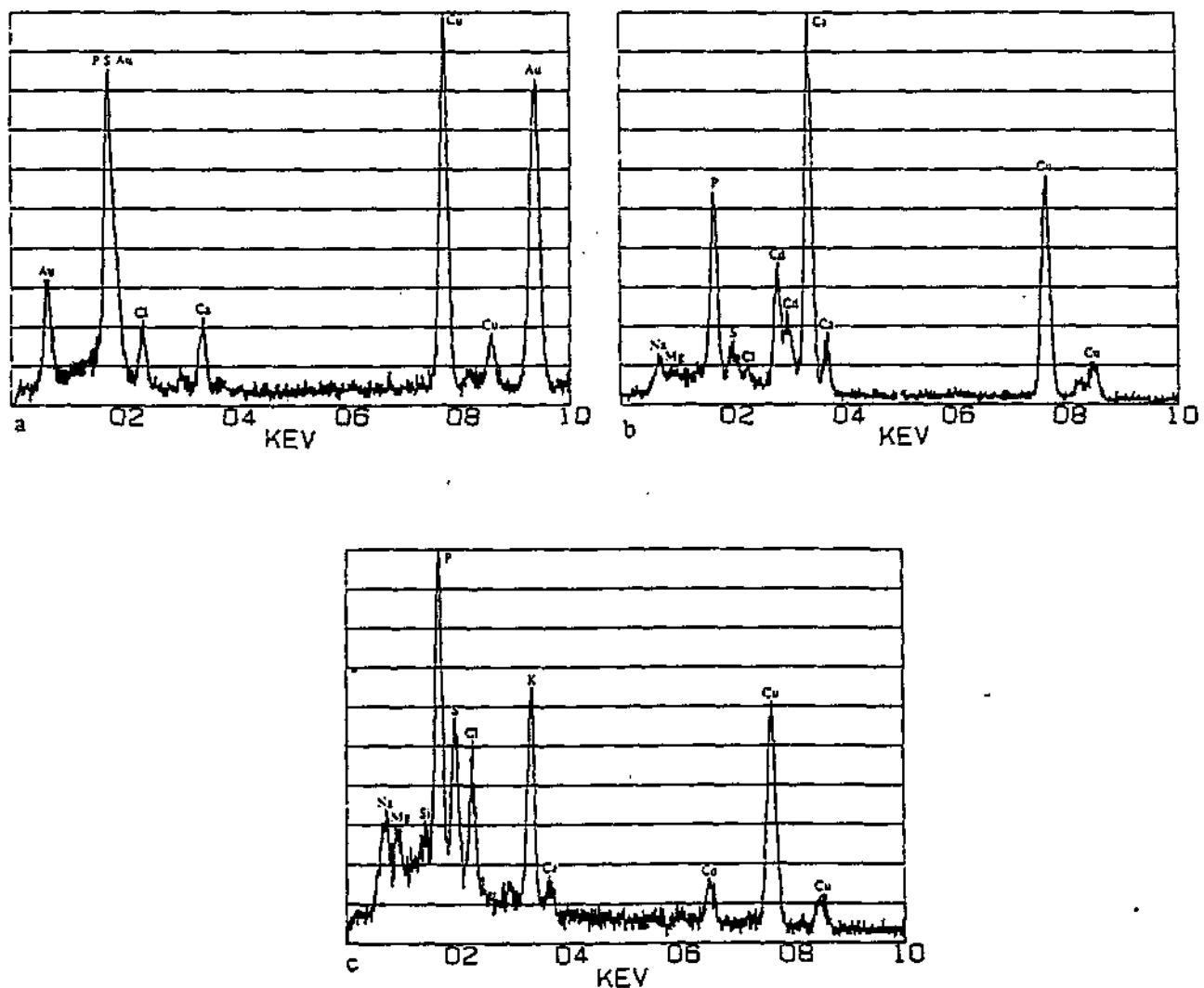


Figure 4.7 EDAX spectra of the electron dense inclusions in a)  $\text{Cu}^{2+}$ , b)  $\text{Cd}^{2+}$  and c)  $\text{Co}^{2+}$  loaded cells after 1 h. Conspicuous P peaks are observed in each of the spectra. The Cu peaks present in (b) and (c) and the Au peaks in (a) are due to grid interference.



#### 4. ACCUMULATION BY VIABLE CELLS

The cellular ion profiles were monitored over time in the presence of high concentrations of the respective heavy metal species (Figure 4.8 - 4.10).

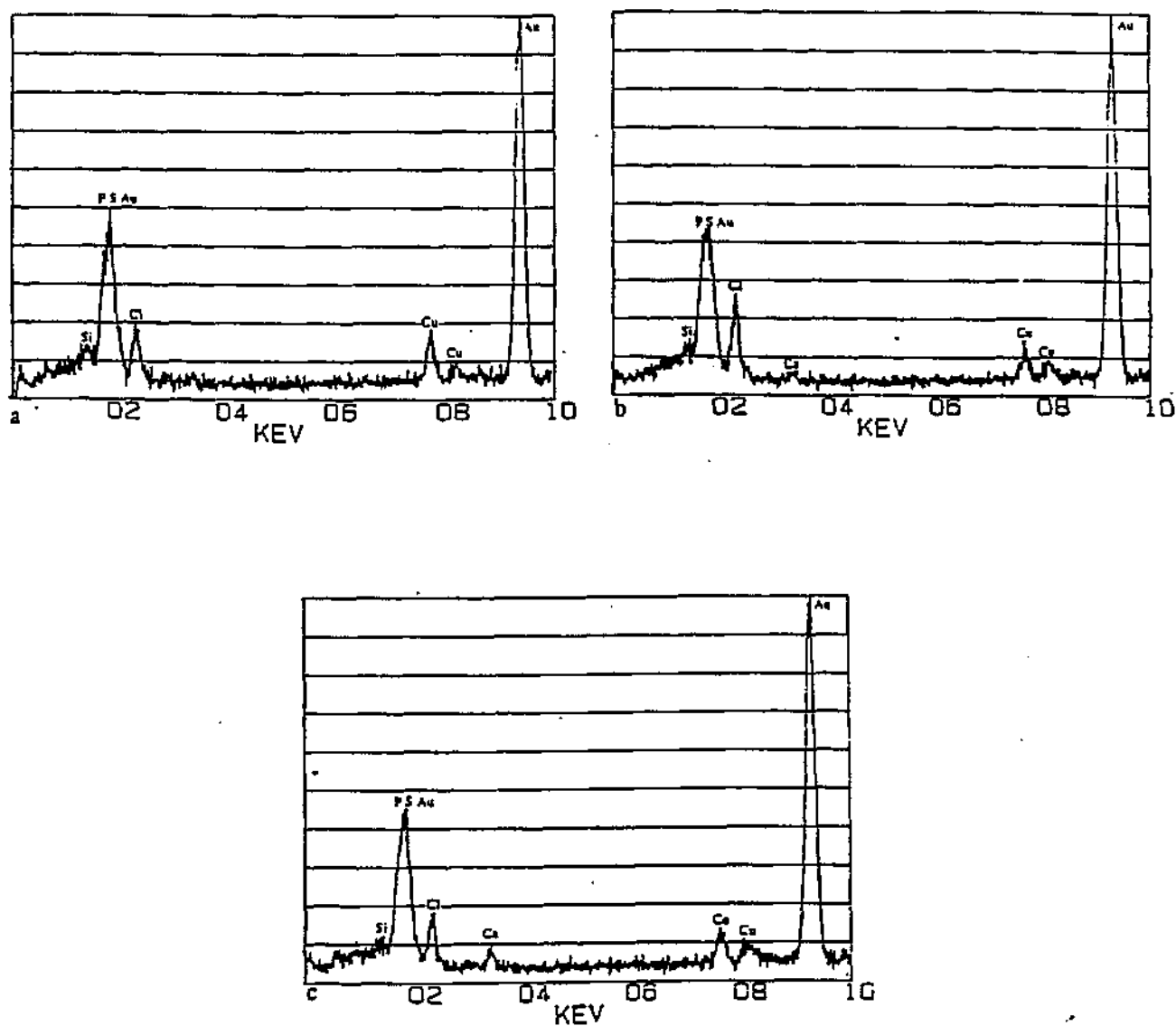


Fig 4.8 Intracellular ion composition of yeast cells exposed to a  $\text{Cu}^{2+}$  containing solution after a) 1, b) 12 and c) 24 h of metal exposure. Au peaks represent grid interference. The absence of physiological ions emphasized the ongoing ion exchange.

#### 4. ACCUMULATION BY VIABLE CELLS

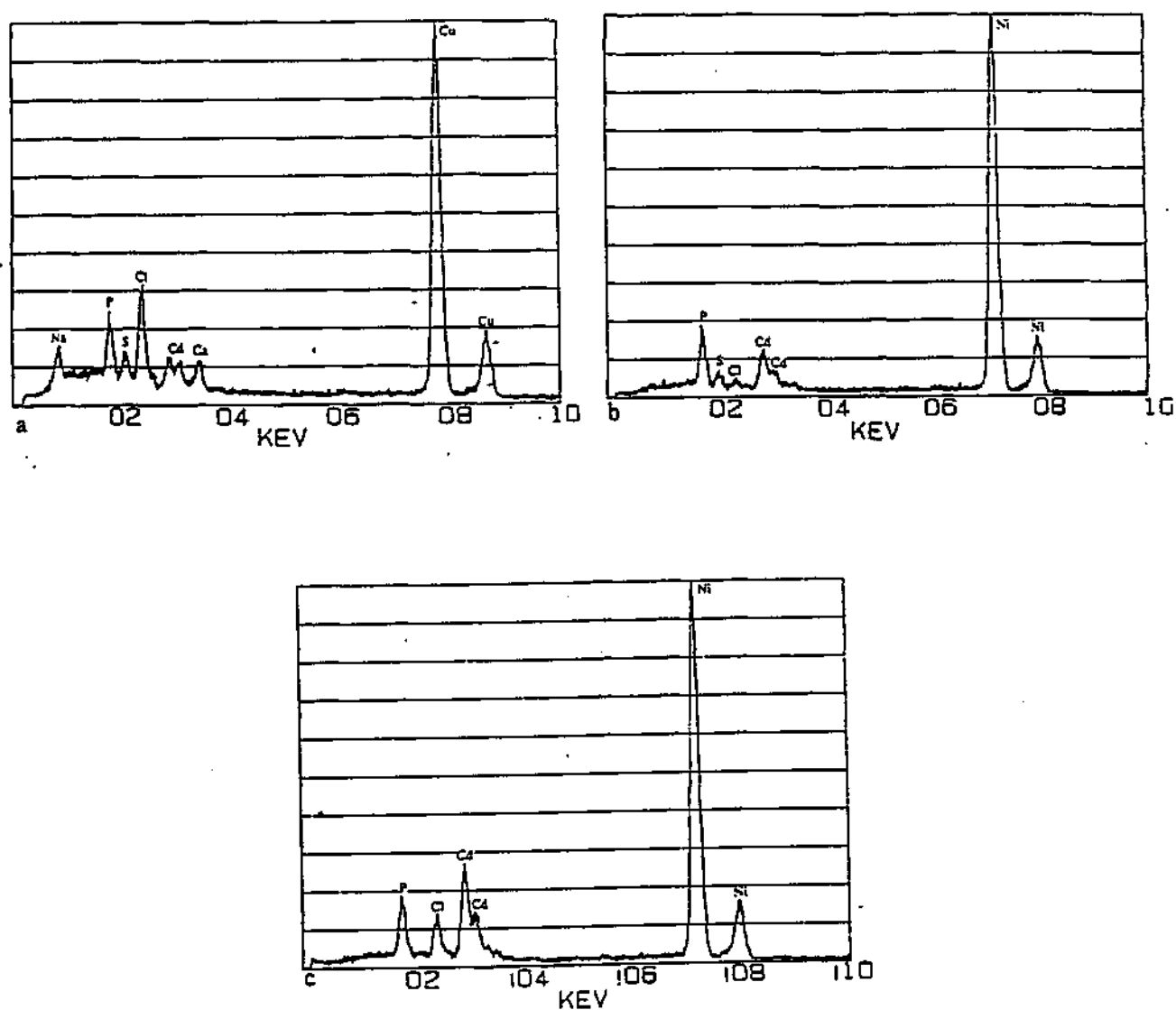


Fig 4.9. Intracellular ion composition of yeast cells exposed to a  $\text{Cd}^{2+}$ -containing solution after a) 1, b) 12 and c) 24 h. Any  $\text{K}^+$  present in the sample would be masked by  $\text{Cd}^{2+}$  peaks. Cu and Ni grids were used. The disappearance of the physiological cations implies ion exchange.

#### 4. ACCUMULATION BY VIABLE CELLS

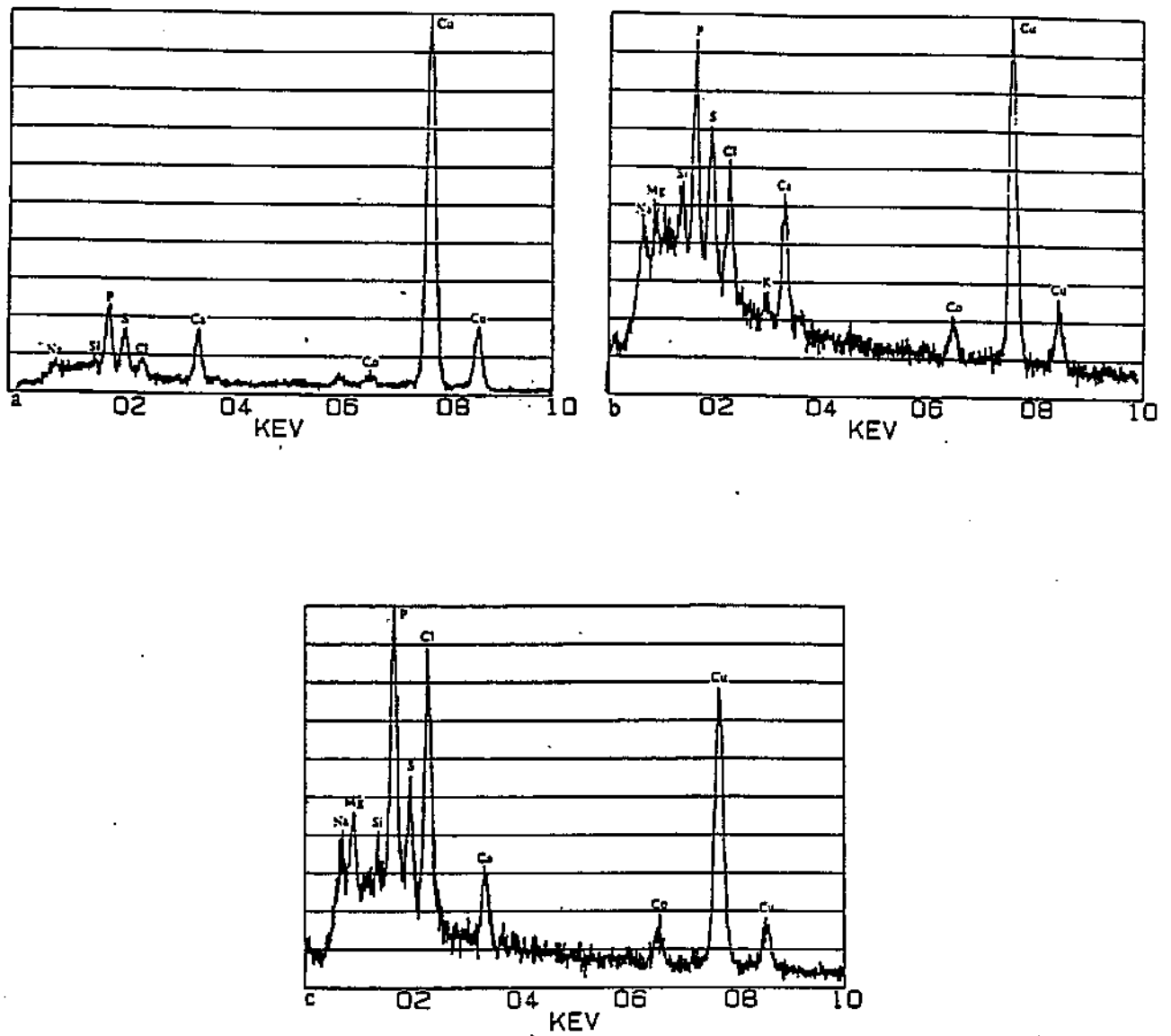


Fig 4.10. Intracellular ion composition of yeast cells exposed to a  $\text{Co}^{2+}$ -containing solution after a) 1, b) 12 and c) 24 h. Cu peaks originate from the grids used in the experiment.

#### 4. ACCUMULATION BY VIABLE CELLS

These spectra suggested a varied cellular response dictated by the heavy metal ions. The response elicited by  $\text{Cu}^{2+}$  (Fig 4.8) was similar to that of  $\text{Cd}^{2+}$  (Fig 4.9), whilst in the presence of  $\text{Co}^{2+}$  the cell responded differently (Fig 4.10). Though  $\text{Cu}^{2+}$  and  $\text{Cd}^{2+}$  elicited similar cellular responses, the pattern of accumulation of these two elements by the cells differed. At the onset of exposure of the yeast cells to  $\text{Cu}^{2+}$  initial, rapid accumulation of the metal by the cells appeared to occur with the intensity of the  $\text{Cu}^{2+}$  peaks in the EDAX spectra not increasing after 1 hr (Fig 4.8). In contrast,  $\text{Cd}^{2+}$  accumulation occurred gradually, with the intensities of these peaks becoming more prominent with time (Fig 4.9).  $\text{Co}^{2+}$  accumulation also occurred gradually, though saturation appeared to occur at an earlier stage than for  $\text{Cd}^{2+}$  (Fig 4.10).

Over time, exposure to, and accumulation of  $\text{Cu}^{2+}$  and  $\text{Cd}^{2+}$  by yeast cells resulted in the decline of intracellular metals. Not all the cellular cations were affected to the same extent, the decline in the amount of  $\text{Na}^+$ ,  $\text{Mg}^{2+}$  and  $\text{K}^+$  occurred in preference to that of  $\text{Ca}^{2+}$ , suggesting selective ion exchange or alternatively high levels of intracellular  $\text{Ca}^{2+}$ . The onset of the decline of these cations occurred rapidly. After 1 hr, analysis of  $\text{Cu}^{2+}$  and  $\text{Cd}^{2+}$  loaded cells failed to detect any physiological cations remaining within the cells. In contrast,  $\text{Co}^{2+}$  interaction with yeast cells failed to trigger an ion-exchange based decline in physiological cations, and after 24 hrs, detectable amounts of  $\text{K}^+$ ,  $\text{Na}^+$  and  $\text{Mg}^{2+}$  remained within the cells. A similar phenomenon was noted by Okorokov (153) who found that  $\text{Co}^{2+}$  translocation into yeast cells did not result in any  $\text{K}^+$  efflux from the cells.

##### 4.3.3. THE EFFECT OF METALS ON MEMBRANE INTEGRITY

Membrane integrity of metal exposed cells was established using a diacyl derivative of fluorescein, FDA. FDA only fluoresces after uptake into the cells and subsequent decomposition to fluorescein by cellular hydrolases. The decomposition of FDA within the cells occurs within a few minutes and the resultant fluorescein shows very small permeability across the cell plasma membrane and is thus contained within the cell (172). The presence of fluorescein outside the cell thus indicates loss of plasma membrane integrity.

Extracellular fluorescence of metal treated cells (Fig 4.11) implicated  $\text{Cd}^{2+}$  as a predominant membrane disrupting agent. The effect of  $\text{Cu}^{2+}$  and  $\text{Co}^{2+}$  on membrane permeability appeared to be similar, and was less severe than that of  $\text{Cd}^{2+}$ . (Final fluorescence values were determined taking

#### 4. ACCUMULATION BY VIABLE CELLS

the values obtained from the control cells (no metal ions present) into account) The  $\text{Cu}^{2+}$  and  $\text{Co}^{2+}$  induced fluorescence intensities of the supernatants comprised 56% and 60% respectively of that induced by  $\text{Cd}^{2+}$ . Corresponding quantitative metal determination revealed that marginally less  $\text{Cd}^{2+}$  was accumulated by yeast cells than  $\text{Co}^{2+}$  or  $\text{Cu}^{2+}$  ( $2.76 \mu\text{mol Cd}^{2+}/\text{g yeast}$ , compared to  $2.94 \mu\text{mol Cu}^{2+}/\text{g yeast}$  and  $2.96 \mu\text{mol Co}^{2+}/\text{g yeast}$ ).

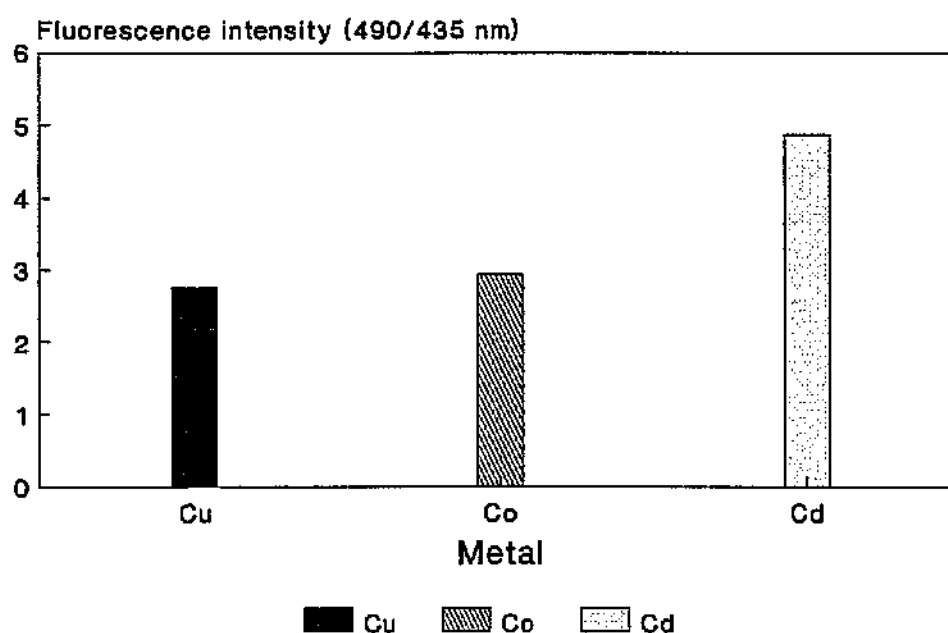


Fig 4.11. Fluorescence determination of the supernatant of  $\text{Cu}^{2+}$ ,  $\text{Cd}^{2+}$  and  $\text{Co}^{2+}$  exposed cells as an indicator of the effect of metals on plasma membrane integrity of yeast cells.

#### 4.4. DISCUSSION

While numerous other authors have provided evidence regarding internalization and compartmentalization of heavy metal cations, the benefits of using X-ray diffractive analysis (EDAX

#### 4. ACCUMULATION BY VIABLE CELLS

spectra) for this purpose include the ease with which metal ion deposition and the subsequent cellular response can be monitored over time.

Distribution of metal cations within yeast cells occurs between the soluble and insoluble fractions. Assymetrical distribution of metal ions occurs with metal ions generally having a greater preference for the insoluble fraction than the soluble fraction. Work done on *S. cerevisiae* and *K. marxianus* (82) proved accumulation of  $\text{Cu}^{2+}$ ,  $\text{Cd}^{2+}$  and  $\text{Ag}^{3+}$  by the insoluble fraction to be the main mechanism of tolerance and accumulation, with 21%  $\text{Cd}^{2+}$ , 46%  $\text{Cu}^{2+}$  and 31%  $\text{Ag}^{3+}$  associated with the vacuole. Similar affinities for vacuolar deposition were exhibited by other ions. Perkins and Gadd (94) found that 35% of  $\text{Li}^{+}$  was accumulated in the vacuoles of *S. cerevisiae* cells. These organelles have also been shown to be the major Fe storage compartment in the yeast cell and the only compartment capable of greatly increasing its Fe content when subjected to high external levels of Fe (81).

The role played by the vacuole in  $\text{Cu}^{2+}$ ,  $\text{Cd}^{2+}$  and  $\text{Co}^{2+}$  sequestration was emphasized during the present study. Vacuolar ion deposition occurred at an early stage, often prior to the detection in the cytosol (Table 4.1). After 1 h the amounts of  $\text{Co}^{2+}$  and  $\text{Cd}^{2+}$  deposited within the vacuole exceeded 1% of its composition, yet this was inadequate for cellular detection. In contrast, rapid uptake and distribution of  $\text{Cu}^{2+}$  occurred with adequate amounts of  $\text{Cu}^{2+}$  being accumulated to enable cellular detection after 1 h.

White and Gadd (167) described an increase in vacuolar  $\text{Co}^{2+}$  accumulation in the presence of elevated levels of external  $\text{Co}^{2+}$ . In comparison vacuolar accumulation of  $\text{Cu}^{2+}$  and  $\text{Cd}^{2+}$  under identical conditions was far less marked, instead a significant increase in accumulation by the soluble fraction was noted. Similar to the darkened deposits observed during the present study (Fig 4.5),  $\text{Cd}^{2+}$  was noted as dark deposits in the cytosol of bacterial cells on uptake in the presence of elevated external concentrations of this metal (174). The  $\text{Cd}^{2+}$  was shown to interact with phosphorous groups within the cytosol. Roomans (cited by 16), when using energy dispersive X-ray analysis, showed that  $\text{Mg}^{2+}$ ,  $\text{Sr}^{2+}$  and  $\text{Ca}^{2+}$  are also sequestered as phosphorous-rich cytoplasmic granules. Similarly EDAX spectra of the electron dense cytoplasmic inclusions in  $\text{Cu}^{2+}$ ,  $\text{Cd}^{2+}$  and  $\text{Co}^{2+}$  treated cells in the present study yielded conspicuous phosphorus peaks. Presumably phosphates are contained within these granules, though this does not necessarily contradict with the view of vacuolar polyphosphate concentration. However, the presence of cytosolic polyphosphates as an

#### 4. ACCUMULATION BY VIABLE CELLS

adaptive mechanism to excessive levels of heavy metals cannot be excluded (173).

An observation drawn from the present study was the inability of some cells to accumulate detectable levels of metal ions. Similar phenomena were noted by others during  $\text{Cd}^{2+}$  accumulation by *S. cerevisiae* (173) and  $\text{UO}_2^{2+}$  uptake by *Streptomyces* sp. (cited by 173), which suggests metabolic driven accumulation of metal ions.

Two distinct cellular responses were detected in response to metal accumulation. Uptake of  $\text{Cd}^{2+}$  and  $\text{Cu}^{2+}$  triggered the loss of the physiological cations:  $\text{K}^+$ ,  $\text{Na}^+$  and  $\text{Mg}^{2+}$  in a distinct ion-exchange process, whereas in the presence of  $\text{Co}^{2+}$  no release of intracellular ions (*ie.* ion-exchange) occurred.  $\text{Cu}^{2+}$  and  $\text{Cd}^{2+}$ -induced cellular cation loss have been reported on previous occasions (36, 39, 175 - 179).  $\text{Na}^+$ ,  $\text{K}^+$  and  $\text{Mg}^{2+}$  ions are distributed between the vacuole and the cytosol of yeast cells, with  $\text{Na}^+$  and  $\text{K}^+$  ions predominantly concentrated within the cytosol (73). The rapid loss of cellular  $\text{K}^+$  during this and other studies on  $\text{Cu}^{2+}$  and  $\text{Cd}^{2+}$  uptake (39, 105, 178, 180) may be enhanced by the effect of these metals on the permeability of the plasma cell membrane.  $\text{Co}^{2+}$  uptake is, however, not necessarily coupled to  $\text{K}^+$  loss (4, 175). Similar to the present study, Okorokov (153) and Norris and Kelly (4) observed no loss of  $\text{K}^+$  during  $\text{Co}^{2+}$  accumulation. No simple relationship exists between  $\text{Cu}^{2+}$  and  $\text{Cd}^{2+}$  uptake and the amounts of  $\text{K}^+$  released. Norris and Kelly (4) approximated the release of 4  $\text{K}^+$  ions for each  $\text{Cd}^{2+}$  ion accumulated, whereas Kessels, *et al* (36), observed the loss of 22  $\text{K}^+$  ions per  $\text{Cd}^{2+}$  ion accumulated. In addition, the release of  $\text{K}^+$  appears to be an integral component of intracellular  $\text{Cu}^{2+}$  accumulation. After  $\text{Cu}^{2+}$  treatment, approximately 30% of the total  $\text{K}^+$  remained within the cells (39). In addition  $\text{Cu}^{2+}$  and  $\text{Cd}^{2+}$  have been found to cause the loss of  $\text{Mg}^{2+}$  from yeast cells (4, 5).  $\text{Ca}^{2+}$  release from cells is least affected by  $\text{Cu}^{2+}$ ,  $\text{Cd}^{2+}$  and  $\text{Co}^{2+}$  (175).  $\text{Ca}^{2+}$  stores remained undepleted in  $\text{Cu}^{2+}$ ,  $\text{Co}^{2+}$  and  $\text{Cd}^{2+}$  exposed cells in the present study (Fig 4.8 - 4.10).

$\text{Cu}^{2+}$  and  $\text{Cd}^{2+}$ -induced cellular ion leakage from yeast cells can also occur as a result of selective permeabilization of the plasma cell membrane by the metals. In addition to  $\text{K}^+$ ,  $\text{Na}^+$  and  $\text{Mg}^{2+}$ , other studies have shown that low molecular weight substances inclusive of inorganic phosphate, 260 nm absorbing materials and ribose containing molecules are released from the cell (39, 177). The release of cellular ions is indicative of the loss of cell viability due to heavy metal toxicity. Cadmium toxicity is reported to be caused by structural lesions in the plasma membrane (35, 178, 180), thereby explaining the elevated fluorescence level noted in the supernatant of  $\text{Cd}^{2+}$  treated cells

in the present study.

#### 4.5. CONCLUSIONS

In conclusion, the present study has investigated the uptake of  $\text{Cu}^{2+}$ ,  $\text{Cd}^{2+}$  and  $\text{Co}^{2+}$  into yeast cells, their subsequent cellular deposition and the response elicited by viable yeast cells. The accumulation of the above-mentioned metals is metabolism-dependent with intracellular deposition primarily occurring in the vacuoles, although cytosolic deposition does occur. Accumulation of heavy metals within the cytosol often occurs as granular deposits. The uptake of heavy metal cations by viable yeast cells has been shown to elicit certain cellular responses.  $\text{Cu}^{2+}$  and  $\text{Cd}^{2+}$  accumulation results in the loss of the physiological cations,  $\text{Na}^+$ ,  $\text{K}^+$  and  $\text{Mg}^{2+}$ . In contrast,  $\text{Co}^{2+}$  has no such effect. Not all the physiological cations are affected, eg.  $\text{Ca}^{2+}$  stores within the yeast cell remain undepleted. Loss of these intracellular cations most likely occurs via an ion-exchange mechanism as all three heavy metals induce plasma cell membrane permeabilization.

Further investigations in this study were aimed at using yeast cells as a biomass for heavy metal accumulation from waste water.



## 5. BIOACCUMULATION OF HEAVY METALS FROM WASTE WATER BY VIABLE *S. cerevisiae* CELLS

### 5.1. INTRODUCTION

The bioaccumulation of heavy metals has received a great deal of attention in recent years, not only as a scientific novelty, but also for its application potential in industry. It is necessary to differentiate between the process of bioaccumulation and biosorption. Although Gadd and White (98) refer to the latter as the uptake of metals by viable or non-viable biomass via various mechanisms, biosorption remains the physico-chemical property of non-viable biomass to retain and concentrate metallic elements from solution via non-energy dependent processes. In comparison, the bioaccumulation of metal by viable microorganisms occurs by a number of processes, such as intracellular uptake by transport, adsorption to cell walls and entrapment in extracellular capsules, precipitation and biotransformation reactions. Both of these processes can be used in the bioremediation of metal containing water.

One of the most ubiquitous biomass types available on a large scale is *S. cerevisiae*. Depending on the manner of propagation, the yeast strains are either referred to as "bakers yeast" (aerobic propagation) or "brewers yeast" (anaerobic propagation). Although this biomass has previously been referred to as a mediocre biosorbent (138) its ready availability and low cost in certain countries make it a favourable choice of biosorbent in these cases. Furthermore, yeast cells retain their ability to accumulate a broad range of heavy metals to varying degrees, under a wide range of external conditions (181). For example, *S. cerevisiae* has been shown to accumulate Ag (4.7 mg/g), Cd (11 - 40 mg/g), Co (4.7 mg/g) (181), Cu (6 - 40 mg/g) (181, 182), U (55 - 140 mg/g) (182), Th (70 mg/g) and Zn (14 - 40 mg/g) (138, 182). Earlier investigations in this study also showed that *S. cerevisiae* was capable of accumulating Cd, Cu and Co.

Obviously the bioavailability and subsequent amounts of the respective metals accumulated are not fixed, but remain as variables, moderated by various factors, such as the chemical and physical properties of the metals (165), cellular physiology (15) and the ambient conditions (181, 183, 184). Inclusive in the range of chemical parameters which influence the uptake of metals are ionic radius, ionic charge, preference for coordination with certain ligands, solubility and subsequent availability

of the metal ions (165).

Metal accumulation is susceptible to both incubation temperature and ambient pH (15, 181, 184). The extent to which temperature affects the uptake depends on the species of metal in question. Brady *et al.* (181), reported minimal temperature related effects on the bioaccumulation of  $\text{Cu}^{2+}$  over a temperature range of 5 - 40°C, although maximum accumulation occurred between 25 - 30°C. Accumulation of uranium by *S. cerevisiae* is highest at 40°C. In comparison, the susceptibility of *S. cerevisiae* to  $\text{Cd}^{2+}$  is greatly enhanced by elevating the incubation temperature from 25°C to 37°C. An elevated incubation temperature also enhances the susceptibility of yeast to  $\text{Hg}^{2+}$ , although the effect is less pronounced (184). Accumulation processes that depend on cellular metabolism such as the second phase of the uptake procedure are those most likely to be affected by variances in temperature. Active uptake is most likely to be inhibited at low temperatures, whereas elevated temperatures increase the fluidity of the lipids in membranes and subsequently affect the membrane integrity.

Transport of cations into yeast cells is influenced by both the intracellular and extracellular pH (15). The alteration of ambient pH over a wide range does not measurably alter the intracellular pH suggesting that the peripherally located binding sites are influenced to a greater extent by the variability of the extracellular pH than the constancy of the intracellular pH (40, 135). Ambient pH is a major factor affecting the amount of metal accumulated owing to the competition between metal cations and  $\text{H}^+$  ions for uptake. In general, low external pH reduces both the surface binding and the intracellular influx of ions (135). The biological availability of metals is also determined by the charge. Shifts in pH affect metal bioaccumulation by changing the metal speciation. A low pH increases metal solubility and mobility whilst at neutral or high pH, insoluble oxides and hydroxides tend to form. The optimal pH for metal accumulation remains species specific, eg. maximum  $\text{Cu}^{2+}$  accumulation by yeast occurs between pH 5.0 - 9.0, with rapid decreases in accumulation at either extreme of the pH range (181). Uptake of  $\text{Ni}^{2+}$  increases with increasing pH up to pH 5.0, while the maximal uptake rate for  $\text{Ca}^{2+}$  occurs at pH 7.0 and is reduced by 85% at pH 4.5 (15). Jones and Gadd (145) found that the uptake of divalent ions by *S. cerevisiae* is significantly reduced below pH 5.0.

The metabolism-dependant uptake of metal ions can be influenced by the presence of competing metal cations, or even inhibited by glucose analogues or lack of glucose. The uptake of  $\text{Ni}^{2+}$ ,  $\text{Co}^{2+}$

## 5. HEAVY METAL BIOACCUMULATION

and  $\text{Zn}^{2+}$  is low in starved *S. carlsbergensis* cells, yet the addition of, or pretreatment with glucose results in a 5 - 20 fold increase in the amount of metal accumulated (25). Contrasting results presented by Brady *et al.* (181), report no enhanced accumulation of  $\text{Cu}^{2+}$ ,  $\text{Cd}^{2+}$  and  $\text{Co}^{2+}$  by *S. cerevisiae* cells in the presence of glucose. The difference could, however, reflect the growth phase of the cells. Non-energy dependent accumulation may occur in stationary phase cells, whilst developing cells in log phase may require an additional energy source.

In yeast an energy-dependent influx of heavy metal cations has been demonstrated with an affinity series of  $\text{Mg}^{2+} > \text{Co}^{2+} > \text{Zn}^{2+} > \text{Mn}^{2+} > \text{Ni}^{2+} > \text{Ca}^{2+} > \text{Sr}^{2+}$  (25). The selectivity of heavy metal accumulation can be further influenced by the presence of competing monovalent or divalent metal cations. Monovalent cations eg.  $\text{K}^+$  may antagonize the uptake of divalent cations such as  $\text{Ca}^{2+}$  or  $\text{Mg}^{2+}$  and *visa versa* (15). Mutual interactions occur between divalent cations. In the presence of specific metal cations, uptake of other divalent cations may be enhanced. For example, the uptake of  $\text{Zn}^{2+}$  is increased specifically by  $\text{Cu}^{2+}$ , whereas the uptake of  $\text{Mn}^{2+}$  remains unaffected (16). Similarly  $\text{Co}^{2+}$  enhances  $\text{Zn}^{2+}$  uptake, with the reciprocal also being true (25). In comparison  $\text{Ca}^{2+}$  inhibits  $\text{Zn}^{2+}$ ,  $\text{Co}^{2+}$  (25) and  $\text{Cd}^{2+}$  uptake (4). The presence of  $\text{Mg}^{2+}$  results in a minimal reduction of  $\text{Cd}^{2+}$  accumulation. The inhibition of metal cation influx by other metal has been reported to be related to the ionic radii (4), though this is based on the assumption that a general mechanism for uptake of divalent cations exists (16, 25). In general, a mixture of heavy metals can produce three possible types of behaviour: synergism, antagonism or non-interaction, where the effects produced are either greater than, less than or the same as the individual effects of the constituents in the mixture (185).

A relationship exists between metal uptake and the ambient metal concentration.  $\text{Cu}^{2+}$  accumulation by yeast has proven to be dependent on the ratio of external free metal concentration to the available biomass (181). Similar effects have been noted for the accumulation of  $\text{UO}_2^{2+}$ , where accumulation was dependent on uranyl ion concentration. The movement of  $\text{Hg}^{2+}$  into yeast cells is also a function of the external  $\text{Hg}^{2+}$  concentration (186).

A central aim of this study has been to forge a link between academic interest and industrial applicability. While earlier chapters in this report have focussed on more academic aspects of metal accumulation such as mechanisms of metal uptake and sites of deposition, the object of the study reported in this chapter was to examine the effectiveness of *S. cerevisiae* biomass to accumulate

## **5. HEAVY METAL BIOACCUMULATION**

metals from waste water. Although metal uptake in viable yeast cells have been studied on previous occasions, this study investigates the bioaccumulation of metal ions from multi-metal solutions in which the aqueous phase differed from those used previously. Instead of using a spiked metal containing solution, waste water was obtained from industrial electroplating plants. This waste water was obtained from three different plants (effluents A, B and C), each differing in metal species and content. The capacity of native bakers yeast cells for metal ion removal from these solutions was determined and the effect of glucose and external pH on this uptake monitored.

### **5.2. METHODS AND MATERIALS**

#### **5.2.1. METAL EQUILIBRATION**

Similar to the method of Tsezos (187), Kuyucak and Volesky (150) and others, the yeast biomass was brought into direct contact with the effluent in batch reactors. Washed viable yeast cells were mixed with the respective effluents (A, B or C) at known concentrations (0.1 g (wet wt)/ml). Equilibration of the yeast-effluent solutions proceeded for 25 h at 25°C with gentle shaking. At 1, 5, and subsequent 5 hourly intervals, 20 ml fractions were removed, centrifuged (3000 g x 10 min) and the supernatant analysed to determine the residual metal concentration (Varian 1275 Atomic Absorption Spectrophotometer). In the absence of yeast, loss of metal due to metal-glass interactions was ascertained from control fractions. The external pH was monitored throughout the duration of the experiment.

#### **5.2.2. OPTIMIZATION STUDIES**

##### **5.2.2.1. BIOMASS RATIO DETERMINATION**

Due to the number of contaminating metal elements therein and the severity of the Cd problem (extremely high levels) all further optimization studies were performed using effluent A. Additional trials were conducted to determine the optimum yeast : metal ratio for metal accumulation. Yeast was suspended in effluent in 0.1, 0.25, 0.5, and 1.0 g/ml (wet wt) ratios, shaken for 15 h (completion of yeast metal equilibration) at 25°C, and the efficiency of metal ion removal determined. The 0.5 g/ml ratio of yeast : waste water attained good metal removal and was used in all subsequent experiments for this section.

**5.2.2.2. GLUCOSE SUPPLEMENTATION**

The effect of an energy source on the efficiency of metal removal was ascertained. The importance of glucose as an energy source was determined by comparing the metal removal by glucose-treated cells to that of untreated cells. In addition, the effect of pretreating the cells with glucose was compared to direct supplementation of glucose to the yeast-effluent solutions.

Suspended yeast cells (0.5 g/ml H<sub>2</sub>O) were pretreated with glucose following the method of Perkins and Gadd (42). Glucose was added to the yeast suspension to a final concentration of 50 mM, 30 min prior to effluent addition. After 30 min the suspension was centrifuged and the pelleted yeast cells washed. The pelleted yeast cells were resuspended in Effluent A (0.5 g/ml) and the metal removal procedure commenced.

The effect of direct glucose addition over time was monitored through the supplementation of the yeast-effluent solution with glucose at 0, 5 and 10 hourly intervals and metal accumulation determined after 15 h. Glucose was added to obtain a final concentration in solution of 50 mM.

**5.2.3. BIOACCUMULATION FROM WASTE WATER USING BATCH REACTIONS**

Multiple metal containing effluents (A, B and C) collected from electroplating factories were treated using batch reaction systems. The percentage metal removed from each of the effluents during 15 h continuous batch systems were compared to those of 3 x 5 h batch reaction systems run in series. The latter involved suspending yeast in effluent (0.5 g/ml) for 5 h at 25°C with gentle shaking. After 5 h the suspensions were spun down (4000 g x 10 min) and the supernatant added to fresh yeast. On completion of incubation (after 15 h) both continuous and series batch systems were spun down and the percentage metal removed, determined.

Identical experiments were conducted using glucose pretreated cells. Optimal pH conditions were also introduced into some of the reactions. The pH of effluents A, B and C varied, viz. pH 6.0, 3.6 and 2.2, respectively. Using NaOH the pH of B was altered to pH 5.0 (precipitation occurred at higher pH values) and that of C from pH 2.2 to pH 6.0. As for previous experiments, the pH was monitored for the duration of incubation.

## 5. HEAVY METAL BIOACCUMULATION

Comparative bioaccumulative analysis was undertaken using a spiked metal solution containing multiple metals in solution. Metal uptake from a stock solution containing 50 mg/l of Zn, Cr, Cu, Cd and Ni was compared to that from industrial effluent. Experimental parameters remained identical to those used previously.

### 5.3. RESULTS

The electroplating effluents used during this study were obtained from three different metal plating factories. All contained metals ions in excess of the stipulated criteria for both drinking and river water (Table 5.1).

Table 5.1. Heavy metal profiles for electroplating effluents A, B and C. Metal levels of the effluents are compared to suggested median levels for drinking and dam/river water. The levels are expressed as mg/l.

	Metal Concentration (mg/l)				
	Drinking water	Dam/river water	A	B	C
Cd	0.01	0.003	16.0	< 0.05	< 0.05
Cr	0.05	0.05	< 0.05	71	4
Cu	1.00	0.005	0.1	0.5	30
Ni	0.05	0.05	0.1	< 0.05	15.6
Zn	5.00	0.1	260	460	0.3

With the exception of  $Zn^{2+}$  removal from effluent A and C, the majority of metal ions were taken up during the initial stages of equilibration (Fig 5.1 - 5.3). The rate of accumulation ( $\mu\text{g/g/hr}$ ) of metals decreased over time with the onset of biomass saturation. Complete biomass saturation was assumed to have occurred after 15 h. No adjustments were made to the pH of the yeast-effluent solutions prior to equilibrium, yet in the presence of yeast cells the external pH was regulated and preferentially maintained between pH 4.0 - 5.0. The greatest change in the external pH of effluent

## 5. HEAVY METAL BIOACCUMULATION

A and B occurred within the first hour (Fig 5.1 and 5.2). After 25 hrs pH values within the same range were recorded for effluents A and B, viz. pH 5.01 and pH 5.33, respectively. The initial pH of the yeast-effluent solution for C was lower than that of A and B (viz. pH 2.01). During equilibration an active cellular response to this acidic environment was maintained, resulting in an increase in the alkalinity of the solution to a final pH of 3.81. In the absence of metal ions the pH of the solutions of yeast cells suspended in Milli-Q water gradually increased over time.

Pretreatment of the yeast cells with glucose enhanced heavy metal ion uptake from effluent A (low amounts of  $\text{Cu}^{2+}$  and  $\text{Ni}^{2+}$  were present in this effluent, hence the graphic representation was limited to  $\text{Cd}^{2+}$  and  $\text{Zn}^{2+}$  accumulation) (Fig 5.4). In contrast to pretreatment, direct addition of glucose to the yeast-effluent A suspension did not stimulate metal removal, when compared to the control (no glucose addition). Glucose was supplemented directly to respective yeast-effluent solutions at 0, 5 and 10 hrs. The lack of response to the treatment suggests an inability of the cells to utilize glucose in the presence of metal ions.

The effect of time, glucose pretreatment and pH modification on the metal removed from the three effluents can be compared in Fig 5.5 - 5.7. Under these conditions, increased metal accumulation was recorded from multiple shorter incubation periods in series. Metal accumulation is an energy dependent process. Glucose pretreatment had a greater effect on bioaccumulation than an increase in the external pH. The combined treatment (*ie.* glucose pretreatment and pH modification) was marginally less effective regarding metal uptake than glucose treatments. (Note: pH treatment was not required for effluent A due to an influent pH 6.0) Though a trend can be established regarding the metal bioaccumulation, due to the variation in the initial concentrations of metals present in the respective effluents, it is difficult for a quantitative comparison to be drawn regarding the amount of metal accumulated.

## 5. HEAVY METAL BIOACCUMULATION

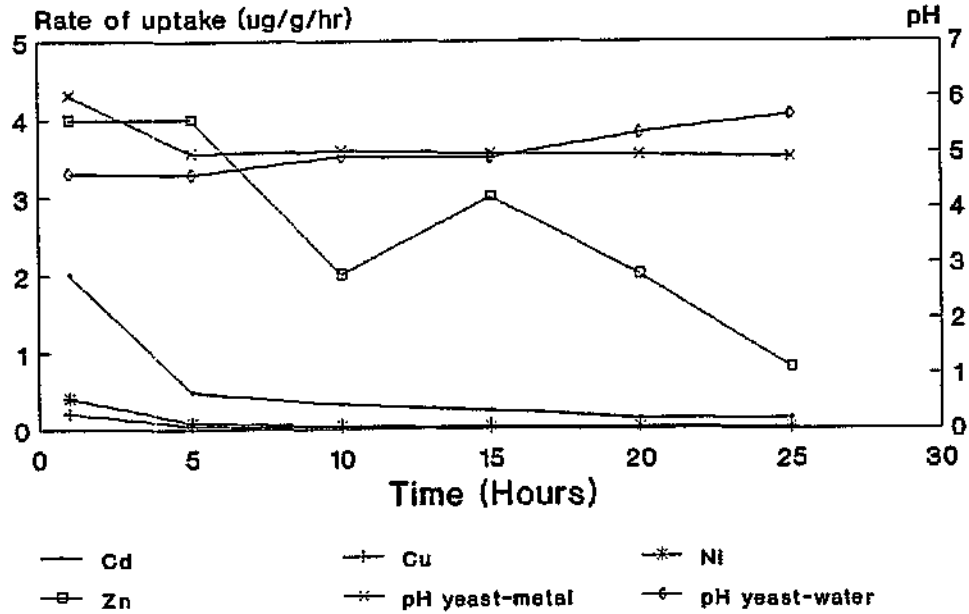


Figure 5.1. The rate of bioaccumulation of metal ions from effluent A over time ( $\mu\text{g/g biomass/h}$ ) by viable yeast cells. The change in pH of yeast-metal solutions can be compared to that of a yeast-water solution over the same period of time.

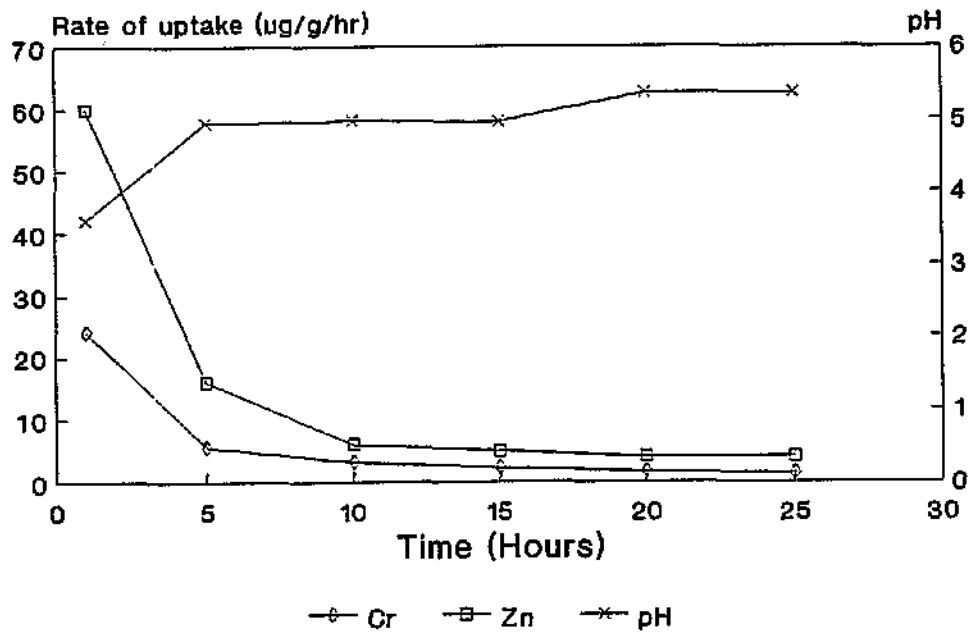


Figure 5.2. The rate of bioaccumulation of metal ions from effluent B over time ( $\mu\text{g/g biomass/h}$ ) by viable yeast cells. The effect of time and metal bioaccumulation on the external pH was monitored.



### 5. HEAVY METAL BIOACCUMULATION

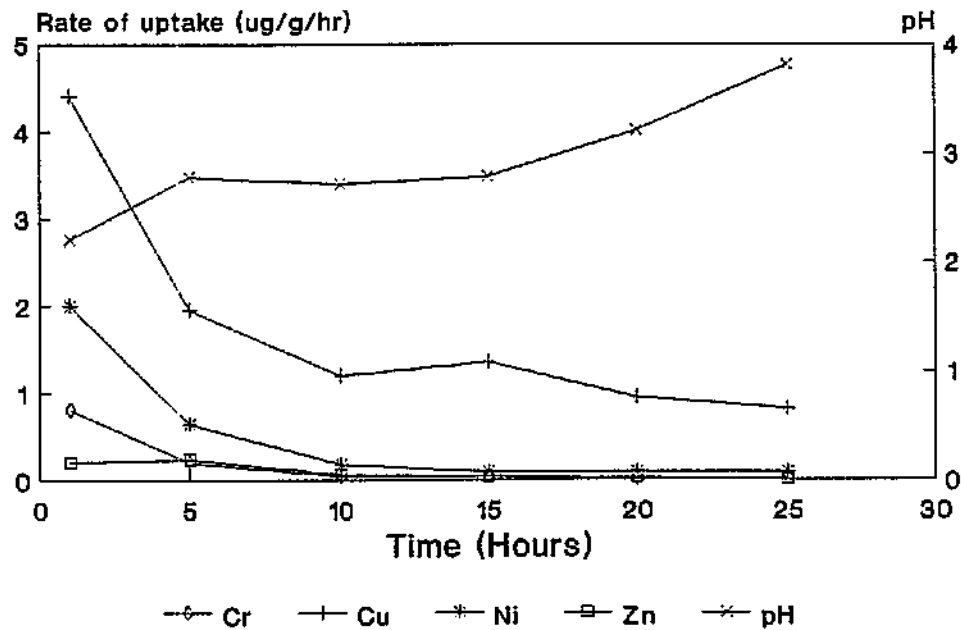


Figure 5.3. The rate of accumulation of metal ions from effluent C over time ( $\mu\text{g/g biomass/h}$ ) by viable yeast cells. The effect of time and metal bioaccumulation on the external pH was monitored.

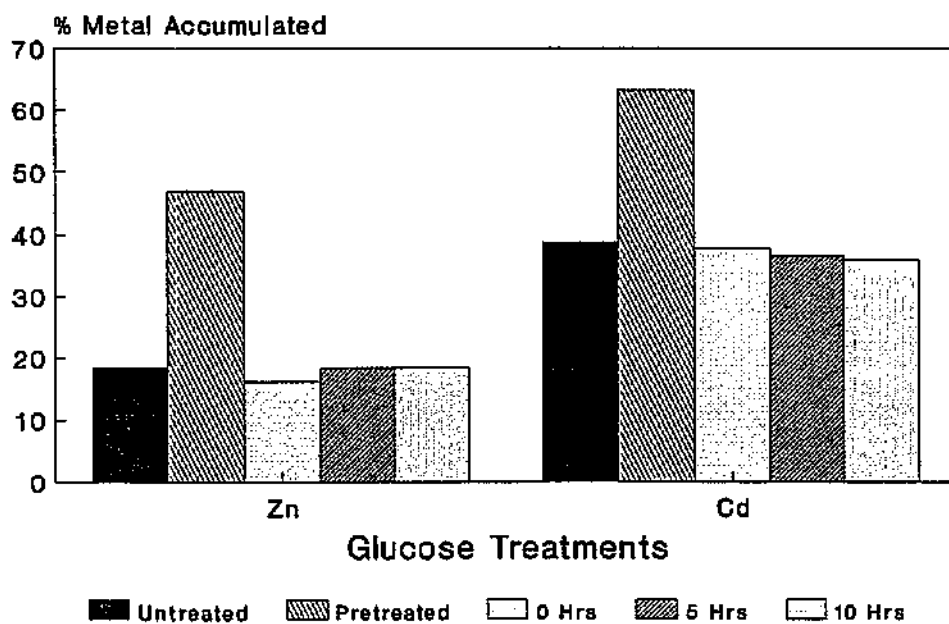


Figure 5.4. The effect of a metabolizable energy source on the uptake of  $\text{Zn}^{2+}$  and  $\text{Cd}^{2+}$  from effluent A by viable yeast cells. Glucose treatment involved either a 30 min pretreatment period or direct addition of glucose at 0, 5 and 10 h respectively.

## 5. HEAVY METAL BIOACCUMULATION

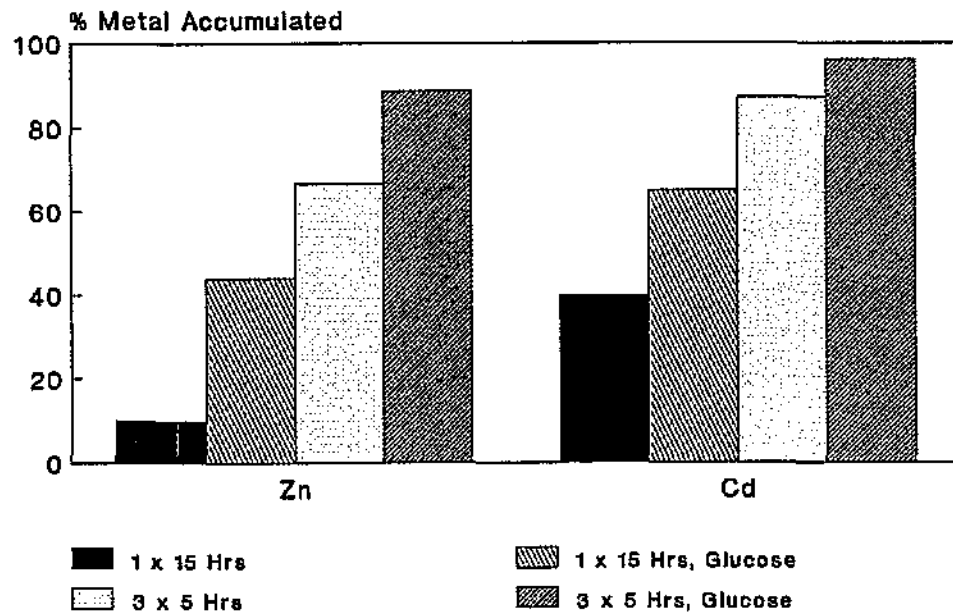


Figure 5.5. Percentage metal removed from effluent A by treated and untreated viable yeast cells in batch systems. The effect of an extended period of incubation on metal removal, was compared to multiple shorter periods of incubation. Stipulation of glucose, pH or both in the legend (Fig 5.5 - 5.7) indicates the effect of the respective treatment on metal removal.

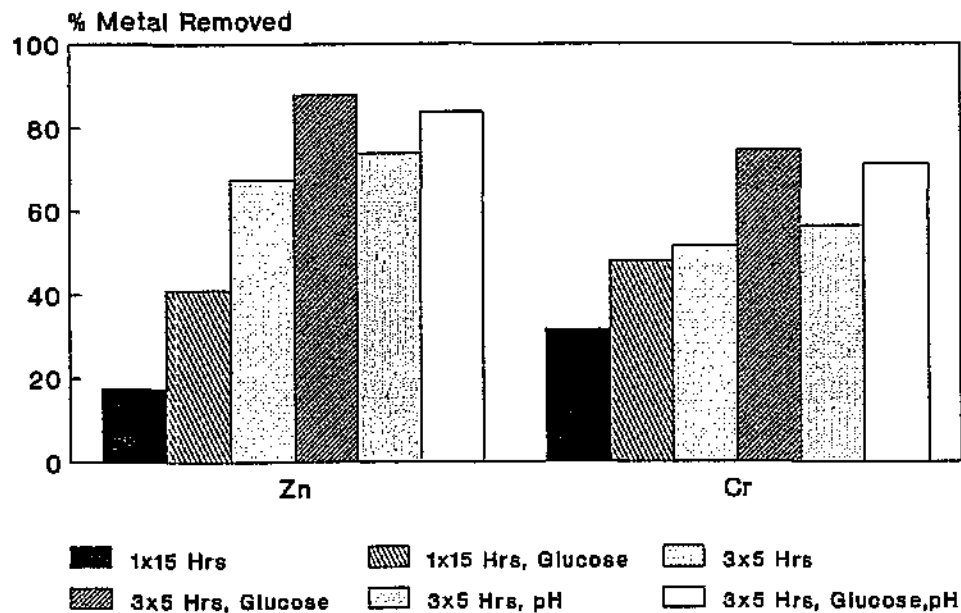


Figure 5.6. Percentage metal removed from effluent B by treated and untreated viable yeast cells in batch systems. The effect of time, pH modification and glucose treatment was observed.

## 5. HEAVY METAL BIOACCUMULATION

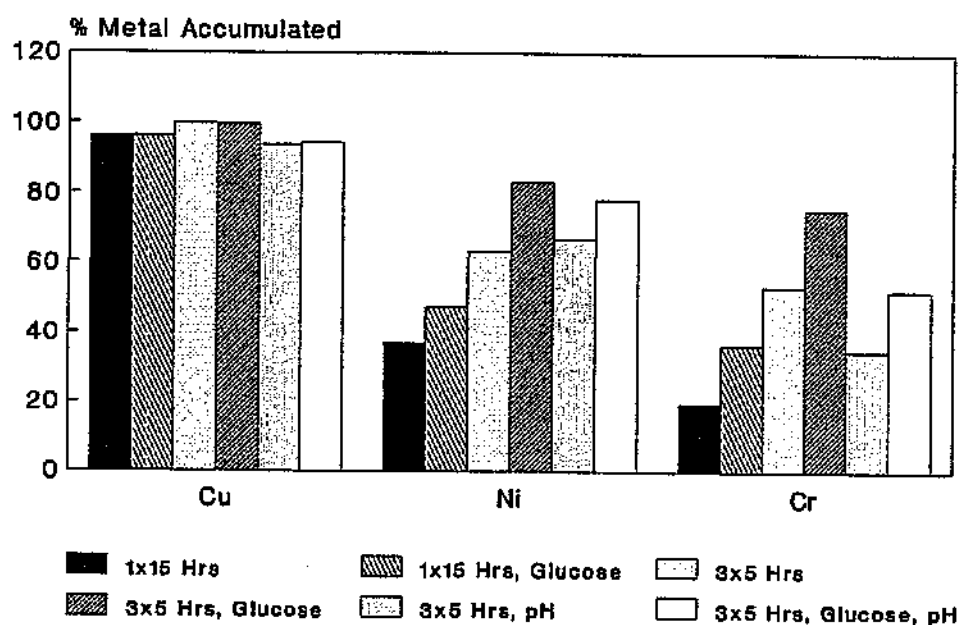


Figure 5.7. Percentage metal removed from effluent C by treated and untreated viable yeast cells in batch systems. The effect of time, pH modification and glucose pretreatment was monitored.

The amount of metal accumulated by the yeast cells from the respective electroplating effluents was quantified (Table 5.2) and this was compared to the results obtained for metal uptake from a spiked multi-element solution (Table 5.3).

## 5. HEAVY METAL BIOACCUMULATION

Table 5.2. Metal accumulation ( $\mu\text{g}$  metal/g (wet mass)) by yeast from electroplating effluents: A, B and C. The effect of time, pH modification and glucose pretreatment on metal uptake is compared. The effect of the respective treatments are indicated as h, glucose, pH or a combination of the three.

	Effluent A		Effluent B		Effluent C		
	Zn ( $\mu\text{g/g}$ )	Cd ( $\mu\text{g/g}$ )	Zn ( $\mu\text{g/g}$ )	Cr ( $\mu\text{g/g}$ )	Ni ( $\mu\text{g/g}$ )	Cr ( $\mu\text{g/g}$ )	Cu ( $\mu\text{g/g}$ )
1 x 15 h	90	12.2	160	45	11.6	1.5	56.4
1 x 15 h, glucose	230	19.9	380	68	14.8	2.8	56.6
3 x 5 h	360	27.1	620	73	19.8	4.1	58.6
3 x 5 h, glucose	480	29.9	810	106	26	5.8	58.5
3 x 5 h, pH			680	80	20.8	2.7	55.5
3 x 5 h, glucose, pH			770	101	24.4	4.0	55.4

Table 5.3. Metal accumulation ( $\mu\text{g}$  metal/g (wet mass) yeast) from a spiked solution containing  $\text{Cu}^{2+}$ ,  $\text{Cd}^{2+}$ ,  $\text{Cr}^{3+}$ ,  $\text{Zn}^{2+}$  and  $\text{Ni}^{2+}$  in 50 mg/l concentrations. The initial pH (pH 1.1) was adjusted to pH 4.5 except during the first experiment. The effect of time pH modification and glucose pretreatment on metal uptake is compared. The effect of the respective treatments are indicated as h, glucose, pH or a combination of the three.

	Cd ( $\mu\text{g/g}$ )	Cr ( $\mu\text{g/g}$ )	Cu ( $\mu\text{g/g}$ )	Ni ( $\mu\text{g/g}$ )	Zn ( $\mu\text{g/g}$ )
1 x 15 h	25.6	8.7	45.7	22.8	9.0
1 x 15 h, pH	57.4	13.6	76.8	38.4	42.4
1 x 15 h, glucose, pH	60.4	31.0	83.3	45.2	48.0
3 x 5 h, pH	72.8	29.0	87.6	59.8	72.0
3 x 5 h, glucose, pH	76.6	42.0	88.0	59.8	74.0

An apparent uptake series ( $\mu\text{g/g}$ ) of  $\text{Cu}^{2+} > \text{Cd}^{2+} > \text{Zn}^{2+} > \text{Ni}^{2+} > \text{Cr}^{3+}$  by the yeast biomass was established. The amount of metal accumulated from the 50 mg/l spiked solution was not indicative of yeast saturation. For example, 74  $\mu\text{g/g}$  of  $\text{Zn}^{2+}$  was accumulated from the spiked solution

## 5. HEAVY METAL BIOACCUMULATION

compared to the 770  $\mu\text{g/g}$  removed from effluent B under similar conditions. Similarly 88  $\mu\text{g/g}$   $\text{Cu}^{2+}$  was accumulated from the spiked solution (Table 5.3) compared to 55.4  $\mu\text{g/g}$  from effluent C (Table 5.2). These results (Table 5.2 and 5.3) indicate the dependency of accumulation on the ratio of external free metal ions to the available biomass. The external metal concentration affects both the metal binding equilibrium and the concentration gradient across the cell membranes. The amount of bioaccumulation is subjected to change in response to variations in the external concentrations.

### 5.4. DISCUSSION

#### 5.4.1. EFFECT OF pH AND GLUCOSE TREATMENT ON METAL BIOACCUMULATION

The results obtained from the present study substantiate the reports that a low external pH reduces metal accumulation by viable yeast cells (10, 25, 38, 185, 189). This effect is particularly noticeable regarding the amount of metal accumulated from spiked laboratory solutions (Table 5.3). Adjustment of the pH from pH 1.1 to a more alkaline pH 4.5 resulted in a 124% increase of  $\text{Cd}^{2+}$  accumulation and an increase of 371% in  $\text{Zn}^{2+}$  accumulation.  $\text{Cu}^{2+}$ ,  $\text{Cr}^{3+}$  and  $\text{Ni}^{2+}$  uptake also increases in the presence of favourable pH conditions. The pH of a solution affects the chemical speciation of metals thereby regulating their biological availability. At pH 4.5 the majority of the metals exist in their ionic form facilitating enhanced accumulation (150). The uptake of divalent cations by *S. cerevisiae* has been found to be significantly reduced below pH 5.0 (145). Optimal pH ranges exist for the uptake of specific metals into microbial cells.  $\text{Ni}^{2+}$  uptake into *S. cerevisiae* increases with increasing medium pH until pH 5.0, and pH 4.0 in *N. crassa* (16, 135), whilst the greatest accumulation of  $\text{Mn}^{2+}$  occurs between pH 5.0 - 7.0 and  $\text{Ca}^{2+}$  until pH 8.0 (16). Maximum bioaccumulation is not only species specific, but also depends on the type of biomass, for example  $\text{Zn}^{2+}$  accumulation by *C. utilis* occurs at pH 4.8, but at pH 6.5 for *N. vasinfecta*.

Pretreatment of yeast cells with glucose resulted in elevated levels of metals being accumulated. Accumulation of  $\text{Zn}^{2+}$  from effluent A is increased by 2.5 times and that of  $\text{Cd}^{2+}$  by 1.6 times by pretreating the cells with glucose (Fig 5.4). These and other results confirm the energy dependent nature of divalent metal cation uptake into yeast cells, though direct addition of glucose to the suspension failed to result in an increased metal uptake, suggesting the inability of the yeast cells to internalize the glucose. In the presence of high metal ion concentrations, glucose may be unable to enter into the cells due to the utilization or inhibition of the glucose uptake system by metal ions.

## 5. HEAVY METAL BIOACCUMULATION

In some instances the direct addition of glucose to yeast-metal suspensions has however been able to stimulate metal accumulation, eg.  $\text{Mn}^{2+}$  (38) and  $\text{Ca}^{2+}$  (190). Substitution of glucose by analogues, fails to enhance metal accumulation, eg. in the presence of sorbose no elevated levels of  $\text{Mn}^{2+}$  were accumulated (38).

### 5.4.2. THE RELATIONSHIP BETWEEN BIOACCUMULATION AND AMBIENT METAL CONCENTRATION IN A MULTI-ION ENVIRONMENT

A relationship exists between intracellular metal ion accumulation and the ambient metal concentration (Table 5.2 and 5.3). For example, in the presence of excessive concentrations of  $\text{Zn}^{2+}$  (effluent B) greater amounts of  $\text{Zn}^{2+}$  were sequestered by the yeast biomass than from effluent A, which had a lower initial concentration of  $\text{Zn}^{2+}$ . Similarly, in the presence of low quantities of metals, eg.  $\text{Cr}^{3+}$ ,  $\text{Ni}^{2+}$  (effluent C) or  $\text{Cd}^{2+}$  (effluent A) less of that metal was accumulated by the yeast cells, suggesting that the amount of metal accumulated is partially determined by the ratio of free external metal concentration to the available cell biomass. This trait has been noted previously in *S. cerevisiae* cells (181), viz. the dependency of  $\text{UO}_2^{2+}$  uptake on ambient uranyl ion concentration. Moreover this type of bioaccumulation is not limited to *S. cerevisiae*, similar uptake patterns have been noted in other microorganisms, eg. the bacteria *S. longwoodensis* (123), *Pseudomonas sp* (191) and *C. vulgaris* (185).

The presence of multiple metal species in solution affects the quantity and pattern of uptake of a specific species of metal ion. The apparent affinity series of  $\text{Cu}^{2+} > \text{Cd}^{2+} > \text{Zn}^{2+} > \text{Ni}^{2+} > \text{Cr}^{3+}$  (Table 5.3) verifies the presence of mutual interactions between metal cations. Both bioaccumulation and biosorption (concept expanded upon in chapter 6) can be of a competitive nature. The bioaccumulation of specific metal ions is often inhibited in the presence of a second or third metal species. The inhibition may arise due to one or more metal species complexing with the same surface ligand, or alternatively utilizing the same uptake mechanism. The interaction of multiple metal species is not necessarily always inhibitory, the uptake of  $\text{Zn}^{2+}$  is increased by  $\text{Cu}^{2+}$ , whereas the uptake of  $\text{Mn}^{2+}$  remains unaffected (16). In the absence of added substrate,  $\text{Co}^{2+}$  enhances  $\text{Zn}^{2+}$  uptake and *visa versa*. Inhibition of metal ion uptake due to the influence of additional metal ions may vary in specificity.  $\text{Ca}^{2+}$  inhibits both  $\text{Zn}^{2+}$  and  $\text{Co}^{2+}$  uptake (25). Uptake of  $\text{Cd}^{2+}$  by *A. nodosum* from a Cd-Cu solution is sensitive to the presence of  $\text{Cu}^{2+}$ . An approximate 20% decrease in  $\text{Cd}^{2+}$  equilibrium uptake occurs due to the presence of  $\text{Cu}^{2+}$  yet the reverse is not true.  $\text{Cu}^{2+}$  and

## 5. HEAVY METAL BIOACCUMULATION

$\text{Zn}^{2+}$  each inhibit the uptake of the other by approximately 80% (110).  $\text{Cd}^{2+}$  and  $\text{Zn}^{2+}$  also have a similar effect on the uptake of each other. A decrease in excess of 20% is noted in the equilibrium sorption of both  $\text{Cd}^{2+}$  and  $\text{Zn}^{2+}$  (110). The decrease in  $\text{Cd}^{2+}$  accumulation is due to inhibition of its internalization by  $\text{Zn}^{2+}$  as previous reports state the absence of effect of  $\text{Zn}^{2+}$  on surface binding of  $\text{Cd}^{2+}$  ions (185). The extent of inhibition of uptake of a specific metal ion varies, depending on the type of metal present.  $\text{Co}^{2+}$  uptake in *S. cerevisiae* is inhibited in the decreasing order by  $\text{Ca}^{2+} > \text{Cd}^{2+} > \text{Mn}^{2+} > \text{Ni}^{2+} > \text{Zn}^{2+}$ , whilst a  $\text{Cd}^{2+}$  uptake inhibition series exists of  $\text{Ca}^{2+} > \text{Ni}^{2+} > \text{Mg}^{2+} > \text{Zn}^{2+} > \text{Mn}^{2+} > \text{Ca}^{2+}$  (4).

### 5.5. CONCLUSIONS

Viable yeast biomass has proven to be capable of accumulating heavy metal cations from aqueous solutions. This ability has many potential applications regarding the removal of metals from either simulated or metal containing waste water solutions. The mechanisms of accumulation and quantities of metal taken up are affected by the ratio of ambient metal concentration to biomass quantity, external pH and the presence of multiple elements in solution. Due to the energy dependent nature of bioaccumulation, the amount of metal sequestered by glucose-pretreated cells far exceeds that taken up by cells in the absence of an energy source. Direct addition of glucose to the biomass-metal environment, does not appear to have any effect on metal accumulation.

Due to the energy-dependent nature of bioaccumulation, the successful implementation of such a system in an industrial bioremediation process would be limited. As an alternative, the substitution of viable cells by non-viable cells may enhance the potential of such a process on a large scale and will consequently be dealt with in subsequent chapters (6 and 7).

## 6. BIOSORPTION OF HEAVY METAL CATIONS BY IMMOBILIZED NON-VIABLE YEAST BIOMASS

### 6.1. INTRODUCTION

Recent waste water bioremediation techniques for heavy metal removal have focussed on biosorptive mechanisms rather than bioaccumulation by microbial cells for the removal of metal cations from solution. Biosorption is a property of non-viable biomass to retain and/or concentrate metal ions from solutions via adsorption or a non-active absorption processes (138), and acts as a potential bioremediation tool which can be implemented using several types of microbial biomass (see chapter 1).

The advantages of non-viable microbial cells are numerous. Inactive biomass has the advantage of being independent of a supply of nutrients for cell growth and maintenance, nor does it involve any time loss due to culture propagation or contamination (97, 139). Moreover, all living cells are prone to the toxic effects of effluents, and in fact the concentration of metals in non-viable biomass often exceeds that of viable biomass due to the inactivation of the resistance mechanisms of the viable yeast cells (97,192). Killed cells can also be stored or used for extended periods of time at room temperature without the onset of putrefication (139).

The chemical composition of microbial cells, and particularly the cell wall or envelope largely determines the biosorbent property of non-viable microbial cells (107, 192). The cell walls and envelopes of microbial biomass are mainly composed of polysaccharides, proteins and lipids and offer abundant ligands for metal interaction, eg. carboxylate, hydroxyl, sulphhydryl, phosphate and amino groups, which differ in their affinity and specificity for metal ions (185). Surface biosorption, a physico-chemical phenomenon based on ion-exchange, coordination, complexation, chelation, adsorption and microprecipitation, occurs relatively rapidly and can be reversible (185, 192). In addition to the external physico-chemical factors, eg. pH and temperature, the solution chemistry of the metal largely influences biosorption (192). The equilibrium amount of metal bound onto the cell surface would therefore be determined by the relative affinities of the binding sites for the toxic metals and other cations present as well as the residual concentrations of these metals remaining in solution (185).



## 6. BIOSORPTION BY NON-VIABLE YEAST BIOMASS

The surfaces of yeast cells have been associated with ion exchange and complexation reactions as well as the formation of stable complexes (192). Strandberg (195) postulated that the polyphosphate and carboxyl groups on the cell surface of *S. cerevisiae* are active in the complexation of uranium. The phosphoryl groups appear to form stable complexes with uranium, whilst the carboxyl groups only become involved at the onset of saturation of the phosphoryl groups. Non-viable strains of bakers and brewers yeast have also been shown to remove greater amounts of cadmium and zinc from solution than live cultures (180, 182). Similarly *S. cerevisiae* has demonstrated a preference to accumulate cobalt and lead via biosorptive mechanisms in preference to bioaccumulative pathways.

Biosorption is not limited to a specific microbial species, but extends to a wide range of biomass types, eg. yeasts, fungi, algae, bacteria and moss (see chapter 1). Volesky and Holan (192) reviewed the metal accumulating abilities of all documented biomass types. The biosorptive capacities vary depending on the microbial strain and metal species present. Some biosorbents are involved in the adsorption of a range of metals with no specific binding priority whilst others are specific for selected metals (138, 185, 192, 193). Conclusive evidence proved that whilst bacterial and fungal biomass types prove to be adequate biosorbents, marine algae (111, 138) and sphagnum peat moss (138, 143, 144, 194) are superior metal chelators. The utilization of biomass species as bioremediation tools does not depend solely on their metal sorption capacity, since the availability of the biomass and cost factors are also important criteria regarding their implementation. Whilst non-viable biomass of the yeast *S. cerevisiae* may only exhibit a moderate level of biosorbent activity when compared to other microbial species (138), it remains the most widely used yeast and waste product in the fermentation industry in South Africa and subsequently is a freely available source of biomass suited as a bioremediation tool.

The cost effective nature of bioremediation remains its primary drawcard (192). Conventional methods for removing metals from industrial waste solutions, eg. chemical precipitation, chemical oxidation or reduction, filtration, electrochemical treatment, membrane technology and evaporation recovery may be ineffective or extremely expensive especially when treating high-volume, low-concentration effluent. The use of ion exchange resin for purification of waste waters has also been excluded due to the high cost of the materials required. In comparison non-viable biosorbents can easily be used for remediation of waste water and particularly in cases where combined purification and recovery are required. The importance of biomass in metal recovery has been reviewed in the light, that not only are the metal uptake capacities high, but selective metal recovery can also occur

## 6. BIOSORPTION BY NON-VIABLE YEAST BIOMASS

(192). The successful industrial application of this method does however require a high capacity biosorbent, with suitable physical properties, and a thorough knowledge of the system under operating conditions (196).

Some methods of killing cells may improve the biosorptive properties of the biomass. For example, *S. cerevisiae* cells when killed by heat drying and grinding increase their ability to accumulate a range of metals (139). Heat-killed *Chlorella* cells also accumulate greater amounts of metals than live *Chlorella* cells (108). Alternative mechanisms of producing non-viable biomass include chemical modification, and in some instances immobilization. Immersion in formaldehyde both kills and cross-links cells, thereby immobilizing them. Non-viable *R. arrhizus* biomass, killed by 1% formaldehyde solutions has proven to be extremely durable and is therefore able to endure greater chemical and physical stress conditions than living biomass (192).

To facilitate the separation of biomass from solution and to improve biomass performance and its physical characteristics, non-viable biomass is commonly immobilized either in a granular or polymeric matrix (144). Many methods of immobilizing cells have been developed. Immobilized non-viable biomass killed and cross-linked using extreme chemical and physical conditions may possess very different metal accumulating properties compared to the original living biomass (188). For bioremediation purposes the microbial biomass need to be immobilized in a particulate form that preserves its biosorptive properties (197). Immobilization can also improve performance in column reactors and enhance reusability (192), eg. immobilized *Candida tropicalis* cells used in the degradation of phenol, exhibited a half-life of between 20 and 40 days, whereas free cells could only be used for 20 h (197).

Evaluation of immobilized biosorbents depends on a number of criteria (192). Both the metal uptake and desorption properties are important, though ultimately the maximum metal loading capacity remains one of the most important features characterizing its performance, especially at high metal concentrations. In addition, the rate of metal uptake and release, selectivity of biosorption and desorption, mechanical and physical properties, efficiency of implementation and operation and economic feasibility of production and implementation of the biomass remain important selection criteria (192).

## **6. BIOSORPTION BY NON-VIABLE YEAST BIOMASS**

Immobilization of biomass with the intent to use it for the treatment of industrial waste water has been investigated by a number of researchers (198). Immobilizing polymers tested have included agar, agarose,  $\kappa$  - carrageenan, collagen, polyacrylamide, polyurethane and cellulose, though not all of these polymers have proven to be suitable for industrial purposes, often due to poor mechanical strength and durability, toxicity or high production costs (198).

Two immobilizing polymers, viz. polyvinylalcohol (PVA) and polyethylenimine (PEI) appear to possess the required criteria for this type of work. PVA, is a non-toxic polymer, which can be produced cheaply on industrial scale as durable beads, whilst the embedding and cross-linking procedure involving PEI is a simple process, also producing durable beads.

In the present study the production of three types of immobilized non-viable yeast biomass was undertaken and their metal accumulating capacity determined. Two immobilized systems employing PVA, viz. PVA Na-alginate and PVA Na-orthophosphate beads were compared to alkali-treated PEI:glutaraldehyde (GA) pellets with respect to their mechanical properties and metal adsorption properties. Bearing in mind that the ultimate purpose of the development of these biomass types was for their utilization in the bioremediation of industrial waste water, the metal affinities of the respective biomass types were determined. A Cu-solution was used as a standard for this work. Additional experiments using the selected biomass type focussed on adsorption isotherms using batch reactions, and the optimization of fixed bed reactor columns, with respect to pH and breakthrough volumes using single and multi- element solutions. The multi-element solutions contained Cu, Cd, Cr, Ni and Zn.

## **6.2. METHODS AND MATERIALS**

### **6.2.1. BIOMASS PREPARATION**

#### **6.2.1.1. POLYVINYLALCOHOL (PVA) Na-ORTHOPHOSPHATE IMMOBILIZATION**

The standard washing procedure was applied to commercial *S. cerevisiae* cells. 70 g (wet weight) of the washed yeast was suspended in Milli-Q water to obtain a 51% (w/v) solution.

## 6. BIOSORPTION BY NON-VIABLE YEAST BIOMASS

The immobilization procedure followed was an adapted version of the method outlined by Chen *et al.* (1999). A 20% (w/v) aqueous solution of PVA (Av MW 70 000 - 100 000, Sigma Chemical Co) was prepared by adding 33 g of PVA to 165 ml of Milli-Q water. The solution was heated to 70°C to enable the PVA to dissolve and was subsequently cooled down to 55°C prior to being mixed with the yeast suspension. The final suspension contained 23% (w/v) cells (wet wt) and 10.8% (w/v) PVA.

The immobilized yeast was further cooled down to 45°C and the PVA-cell suspension extruded via a peristaltic pump through a needle (Terumo needle: gauge 1.2 mm x 38 mm) into 2 l of saturated boric acid (Sigma Chemical Co) and stirred for 2 h. Spherical bead formation (3 mm diameter) resulted from cross-linking the PVA with the saturated boric acid.

To initiate the gelling and hardening, the beads were transferred from the boric acid solution, washed using Milli-Q water and placed in 2 l of 1.0 M Na-dihydrogen orthophosphate for 2 h. On removal from the phosphate solution the PVA beads were washed using Milli-Q water and freeze-dried for 36 h.

### 6.2.1.2. PVA Na-ALGINATE IMMOBILIZATION

Following the method of Shindo and Kakimura (200), washed yeast cells were immobilized as hollow PVA beads. The hollow structure of the beads prevents disintegration.

Using 21 g (wet wt) a 10% (w/v) suspension of washed yeast in Milli-Q water was prepared. 13.2 g of PVA was suspended in 165 ml of Milli-Q water. To this 3.3 g of alginic acid (low viscosity, Na-salt, Sigma Chemical Co) was added with stirring.

The PVA Na-alginate suspension was heated with stirring and maintained at 95°C for 20 min to dissolve the components. On cooling (45°C), the suspension was added to the yeast and mixed thoroughly. Bead formation was attained by dropping the PVA-yeast solution into 2 l of 2% (w/v)  $\text{CaCl}_2 \cdot 2\text{H}_2\text{O}$  through a thin needle (Terumo needle: gauge 1.2 mm x 38 mm). Spherical beads with an approximate diameter of 3 mm were formed. These were gently stirred for 2 h, the  $\text{CaCl}_2$  drained and the beads rinsed with Milli-Q water. Lyophilization for 24 h yielded dried hollow PVA beads.

### 6.2.1.3. POLYETHYLENIMINE (PEI) AND GLUTARALDEHYDE (GA) IMMOBILIZATION

#### 6.2.1.3.1. IMMOBILIZATION

200 g (wet wt) of washed yeast and 20 ml Milli-Q water were blended to a smooth paste (Waring commercial blender) before being treated with embedding and cross-linking agents. 25% (v/v) GA (50% aqueous glutaraldehyde, Sigma Chemical Co) was added to the biomass-water paste and blended until smooth. 33% (v/v) PEI (50% aqueous PEI, Aldrich Chemical Co) was added and mixing initiated until a moist dough was obtained. Similar to the method used by Brierley and Brierley (140), the ratios of PEI:GA:yeast were varied to obtain a stable complex. Initial ratios of PEI:GA:yeast (ml:ml:g) of 1.2:1:40, 1.2:1:50 and 1.2:1:65 were tested. The moist dough was crumbled to form granules which were oven-dried for 12 h at 80°C.

#### 6.2.1.3.2. HOT ALKALI TREATMENT

Dried, immobilized yeast biomass pellets were suspended in 3% (w/v) KOH solutions (0.1 g/ml) and heated to 70°C. The granulated material was separated from the caustic solution by settling, the latter retained whilst the pellets of granulated material were washed thoroughly with Milli-Q water. The washing procedure was repeated twice and the rinsing water added to the caustic solution.

Reconstitution of the alkali-soluble components was achieved through acidification. 32% HCl (AECI Ltd) was slowly added with stirring until pH 6.0. The decrease in pH resulted in the reconstitution and precipitation of the alkali-soluble fractions. Subsequent centrifugation (5000 g x 10 min) pelleted out the reconstituted biomass.

The washed, reconstituted biomass was added to the alkali-insoluble fraction. Both fractions were heat dried (80°C) overnight.

### 6.2.2. DETERMINATION OF STRUCTURAL PROPERTIES

Scanning electron microscopy (JOEL JSM 180 SEM) of gold coated biomass samples provided information regarding the porosity of the pellets and the surface area available for metal binding.

## **6. BIOSORPTION BY NON-VIABLE YEAST BIOMASS**

Subjective stability tests were performed on the PVA and PEI:GA biomass types ( untreated and 3% KOH treated 1.2:1:40, 1.2:1:50 and 1.2:1:65 PEI:GA biomass preparations were tested). Dried biomass granules were soaked overnight in Milli-Q water at room temperature (20°C). The moist biomass granules were handled manually to determine their physical stability. Poor stability was reflected by disintegration of the pellets, whilst the stable preparations retained their integrity under handling pressure.

### **6.2.3. DETERMINATION OF THE BIOMASS BIOSORPTIVE PROPERTIES**

#### **6.2.3.1. METAL ACCUMULATION IN PACKED-BED COLUMNS**

All polymers were found to bind very little metal in the absence of biomass. 5 g (dry wt) of PVA Na-alginate and PVA Na-orthophosphate pellets were rehydrated (2% (w/v)  $\text{CaCl}_2$  solution and Milli-Q water respectively) and rinsed prior to being packed into columns. LKB glass chromatography columns (internal diameter 16 mm) were used for this purpose. Both packed columns measured column volumes of 40 ml. 10 g (dry wt) of 3% KOH treated 1.2:1:40 PEI:GA biomass was soaked for 1 hr in Milli-Q water followed by two water rinses. The wet biomass was packed into similar glass columns as a slurry. Excess water was drained and the biomass evenly compacted (column volume: 40 ml). All columns were packed in duplicate.

To determine the metal biosorptive capacity of the pellets, 300 ml of 100 mg/l Cu-solution (pH 1.4 and pH 5.5, respectively) was pumped through the relevant columns. The influent Cu-solution was pumped upwards (to prevent compacting of the column) through the column at a flow rate of 55 ml/hr. 10 ml aliquots of the column were collected (LKB 2112 fraction collector) and analysed with respect to pH and  $\text{Cu}^{2+}$  accumulation (1275 Varian Atomic Absorption Spectrophotometer).

#### **6.2.3.2. BIOMASS REGENERATION AND METAL REACCUMULATION**

One column volume (40 ml) of Milli-Q water was flushed through the columns exposed to the pH 1.4 Cu-solution. Desorption of the bound metal was achieved by pumping 2 column volumes of 1 mM EDTA upwards through the column (flow rate 55 ml/hr). A final rinse of 2 column volumes of Milli-Q water completed the desorption procedure.

## **6. BIOSORPTION BY NON-VIABLE YEAST BIOMASS**

On removal from the columns the biomass types were rinsed in Milli-Q water. The PVA-biomass preparations were lyophilized (section 6.2.1.1. and 6.2.1.2.), whilst the PEI:GA biomass was dried overnight, reconditioned with an alkali solution (section 6.2.1.3.2.) and oven-dried. Any change in biomass weight due to desorption and reconditioning procedure was ascertained by comparing the dry weight of the regenerated pellets to their initial dry weight.

The rehydration, packing and metal accumulation procedures outlined in section 6.2.3.1. were repeated for each of the biomass columns and the Cu removal determined using the standard atomic absorption procedure.

### **6.2.4. METAL BIOSORPTION TESTS**

The effect of metal ion concentration on the PEI:GA biomass biosorption performance was evaluated by contacting the biomass pellets with respective  $\text{Cu}^{2+}$ ,  $\text{Cd}^{2+}$ ,  $\text{Cr}^{3+}$ ,  $\text{Ni}^{2+}$  and  $\text{Zn}^{2+}$  metal solutions of increasing concentrations (0.5, 1.0, 5.0, 10.0, 25.0, 50.0 and 100.0 mg/l solutions).

4 g (wet wt) of hydrated biomass was placed in acid washed glass flasks and suspended in 25 ml of the relevant concentration of metal solution and the pH adjusted to pH 5.5 - 5.6. After gentle shaking for 2 h at room temperature the biomass was separated from the metal solution. Metal biosorption was determined indirectly by measuring the concentration of the metal remaining in the solution. To minimize any error due to adsorption of the metal to the flask walls, the experimental criteria of the control flasks remained identical to those of the test flasks. The control flask contained either no biomass (*ie.* only the relevant concentration of the metal solution adjusted to the correct pH), or alternatively aliquots of yeast suspended in ultra-pure Milli-Q water.

### **6.2.5. FIXED-BED BIOSORPTION USING PEI:GA BIOMASS**

#### **6.2.5.1. BREAKTHROUGH DETERMINATION OF INDIVIDUAL CATION SPECIES**

PEI:GA biomass fractions (10 g dry wt) were rehydrated and packed into columns as for section 6.2.3.1. Stock solutions (1000 mg/l) of  $\text{Cu}^{2+}$ ,  $\text{Cd}^{2+}$ ,  $\text{Cr}^{3+}$ ,  $\text{Ni}^{2+}$  and  $\text{Zn}^{2+}$  (SARchem) were diluted to 100 mg/l. Using 3% KOH the pH of each of these solutions was adjusted to pH 5.5. 1.5 l of the respective metal cation solutions were pumped upwards through separate columns (column volume;

40 ml, column height: 20 cm). A flow rate of 55 ml/hr was maintained throughout the duration of the experiment.

Aliquots (10 ml) of the eluants were collected and quantitatively analysed using a GBC 909 Atomic Absorption Spectrophotometer to determine metal accumulation and breakthrough. pH profiles for each of the column eluents were established.

#### **6.2.5.2. MULTI-ELEMENT COMPETITION AND EFFECT OF SOLUTION pH ON BREAKTHROUGH DETERMINATION**

Due to differences in the molecular weights of the metal ion species, competition and affinity studies were conducted using equimolar metal solutions, containing the 5 metal species. In an attempt to remain within the same concentration range of the individual metal cation solutions (except for Cd) the eventual concentration of the metal cations in the equimolar solutions were established as 1.5 mM (mg/l concentrations for the respective metals of 77.99 mg/l Cr; 88.05 mg/l Ni; 95.32 mg/l Cu; 98.07 mg/l Zn and 168.62 mg/l Cd ).

To determine the effect of pH, three equimolar solutions of pH 1.5, 2.5 and 4.5 were prepared. Adjustments to the pH were made using 3% KOH. The respective multi-cation solution (0.5 l) was pumped upwards through the column at a flow rate of 55 ml/hr. The experiment was conducted in triplicate, exposing fresh biomass to different pH solutions. Sample collection and analysis proceeded as outlined in section 6.2.5.1.

### **6.3. RESULTS**

#### **6.3.1. IMMOBILIZED AND STRUCTURAL PROPERTIES OF THE BIOMASS**

Multiple criteria established the basis for successful immobilization. Though % yield of the final product remains important, evaluation is also gauged by the simplicity of the procedure. The % yield (dry wt of end product expressed as a % of the initial wet wt) of the PVA immobilized biomass fractions, viz 54.2% for PVA Na-alginate and 38.6% for PVA Na-orthophosphate, compared favourably to that of the alkali PEI:GA biomass (15 - 17%). The low % yield of PEI:GA biomass can be ascribed to the alkaline treatment of the immobilized biomass. Hot alkali solubilizes the



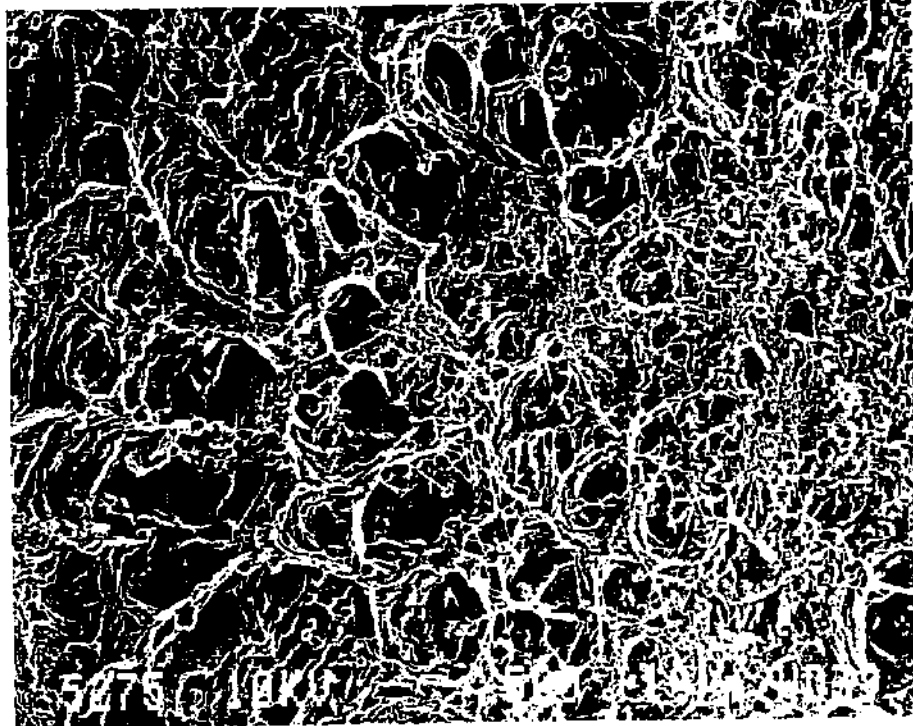
mannan and some of the  $\beta$  1-6 glucan fractions of the cell wall, although some of the material may be reclaimed using acid. Alkali treatment was limited to immobilized biomass. Brierley *et al.* (140), reported that the alkaline treatment of native yeast biomass resulted in the unacceptable loss of biomass. Embedding and cross-linking enhanced the stability of the product, thereby limiting biomass loss. Initial PEI:GA immobilization resulted in a 29% yield which mirrors the dry wt : wet wt ratio for yeast suggesting no initial loss of biomass during immobilization.

The simplicity of the cross-linking and embedding immobilization of the PEI:GA biomass exceeded that of the PVA bead formation, with respect to both the number of solutions and time required for the immobilization procedure. Additional drawbacks related to the PVA beads included limited quantities of yeast immobilized per batch. Attempts to increase the batch size resulted in numerous complications. In comparison, the batch size of PEI:GA biomass could be increased successfully, whilst still maintaining the integrity of the pellets.

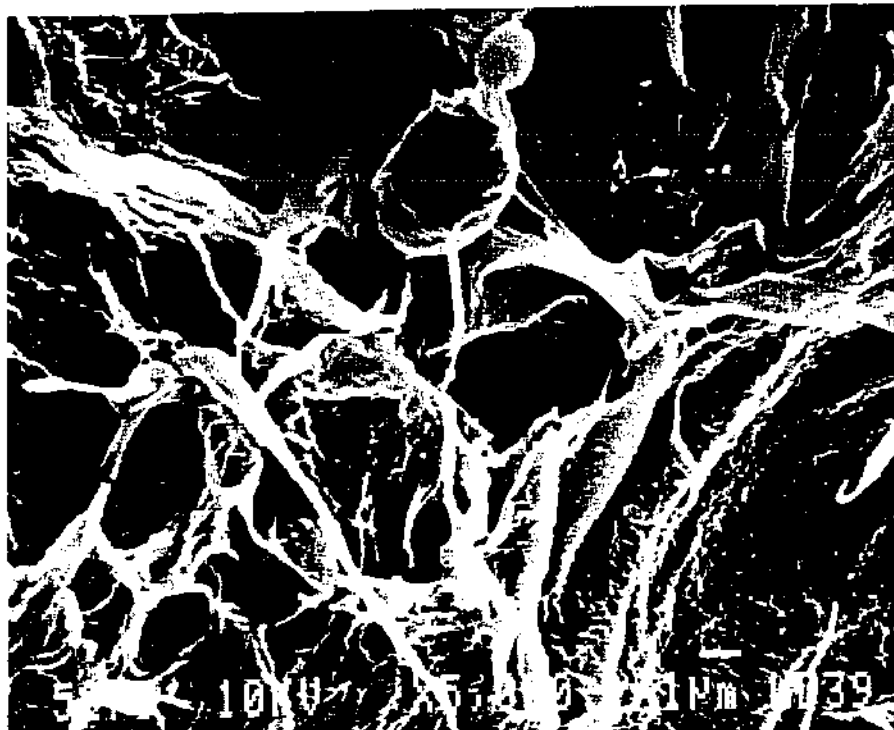
Electron micrographs (Fig 6.1 - 6.6) of the three biomass types reveal enlarged surface areas available for metal-biomass interactions. Noticeably porous were the two PVA based bead types (Fig 6.1 - 6.4), whilst PEI:GA pellets appeared more compact and dense (Fig 6.5 and 6.6). Although similar in shape, colour and structure to the naked eye, micrographs revealed differences in the microstructure of the PVA beads. PVA Na-alginate beads exhibited a lattice structure (Fig 6.1 and 6.2) whilst PVA Na-orthophosphate beads were more sponge-like in appearance (Fig 6.3 and 6.4). Although porous, both bead types possessed sufficient integrity to withstand the elevated pressures of column conditions. Attrition tests (grinding and manual handling) appeared not to affect either their physical properties or metal accumulating capacities.

At low magnification (Fig 6.5) PEI:GA immobilized yeast cells appeared as solid compact pellets with limited available access to the interior of the pellet. The rough, undulating nature of the pellet surface increased the external binding area. Under high magnification (Fig 6.6) pores in the exterior of the pellet become apparent. Although the latter would increase the accessibility of the pellet interior to metal cations, the general structure of the pellet suggested the majority of metal cation interaction to occur between surface ligands. In order to attain maximum metal biosorption, the ratio of surface : metal solution should be kept high. This necessitates the production of the smallest possible pellets without compromising on the physical integrity of the granules. Pellets containing 1.2:1:40 (ml:ml:g) PEI:GA yeast exhibited the highest level of stability, whilst an increase in the amount of yeast added

to disintegration and flaking on application of pressure.



6.1.

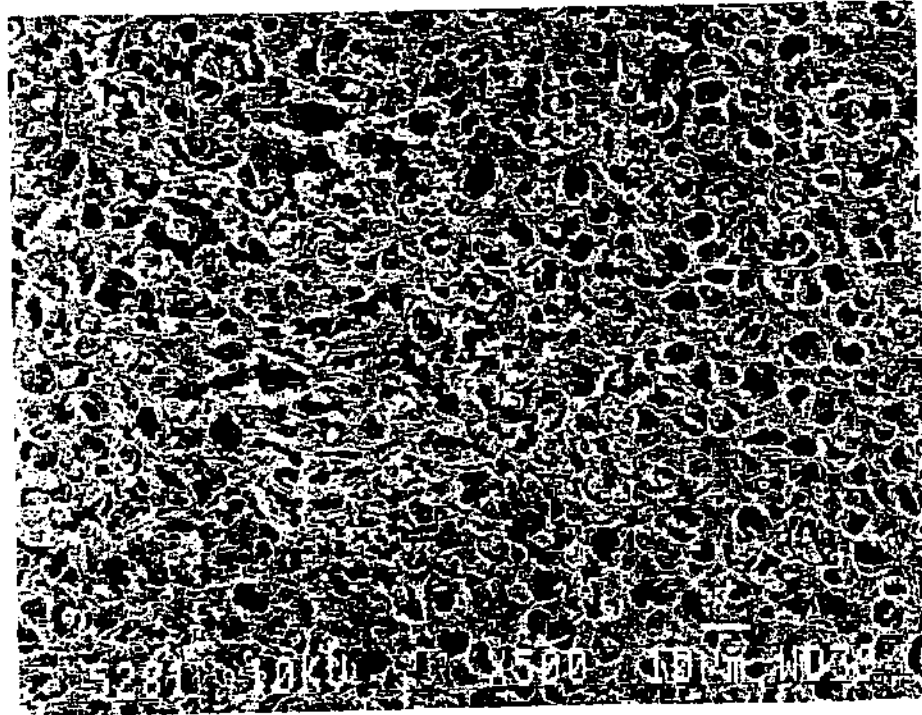


6.2.

Figure 6.1 - 6.2. Scanning electron micrographs of the surface of yeast containing PVA Na-alginate pellets at 6.1) 500x and 6.2) 5 000x magnification. Note the lattice structure of the pellet due to cross-linking.

6. BIOSORPTION BY NON-VIABLE YEAST BIOMASS

6.3.



6.4.

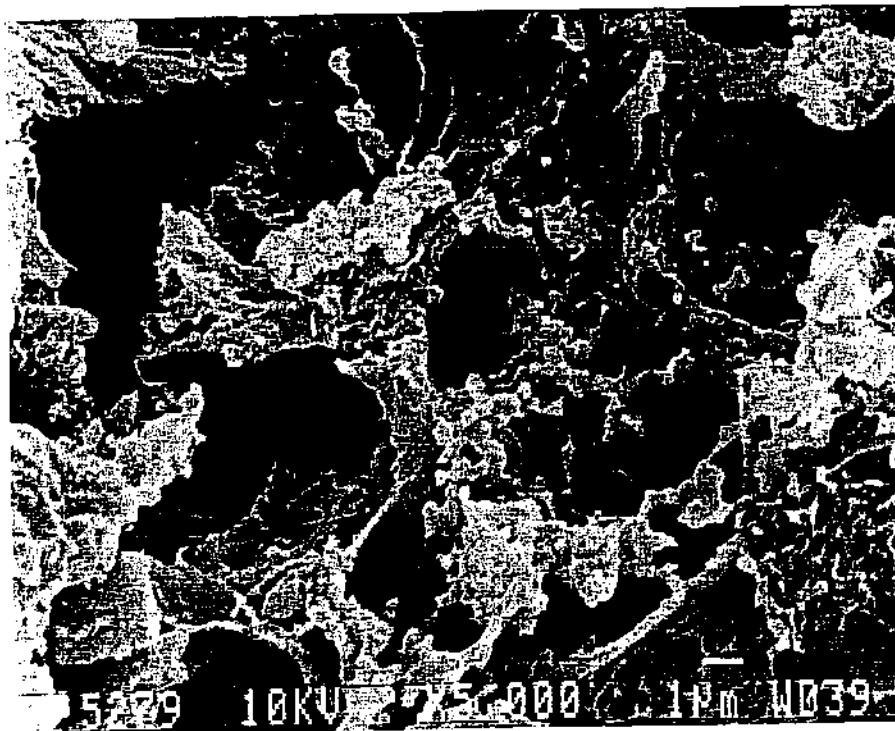
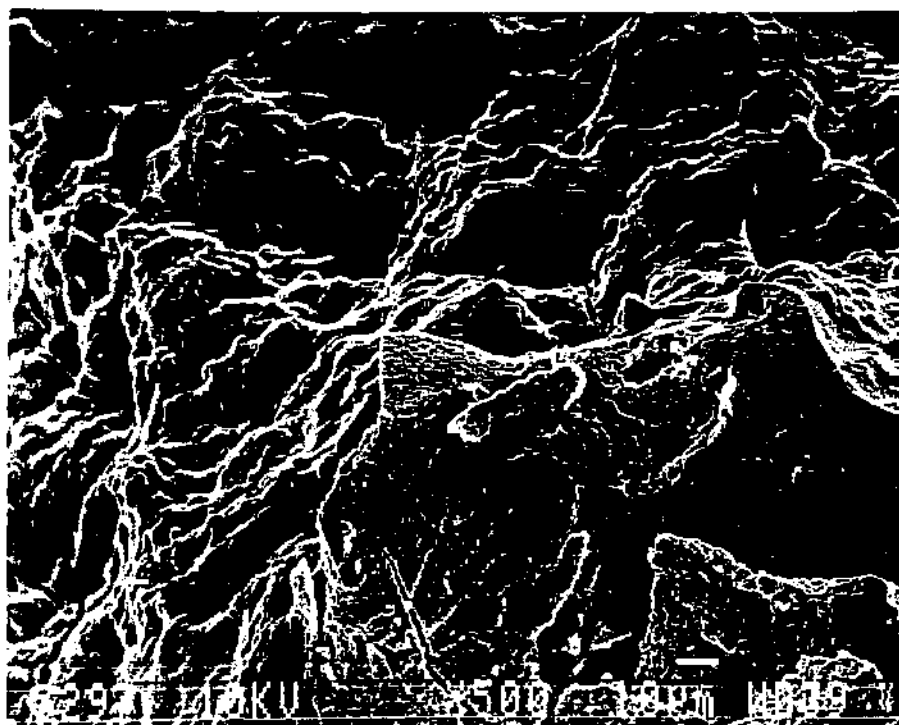


Figure 6.3 - 6.4. Scanning electron micrographs of the surface of yeast containing PVA Na-orthophosphate pellets at 6.3) 500x and 6.4) 5 000x magnification. The external appearance is sponge-like.

## 6. BIOSORPTION BY NON-VIABLE YEAST BIOMASS

6.5.



6.6.

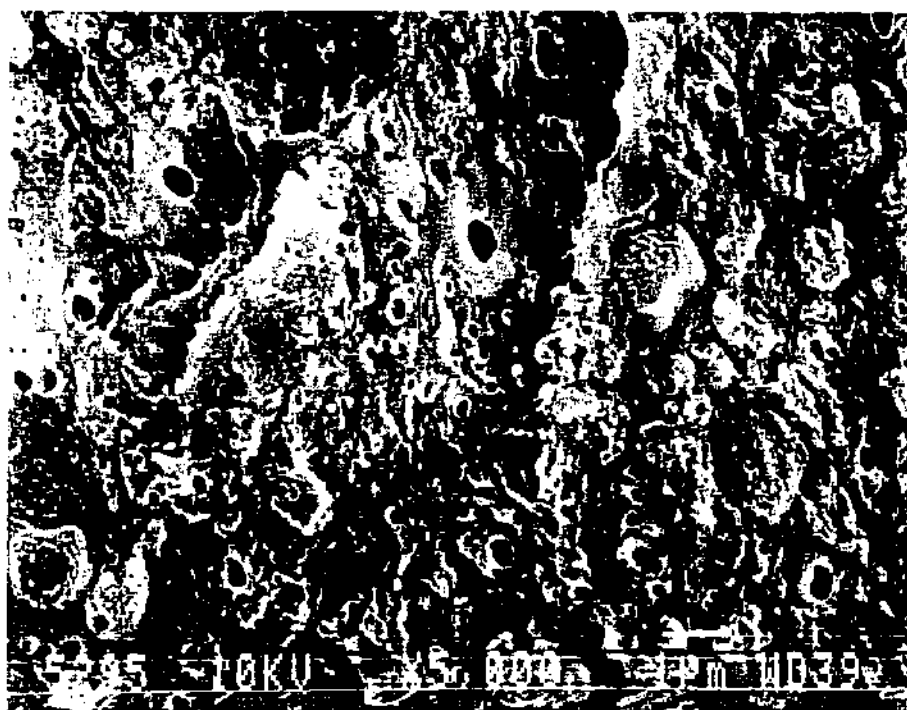


Fig 6.5 - 6.6. Scanning electron micrographs of KOH treated PEI:GA biomass pellets at 6.5) 500x and 6.6) 5 000x magnification. Note the initial compact appearance of the granules, though pores do become apparent at higher magnifications.

## 6.3.2. METAL ACCUMULATION

The biosorbent capacities of the three types of biomass pellets can be compared in Fig 6.7 - 6.9. The polymers form a very small portion of the immobilized biomass. Subsequently the contribution thereof to biosorption can be regarded as minimal. Immediately apparent is the effect of the influent pH on metal accumulation and its resultant effect on the onset of the breakthrough volumes (80% metal accumulation) of the columns, most noticeably so for KOH PEI:GA (Fig 6.7) and PVA Na-alginate (Fig 6.8) pellets. The pH profile of the PEI:GA column was initially influenced by the residual alkalinity of the PEI:GA biomass. An influent acidic solution (pH 1.4) results in low breakthrough volumes for all three biomass types, viz. 10 ml for PVA Na-alginate and Na-orthophosphate and 100 ml for PEI:GA pellets, respectively. An increase in the pH of the influent solution viz. pH 1.4 to pH 2.5 had a dramatic effect on the breakthrough volume of the PEI:GA biomass though the onset of saturation still elicited an almost immediate decline in biosorption by the column biomass.

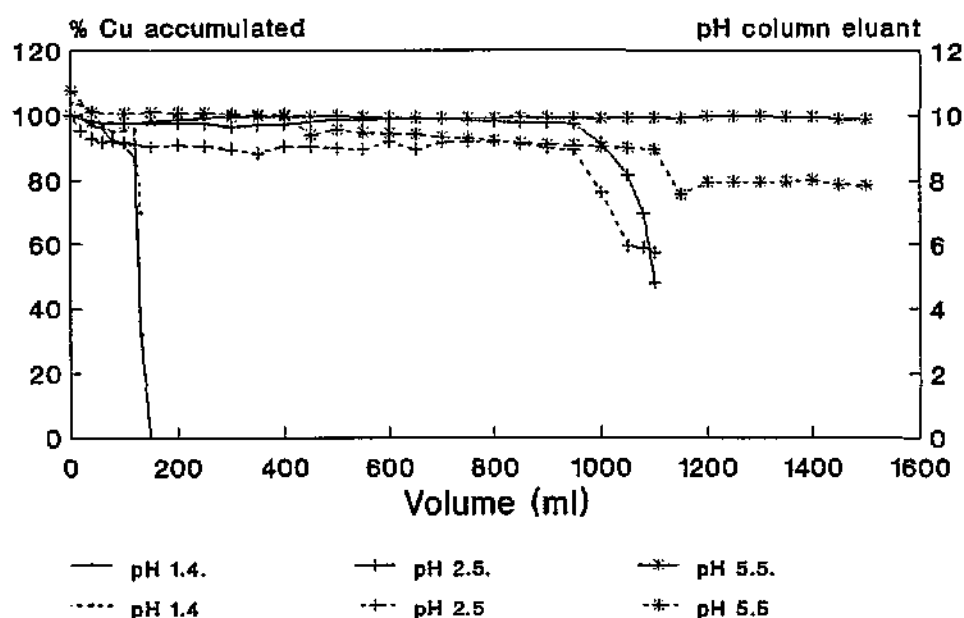


Figure 6.7. The effect of pH of the influent solution on Cu-accumulation and breakthrough volume of KOH treated PEI:GA biomass within a fixed-bed reactor. The corresponding dotted lines represent the pH profile of the column at that influent pH.

## 6. BIOSORPTION BY NON-VIABLE YEAST BIOMASS

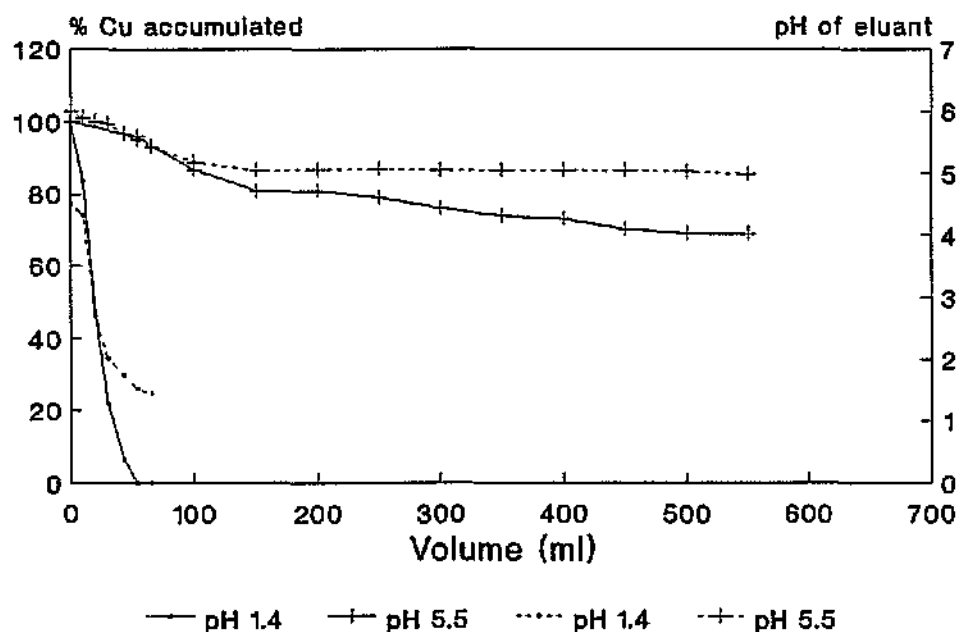


Fig 6.8. The effect of pH of the influent metal solution on Cu-accumulation and breakthrough volume of PVA Na-alginate pellets in a fixed-bed reactor. The corresponding dotted lines represent the pH profile of the column at that influent pH.

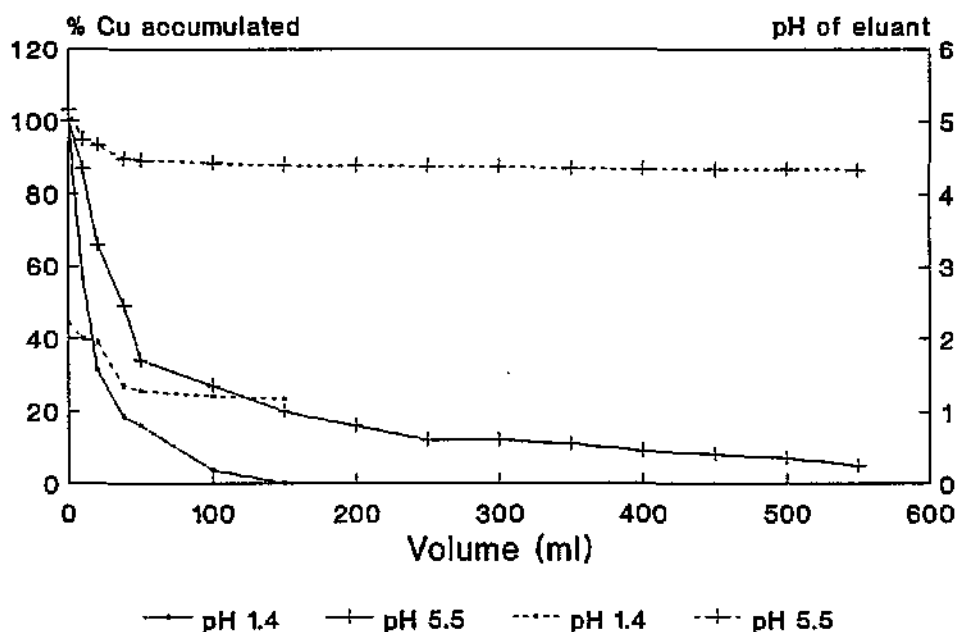


Fig 6.9. The effect of pH of the influent metal solution on Cu-accumulation and breakthrough volume of PVA Na-orthophosphate pellets in a fixed bed reactor. The corresponding dotted lines represents the pH profile of the column at that influent pH.

## 6. BIOSORPTION BY NON-VIABLE YEAST BIOMASS

Cu biosorption appeared to favour an influent pH of pH 5.5. At higher pH values precipitation of the solution occurred within the columns. After processing 1.5 l of the influent Cu-solution (pH 5.5), breakthrough had not yet occurred in the PEI:GA column. A gradual decline in the amount of  $\text{Cu}^{2+}$  accumulated by the PVA Na-alginate pellets at this pH occurred over time with the onset of saturation. In contrast, PVA Na-orthophosphate pellets accumulated only slightly more  $\text{Cu}^{2+}$  from the alkaline solution than from the acidic one (Fig 6.9).

The breakthrough volumes of the respective biomass types in the columns were determined by the pH of the column. This phenomenon occurred at the interchange between alkali or neutral pH to mildly acidic conditions within the column. For example, breakthrough (1014 ml) of the PEI:GA column (influent pH 2.5) occurred as a result in the decline of pH from pH 7.6 to pH 6.15. The column eluant of the two PVA columns remained acidic (pH 5.90 and pH 5.14 respectively) despite an influent pH of 5.5, which explains the low metal biosorption in these columns.

Biomass saturation and subsequent breakthrough of native and regenerated biomass columns (Fig 6.10 - 6.12) mirrored pH activity. Accumulation and reaccumulation of metals for each of the respective biomass types exhibited similar trends, though regenerated PVA beads appeared to be slightly better metal accumulators than the native pellets (Fig 6.11 and 6.12). Although the onset of Cu-saturation (80% metal accumulation) of PVA beads occurred at low influent volumes, the metal bound to the pellet was not eluted during breakthrough. In comparison, Cu-saturation of the PEI:GA biomass (Fig 6.10) resulted in the release of all complexed  $\text{Cu}^{2+}$  (represented by the negative accumulation values). The majority of the metal was released as a result of biomass saturation, though any residual metal was eluted by the remaining influent Cu-solution. The pH-induced breakthrough affected the binding capacity of the PEI:GA pellets. Subsequent to breakthrough, no  $\text{Cu}^{2+}$  was accumulated.

## 6. BIOSORPTION BY NON-VIABLE YEAST BIOMASS

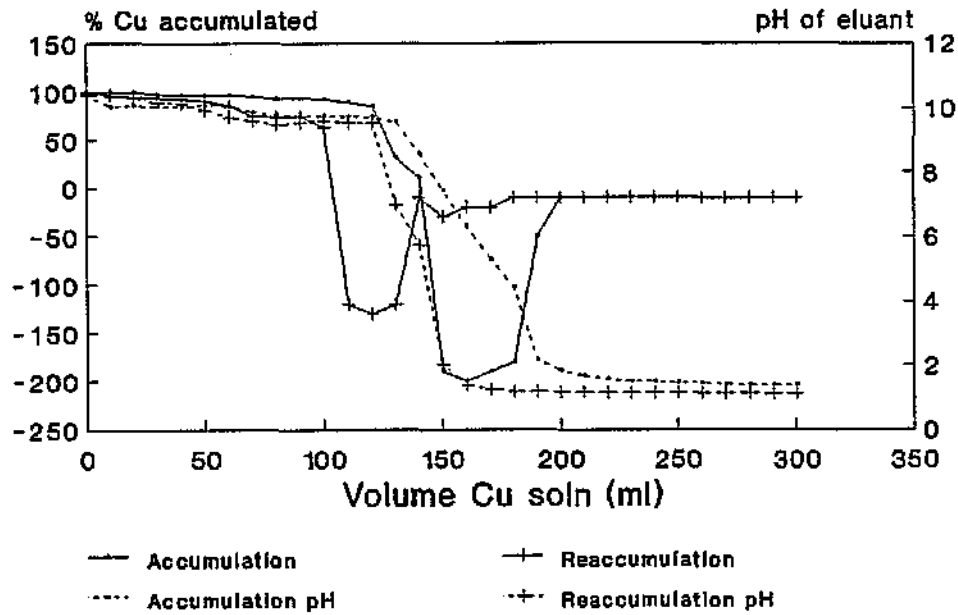


Fig 6.10. A comparison between  $\text{Cu}^{2+}$  biosorption by fresh and regenerated KOH treated PEI:GA biomass pellets. The influent metal solution was at pH 1.4, whilst the dotted lines represent the respective pH profiles.

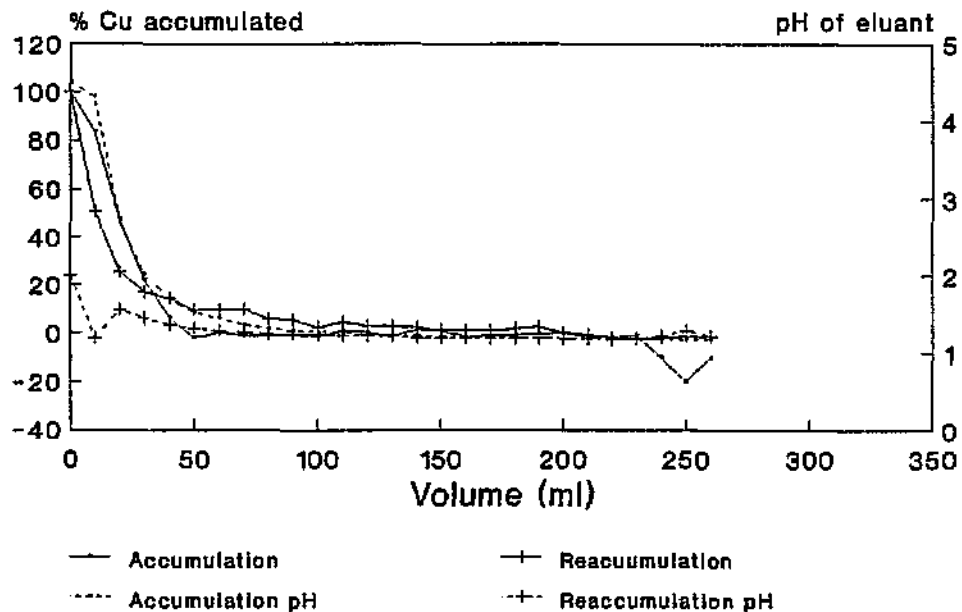


Fig 6.11. A comparison between  $\text{Cu}^{2+}$  biosorption by fresh and regenerated PVA Na-alginate pellets. The influent solution was maintained at pH 1.4, whilst the dotted lines represent the respective column pH profiles.



## 6. BIOSORPTION BY NON-VIABLE YEAST BIOMASS

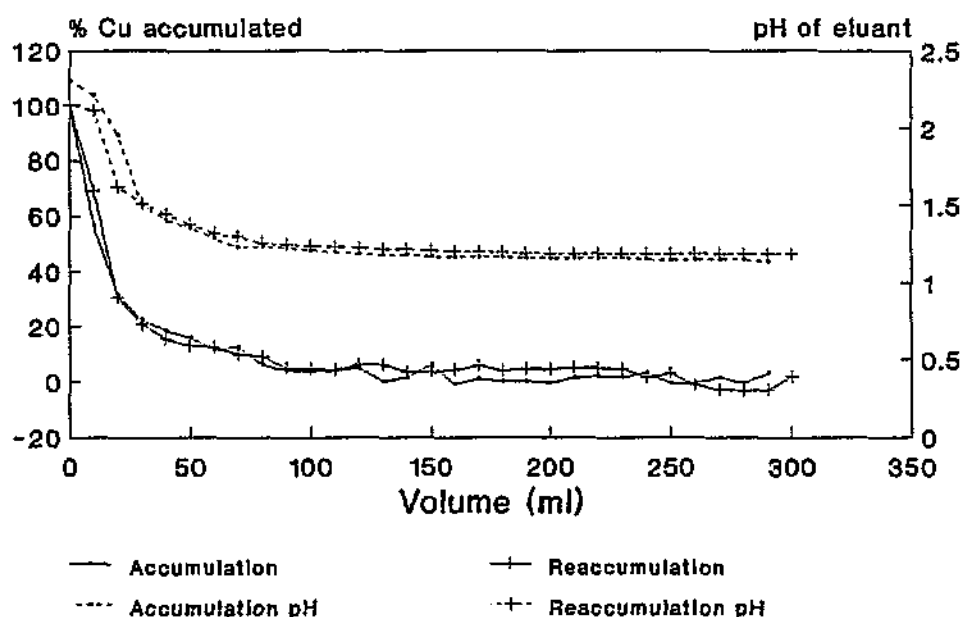


Fig 6.12. A comparison between  $\text{Cu}^{2+}$  biosorption by fresh and regenerated PVA Na-orthophosphate. The influent metal solution was maintained at pH 1.4, whilst the dotted lines represent the pH profiles of the respective columns.

### 6.3.3. COLUMN BIOSORPTION

Fixed column reactors behave in accordance with the theoretical plate theory, and due to the multiple equilibrium plates are surmised to remove metals more efficiently than batch reactors which permit only a single equilibration. Breakthrough should thus occur gradually at the onset of saturation of the majority of the theoretical plates. On passing the respective metal-solutions through columns containing the granular biosorbent (PEI:GA biomass) complete removal of the Cd and Cu from 1.5l of the respective metal solution was attained (Fig 6.13). Less efficient was the removal of Zn, Ni and Cr, though subsequent to the onset of breakthrough of these elements, biosorption of the metals still occurred, though at lower efficiencies, until the onset of complete saturation. Initial breakthrough of Cr occurred after 550 ml of the influent solution had been processed, a further 350

## 6. BIOSORPTION BY NON-VIABLE YEAST BIOMASS

ml was processed less efficiently, until the onset of total saturation. Similar trends regarding the biosorption of Ni and Zn were apparent at greater volumes of the influent solutions. The ability of the biosorbent in columns to remove a single metal from solution decreased in the order of Cu, Cd, Zn > Ni > Cr, with the onset of the respective breakthrough volumes at 750 ml for Cr, 1200 ml for Ni, and those for Cd, Cu and Zn undetermined.

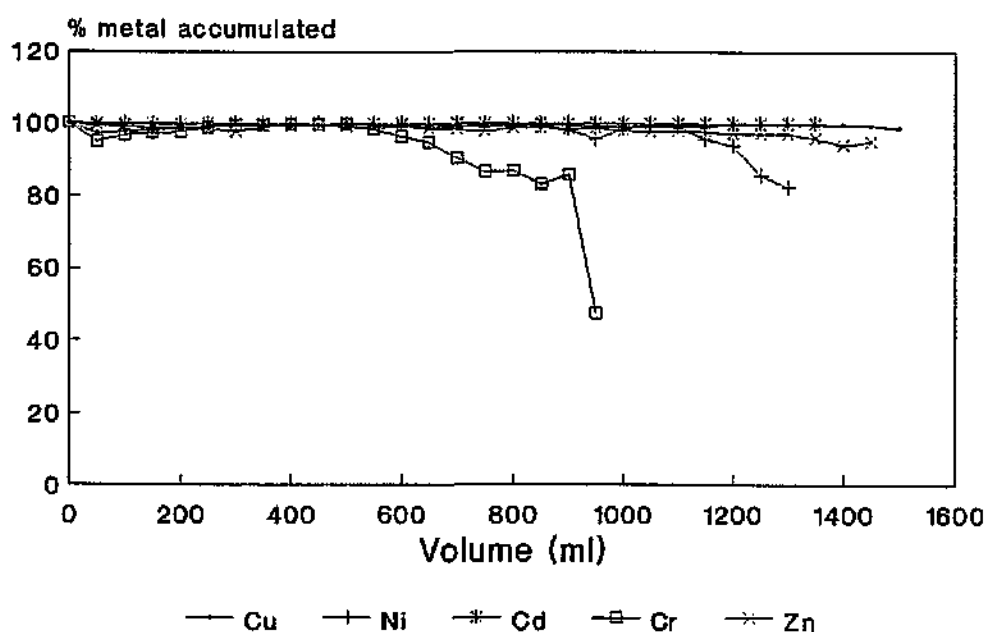


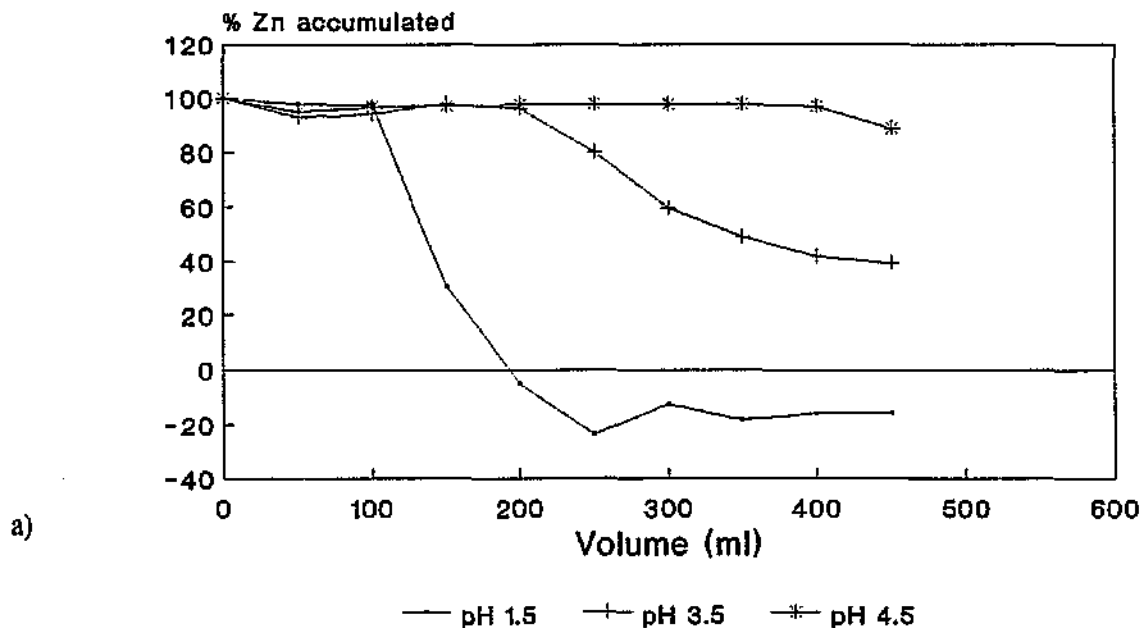
Fig 6.13. Comparison of metal biosorption by KOH treated PEI:GA biomass in fixed bed reactors from respective single element solutions (100 mg/l, pH 5.5).

The introduction of multiple metal cations in solution greatly affected the metal accumulating ability of the PEI:GA biomass (Fig 6.14a - e). Due to the superior metal binding abilities of PEI:GA biomass compared to those of the PVA pellets, the former was preferentially used as the biosorbent. Competition between the metal ions for binding sites on this biomass resulted in the reduction of the breakthrough volume of the columns. Due to the nature of the influent solution (*ie.* the number of different ion species) the pH thereof was unable to be raised above pH 4.5 without precipitation occurring. However, the metal accumulating ability of the biomass was limited at extremely low pH values. An increase in the pH of the influent solution from pH 1.5 to pH 2.5 markedly increased the amount of metal accumulated, especially Zn, Cu and Cr (Fig 6.14a - c). At the onset of breakthrough

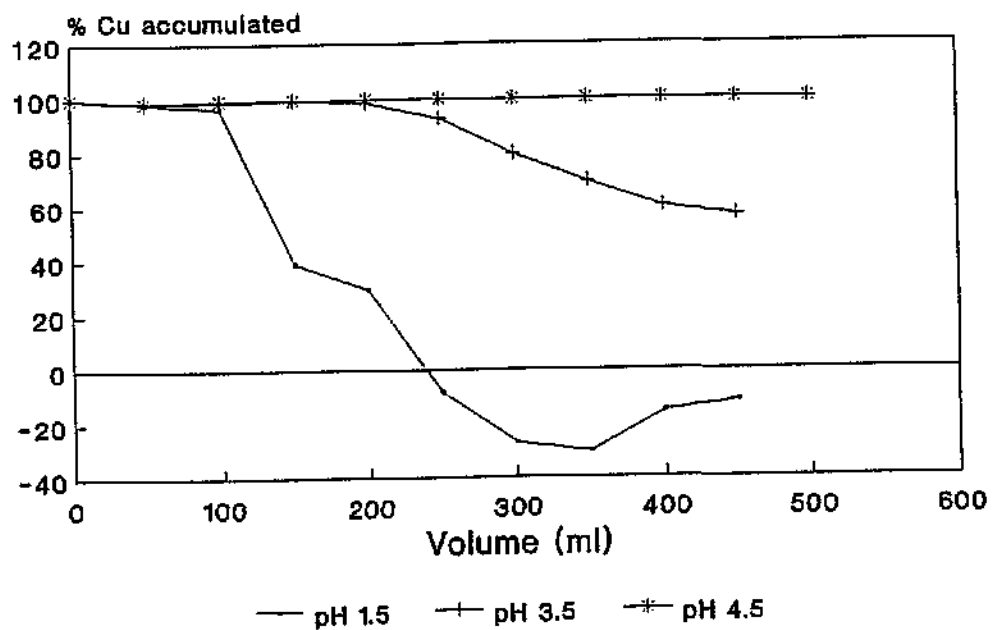
## 6. BIOSORPTION BY NON-VIABLE YEAST BIOMASS

at pH 1.5, biosorption of these metals rapidly ceased, and at higher influent volumes of the metal solution, elution of previously bound metals from the columns occurred. The elution of these bound metals from solution confirms the pH sensitivity of the biosorption of these metals, viz. Cu, Zn and Cr.

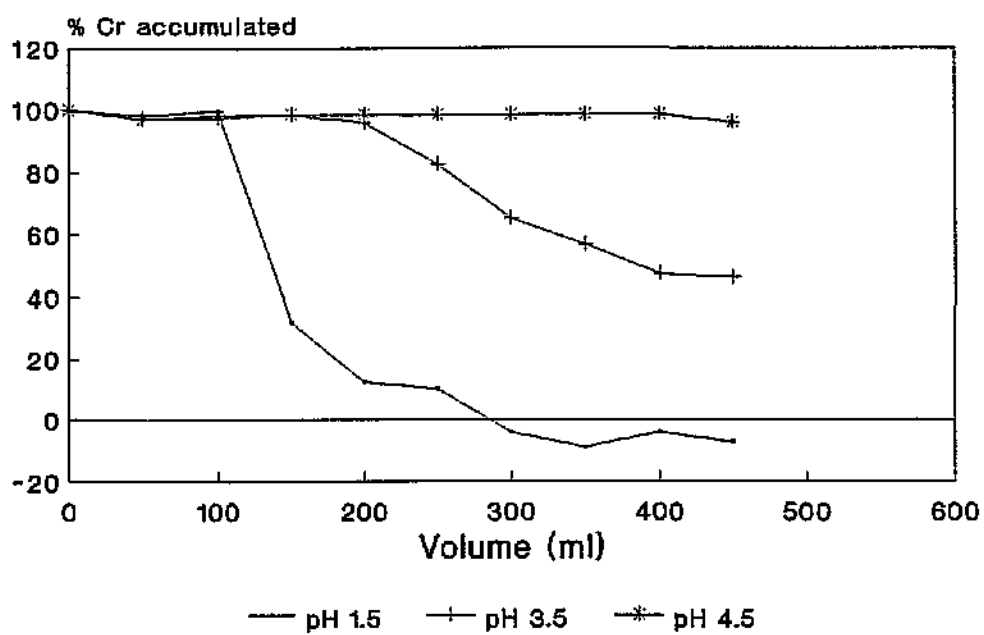
The valency of the metal is largely determined by pH of the influent solution. An increase in the pH of this solution results in a change of speciation occurring and at pH 4.5 the majority of the metals exist as divalent cations, thereby enabling maximum biosorption to occur in the columns (150). Under these conditions (pH 4.5) an affinity series for the biosorption from a multi-element solution of  $\text{Cu} > \text{Zn}, \text{Cr} > \text{Ni} > \text{Cd}$  exists. The preferential biosorption of individual metal ions from a mixed metal solution, suggests the partial specificity of the available binding sites for each metal.



## 6. BIOSORPTION BY NON-VIABLE YEAST BIOMASS



b)



c)

# 6. BIOSORPTION BY NON-VIABLE YEAST BIOMASS

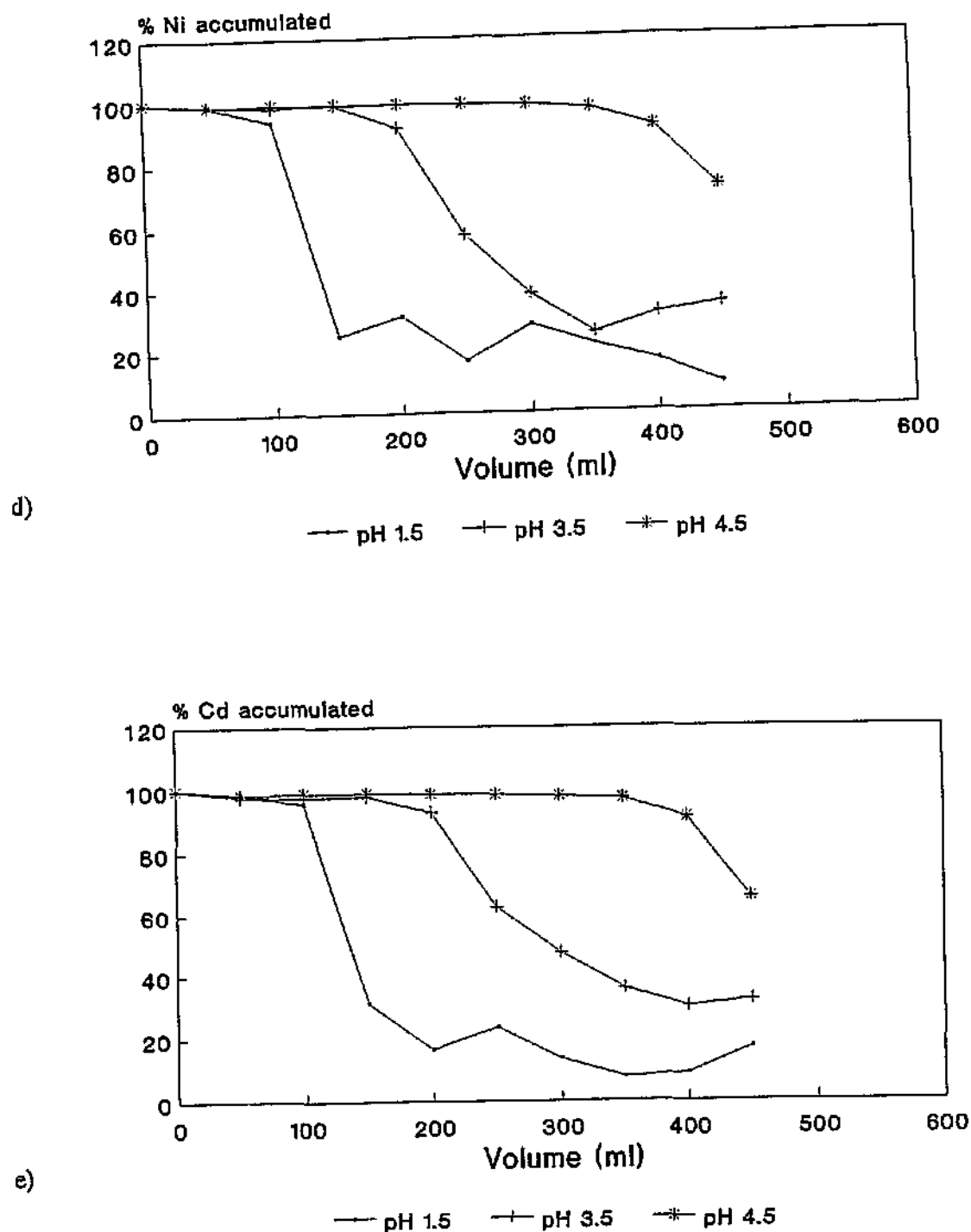


Figure 6.14. Effect of pH on the % metal accumulated by PEI:GA biomass in columns and the respective breakthrough volumes of multi-element equimolar solutions, a) Zn, b) Cu, c) Cr, d) Ni and e) Cd.

## 6.3.4. PEI:GA BIOMASS SORPTION CAPACITY

The results presented in Fig 6.15 indicate the correlation between biosorption of metal cations and the ratio of external free metal ion concentration to the available biomass. Biosorption of metal cations is dependent on this external metal concentration. The linear nature of the graphs indicates continued biosorption, whilst the levelling off reflects the onset of saturation. The biomass accumulated metal cations at varying concentrations, but did not appear to be specific for a single metal species, though Cd saturation was reached before that of other metals. In comparison, at ambient concentrations of 100 mg/l continued biosorption of Ni and Zn occurred. The affinity of the biomass for different metal cations varied at different external concentrations of the metals.

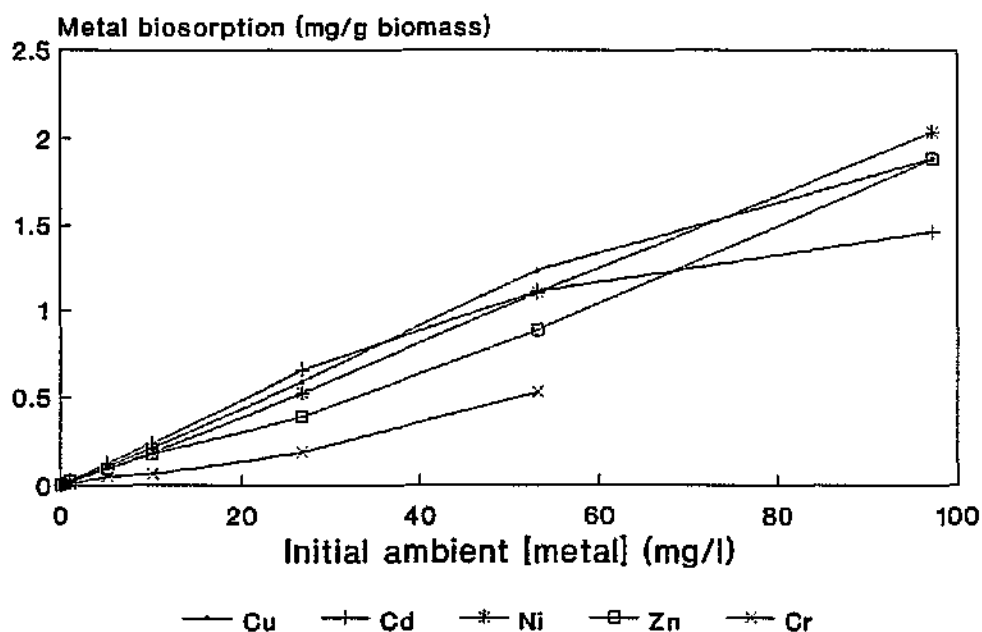


Fig 6.15. Adsorption isotherms indicating the relationship between initial ambient metal concentration and metal biosorption by PEI:GA biomass in batch reaction studies.

## 6.4. DISCUSSION

The three granular biosorbents produced in this study, viz. PVA Na-alginate, PVA Na-orthophosphate and PEI:GA biomass fulfilled the necessary physical requirements, viz. that of mechanical strength, rigidity and porosity. The microstructure and surface area available for metal binding of both types of PVA pellets exceeds that of the PEI:GA pellets, and can be ascribed to the gel lattice formation initiated during cross-linking. The porosity of the PEI:GA biomass pellets improved on treatment with hot alkali, though this also results in a loss of biomass due to the solubilization of predominantly the mannan and some of the  $\beta$  1-6 glucan cell wall fractions in the alkali. Due to the role these components play in metal adsorption, the loss of these fractions needs to be minimized. Brierley *et al.* (140), favoured alkali treatment of immobilized biomass to that of raw material, due to a diminished biomass loss.

The metal accumulating capacity of the fixed-bed reactor containing PEI:GA biomass exceeds that of the PVA pellets under identical conditions. Arguably the amount of yeast (wet wt) contained per column (column volume: 40 ml) for both PVA productions was less than that of the alkali preparation, though the efficiency of metal accumulation of the PEI:GA pellets still exceeds that of the other two pellet types. Due to the spatial limitations, the feasibility of utilizing the PVA types of biomass in fixed-bed reactors is limited.

Hot alkali-treatment enhances the metal loading capacity of the PEI:GA biomass (results not shown), through increasing the porosity of the biomass and increasing the alkalinity of the granules themselves. Though washed extensively, residual alkali may remain behind in the biomass pores, thereby influencing the biomass metal accumulating pattern. As noted by Brierley *et al.* (cited by 139), not all caustic treated biomass has the same capacity or affinity for metals. For example, the pretreatment of *Penicillium* biomass with NaOH greatly reduces its uptake capacity and in a previous study, alkali-treated native *S. cerevisiae* cells were found to bind less metal than the untreated cells (139).

PEI:GA biomass is capable of binding individual metal ion species from both single and mixed metal solutions. Regenerated biomass, though not as efficient as fresh KOH treated PEI:GA pellets mirror the binding pattern of the latter whilst managing to attain 65% Cu removal after processing 100 ml of influent solution. Metal accumulation in fixed bed columns is largely dependent on the pH of the

## 6. BIOSORPTION BY NON-VIABLE YEAST BIOMASS

influent solution; the greater the acidity of the influent solution, the less metal accumulated. Similarly, from batch studies (data not represented) at very high influent pH values very little metal accumulation by PEI:GA biomass occurs. The majority of metals occur as divalent cation species between pH 4.0 - 6.0 thereby facilitating easy accumulation.

As a general biosorbent the PEI:GA biomass has extensive potential. Although the affinity of the biomass for the respective metal cations varies depending on the metal ion species and ambient concentration thereof (Fig 6.15), the mechanism of biosorption appears to be similar. Comparison of the breakthrough volumes of single element solutions to those containing multiple metals (Fig 6.13 and 6.14) confirms the competitive nature of metal biosorption. If the cation-ligand interactions were metal species specific, the breakthrough volumes for the respective metals in a multi-element solution would remain relatively similar to those in a single element solution. Yet due to the competitive nature of the biosorption and limited number of binding sites, the breakthrough volumes of the multi-cation solutions are greatly reduced in comparison to single element breakthrough volumes. Further reductions in the amount of metal accumulated can result from steric hinderance by surface-bound metal ions.

Biosorption of the individual metals by the PEI:GA biomass is largely dependent on the ratio of external free metal ion concentration to the available biomass. The biological availability of metals is determined by their chemical speciation (charge). Shifts in pH affect the metal biosorption, by changing their solution chemistry, the nature of functional groups in the biomass as well as the competition of metallic ions with hydrogen and other monovalent ions for the binding sites (139, 150). Similar to the results obtained from the present study, Kuyucak and Volesky (150), noted that almost all the metallic species being studied, viz. U, Zn, Cd, Co and Cu, with the exception of Au were ionized as various cationic species between pH 4.0 - 5.0. Due to the nature of the metal biosorption, subsequent desorption of the metal ions is readily achieved by changing the pH of the influent solution. Mild solutions of acids, eg. hydrochloric, nitric and sulphuric are often used as desorption agents (197) due to the high solubility of metals in these solutions.



## 6.5. CONCLUSIONS

The three preparations of non-viable biomass, viz. PVA Na-alginate, PVA Na-orthophosphate and alkaline treated PEI:GA granules, produced during the present study all exhibit excellent mechanical stability. However, the metal biosorption capacity of the PEI:GA biomass exceeds that of the other two biomass types. PEI:GA biomass has proven to be an efficient metal accumulator, with the amount of metal accumulated largely dependent on the ratio of free metal ion concentration to available biomass. The availability of the metals is influenced by the solution pH. At low pH the affinity of the biomass for metals decreases and subsequently breakthrough occurs at low volumes of the influent solutions. Enhanced metal biosorption by the biomass in columns occurs at higher pH values, eg. pH 4.5 - 6.0. Biosorption is of a competitive nature. In the presence of multiple elements a decline occurs in the amount of complexed metal and the resultant breakthrough volumes of the individual metal ions occurs at lower influent volumes.

The data from this aspect of the study indicated that the immobilized non-viable yeast biomass could be successfully used for the bioremediation of effluents such as those from electroplating industries. An attempt at such an application of bioremediation is described in the following chapter.

## 7. APPLICATION OF METAL BIOSORPTION BY NON-VIABLE YEAST BIOMASS TO AN ELECTROPLATING EFFLUENT

### 7.1. INTRODUCTION

The most extensive, though not the sole use of bioremediation was possibly that which involved the clean up efforts in Alaska resulting from the Exxon Valdez oil spill in the 1980's (201). The publicity generated by this event sparked off world wide interest in bioremediation, though awareness of numerous other applications has remained limited. The development of bioremediation processes for water is one of the main applications of biological treatment systems, inclusive of the clean up of ground water, soils, lagoons, sludges and process waste streams. In the last decade the application of biological based technology has branched out to the treatment of metal containing water with areas of application covering detoxification of metal-bearing waste water, decontamination of radioactive waste water, recovery of metals from ore processing solutions and the concentration and recovery of rare and strategic metals from sea water (192). The biosorption processes are based on solid-liquid contact, not dissimilar to those used for ion-exchange or activated carbon application (192). However, biosorbents have most successfully been applied in the treatment of low-concentration, high-volume waste streams, eg. mine waste water streams (202), with very few studies having been conducted using high-concentration metal effluent, eg. industrial effluent. Several methods already exist for the treatment of this type of waste, such as electroplating effluent. Reverse osmosis, electrodialysis, diffusion dialysis, electrolytic metal recovery, evaporation and ion-exchange have all been implemented as treatment systems (203). An alternative approach employed an integrated waste treatment system (204), yet its sorbent material was rather inefficient and non-regenerative. Biosorptive treatment of this effluent using bioreactor tanks would therefore offer a novel and cost effective approach to a difficult problem.

When designing bioreactors, numerous options exist depending on the required criteria, though the types of reactors used in industry for carrying out heterogenous solid-liquid contact reactions can be classified in two broad categories (192, 205, 206). These are reactors in which the solid state particles remain in a fixed position relative to one another, eg. fixed bed, trickle bed and moving bed reactors or secondly reactors in which the solid state is suspended in a fluid and constantly moving about, eg. fluidized bed and slurry reactors (206). For the purposes of bioremediation of

## **7. APPLICATION OF BIOSORPTION BY NON-VIABLE YEAST BIOMASS**

metal containing waste water, variations to both of these categories accomplishes appropriate contact between the solution and solid biosorbent phase (192). For example, fixed packed bed reactors in their most basic form consist of cylindrical tubes or columns packed with biosorbent pellets (206), through which the metal-bearing liquid percolates (192). The principle of metal biosorption within these columns is based on theoretical plate or multi-equilibrium theory. The line of saturation of the biomass progresses through the bed in the direction of the flow until onset of total biomass saturation at the breakthrough volume. Depending on the nature of the biosorbent an upwards or downward line of flow can be selected (192).

Stirred tanks in the form of batch or continuous flow reactors can be used, though the latter is preferred by chemical and bioremediation industries (192, 205). Different multi-step modifications can be developed for the basic continuous flow stirred tank scheme. Multi-step or phase modification such as the introduction of multiple bioreactors, or recycling of the metal solution in combination with biomass regeneration can not only increase the operating efficiency of the system, but also its operating costs (192).

Several multi-component fixed bed adsorption models (204, 207 - 209) have been applied to metal removal from metal-contaminated waste water (141, 144, 210, 211). Treatment of acid mine drainage water by a three-column circuit, containing a lead-load column, scavenger column and an elution column has successfully removed Ni, Co, Cu and Zn from acid mine drainage water to within the stipulated water criteria limits (144, 210, 211). Elsewhere, p-chlorophenol and mercuric ions were removed from waste water using fixed bed columns (211).

Equally successful has been the removal of metal ions from acid mine drainage water using low maintenance circuits (144, 212). These low maintenance circuits, viz, a trough and bucket system are based on continuous flow principles, yet have been designed for field application in remote areas. Both systems utilize porous bags containing the biomass and in the absence of stirrers, a hydraulic gradient is used to circulate the water.

Biosorbent technology especially on an industrial scale is still in its infancy. Though examples of successful application have been cited, the scope for bioremediation extends far beyond the treatment of relatively dilute mine waste water. Industrially produced waste water, eg. tannery or electroplating effluent, due to the nature of the processes often contain several metals in excess of those found in

## **7. APPLICATION OF BIOSORPTION BY NON-VIABLE YEAST BIOMASS**

mine water, though in smaller volumes. Ultimately a system equipped to handle low-volume, high metal content waste water is required.

In the present study the application of a bioremediation process for the treatment of electroplating waste water was investigated. The systems studied and the effluents used are based on the results of the small scale investigations with electroplating effluent as described in chapter 6. The PEI:GA immobilized biomass developed previously (see chapter 6) was used in preference to the PVA type biomass pellets for the duration of this study, due to its superior metal accumulating properties and mechanical strength. The primary objectives of this investigation was to evaluate the biomass performance during the treatment of the industrial effluent and to compare the applicability of two types of bioremediation systems. Samples of water were obtained from several factories, but the particular waste water used in the present study (effluent A in chapter 6) was selected due to the number and levels of the metal species contained therein. Efficiency of metal biosorption and subsequent metal removal by the biomass was investigated using continuous-flow fixed bed and stirred bioreactors as single or multiple reactors which operated either independently or as part of a biphasic process. Comparative estimations of the efficiency of metal removal and the feasibility of industrial applicability were drawn between the two systems.

### **7.2. MATERIALS AND METHODS**

#### **7.2.1. ELECTROPLATING EFFLUENT**

The electroplating effluent (effluent A) was obtained from a factory operating three plating lines, viz. acid/zinc, zinc/cyanide and cadmium/cyanide lines. Run-off and discharge water from all three systems were combined prior to disposal, resulting in the discharge of an extremely toxic waste product. The levels of the respective metal ions varied depending on which process was being flushed out. Corresponding fluctuations in the pH of the raw effluent occurred. A pH range between pH 1.0 - 7.0 was noted.

The present waste disposal system is relatively primitive consisting of two compartmented tanks in series (Fig 7.1). These tanks are fed directly from the factory floor and serve as settling tanks for the precipitation of excess metal ions. The effluent undergoes no further treatment and the remaining liquor is flushed directly into the sewage disposal system. Sampling was conducted at two points

## 7. APPLICATION OF BIOSORPTION BY NON-VIABLE YEAST BIOMASS

along the waste disposal line. Initial samples were provided from the site where the raw effluent entered into the settling tanks (subsequently referred to as raw effluent) whilst the second samples were collected at the point where the waste water left the settling tanks prior to disposal in the sewage system (subsequently referred to as post settling tank (PST) effluent). The pH of the PST effluent ranged between pH 1.5 - 6.0. Depending on the nature of the raw effluent, varying concentrations of metal ions were precipitated in the slurry within the tanks, yet the level of the metal ions in the liquor frequently exceeded the permitted criteria (Table 7.1). Raw effluent was examined in the initial studies in order to determine whether bioremediation of this effluent would eliminate the need for settling tanks.

Table 7.1. Levels of metal (mg/l) present in raw and PST electroplating effluent compared to stipulated national drinking water and aquatic ecosystems criteria (median levels).

	Cu	Cd	Cr	Ni	Zn
Drinking water criteria	1.0	0.01	0.05	0.05	5.0
Dam/River water (aquatic life) criteria	0.005	0.003	0.05	0.05	1.0
Raw effluent	2.0 - 2.5	20 - 80	60 - 70	2.0 - 3.0	1000 - 3500
PST effluent	0.2 - 1.0	20 - 80	5 - 50	0.2 - 1.2	300 - 1500

### 7.2.2. CONTINUOUS-FLOW FIXED BED REACTORS

#### 7.2.2.1. PROCESSING OF RAW EFFLUENT

Using 2M KOH the pH of raw effluent (initial pH 1.5) was adjusted to pH 2.5, 3.5, 5.0 and 6.0 respectively to determine the pH optimum for the biomass under experimental conditions (pH optimum for metal biosorption from spiked aqueous solutions was previously established between pH 4.5 - 6.0). Precipitated matter (brought about as a result of increased solution pH) in the pH 5.0 and 6.0 solutions was allowed to settle out and subsequently discarded prior to use. The pH modification of the raw effluent served a dual purpose, not only to ascertain an optimum pH range for metal removal, but also to remove the excess metal ions present in solution.

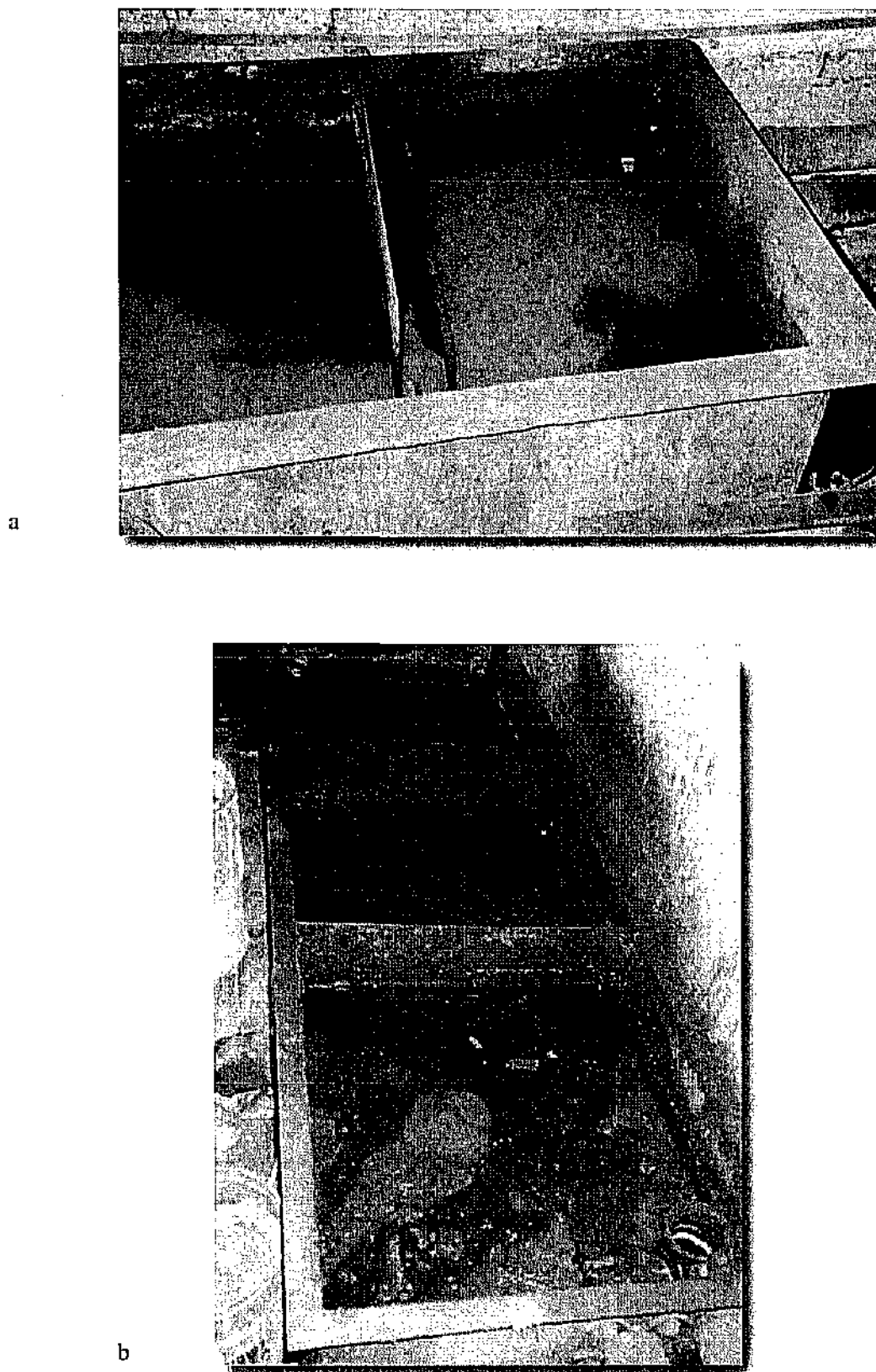


Fig 7.1. The waste water treatment tanks operated in the electroplating factory. Two sets of tanks were linked in series allowing precipitation of metals to occur (a-b). The difference in colour of the effluent is due to pH change. Note the precipitated sludge in the first tank.

## **7. APPLICATION OF BIOSORPTION BY NON-VIABLE YEAST BIOMASS**

The respective raw effluent solutions were pumped upwards through the PEI:GA biomass packed glass columns. Untreated raw effluent (pH 1.5) was used as the control. All experimental criteria, viz. dry wt (g) biomass used, biomass preparation and column volume and height remained identical to that described in section 6.2.3.1. The flow rate was maintained at 55 ml/hr, permitting a contact time in excess of 1 hr between the biomass and metal solution. The pH and metal content of the column eluant fractions were compared to those of the pre-column effluent.

### **7.2.2.2. DUAL COLUMNS IN SERIES**

1.4 l of pH 5.0 aw effluent (initial pH 2.23) was pumped through columns linked together in series with the eluant from column 1 fed directly to column 2. Both columns were identical with respect to dimensions and biomass load, and a flow rate of 55 ml/h was maintained. From column 2, 10 ml fractions were collected and the metal content and column pH profile analysed. The success of the metal removal in this and following systems was often gauged by the breakthrough volumes for Zn and Cd (based on the high levels of these metals within this solution and the extreme toxicity of Cd in solution).

### **7.2.2.3. SINGLE AND DUAL REACTOR TREATMENT OF PST EFFLUENT**

pH modification of the PST effluent used in this particular experiment was not required (influent pH 5.58). 1.4 l volumes of PST effluent were pumped through respective single and dual column systems (flow rate 55 ml/h). Column parameters and experimental criteria remained unchanged to previous experiments. Fractions of column eluant (10 ml) were collected and analysed accordingly.

### **7.2.2.4. PROCESS SCALE UP: EXPERIMENTAL PARAMETERS**

Perspex LKB Chromatography columns were adapted (silicon sealed and water-proofed) to fulfill the necessary requirements. The columns had an internal diameter (ID) of 3.7 cm, column height of 30 cm and total volume of 325 ml.

Three columns were run, each differing with respect to the biomass load, viz. 85, 90 and 95 g (dry wt). Prior to packing, the biomass was rehydrated and rinsed three times using Milli-Q water. The wet pellets were contained within the column by two fine mesh sieves to prevent fouling of the inlet

## **7. APPLICATION OF BIOSORPTION BY NON-VIABLE YEAST BIOMASS**

and outlet ports. The influent pH values of each of the columns ranged from pH 5.3, 5.26 to 5.05. PST effluent (5.0 l) was pumped upwards through the fixed beds at a flow rate of 4.5 l/hr, and 10 ml fractions were collected every 200 ml and analysed for metal content and pH.

### **7.2.3. CONTINUOUS-FLOW STIRRED BIOREACTORS**

#### **7.2.3.1. BIOREACTOR DESIGN**

Cylindrical bioreactors made from perspex served as reactor tanks. All three bioreactors were of identical dimensions, each containing a single inlet port at the base of the tanks and three outlet ports at calibrated 2.5 l volumes. The height of the bioreactors measured 430 mm, ID 172 mm and contained a total volume of 10.0 l. The design of the tanks enabled operation at 2.5, 5.0 and 7.5 l capacity thereby facilitating scale-up. The reactor tanks were not sealed entities allowing easy access to the biomass and enabling constant top-stirring thereof (60 - 100 Upm).

#### **7.2.3.2. SINGLE BIOREACTOR SYSTEM**

7.0 l of PST (initial pH 1.98, final KOH-modified PST pH 5.0) was pumped through the bioreactor containing 100 g (dry wt) of washed biomass. A flow rate of 5.0 l/hr was established and entry into the tank was facilitated via the bottom port. The tank was operated at 2.5 l capacity with continuous stirring. 10 ml fractions were collected from every 0.1 l of eluant for the first 3 l and subsequently from every 0.5 l. These fractions were analysed with respect to pH change and metal content using the standard protocol in order to determine the metal loading capacity and breakthrough volumes of the bioreactors.

To determine the effect of scale up on the operating efficiency of the biomass, the experiment was repeated using 200 g (dry wt) of biomass and 5.0 l capacity of the bioreactor. 9.5 l of PST, pH 6.0 (initial pH 1.93) was pumped through the system at the set flow rate of 5.0 l/hr. The collection and analysis procedure of the fractions proceeded as before. Due to the decline in efficiency of metal biosorption brought about by increasing the bioreactor volume, the bioreactor was not operated at its full capacity (7.5 l).



#### **7.2.3.3. DUAL BIOREACTORS LINKED IN SERIES**

The development of a dual bioreactor system required the eluant from tank 1 to be pumped directly into tank 2. Sampling points were established at the outlet ports of both tanks where 10 ml fractions were collected at 0.5 l intervals and analysed accordingly. The influent pH of the PST effluent was maintained at pH 6.0 (initial pH 2.02 - 2.43) and the operating capacity of tank 1 at 5.0 l, whilst that of tank 2 was increased from 2.5 l to 5.0 l after the initial experiment in order to establish its metal loading capacity. This operating capacity was maintained for subsequent experiments.

The breakthrough volume of tank 1 and effect of biomass replacement therein on the total metal removal required large influent volumes of PST to be pumped through the system. 10.0 l was sampled from both tanks with sampling occurring every 0.5 l. To determine the effect of biomass substitution on the total metal removal, the biomass in tank 1 was replaced subsequent to collecting every 4.5 l of eluant. A total of 20.0 l was pumped through the system, necessitating 4 biomass changes.

#### **7.2.3.4. DETERMINATION OF MAXIMUM LOADING CAPACITY**

The evaluation of the performance of the bioreactor system necessitated the introduction of a third tank to ascertain its efficiency as a scavenger tank in removing the remaining metals from solution. Two variations of the system were tested, each containing triple bioreactors linked in series (Fig 7.2).

In system 1 each of the tanks was operated at 2.5 l (200 g biomass (dry wt)) capacity. 55 l of influent PST was prepared to pH 5.4, yet due to the residual volumes remaining within each of the tanks only 40 l of effluent was sampled from each bioreactor. The biomass in tank 1 was replaced with fresh material subsequent to every 5.0 l of eluant collected. Biomass replacement in tank 2 occurred at the onset of saturation (approximately 22.0 l), with the biomass from the second bioreactor being replaced with that from tank 3. Tank 3 was supplied with freshly prepared biomass.

## 7. APPLICATION OF BIOSORPTION BY NON-VIABLE YEAST BIOMASS

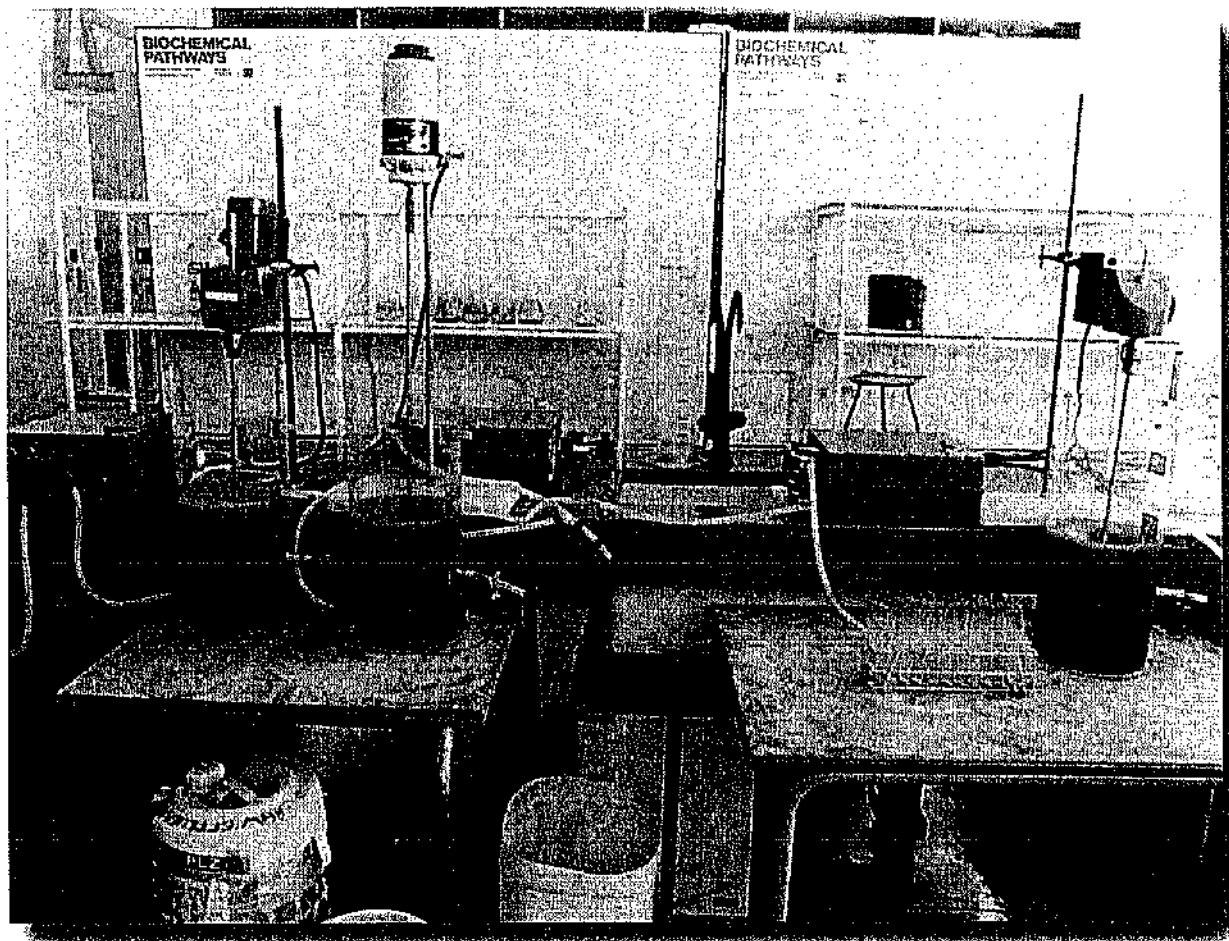


Fig 7.2. The continuous-flow stirred tank bioreactor system. Three bioreactors operating at 5.0 l capacity were linked together in series, with the eluant from one tank being fed directly into the next. Sampling points were established at the outlet of each of the bioreactors.

The experimental criteria for system 2 remained unchanged though changes to the influent pH (pH 4.5) and biomass substitution in this reactor were implemented. At the onset of saturation in tank 2 (22.0 l), the biomass was replaced with fresh material whilst that in tank 3 remained unchanged. 75.0 l of PST effluent was prepared with 40 l being sampled from each of the tanks. The remainder of the effluent was lost either due to pH induced precipitation or as residual fluid in the bioreactors. A crucial step in the success of both bioreactor systems was the washing procedure of the biomass prior to bioaccumulation. Extensive washing and rinsing of the biomass in Milli-Q water was required to remove the residual alkali from the PEI:GA pellets. In the presence of very high alkalinity flocculation and precipitation occurred within the tanks.

### 7.3. RESULTS

#### 7.3.1. CONTINUOUS-FLOW FIXED BED REACTORS

##### 7.3.1.1. SINGLE AND MULTI-PHASED RAW AND PST EFFLUENT TREATMENT

##### 7.3.1.1.1. RAW EFFLUENT

Fixed bed bioreactors can be operated either independently as in this study or as the second phase of a biphasic process, where the biological phase was preceded by the initial chemical phase involving pH modification of the raw effluent. Chemical modification served a dual purpose, viz. priming of the effluent for further use and the precipitation of excess metals. The increase in the pH of the effluent resulted in the decrease in solubility of the metal ions in solution and caused the subsequent precipitation of the metals predominantly as insoluble hydroxides (181), eg. at pH 5.0 and 6.0 (Table 7.2). The increase of influent pH decreased the influent metal concentration and thereby correspondingly extended the lifespan of the column biomass prior to breakthrough occurring.

Table 7.2. The effect of pH on the metal concentration of the influent raw effluent and the resultant breakthrough volumes (BV) in each of the small-scale single columns. Due to variations in the initial metal ion concentrations the metal levels are expressed as % of the initial concentrations. The breakthrough volumes (l) reflects the carrying capacity of the columns. The effluent was run through single columns.

	Cu		Cd		Cr		Ni		Zn	
	%	BV (l)	%	BV (l)	%	BV (l)	%	BV (l)	%	BV (l)
Raw effluent (pH 1.45)	100	0.16	100	0.13	100	0.45	100	0.14	100	0.12
pH 2.5	99	> 0.3	99.8	0.21	100	0.27	98.2	0.25	99.8	0.19
pH 3.5	79.7	> 0.3	94.5	0.22	100	0.30	87.2	0.28	99.8	0.19
pH 5.0	63.2	> 1.1	95.9	0.5	20.5	> 1.1	96.3	> 1.1	89.2	0.46
pH 6.0	25.6	> 1.1	98	0.48	0.0	> 1.1	87	> 1.1	82	0.46

## **7. APPLICATION OF BIOSORPTION BY NON-VIABLE YEAST BIOMASS**

From Table 7.2 it is apparent that pH and metal concentration are closely related to breakthrough volumes. Adsorption increased with increasing pH until a pH plateau was reached and subsequently the breakthrough volume of the columns remained unchanged over the volumes measured, regardless of fluctuations in pH, eg. pH 5.0 and 6.0. From preliminary batch reaction studies (results not reported) it was determined that the plateau was not unlimited, but for most metals probably extended between pH 5.0 - 7.0, after which a decline occurred in the amount of metal accumulated. The results presented in Table 7.2 were obtained from separate experiments. Initial experiments were run using smaller influent volumes of effluent and based on the results obtained from these experiments, larger influent volumes were used for subsequent experiments. Consequently instances where breakthrough volume has not yet been attained, (eg. Cu, Cr and Ni) indicate that breakthrough had not been reached for the total volume of effluent used.

Since optimal operating conditions for the treatment of raw effluent were achieved between pH 5.0 and 6.0, the feasibility of using influent raw effluent instead of PST effluent in a biphasic system had to be considered. The precipitation of metals from raw effluent due to alkali treatment was therefore compared to the effectiveness of metal removal in the settling tanks (PST effluent) (Fig 7.3). Though the initial concentration of metals in both solutions varied (Table 7.1), the data in Fig 7.3 represents the general trend of metal removal by pH adjustment or settling. Although the PST effluent used in Fig 7.3 had an influent pH of 4.6, the pH values for PST effluent ranged between pH 1.5 - 6.0. However, the data shown in Fig 7.3. is representative of all the PST effluents. With the exception of Cd, the amount of metal precipitated out from the raw effluent by the settling tanks exceeded the metal removal by the chemical treatment. 99.2% of Cr was removed from the raw effluent by settling, thereby almost totally eliminating it as a problem metal whilst Cu, Ni and Zn removal in the settling tanks varied between 60 - 85%. The amount of Cd in the PST solution actually exceeded the initial levels from the raw effluent by 1.5 times due to conditions within the settling tanks enabling the mobilization of sludge Cd into solution, and thereby compounding the problem of removing this metal.

## 7. APPLICATION OF BIOSORPTION BY NON-VIABLE YEAST BIOMASS

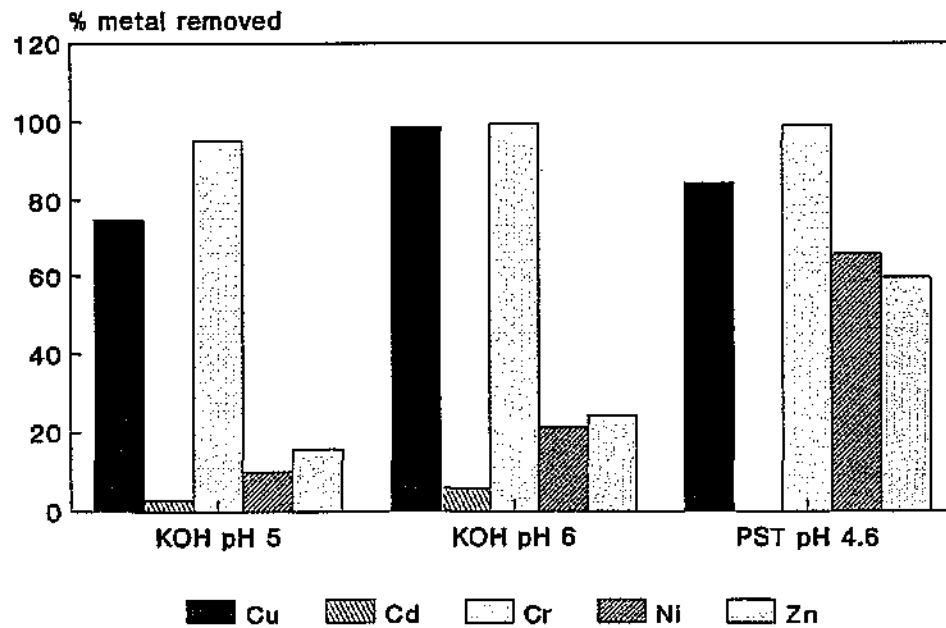


Fig 7.3. Comparison between alkali (KOH) treatment and settling tanks as a means of precipitating out excess metal from raw effluent. Levels of Cd in PST were 1.5 times higher than those in the raw effluent.

The introduction of a second column into the system had a minimal effect on the breakthrough volume or the amount of metal removed from the raw effluent (Fig 7.4). The onset of breakthrough (*ie.* 80% removal of metals) of Zn occurred at 400 ml and that of Cd at 520 ml compared to 460 ml for Zn and 500 ml for Cd in a single column (Table 7.2). This suggests a change in the metal chemistry in the solution, which lowers the affinity of the biomass in the second column for the metals.

## 7. APPLICATION OF BIOSORPTION BY NON-VIABLE YEAST BIOMASS

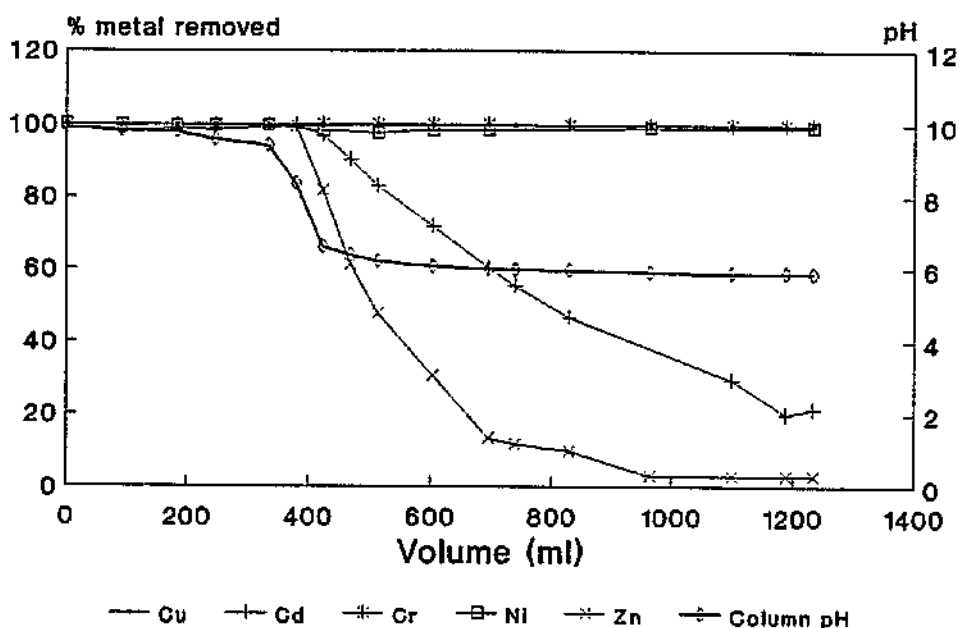


Fig 7.4. Metal removal from raw effluent (pH 5.0) using dual bioreactor columns linked in series.

### 7.3.1.1.2. PST EFFLUENT

Appropriate treatment of the PST effluent was determined by the influent pH. High acidity ( $\text{pH} < 4.5$ ) necessitated chemical priming using KOH, whilst an influent  $\text{pH} > 4.5$  enabled the implementation of a single phase system (*ie.* no chemical treatment).  $\text{pH} 4.5$  was selected as the cut-off pH for chemical treatment, since even mild alkali modification at this influent pH resulted in a large increase in the alkalinity of the system. The onset of breakthrough occurred at 400 ml for Cd and Zn from untreated PST effluent ( $\text{pH} 4.5$ ) pumped through a single column (Fig 7.5). The amount of metal removed was increased by the introduction of a second column into the system (Fig 7.6). Constant operating efficiency of the first column was assumed to occur in the dual column system, thereby implying a lower operating efficiency for the second column. The cumulative effect of both columns resulted in 80% removal of Cd and Zn occurring for 630 and 550 ml effluent respectively. However, the residual level of these two metals in the processed solutions, *viz.* 9.76 mg/l of Cd and 106 mg/l for Zn still remained in excess of the stipulated water quality criteria.

# 7. APPLICATION OF BIOSORPTION BY NON-VIABLE YEAST BIOMASS

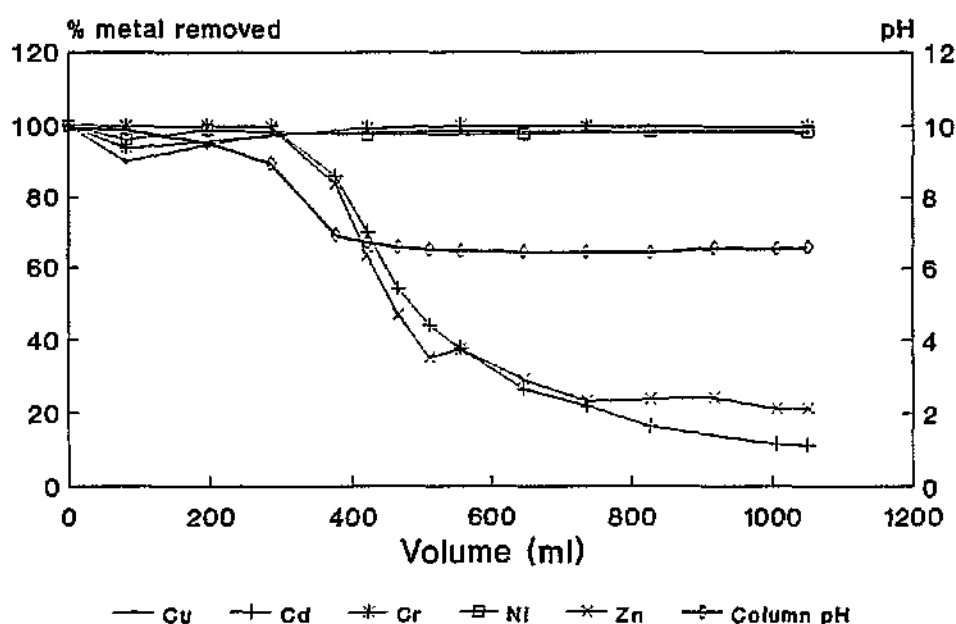


Fig. 7.5. Metal removal from PST effluent (pH 4.5) using a single column system. No prior chemical modification of the effluent was necessary.

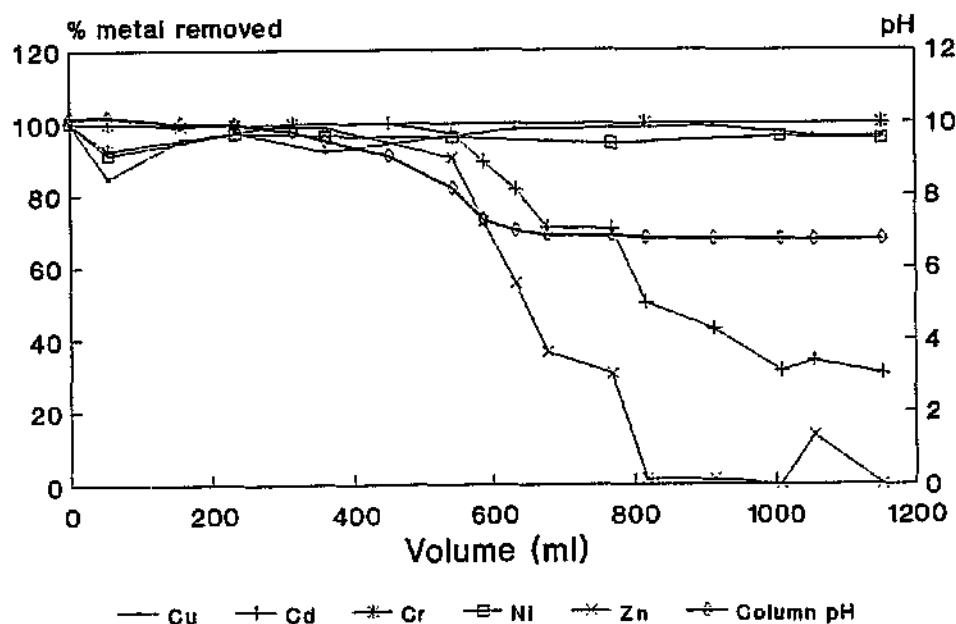


Fig 7.6. Metal removal from PST effluent (pH 4.5) using dual columns in series. No prior chemical modification of the effluent was necessary.

**7.3.1.2. PROCESS SCALE UP**

Using PST effluent, scale-up of fixed bed columns from a 40 ml (10 g (dry wt)) capacity to a column capacity of 325 ml (85 - 95 g (dry wt)) failed to produce any corresponding increase in metal removal (Cd used as a standard) (Table 7.3). Similar to smaller scale columns, the decline in metal accumulation was influenced by the pH profile within the columns with breakthrough occurring due to a drop in the pH of the column effluent. Furthermore, total biomass contained within the columns, column performance and biomass characteristics under operating conditions also influenced the breakthrough volumes.

Table 7.3. The effect of process scale-up on the breakthrough volumes and final concentrations of Cd in solution. The breakthrough volumes (BV) were predominantly affected by the biomass capacity of the column.

Column No.	Biomass (g (dry wt))	BV (l)	Final [Cd] (mg/L)
1	10	1.1	45.6
2	85	4.3	46.0
3	90	3.5	48.5
4	95	4.0	46.7

Several problems were experienced during process scale-up. The column containing immobilized biomass was unable to maintain its integrity under high pressure (created by the flow rate of 4.5 l/hr), resulting in compacting and channelling of the biomass. Compacting was not alleviated by the upward flow of the effluent or by increasing the amount of biomass contained within the column. A cut-off point for the biomass loading capacity and flow rate of the column existed, beyond which counter pressure developed, resulting in leakage of the column.

**7.3.2. CONTINUOUS-FLOW STIRRED BIOREACTORS**

Pretreatment of the PST effluent proved to be an integral part of the process in these experiments, since PST effluent in these studies was pH 1.98. Not only did this prime the effluent for further treatment, but also resulted in the removal of metal, eg. 67% of Cu, 5% of Cd, 99.5% of Cr, 15%



## 7. APPLICATION OF BIOSORPTION BY NON-VIABLE YEAST BIOMASS

of Ni and 26% of Zn removal was achieved through KOH precipitation (typical results from 6 experiments). The minor metals, viz. Cu, Cd and Ni responded well to this treatment, but due to the excessive levels of Zn in the effluent, the residual amount of Zn in the influent solution averaged 850 - 1000 mg/l and Cd 40 - 60 mg/l.

### 7.3.2.1. BIOREACTOR EFFICIENCY

The reactor volume and proportional amount of biomass contained therein, influenced the amount of metal removed from solution (Table 7.4). Though the total amount of metal removal increased, the efficiency of metal removal in the 5.0 l tank depended on the initial concentration and the metal species in question. For example, Cu and Zn removal increased threefold, yet Cd accumulation was limited to approximately 61% of the potential removal capacity and no increase in Ni removal occurred.

Table 7.4. Comparison between the efficiency of metal removal by 2.5 l and 5.0 l tanks. The amount of metal removed is expressed as % of modified PST effluent, and was determined subsequent to 4.0 l of effluent being processed by each of the bioreactors.

	Cu	Cd	Cr	Ni	Zn
2.5 l tank	22.0	25.7	93.3	87.3	22.4
5.0 l tank	77.2	41.5	99.9	83.2	74.1

By increasing the bioreactor volume, yet maintaining the flow rate as in the above experiment, the contact time between the biomass and effluent was extended to ensure maximum metal removal. Batch studies (data not shown) have however indicated that the majority of metal absorption occurred within the first 10 min. For example, in batch studies 82% of Cd was removed within 10 minutes, whilst after an hour only 85% of removal had been achieved. Thus in larger volume bioreactors, the flow rate can be increased, without negatively effecting the amount of metal removed, thereby increasing the operational efficiency of such a system.

### 7.3.2.2. DUAL BIOREACTORS IN SERIES

The decline in efficiency of removal of certain metals, eg. Cd and Ni with increased bioreactor

#### 7. APPLICATION OF BIOSORPTION BY NON-VIABLE YEAST BIOMASS

capacity, reduced the feasibility of operating the bioreactor to at its full capacity (7.5 l). Operating a second bioreactor coupled in series provided a more efficient alternative. Though the majority of the metal removal occurred in tank 1 (Table 7.5), optimum metal removal was achieved by operating both tanks at 5.0 l capacities.

Table 7.5. Comparison of efficiency of metal removal from PST effluents between two dual bioreactor systems, viz. 5.0 l and 2.5 l or 2 x 5.0 l tanks. Total metal removal from PST effluent and the metal concentrations (mg/l) of the influent and eluant solutions was measured. % metal removal and metal concentration were determined after 5.0 l of effluent had been processed.

	Cu	Cd	Cr	Ni	Zn
(%) of metal removal by Tank 1	52.9	39.9	62.2	74.6	47.1
(%) of metal removal by Tank 2 (2.5 l)	-	22.9	12.5	8	22
(%) of metal removal by Tank 2 (5.0 l)	-	34	33.7	13	28
Total removal (%) by 5.0 + 2.5 l system	94	69.2	99.9	83.5	76.1
Total removal (%) by 2 x 5.0 l system	94.8	72.2	99.9	90.6	85.6
[Metal] in influent PST (mg/l)	0.078	58.9	0.066	0.361	809
[Metal] in eluant of 5.0 + 2.5 l system (mg/l)	0.039	19.2	0.006	0.07	279
[Metal] in eluant of 2 x 5.0 l system (mg/l)	0.04	17.2	0.005	0.037	171

With the exception of Cd and Zn, the metal levels in the eluants of both systems fulfilled the required drinking water criteria. Removal of Cd and Zn from PST effluent ranged between 69 - 72% for Cd and 76 - 86% for Zn.

## 7.3.2.3. BREAKTHROUGH DETERMINATION

The onset of breakthrough for Cd and Zn in tank 1 occurred between 4.5 - 5.0 l, depending on the influent concentrations of these metals (Fig 7.7). At this stage approximately 60% of Cd and 70% of Zn are removed from the effluent. The estimated breakthrough volume of tank 2 was 22 - 25 l depending on the influent Cd and Zn levels. The implementation of biomass substitution in tank 1 extended the lifespan of the second bioreactor. (Data relevant to this is shown in the following section) Subsequent to processing 20.0 l, 99.5% Cd and 98% Zn removal was still being achieved in the second reactor.

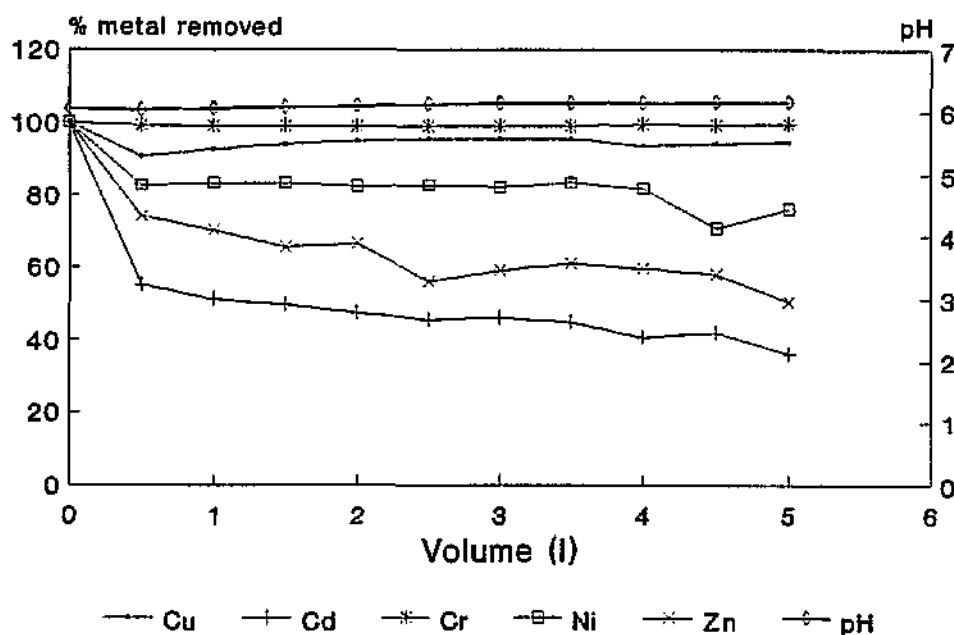


Fig 7.7. Biomass saturation and resultant breakthrough volume of tank 1 in a dual tank system. Depending on the influent concentrations the breakthrough volume of this tank was established between 4.5 - 5.0 l.

### 7.3.2.3. PROCESS SCALE UP

Process scale up involved the introduction of a third bioreactor into the bioremediation system. The first bioreactor was retained as the primary site for metal removal from the PST effluent, whilst the second tank removed the majority of the remaining cations from solution. The aim of a third tank was to provide a scavenging unit to remove the metal still in the water, thereby producing an eluant which complied with the water quality criteria.

The implementation of the third bioreactor within the system, however, had a minimal effect on the efficiency of metal removal and subsequently the total amount of metal removed (predominantly Cd and Zn) from the effluent (Fig 7.8 - 7.10). The majority of metal removal occurred in tank 1, whilst metal removal in tank 2 remained very similar to that attained by the second reactor in a dual reactor series. Fluctuations in the levels of Zn and Cd and to a lesser extent of Ni and Cu in tank 1 indicated the pattern of biomass saturation. The replacement with fresh biomass in tank 1 after every 5.0 l of influent solution resulted in an immediate increase in the amount of metal removal (Fig 7.8). A similar effect was noted in tank 2, where the replacement of the saturated biomass with fresh biomass after 22.0 l resulted in a 22% increase in Zn and 16% increase in Cd accumulation (Fig 7.9). Substitution of the biomass in tank 3 (result obtained from system 1, section 7.2.3.4.- not shown) had no effect on the metal removal in this tank. The trend of metal removal in tank 3 remained similar to that of the unsubstituted tank (Fig 7.10).

The efficiency of Zn and Cd accumulation by the first two tanks complemented each other (Fig 7.11 and 7.12). Zn and Cd accumulation in tank 2 was low when the biomass in tank 1 had been replaced with fresh material. Saturation of this biomass resulted in the biomass of tank 2 accumulating greater quantities of Cd and Zn. This phenomenon was more apparent for Cd accumulation (Fig 7.11) than for Zn removal (Fig 7.12). Replacement of the saturated biomass of tank 2 with that from tank 3 had only a marginal effect on the amount of Zn accumulated (the biomass in tank 3 was replaced with fresh biomass - results not shown). Ni removal within tank 2 was low, yet still remained within the stipulated criteria for drinking water (Fig 7.13). The nominal amount of metal accumulated in tank 3 reduced the feasibility of replacing the biomass in this tank. The most feasible option may be to utilize the biomass in tank 3 until the onset of saturation, whilst replacing the saturated biomass in tank 2 with fresh biomass.

## 7. APPLICATION OF BIOSORPTION BY NON-VIABLE YEAST BIOMASS

The implementation of a third tank in the process failed to produce waste water containing Cd and Zn within the stipulated drinking water criteria, though on average only 18% of the initial Zn and 17% of the initial Cd remained in solution after 40.0 l of the effluent had been processed. Although only 2 - 5% removal of Cu, Cr and Ni was achieved by tank 3, this was adequate for the concentration of these metals to fall within the drinking water standards. This decreased accumulation in tank 3 was thought to be a consequence of the change in the solution chemistry of the effluent. Exposure of the effluent to the biomass in the first two bioreactors resulted in an increase of eluant solution pH ( $> \text{pH } 7.5$ ) and subsequently a change in metal chemistry and a decline in metal sorption. Extensive washing of the biomass contained in tank 2 and 3 with Milli-Q water prior to implementation in the system appeared to reduce the pH induced effect.

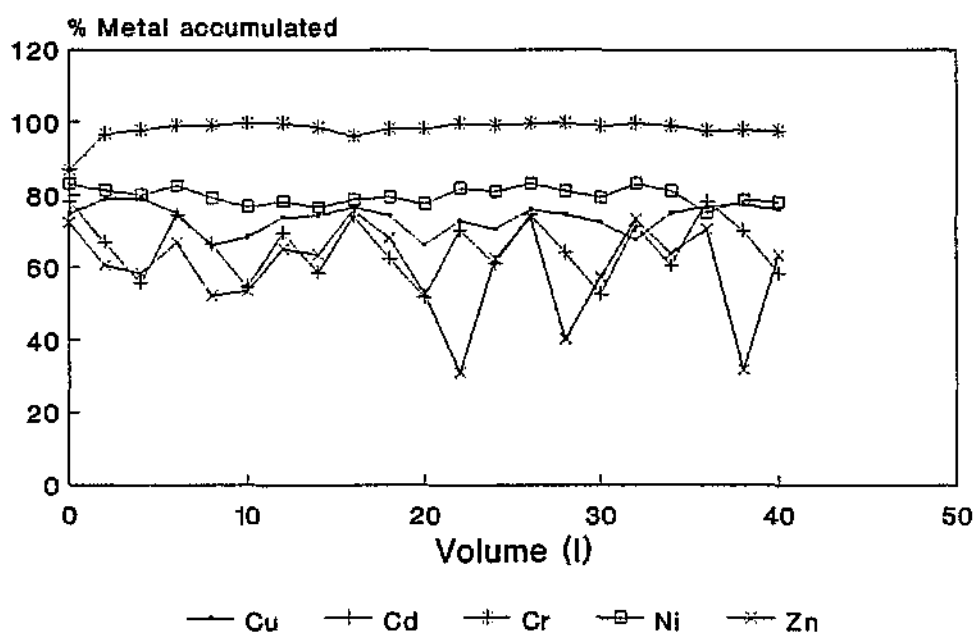


Fig 7.8. Metal accumulation from PST effluent by tank 1 (of a set of triple tanks linked in series). The % metal removed from solution fluctuated depending on the extent of biomass saturation and subsequent replacement with fresh biomass (after every 5.0 l of effluent processed).

## 7. APPLICATION OF BIOSORPTION BY NON-VIABLE YEAST BIOMASS

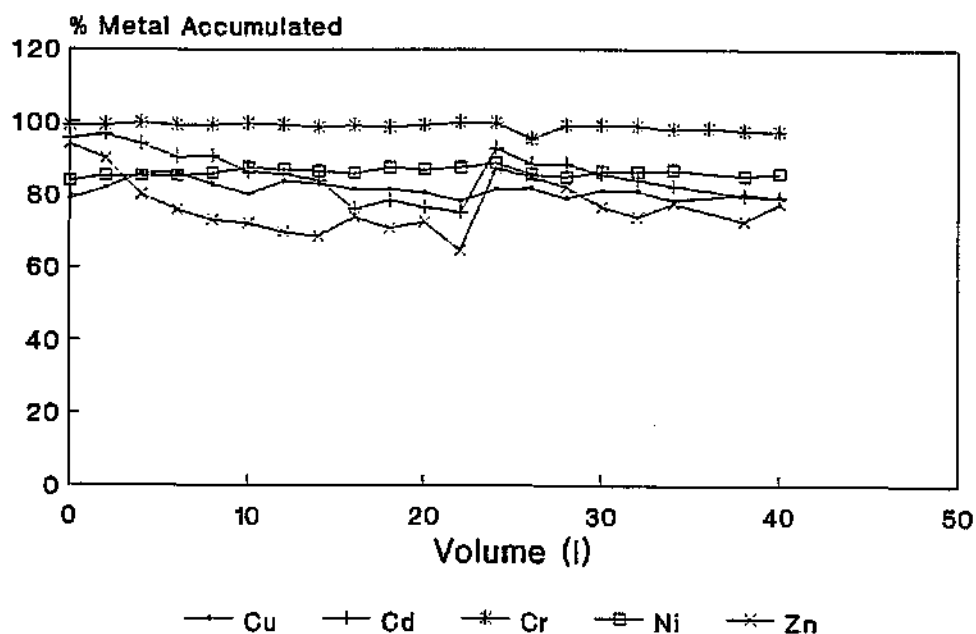


Fig 7.9. Metal removal from PST effluent in tank 2 (triple tanks linked in series). Note the increase in Zn and Cd removal in the presence of fresh biomass (22.0 l).

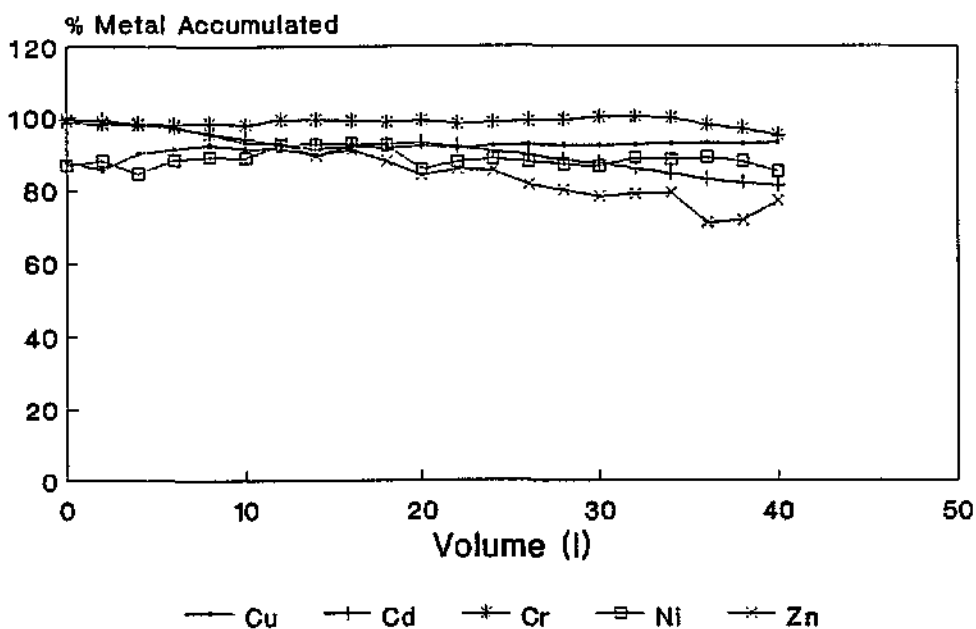


Fig 7.10. Metal removal from PST effluent in tank 3 (triple tanks linked in series). No biomass substitution occurred in the tank.

# 7. APPLICATION OF BIOSORPTION BY NON-VIABLE YEAST BIOMASS

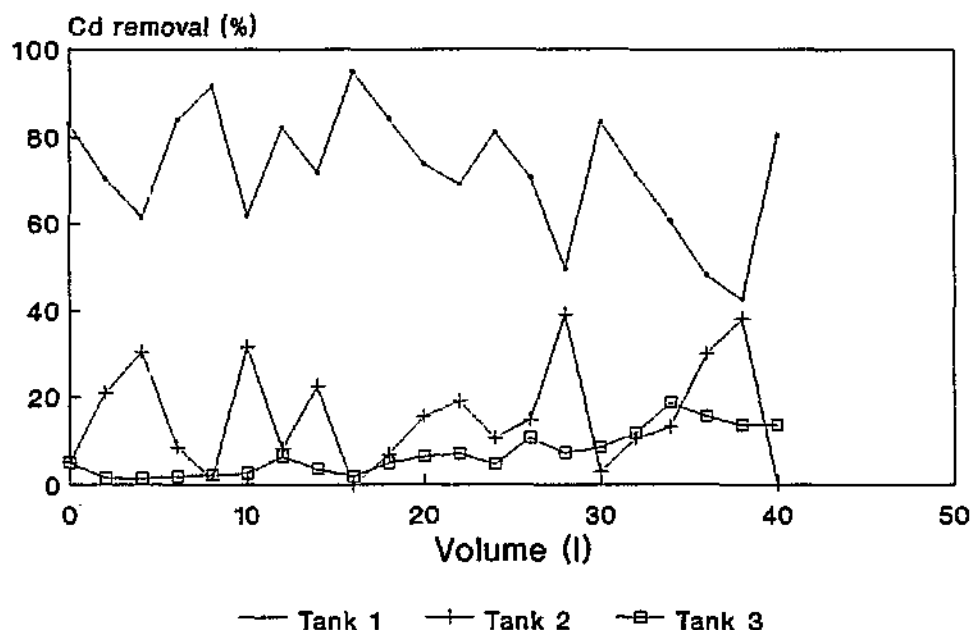


Fig 7. 11. Comparison of the efficiency of Cd removal from the initial influent PST solution by each of the bioreactor tanks. The concentration of Cd in the eluant of the tanks 1,2 and 3 after 40.0 l of PST had been processed was: 19.21 mg/l (tank 1), 9.62 mg/l (tank 2) and 8.64 mg/l (tank 3).

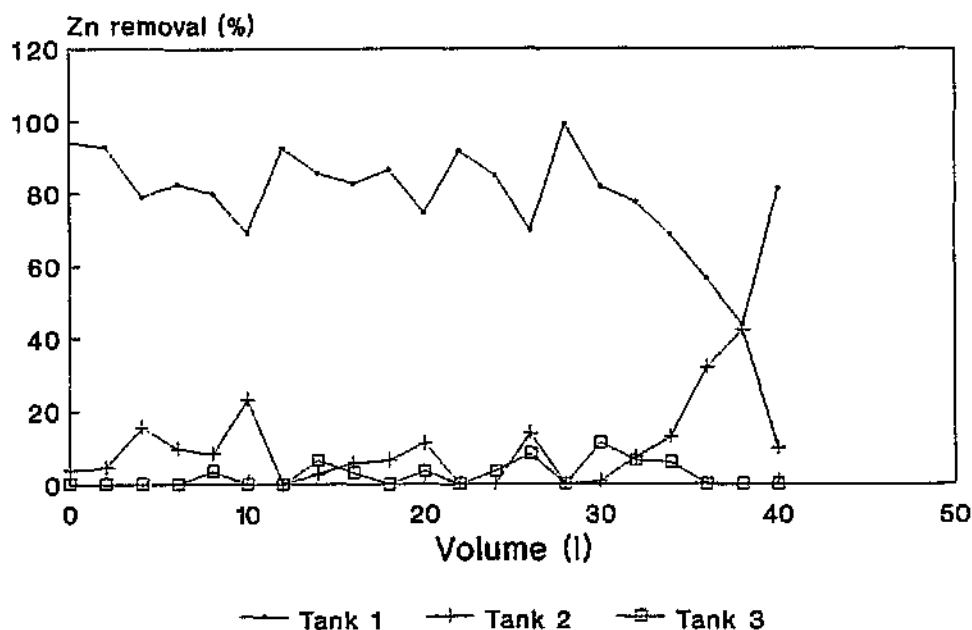


Fig 7.12. Comparison of the efficiency of Zn removal from the initial influent PST solution by each of the bioreactor tanks. The concentration of Zn in the eluant from tanks 1,2 and 3 after 40.0 l of PST had been processed was: 279 mg/l (tank 1), 170 mg/l (tank 2) and 164 mg/l (tank 3).

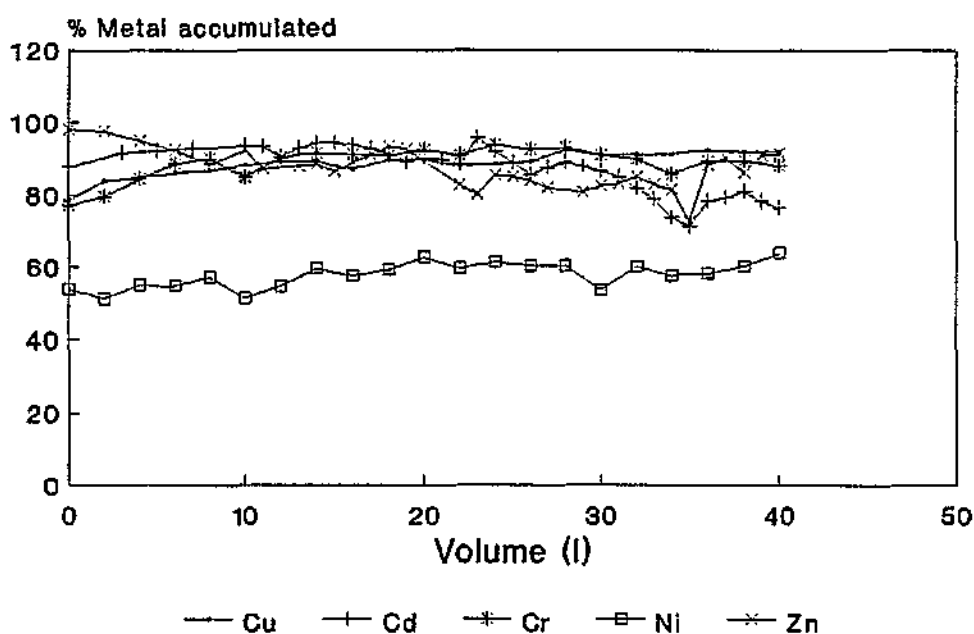


Fig 7.13. Comparative metal accumulation from PST effluent in tank 2 (triple tanks linked in series). The biomass in tank 2 was replaced by that from tank 3 after 22.0 l.

#### 7.4. DISCUSSION

Though chemical precipitation has remained one of the most widely used processes for the removal of metal contaminants from waste waters, depending on the initial metal concentration it is not always capable of achieving sufficiently low levels of metal in the effluent (144). Similarly most biosorbents have only been effectively applied in the treatment of low-concentration, high-volume metal containing waste water (202). Subsequently when faced with high-concentration, low-volume metal containing waste water, eg electroplating effluent the problem is compounded. The implementation of a combined biphasic metal removal system, consisting of primary phase chemical modification followed by a secondary phase bioremediation process offers advantages to both systems.

The results from this study indicate that the primary phase involving the chemical modification of



## 7. APPLICATION OF BIOSORPTION BY NON-VIABLE YEAST BIOMASS

the effluent serves a dual purpose. The addition of KOH to the solution results not only in the precipitation of excess metal ions, but due to the low initial pH of the effluent, it serves to prime the effluent for the secondary bioremediation phase. The optimum pH for metal biosorption by PEI:GA biomass occurs between pH 4.5 - 6.0 (see chapter 6). At these pH levels the solubility of the metals decreases and they precipitate out predominantly as insoluble hydroxides, thereby presenting a more dilute solution for treatment. Though both PST and raw effluent can be treated with alkali to decrease levels of the metal in solution, greater amounts of metal are removed from the raw effluent by the settling tanks than by KOH. Biphaseic treatment of PST in an industrial scheme therefore remains preferable to using modified raw-effluent.

Two alternatives can be considered in the implementation of the secondary stages of the bioremediation process, *viz.* continuous-flow fixed bed reactors or continuous-flow stirred tank reactors. Both are application orientated systems, capable of accumulating metal ions from solution, yet differ with respect to mode of action and performance. Small scale fixed bed reactors allow efficient utilization of the sorbent, due to the improved flow of the effluent through the columns. Using these reactors, the efficiency of metal removal in this study largely depended on the chemistry of the influent solutions and the fixed-bed characteristics. Metal removal from acidic effluent solutions was poor with breakthrough occurring at low volumes, whilst low efficiency can also be attributed to loosely packed columns (data not shown). Correct packing of the column ensures even dispersion of the effluent solution throughout the column. To increase the amount of metal removed from aqueous systems two possibilities can be considered, *ie.* the introduction of a second column into the circuit or secondly, process scale-up. Depending on the nature of the influent solution the introduction of a dual column system can increase the total amount of metal removed from the effluent, though the operational efficiency of the second column may be less than the original column, or in some instances may have no additional effect on removal of a particular metal.

Process scale-up of fixed bed reactor systems did not provide the most effective solution to waste water treatment. Increasing the bed depth of the column by increasing the amount of biomass contained within the column extended the breakthrough volume of the column. Although the breakthrough volume is dependent on the amount of biomass contained therein, the operating efficiency of these columns was extremely low, and was not proportionally increased to that of the smaller scale columns. Compacting and channelling of the biomass occurred within the larger bioreactor columns. Both of these conditions decrease the available surface area of the biosorbent,

## 7. APPLICATION OF BIOSORPTION BY NON-VIABLE YEAST BIOMASS

thereby affecting the ratio of binding ligands : metal ions, which negatively affects the sorption kinetics. In addition, compacting of the biomass causes build-up of counter pressure within the column. To minimize the effect of compacting and channelling, columns of short bed depths with lowered contact time could be utilized.

The alternative to fixed-bed continuous-flow systems, *ie.* continuous-flow stirred tank reactors were more suited to larger scale processes due to the simplicity of the system and the ease with which scale up was achieved. Although scale-up within this system resulted in a slight decline in the overall efficiency of metal removal occurring, this decline is negligible when compared to the efficiency of scale-up of the previous system. Greater efficiency of metal removal is achieved through operating the multiple bioreactors in series at lower operating capacities (5.0 l) in preference to a single bioreactor at maximum capacity (7.5 l). A circuit containing dual bioreactors, operating at 5.0 l capacity and linked in series is more efficient with regard to metal removal than a circuit containing triple bioreactors operating at the same volume. Sorption of the majority of the metals occurs in the first two bioreactors with the third tank appearing to be incapable of removing the remainder of the residual Zn and Cd. A second tank, operating at maximum capacity (7.5 l, 300 g biomass (dry wt)) remains a possibility instead of coupling a third bioreactor to the system.

The majority of metal sorption occurs in the first bioreactor though the onset of biomass saturation takes place at low eluant volumes (4.5 - 5.0 l). Immediate replacement of the saturated biomass with fresh material extends the lifespan of the second bioreactor, resulting in the 200 g (dry wt) of PEI:GA biomass in the bioreactor being capable of treating 22 - 25 l of effluent prior to breakthrough occurring. Though the eluant produced by a dual reactor circuit contained levels of Cu, Cr and Ni within the required levels, the amounts of Cd and Zn remained in excess of required standards for both dual and triple bioreactor systems *ie.* 171 and 174 mg/l for Zn and 8.65 and 17.2 mg/l for Cd. The inability of the unsaturated biomass in the second and third bioreactors to remove significant amounts of metals once again appears to originate from a pH change and change in the solution chemistry of the effluent. Overcoming these problems requires the pH of the reactor eluants to be maintained within the optimum adsorption range of the PEI:GA biomass (*viz.* pH 4.5 - 6.0), or alternatively the implementation of a third type of phase within the circuit such as the use of another type of biosorbent in the system.

Though both of the secondary phase bioremediation systems are capable of removing metal ions from

## **7. APPLICATION OF BIOSORPTION BY NON-VIABLE YEAST BIOMASS**

electroplating waste solutions, several factors define their applicability on an industrial scale. Prior to implementation of either of these systems, the economic feasibility of the initial outlay and subsequent maintenance costs has to be assessed. The cost of implementing these systems will have to be compared to the operating efficiency and percentage metal removal attained. The efficiency of metal removal by small scale fixed-bed continuous flow reactor columns exceeds that of stirred continuous flow tanks, yet several limitations regarding the biomass characteristics (eg. compacting and channelling within the columns) and column parameters (low flow rate, long contact periods) negatively influenced the metal removal in columns from larger volumes. In contrast continuous-flow stirred bioreactor tanks can operate efficiently under a wide range of conditions. Due to the short contact time required for maximum metal-biomass interaction, the flow rate of these systems can be altered without negatively influencing the biomass sorption characteristics. Scale-up of the bioreactor tanks is easily facilitated with a minimal loss of efficiency of metal removal. An additional advantage of stirred reactor tanks is the short contact time required for metal sorption to occur, with the majority of metals being removed within the first 10 min. Moreover constant exposure of the biomass to the effluent solution and resultant increased biosorption is achieved by constant stirring of the biomass-effluent solution, although the cost of providing stirrers and their operation will need to be taken into account.

Metal ion removal from PEI:GA biomass can be achieved through effective desorption methods, eg. EDTA (see chapter 6), though due to environmental considerations mild acidic solutions, eg. inorganic acids (HCl) or organic acids eg. lactic acid are predominantly used. The desorbed biomass can be readily regenerated and utilized effectively in bioreactor tanks. Both packed bed and stirred continuous flow reactor tanks would be able to utilize this regenerated biomass, especially in scavenger bioreactors.

### **7.5. CONCLUSIONS**

While the metal accumulating ability of PEI:GA biomass had already been proven, its efficiency as an industrial applicant remained unknown. Successful metal biosorption was achieved from high-concentration solutions in the present study, though the efficiency of metal removal improved when PEI:GA biosorption was implemented as part of a biphasic and not a single phase remediation system. The initial phase requires chemical treatment in order to precipitate excess metals out of solution and

## 7. APPLICATION OF BIOSORPTION BY NON-VIABLE YEAST BIOMASS

to prime the effluent for bioremediation. Although alkaline solutions (KOH) have been used in this study, low metal or metal free industrial waste solutions may also be used as priming agents in larger scale pilot plants, thereby minimizing costs.

The industrial applicability of the two secondary phase biological systems, *viz.* continuous-flow fixed bed and continuous-flow stirred tank reactors, vary. Due to the long contact time and deep bed depths of the fixed beds, column implementation on a large scale appears to be non-viable. Though the efficiency of the system may be improved by using several shorter columns with a low contact time in series, this will increase the labour intensity of the system.

The implementation of continuous-flow stirred tanks in a large scale system has several advantages. Due to the largely unsophisticated nature of waste treatment systems in most factories the design of the stirred tanks were kept as simplistic as possible, whilst striving to attain efficient metal removal. Single or multiple reactors can be used depending on the metal content and nature of the effluent. In the presence of high-concentration effluents, dual reactors are required for efficient biosorption, with the first bioreactor serving as the prime metal removal site and the subsequent bioreactor(s) scavenging the remainder of the metals.

The implementation of such a system, *ie.* biphasic continuous-flow stirred bioreactors on an industrial scale shows potential especially for the treatment of low volume effluents. Such a system would involve the production of smaller, more cost effective bioreactors, which could be installed and operated on-site. In addition desorption, reconditioning and reuse of the biomass would limit the operational costs of such a plant.

Though only operated on a laboratory scale at this stage, the results obtained from the present study confirm the potential of using microbial matter as biosorbents for bioremediation. This study is one of the first in South Africa to use bioremediation for the removal of heavy metals from high-concentration, low-volume electroplating waste water. In comparison to many of the chemical agents used for waste water purification, the PEI:GA biomass is relatively cheap to produce. The cost of immobilizing 10 kg of commercially purchased biomass varies between R 300 - 350 (approximately \$75 - 80, 1995 prices) compared to an estimated price for ion exchange resins of \$ 300 - 400/10 kg. The cost effectiveness of such a system will be further increased through desorbing the metals from the biomass and reconditioning and reusing the biomass.

## 8. GENERAL DISCUSSION AND CONCLUSIONS

### 8.1. BIOACCUMULATION

Accumulation of heavy metals is an attribute shared by yeast and many other microbial cells. This concept was explored in the present study where metal binding experiments were performed using *S. cerevisiae* in an attempt to establish the cellular responses to heavy metal ions and the mechanisms of interaction between the metal cations and various components of yeast cells. Waste water often contains several different metal ions and the development and optimization of a bioaccumulation process for the treatment of metal containing effluent requires a comprehensive understanding of the mechanisms of metal accumulation.

From this study yeast cells have been shown to be capable of accumulating heavy metals under a wide range of ambient conditions. This uptake of heavy metals by yeast cells appears to be largely influenced by external factors, though it is also influenced by the inherent cellular characteristics. A relationship was established between intracellular metal ion accumulation and the ambient metal ion concentrations. The higher the concentration of the metal ions in solution, the greater the amount of metal accumulated by the yeast. The accumulation of heavy metals by yeast cells appears to be partially non-specific. Although the affinity of yeast-metal interactions varied depending on the respective species of metal ions, the affinity for, and the levels of individual heavy metal cations accumulated from multi-element solutions decreased, compared to the amount of metal accumulated from single ion solutions. Furthermore, the amount of accumulated metal is negatively influenced in the presence of unfavourable pH conditions. Accumulation from very acidic solutions (eg. pH 1.5) was negligible, whilst the amount of metal taken up increased with an increase in the alkalinity of the solution (approximately pH 6.0 - 7.0).

After an initial, rapid phase of accumulation, the rate of accumulation of metals declines over time. In viable cells the predominant mechanism of internalization is energy dependent. The addition and pretreatment of cells with an energy source, viz. glucose, results in enhanced metal uptake, whilst in the absence of an external energy source metal accumulation decreases after the utilization of the available energy source by the yeast cell.

## 8. GENERAL DISCUSSION AND CONCLUSION

Initial yeast-metal contact occurs at the cell wall, followed by internalization and subsequent sequestration. Intracellular metal ion deposition was shown to occur in the soluble cytosol and insoluble vacuolar fractions. Though the primary site for intracellular deposition appears to be the vacuole, granular metal ion deposits did form within the cytosol, eg.  $\text{Cd}^{2+}$  and  $\text{Co}^{2+}$  depositions. The accumulation of heavy metal ions by *S. cerevisiae* cells elicited certain cellular responses. Exposure of the cells to, and the subsequent accumulation of  $\text{Cd}^{2+}$  and  $\text{Cu}^{2+}$  by the cells triggered an ion-exchange phenomenon, whereby  $\text{Na}^+$ ,  $\text{K}^+$  and  $\text{Mg}^{2+}$  (but not  $\text{Ca}^{2+}$ ) were eluted from the yeast cell interior. Not all heavy metal cations bring about this effect. For example,  $\text{Co}^{2+}$  uptake did not result in any change in the intracellular ion-profile of yeast cells. Moreover in the presence of all of these heavy metal cations, permeabilization of the plasma cell membrane occurs.

Two primary sites for cellular heavy metal ion deposition are the yeast cell wall and the vacuole. Based on the results from this study it appears that all of the cell wall components are responsible for metal accumulation, and that isolated cell wall components are better metal accumulators than intact cell walls. Accumulation appears to reflect the spatial arrangement of the cell wall. Mannan, the outermost cell wall polymer exhibited the highest metal binding capacity, whilst in contrast glucan binds relatively low amounts of metals. An apparent affinity sequence for metal accumulation exists of mannan > chitin > glucan > intact cell walls, though not all metals are accumulated to the same extent. The limited amounts of metal accumulated by intact yeast cell walls can be ascribed to spatial limitations, and masking of available binding sites by other cell wall components.

The storage capabilities of the second major metal accumulating organelle, viz. the yeast vacuole warrants further research regarding its accumulating and concentration capabilities of heavy metals from solution. While results from the present study have indicated that metal ions are concentrated within this organelle, the vacuole appears to have a limited, yet indefinite capacity for heavy metal storage. The amount of metal concentrated therein is dependent on the metal species. Metals were accumulated in the order of decreasing ionic size, ie.  $\text{Cu}^{2+} > \text{Co}^{2+} > \text{Cd}^{2+}$ . The majority of vacuolar metal ion accumulation occurred during the initial contact phase (within the first 30 min). Although the uptake mechanism for heavy metals into the vacuole is not clearly understood, according to several other reports the energy dependent  $\text{H}^+$ -ATPase translocation pathway involved in the uptake of amino acids and several other cations, appears to play an important role. The vacuolar ATPase differs from that of the plasma cell membrane and plant V-ATPase systems due to the fact that some ATPase uncouplers, eg. DNP, are ineffective in inhibiting vacuolar metal uptake and translocation.

## 8.2. BIOSORPTION AND EFFLUENT TREATMENT

Though prior knowledge regarding the mechanisms of metal bioaccumulation by viable yeast cells is essential for bioremediation, it is not always feasible to use viable yeast cells in these bioremediation processes. The advantages of using non-viable yeast biomass for bioremediation are numerous, and the ability to recondition and reuse the biomass must be one of the most important.

One of the most effective methods of utilizing non-viable yeast biomass involves immobilization of the yeast cell, though it has remained essential to develop a method of immobilization which is both inexpensive compared to conventional metal removal techniques, and yet does not diminish the biosorptive capacity of the biomass. In addition such a system has to allow for complete metal recovery, as well as the recovery and reuse of the biomass.

In the present study three immobilized non-viable yeast systems were tested. While the three preparations viz. PVA Na-orthophosphate, PVA Na-alginate and hot alkali treated PEI:GA produced biomass, fulfilled the required mechanical and physical criteria, the superior metal accumulating ability of the alkali treated PEI:GA pellets determined their selection as metal biosorbent material.

Due to alkalinity of the PEI:GA pellets, this biomass appeared to preferentially accumulate metal from influent effluent solutions between pH 4.5 - 6.0. In the treatment of metal-containing waste water (using the PEI:GA biomass pellets) two types of bioremediation systems were implemented, viz. continuous-flow fixed bed reactors and continuous-flow stirred tank reactor systems. The designs of both of these systems have successfully been used for the treatment of waste water by other groups, yet due to the different nature of the effluent used in this study, *ie.* low-volume, high-concentration of metals, several adaptations to both systems were necessary. Depending on the metal concentration of the influent waste water effluent the treatment required thereof varied. Industrial waste water containing extremely high levels of heavy metals cannot be adequately treated by bioremediation processes alone. This type of effluent requires initial primary phase chemical treatment, not only to prime the effluent (eg. regarding pH optimum) for further treatment, but also to precipitate out excess metals.

The potential applicability of the two types of secondary bioremediation systems in industry varies. The ideal system should be cost effective and simplistic, yet effective regarding metal removal and

## 8. GENERAL DISCUSSION AND CONCLUSION

should be easily implemented on-site or at larger waste disposal collection sites. Based on these criteria it becomes apparent from the present study that the continuous-flow stirred bioreactor tanks possess greater industrial application potential than continuous-flow fixed bed reactors. Though fixed bed systems can be implemented in industrial systems, due to the nature of the columns several problems may be encountered. When using columns with a deep bed depth, the time required for the bioremediation process is extended. Columns containing short bed depths can be used, yet to achieve effective metal removal several of these will have to be implemented in series.

In contrast, efficient metal biosorption in stirred bioreactors occurs rapidly, thereby enabling a high flow rate to be maintained and larger volumes of the effluent to be processed. An additional advantage noted from the present study is the minimal loss of efficiency of metal removal on increasing the bioreactor capacity up to a certain point. Depending on the type of effluent being treated, the number and operational volume of the tanks used in such a system can vary.

### 8.3. GENERAL COMMENTS

While the knowledge regarding the mechanisms of biosorption and accumulation by the yeast *S. cerevisiae* may not be complete, sufficient information exists to realize the potential of these cells as biosorbent agents. The implementation of biological systems in the place of conventional waste water treatment processes requires the former to be a highly efficient, yet cost effective system. These biological systems must contain biosorbent material which has similar or improved metal accumulating abilities compared to the native biomass and must simultaneously allow for the effective recovery of the metal and regeneration and reuse of the biomass. As of yet the application of biosorbent technology is still in the trial stages with very few systems fully operational under pilot scale or industrial conditions, though several options are available for implementation eg. cross-flow microfiltration units or alternatively immobilized preparations. The bioremediation processes need not operate as complete systems, and a particular process can be designed for a specific application and need not be used as a general bioremediation tool. The use of different types of biomass in specific bioreactors in a biosorption system also offers possibilities for producing a product which will meet stipulated water criteria with respect to heavy metal concentrations.



## **9. THE USE OF FORMALDEHYDE CROSS-LINKED *S. CEREVISIAE* FOR COLUMN REMOVAL OF METALS FROM AQUEOUS SOLUTION AND ELECTROPLATING EFFLUENT**

### **9.1 INTRODUCTION**

A variety of microorganisms are capable of accumulating heavy metals from aqueous solutions and their potential in bioremediation of heavy metal contaminated wastewater has been extensively investigated (138). Most microbial biomass consists of small particles with low density, poor mechanical strength and little rigidity. Use of the native biomass in conventional processing operations for treatment of metal bearing wastewater is not practical because of solid/liquid separation problems. Immobilization of the biomass can bestow ideal size, mechanical strength, rigidity and porous characteristics to the biological material (140). Among the existing methods for immobilizing the potential microorganisms, entrapment in a polymeric matrix was the most common method. Gel entrapment on a large scale can, however, be prohibitively expensive and limits to diffusion rates within a gel is a major problem (213). In this regard, the development of a economically viable means of immobilization, with its sorptive properties preserved, has been conducted in present study. The yeast *Saccharomyces cerevisiae* was chosen as starting biosorbent because it has been known to effectively accumulate a wide range of heavy metals and can be obtained cheaply as a by-product of fermentation industries (214). Cross-linking of non-viable yeast cells with formaldehyde/HCl was performed and its metals uptake capacities from electroplating effluent investigated.

### **9.2 MATERIALS AND METHODS**

#### **9.2.1 Materials**

Suspension of *Saccharomyces cerevisiae* as a by-product from post malt fermentation was obtained from SA Breweries. The electroplating effluent was collected from a factory (PE Plating, South Africa) operating a chromium-plating line (Table 1). All the chemicals were analytical grade. Formaldehyde, HCl,  $\text{CuCl}_2 \cdot 7\text{H}_2\text{O}$  and  $\text{ZnSO}_4$  were obtained from Saarchem, SA.  $\text{CdSO}_4$  from Riedel-deHaen, Germany.

**Table 9.1** Levels of metals present in electroplating effluent (PE Plating), compared to stipulated criteria (mg/l)

	pH	Cu	Zn	Cd	Cr <sup>6+</sup>	Ni	Pb
Drinking water	Neutral	1.0	5.0	0.01	0.05	0.05	0.05
Dam/River	Neutral	0.005	1.0	0.003	0.05	0.05	0.05
Effluent	7.3-7.5	0.2-1.8	1.2-8.0	0	29.0-31.0	0.05-1.3	4.5-5.2

### 9.2.2 Immobilization

The cross-linking procedure was an adapted version of the method for treatment of algal biomass outlined by Schiewer *et al.* (215). The cells were extensively washed with distilled water to remove any remaining alcohol. After being oven-dried at 60°C for 8 hours, the yeast was crumbled to form granules (3-5mm in diameter), rinsed in the immobilizing solution for 10 min, and dried again at room temperature. The immobilizing solution was made of varying concentrations of formaldehyde ranging from 1-15% in 0.1M HCl. Mechanical strength of the pellets was assessed by resistance to degradation and structural damage as a result of high hydrodynamic pressure in columns, grinding and manual handling. Water-insolubility of the pellets was evaluated by incubating them in distilled water for 5 days.

### 9.2.3 Metal determination

The concentrations of total chromium, copper, zinc and cadmium were determined by atomic adsorption spectrophotometry (GBC 909). The hexavalent chromium was measured colorimetrically using 1,5-diphenyl carbazide (Saarchem) method (216). The difference between the two values was taken as trivalent chromium concentration.

### 9.2.4 Column operation

Glass columns of 16mm internal diameter were used in the operation. 10g (dry wt.) of FA-immobilised yeast was rehydrated in dist. water for 1 hour and then packed into the column (1.6x20cm). The feeding solutions were pumped upwards through the column at a flow rate of

50ml/h. As precipitation of respective metals could occur at various pHs, the influent pHs were kept at natural values of their solutions for column operation. The effluent was collected in 10ml fractions. The working temperature was kept at approximately 18°C. The saturated yeast biomass was regenerated by washing the columns downwards with 0.1M HCl at a flow rate of 50ml/h. After acid washing, the columns were reconditioned with 0.05M NaOH (incubated for 5 min) to bring the pH of the biomass up which was followed by 2 bed volume of distilled water. The term of regeneration efficiency outlined by Martin and Ng (217) was employed to evaluate reusability of the biomass. The regeneration efficiency was defined as the ratio of metal uptake of reaccumulation to that of the first cycle.

Scale-up of column removal of  $\text{Cr}^{6+}$  with 150g FA cross-linked yeast from EPE was performed using a "Perspex" column of 3.6x49cm, at a flow rate of 1 litre/h and pHs of 2.5 and 3, respectively.

### **9.2.5 Desorption of $\text{Cr}^{6+}$ with various desorbents**

The elution 1 were carried out downwards with 1M NaCl/0.05M NaOH or 0.1M NaOH respectively, at a flow rate of 50ml/h. The elution 2 involved in reduction of  $\text{Cr}^{6+}$  to  $\text{Cr}^{3+}$  by FA followed by desorption of the cation Cr with 1N  $\text{HNO}_3$ . Washes of the  $\text{Cr}^{6+}$  with 20ml portions of a mixture of 0.1% FA and 1N  $\text{HNO}_3$  (mixed immediately before use) were performed. The desorbing solution was left in the column for about 6 hours before being released. The portion washes were repeatedly carried out for 4-5 times until the concentrations of the elute were below 100mg/l.

## **9.3 RESULTS AND DISCUSSION**

### **9.3.1 Stability of the cross-linked biomass**

The 13-15% FA/0.1M HCl cross-linked biomass yielded the most mechanically stable and water-insoluble pellets. The cell loading, weight of dried yeast before immobilization versus that after immobilization, was found to be 97.8%. The consumption of immobilizing solution was 78ml per 100g dried yeast. The stability tests showed that grinding and manual handling did not appear to affect the physical properties of the pellets while the granules were still rigid and retained integrity after 5 days incubation. Table 2 shows the diverse stabilities of the cross-linked biomass at varying ratio of FA to 0.1M HCl.

**Table 9.2** Granule stabilities of the yeast biomass cross-linked with differing FA/0.1M HCl ratios.

FA/0.1M HCl (%)	Rinse time (min)	Solubility in cross-linking solution	Solubility in water	Granule stability (subjective test)	Cell loading (%)
1	10	Soluble	-	Not applicable	
4	10	Soluble	-	Not applicable	
8	10	Soluble	-	Not applicable	
10.5	10	Slightly soluble	Insoluble	Hard	93.7
13	10	Insoluble	Insoluble	Hard	97.8
13	5	Insoluble	Insoluble	Hard	
15	10	Insoluble	Insoluble	Hard	97.5
15	5	Insoluble	Insoluble	Hard	

### 9.3.2 Column adsorption of Cu, Zn and Cd from aqueous solutions

The metal cations were effectively removed from aqueous solutions by the biomass column at a flow rate of 50ml/h and the natural pHs of their solutions. The metal uptake capacities of the biomass at 60% saturation for Cu, Zn and Cd were found to be 8.03mg/g, 7.05mg/g and 14.04mg/g, respectively (Fig.1, 2 and Table 3). Values of the metal uptake capacities can also be obtained when the data is calculated on molar base (Table 3), giving values of 0.126mmol/g for Cu, 0.108-0.11mmol/g for Zn and 0.125mmol/g for Cd. The resulting values ranging from 0.1-0.12mmol/g might be adopted to estimate the concentration of binding sites on surfaces of the biomass for these divalent cation metals, under conditions of the experiment, regardless of respective atomic masses. The effects of pH changes in column operation on the onset of the breakthrough for respective metals is significant indicating the ion-exchange nature of the biosorptive process.

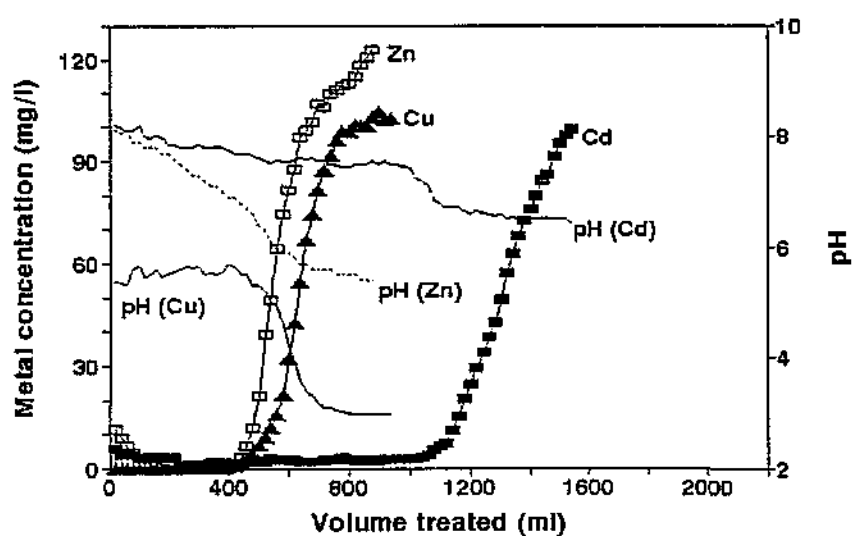


Figure 9.1: Breakthrough curves for column removal of cation metals by yeast biomass from aqueous solutions at respective pHs. Biomass, 10 g; Flow rate, 50 ml/h; Infl. metal conc.: Cu, 127 mg/l; Zn, 130.7 mg/l; Cd, 112.4 mg/l.

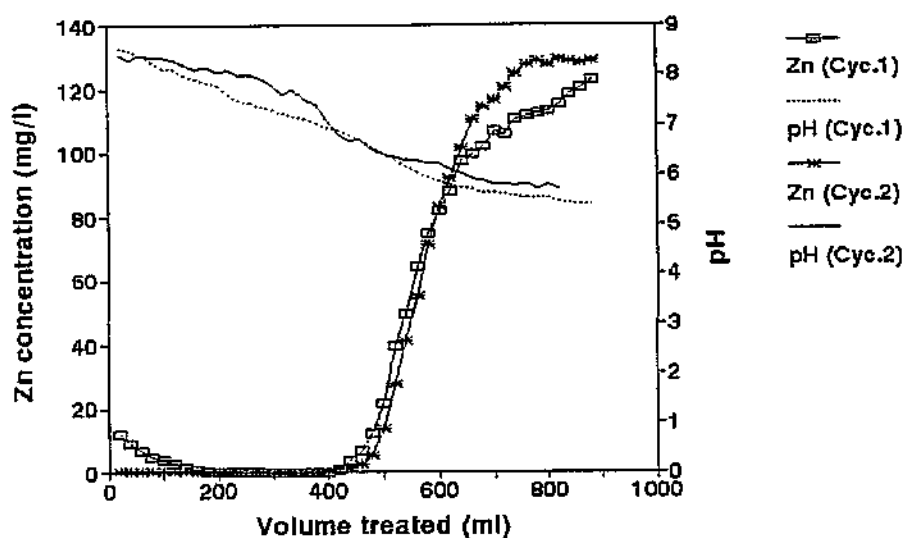


Figure 9.2: Breakthrough curves for removal of Zn by yeast biomass for 2 cycles. Biomass, 10 g; Flow rate, 50 ml/h; Infl. Zn conc., Zn, 130.7 mg/l; Infl. pH, 6.1

**Table 9.3** Column removal of cation metals from aqueous solutions

Metal	Infl. conc. (mg/l)	Infl. pH	Flow rate (ml/h)	Biomass (g)	Metal uptake (mg/g) <sup>a</sup>	Metal uptake (mmol/g) <sup>a</sup>
Cu	127	5.3	50	10	8.03	0.126
Zn	130.7	6.1	50	10	7.05	0.108
Zn <sup>b</sup>	130	6.1	50	10	7.19	0.110
Cd	117	6.7	50	10	14.04	0.125

<sup>a</sup> at 60% saturation of the biomass.<sup>b</sup> Cyc.2

### 9.3.3 Desorption and recovery of cation metals

93-97% recovery of the cation metals was accomplished using 0.1M HCl in a volume of 120ml (Fig.3, 4 and Table 4). The bound metals were desorbed and concentrated to levels as high as 1500mg/l for Cd and 1000mg/l for Cu and Zn, so that recycling of them in electroplating process would be possible or, alternatively, precipitation of the recovered metals could be greatly facilitated. Reaccumulation of Zn by the regenerated biomass remained constant with the metal uptake of 7.19mg/g demonstrating the potential for repeated utilisation of FA cross-linked yeast biomass in treatment of cation metal-laden wastewater (Fig.2 and Table 3). Reconditioning the column biomass with 0.05M NaOH also appeared to improve the uptake capacities of the biomass probably through increasing porosity and alkalinity of the biomass itself.

**Table 9.4** Cation metal recovery with 0.1M HCl

Metal	Metal accumulated (mg)	Metal Desorbed (mg)	Volume used (ml)	Recovery %	Regeneration efficiency %
Cu	87.05	80.98	120	93.03	100
Zn	76.74	74.84	120	97.52	
Cd	144.87	138.50	120	95.6	

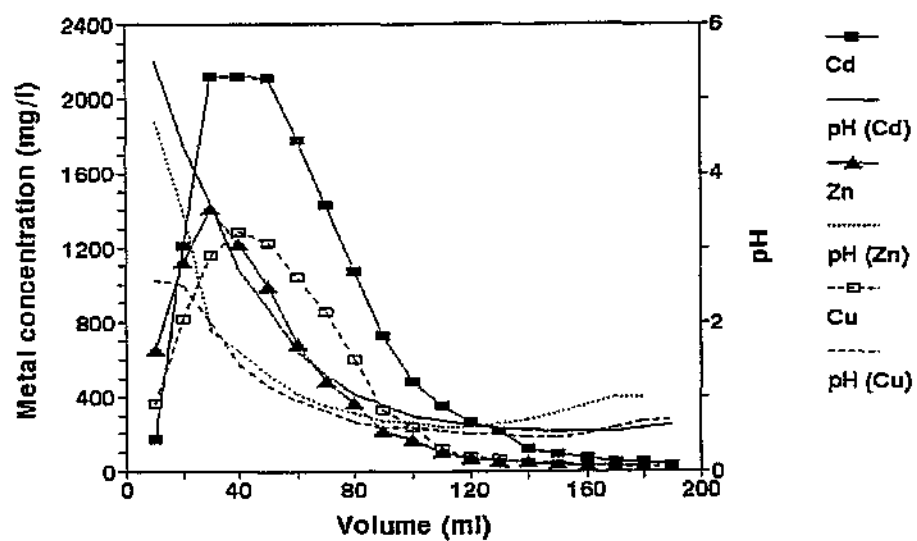


Figure 9.3: Desorption of cation metals with 0.1M HCl. Flow rate, 50 ml/h.

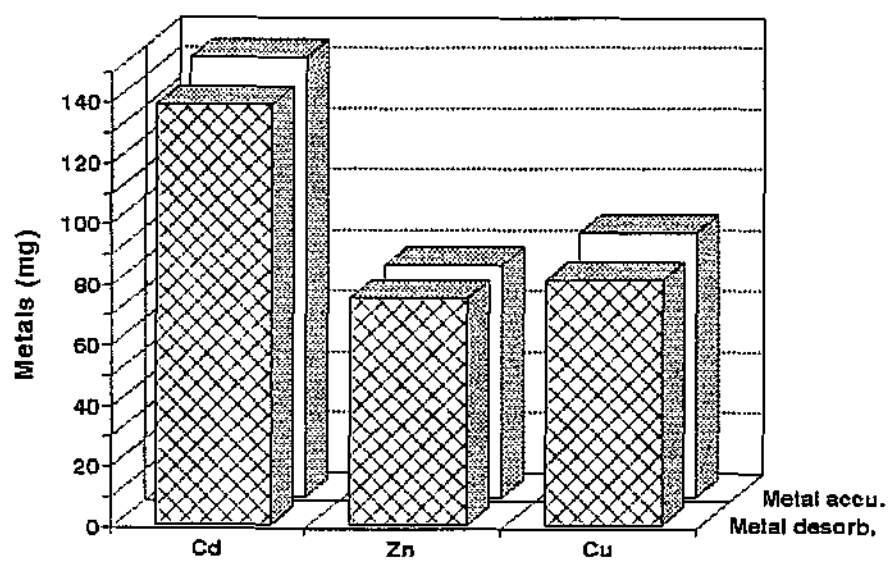


Figure 9.4: Recovery of cation metals from saturated biomass with 0.1M NaCl.

### 9.3.4 Column adsorption of $\text{Cr}^{6+}$ from electroplating effluent

Significant effects of varying influent pHs on adsorption of  $\text{Cr}^{6+}$  onto yeast biomass were observed in Fig.5 and Table 5. Unlike cation metal accumulation, gradual breakthrough of the total Cr (TCr) and  $\text{Cr}^{6+}$  at all pHs occurred in the column elution profiles (Fig.5). At the optimum influent pH of 2.5, the Cr uptake capacity, calculated from the breakthrough curves at 60% saturation, was found to be 6.31mg/g while less metal was accumulated at increasing influent pHs (Table 5). Nevertheless further accumulation of  $\text{Cr}^{6+}$  on the semi-saturated biomass can be expected before it reaches full saturation.

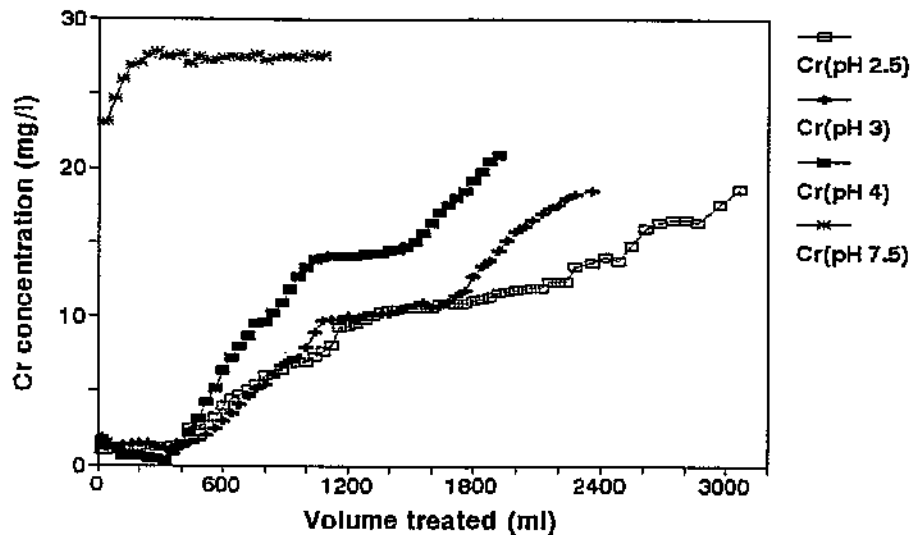


Figure 9.5: Breakthrough curves for column removal of  $\text{Cr}^{6+}$  by yeast biomass from EPE at varying influent pHs. Biomass, 10 g; Flow rate, 50 ml/h; Infl.  $\text{Cr}^{6+}$  conc., 30 mg/l.

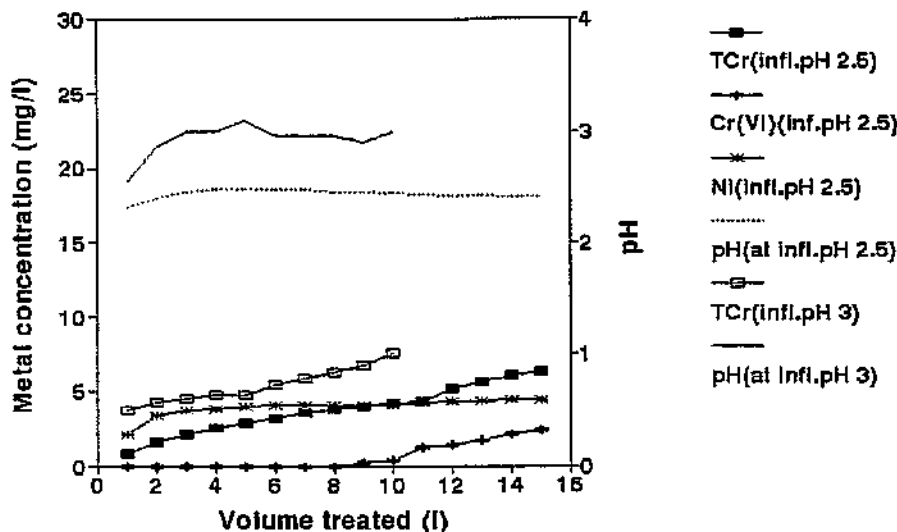


Figure 9.6: Breakthrough curves in scale-up for column removal of  $\text{Cr}^{6+}$  by yeast biomass from EPE at influent pHs of 2.5 and 3. Biomass, 150 g; Flow rate, 11/h; Infl.  $\text{Cr}^{6+}$  conc., 30 mg/l.



Although gradual breakthrough of total Cr and  $\text{Cr}^{6+}$  occurred in the scale-up of the column operations substantial amounts of Cr and  $\text{Cr}^{6+}$  had been accumulated and removed from EPE at 20% saturation at pHs of 2.5 and 3.0, respectively (Fig.6). From the profile, the estimated values of Cr uptake at full saturation are as high as 11.96mg/g for TCr and 13.36mg/g for  $\text{Cr}^{6+}$  at pH of 2.5. Reaccumulation of the effluent (Cycle 2) exhibited little effect on removal of the remaining Cr since most of the Cr leached from the column in cycle 1 was  $\text{Cr}^{3+}$ , which obviously can not be effectively accumulated at such a low pH. Little Ni from EPE had been removed during the column operation at such a low pH. The reduction of  $\text{Cr}^{6+}$  to its trivalent form, along with adsorption, was found to exist in the removal of  $\text{Cr}^{6+}$  by sorbents such as activated carbon, sphagnum moss peat and leaf mould (218, 219). The phenomenon was once again revealed in the present study that there was appreciable amount of  $\text{Cr}^{6+}$  being converted by the FA cross-linked yeast at pH 2.5, probably due to some unknown reducing group on the surface of the biomass or the remaining FA from cross-linking procedure.

**Table 9.5** Column removal of  $\text{Cr}^{6+}$  from electroplating effluent

Infl., conc. (mg/l)	Infl., pH	Flow rate (ml/h)	Biomass (g)	$\text{Cr}^{6+}$ removal (mg/g) <sup>a</sup>	TCr uptake (mg/g) <sup>a</sup>	Volume treated (l) <sup>a</sup>
30	2.5	50	10		6.31	3.07
30 <sup>b</sup>	2.5	50	10		5.10	2.4
30	3.0	50	10		4.97	2.28
30	4.0	50	10		3.67	1.72
30	7.5	50	10		0.34	0
30	2.5	1000	150	2.94 <sup>c</sup>	2.63 <sup>c</sup>	> 15
30	3.0	1000	150	1.85 <sup>d</sup>	1.65 <sup>d</sup>	> 10

<sup>a</sup> At 60% saturation of the biomass.

<sup>b</sup> Cycle 2.

<sup>c</sup> At 20% saturation of the biomass.

<sup>d</sup> At 25% saturation of the biomass.

Other researchers have also observed the similar gradual breakthrough of  $\text{Cr}^{6+}$  in their studies on column adsorption of  $\text{Cr}^{6+}$  with activated carbon, leaf mould, sphagnum moss peat, coconut husk etc.(218-220). The phenomenon of gradual breakthrough, from an application viewpoint, is of importance because a column run is always terminated at some chosen values of metal concentration. Therefore total available metal removing capacity of the sorbent can not be fully utilised in single fixed-bed runs. An investigation into the phenomenon has been reported by Sengupta and Clifford

(221) in their chromate-anion-exchange experiments using basic anion resins(IRA-458 and IRA-68). It was concluded that the early breakthrough is not due to poor column kinetics but is predictable from an equilibrium model by using the appropriate exchange reaction involving both  $\text{HCrO}_4^-$  and  $\text{Cr}_2\text{O}_7^{2-}$ . At low pH  $\text{HCrO}_4^-$  is the only  $\text{Cr}^{6+}$  species in the aqueous phase, while in the exchange phase both the  $\text{HCrO}_4^-$  and  $\text{Cr}_2\text{O}_7^{2-}$  (the presence of  $\text{Cr}_2\text{O}_7^{2-}$  in the solid phase may be viewed as the dimerization of  $\text{HCrO}_4^-$  according to the Donnan equilibrium principle) in the exchanger's solid phase causes a positively curved (concave upwards) isotherm at relatively low  $\text{Cr}^{6+}$  loading of the resin, and this equilibrium property is primarily responsible for the gradual breakthrough of  $\text{Cr}^{6+}$ .

### 9.3.5 Desorption of $\text{Cr}^{6+}$

#### Desorption with NaCl or NaOH

After washing with 0.1M NaOH, very little  $\text{Cr}^{6+}$  (2.27mg) had been recovered with a recovery of only 5.16% (Fig.7 and Table 6). Furthermore the liquor leached from the column was brown coloured during the alkaline desorption and extraction of yeast constituents by alkaline was thought possible. Elution through the column with 1M NaCl/0.05M NaOH improved the desorption efficiency (11.55mg) giving a recovery of 31.5% (Fig.7).

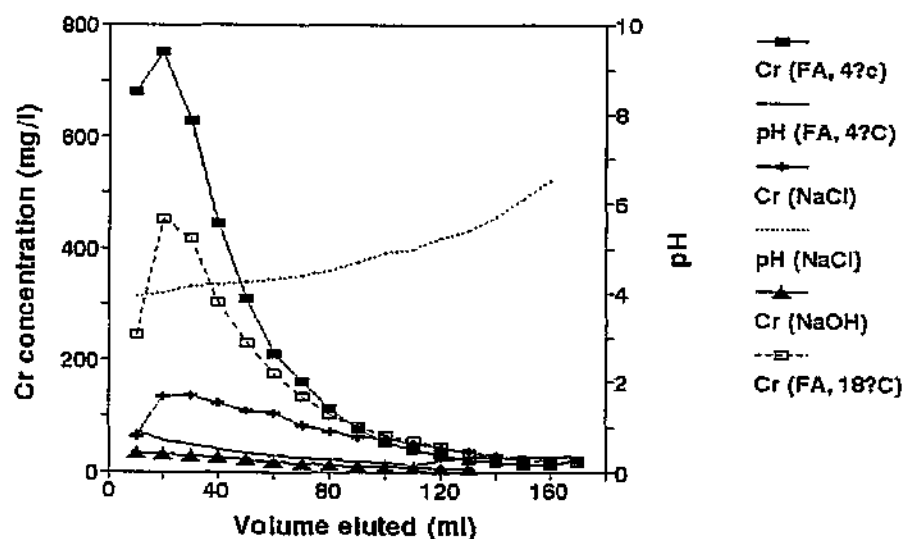


Figure 9.7: Desorption of  $\text{Cr}^{6+}$  with varying desorbents. Flow rate, 50 ml/h.

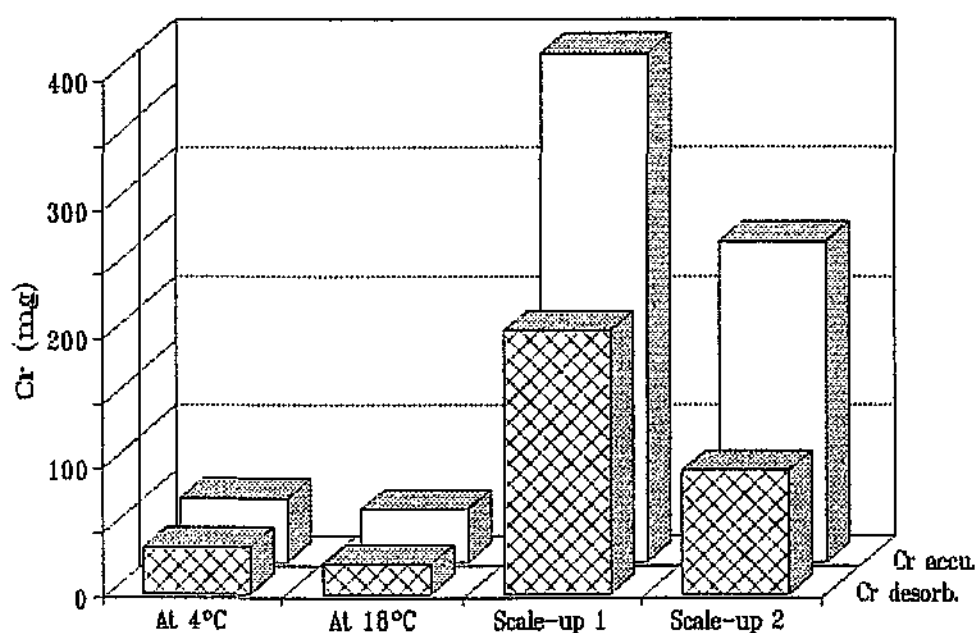


Figure 9.8: Recovery of  $\text{Cr}^{6+}$  from saturated biomass with 0.1% FA/1N  $\text{HNO}_3$ .

### 9.3.6 Reduction and desorption of $\text{Cr}^{6+}$

The methodology was based on the assumption that  $\text{Cr}^{6+}$  which was bound to yeast biomass during adsorption could be reduced by either some unknown reducing groups on the surface of the biomass or by introducing the reductant, formaldehyde, and thereby desorbed by acids. The results of desorption with FA/1N  $\text{HNO}_3$  is presented in Fig.7, 8 and Table 6. Among the regenerating agents the combination of FA and  $\text{HNO}_3$  at 4°C exhibited the best desorbing capacity with a recovery of 72.23%, and subsequently a regeneration efficiency of 83.72%. Applying the same combination of FA and  $\text{HNO}_3$  at 18°C only resulted less Cr recovery (38-56%) than that at low temperature. As the adsorption of Cr to biomass is generally thought as an endothermic, chemisorptive procedure (222), the enhanced process of desorption of Cr from the biomass by lowering the reaction temperature can be expected, which in turn would facilitate the subsequent reuse of the biomass in treatment of Cr-laden waste streams.

**Table 9.6** Chromium recovery with various desorbents

Desorbent/	Cr <sup>6+</sup> accumulated (mg)	Cr desorbed (mg)	Volume used (ml)	Recovery %	Regeneration efficiency %
1% FA/1N HNO <sub>3</sub> <sup>a</sup>	49.66	35.87	120	72.23	83.72
1% FA/1N HNO <sub>3</sub>	41.10	23.07	120	56.13	
1% FA/1N HNO <sub>3</sub> <sup>b</sup>	393.8	203.4	1000	51.65	
1% FA/1N HNO <sub>3</sub> <sup>c</sup>	247.5	95.4	1000	38.56	
NaCl/0.05 M NaOH	36.67	11.55	120	31.5	
0.1M NaOH	44	2.27	120	5.16	

<sup>a</sup> At 4°C.<sup>b</sup> Scale-up 1<sup>c</sup> Scale-up 2

## 9.4 CONCLUSIONS

This study presents a novel method in immobilizing *S. cerevisiae* as a biosorbent for treatment of metal-laden waste effluent, in which the immobilizing cost can be reduced to an affordable extent on industrial scale. The non-viable yeast cross-linked by 13% FA/1N HNO<sub>3</sub> exhibits good mechanical strength and rigidity in continuous-flow operation. No apparent disruption of the biomass after repeated use has been observed. Cu, Zn and Cd were effectively removed from aqueous solutions by the yeast biomass at natural pHs of their solutions. Complete recovery of the bound metals were achieved by washing the column biomass with 0.1M HCl. The recovered metals were concentrated in such small volumes that recycling or precipitation of them can be carried out. The metal uptake capacity of the regenerated biomass remained constant in comparison with cycle 1 thereby reuse of the yeast would be possible.

In the case of Cr<sup>6+</sup>, a gradual breakthrough curve of Cr in column profile was noted, with reduction of Cr<sup>6+</sup> to Cr<sup>3+</sup> occurring. However, Cr<sup>6+</sup> in EPE can be significantly minimised either by accumulation onto the biomass or reduced to its trivalent form so that detoxification of Cr<sup>6+</sup>-laden wastewater can be accomplished. Desorption of bound Cr<sup>6+</sup> with either alkaline or salt could not

facilitate the regeneration. A combination of reduction and desorption with FA/HNO<sub>3</sub> appeared promising in regeneration of the saturated biomass at 4 °C, while applying the same procedure at room temperature did not show satisfactory results, reflecting the thermochemical effect on binding of the metal to yeast biomass.

## 10 THE REMOVAL OF METALS FROM AQUEOUS SOLUTIONS BY IMMOBILISED *SACCHAROMYCES CEREVISIAE*.

### 10.1 INTRODUCTION

The efficiency of a metal bioremediation process is dependant on many factors including the biosorbents maximum binding capacity, affinity, metal bioavailability and the composition of the effluent (192, 222). In this initial study we investigated the uptake kinetics of a range of metals by a polyacrylamide immobilised *S. cerevisiae* biomass. The potential advantages of the biosorbent, such as improved accumulation of metals by the immobilised biomass as found by Garnham *et al* (223), were assessed. The parameters influencing the metal binding capabilities were investigated and the potential advantages of the immobilised biosorbent explored. These parameters investigated were metal concentration, incubation time and pH. Optimum metal pH ranges and incubation times were determined and these parameters used in the equilibrium binding studies. Metal uptake is represented as  $\mu$ mole of metal removed from solution per gram of *S. cerevisiae* ( $\mu$ mol/g). The metals chosen for this study are present in industrial effluents currently under investigation in our laboratory.

### 10.2 MATERIALS

Commercial preparations of *S. cerevisiae* were obtained from Anchor Yeast Inc. (production strain 90 % viability). Copper, cobalt and cadmium chlorides were obtained from Merck, zinc chloride from BDH, chromium chloride from Reidel-de-Haen and nickel chloride from Saarchem. Gold standard was obtained from Saarchem. *N,N,N',N'*-tetramethylethylenediamine (TEMED), *N,N'* methylene-bis-acrylamide and polyacrylamide were purchased from Sigma. Ammonium persulphate, sodium chloride, sodium hydroxide and hydrochloric acid were supplied by Saarchem. HA 0.45 micron nylon filters were purchased from Micron Separations Inc. Ultra-pure deionized water, purified by a milli-Q water system, was used to prepare solutions in all experiments.

### 10.3 METHOD

#### 10.3.1 *S. cerevisiae* immobilisation

Yeast immobilisation as adapted by Brady and Duncan (181) was as follows: 3.75 g acrylamide monomer and 0.2 g *N,N'*-methylene-bis-acrylamide were dissolved in 12 ml deionised water. *S. cerevisiae* (5 g) was washed with 10 ml water and then resuspended in 10 ml 0.9 % NaCl. The acrylamide solution and the cell suspension were mixed together with 1 ml TEMED and 2.5 ml ammonium persulphate. The reaction mixture was cooled and allowed to polymerize, after which it was passed through a 30-mesh sieve. The resultant biomass ( $\pm 50$  g) was conditioned by washing in 0.1 M HCl followed by a 0.05 M NaOH wash and a final rinse in water. The pH was adjusted to 5 and all excess water removed by filtration.

#### 10.3.2 Adsorption kinetic profiles

Immobilised biomass (1g) was weighed into 100 ml conical flasks. The metal solution (10 ml of 200  $\mu\text{mol/l}$  at pH 5) was then added. For determination of the binding rates the contact times were 0.5, 1, 2, 3, 4, 5, 10, 20, 30 and 60 minutes with shaking at ambient temperature. Post incubation 5 ml of the reaction mixtures were filtered through 0.45  $\mu\text{m}$  nylon filters under vacuum and the filtrate analysed for metal.

#### 10.3.3 pH profiles

The pH of the metal solutions was adjusted using NaOH or HCl prior to incubation with the biosorbent. The pH range evaluated was from pH 2 to 6. Batch reactor incubation was as described for equilibrium profiles. The initial metal concentrations were 200  $\mu\text{mol/l}$ .

#### 10.3.4 Equilibrium profiles

Investigations of metal removal by the immobilised biosorbent were conducted over the range of 50 to 2000  $\mu\text{mol/l}$ . Incubation was as above with shaking for 30 minutes. Post-contact, the mixtures were centrifuged at 500 g x 5 min, the supernatant was removed and analysed for metal. For kinetic characterization, the results were analysed using Michaelis-Menten binding isotherms.  $K_d$  and  $B_{\text{max}}$  values were determined using Scatchard and Hanes-Woolf transformation plots.

All the above experiments evaluated the removal the metal chlorides of  $\text{Cu}^{2+}$ ,  $\text{Zn}^{2+}$ ,  $\text{Co}^{2+}$ ,  $\text{Cd}^{2+}$ ,  $\text{Ni}^{2+}$  and  $\text{Cr}^{3+}$ . A gold solution was also investigated, the oxidation state was unknown. The determinations were repeated 5 times per parameter evaluated.

## 10.4 RESULTS

### 10.4.1 Metal removal over time

The immobilised *S. cerevisiae* efficiently removed all the metals investigated from solution. Copper uptake progressively increased up to 20 minutes, reaching an equilibrium of 65 % metal removal (Refer to figure 10.1). The initial concentration was 200  $\mu\text{mol/l}$  and the bioremediation process decreased the copper to well within required drinking water criteria. The biosorbent's ability to remove the other metals was compared to its performance relative to copper and thus an initial concentration of 200  $\mu\text{mol/l}$  was used throughout these investigations. Zinc removal equilibrium was reached in 10 minutes of incubation and the percentage removal was 60 %. Cobalt removal reached an equilibrium of 65-70% in 5 minutes (Figure 10.2). Cadmium removal was high at  $\geq 88$  %, however, equilibrium was relatively slow at 30 minutes. Gold removal was both rapid and high, with a removal of 75 % within the first 3 minutes and reaching 90% within 5 minutes of incubation. Chromium and nickel removal was similar to copper removal, with equilibriums of 65 to 73 % being reached within 20 minutes of contact.

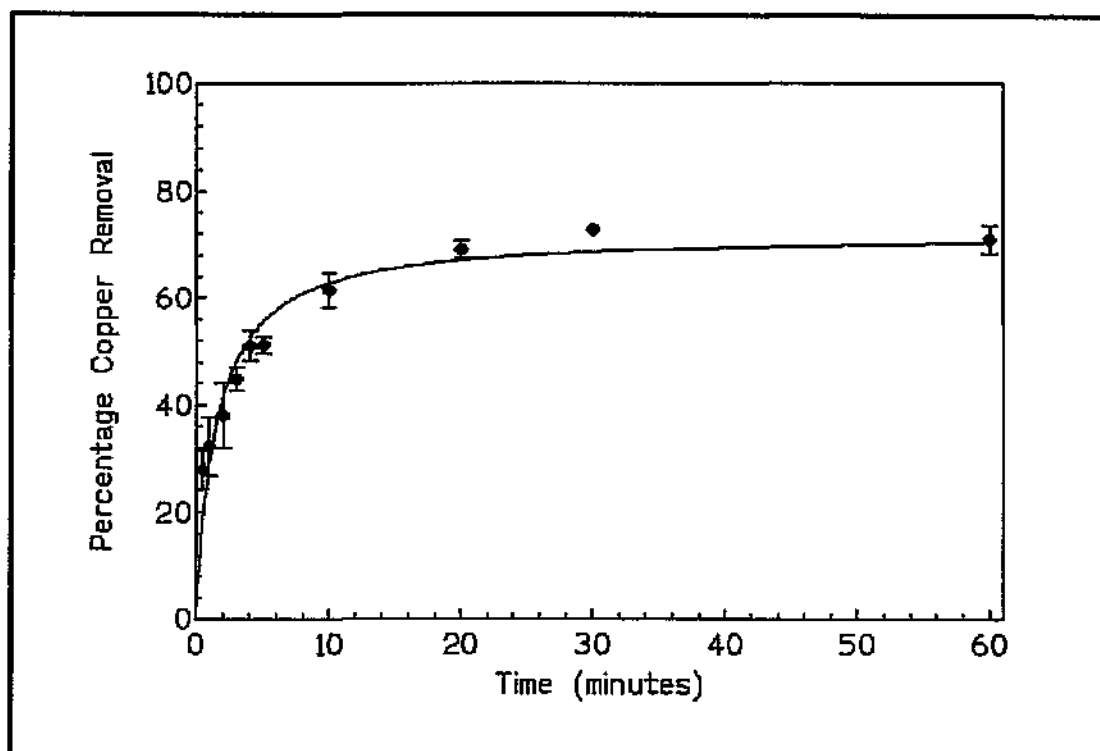


Figure 10.1 : Percentage copper accumulated in batch reactors by immobilised *Saccharomyces cerevisiae* as a function of time ( $n=5$ ,  $\pm$ SD). Initial copper concentration was 200  $\mu\text{mol/l}$ .



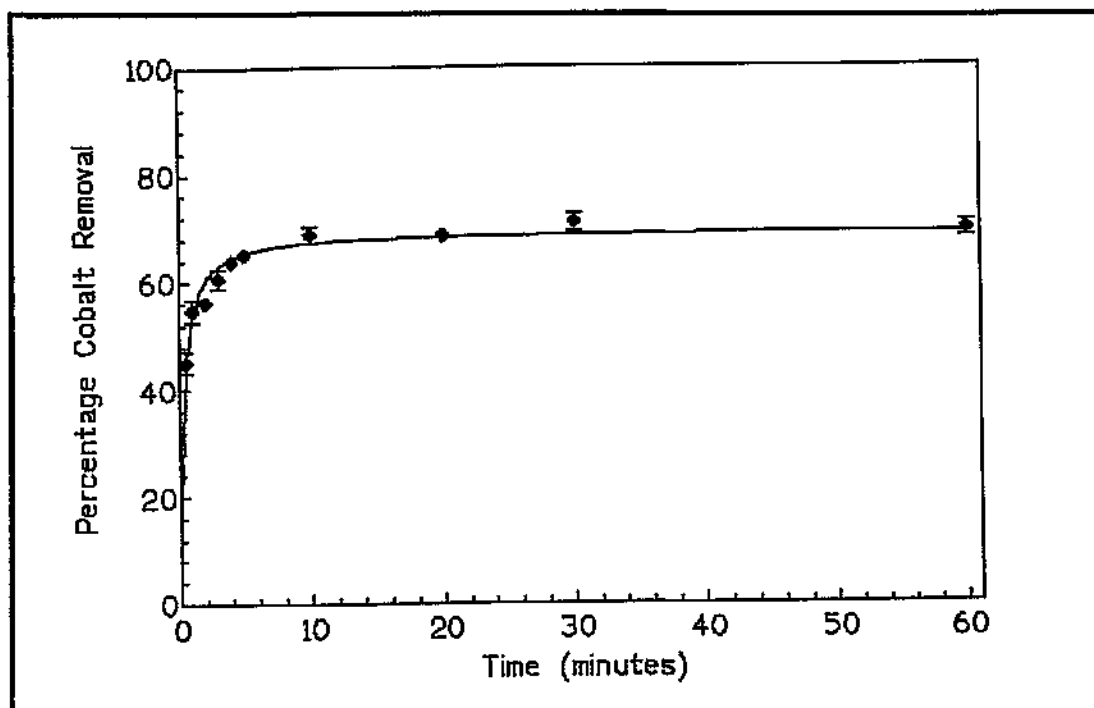
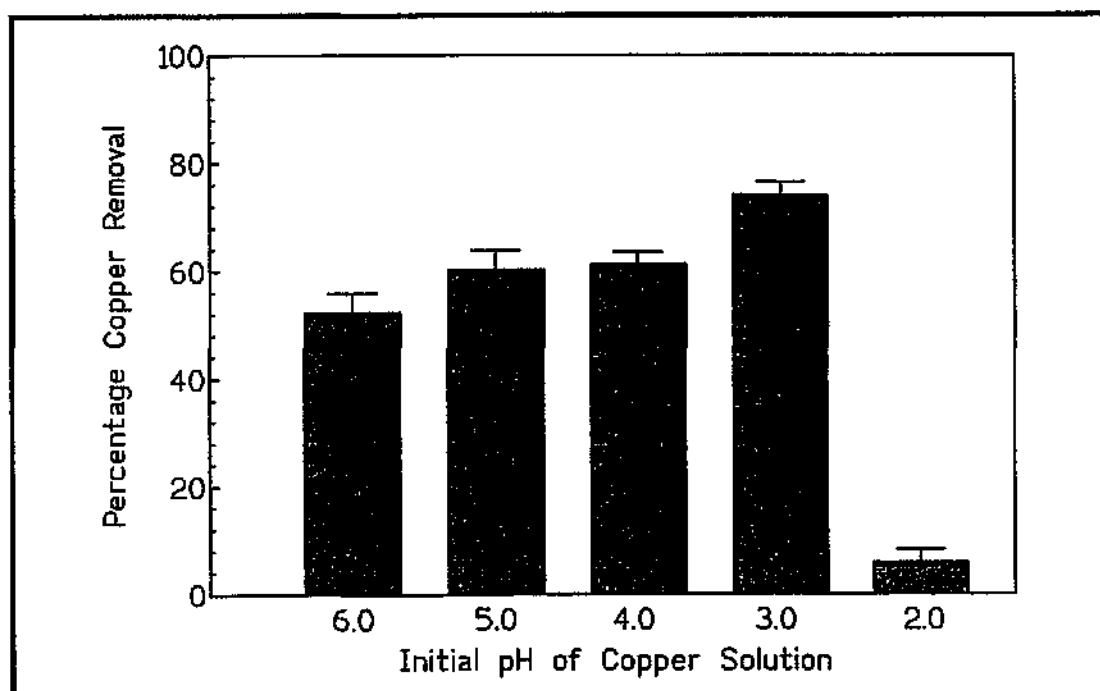


Figure 10.2 : Percentage cobalt removed in batch reactors by immobilised *Saccharomyces cerevisiae* as a function of time ( $n=5$ ,  $\pm$  SD). The initial cobalt concentration was  $200 \mu\text{mol/l}$ .

#### 10.4.2 Effect of pH on bioaccumulation

The bioaccumulation of divalent cations is pH dependant. By adjusting the pH of the metal solutions prior to biosorbent contact, a profile of optimum pH for metal removal was generated. Copper, chromium and nickel removal from solution by *S. cerevisiae* was maximized in the pH range 3 to 5 (60-70%), and was substantially reduced at pH 2 to  $\leq 7\%$  (Refer to figure 10.3). Zinc removal was not effected between pH 3 and 6 (60%), but only 34 % was accumulated at pH 2 as presented in Figure 10.4. Cadmium and cobalt removal was high ( $\geq 70\%$ ) between pH 4 and 6, but was reduced from pH 3 (Refer to Figure 10.5). At pH 2 removal was 25 and 5 % respectively. The gold investigated was effectively removed from solution at a lower solution pH values. At pH 3 and below removal was in excess of 80 % (Refer to Figure 10.6).



**Figure 10.3 :** Removal of copper from aqueous solutions of varied pH in batch reactors by immobilised *Saccharomyces cerevisiae* ( $n=5$ ,  $\pm$  SD). The pH of the copper solutions was adjusted using HCl and NaOH and the initial concentration was  $200 \mu\text{mol/l}$ .

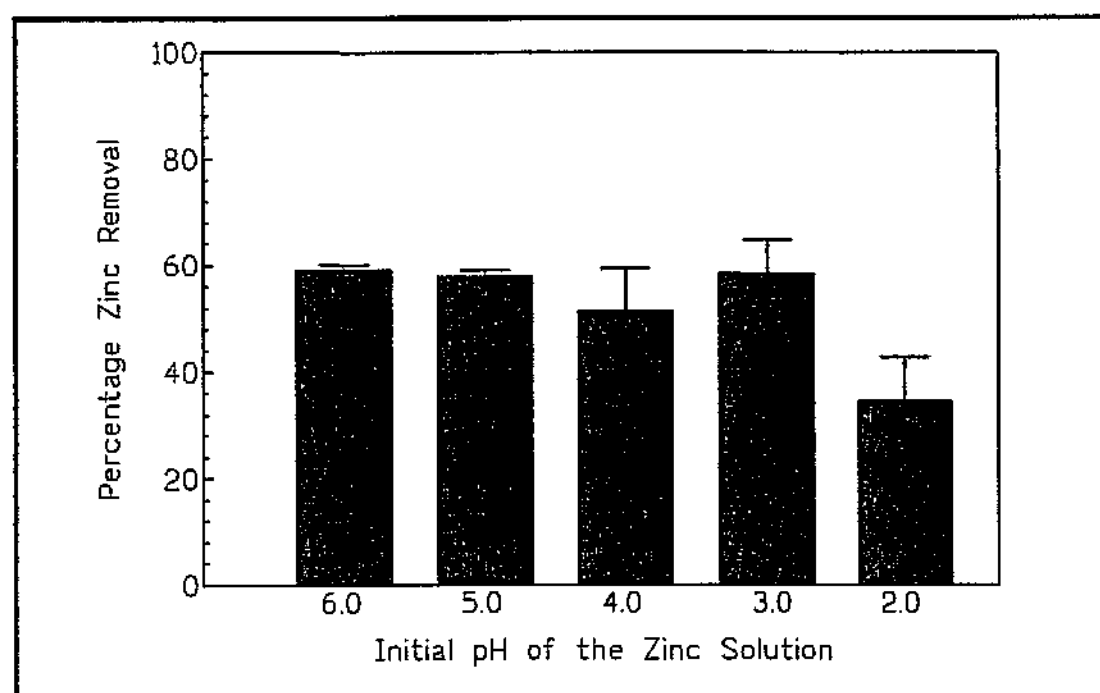


**Figure 10.4 :** Removal of zinc from aqueous solutions of varied pH in batch reactors by immobilised *Saccharomyces cerevisiae* ( $n=5$ ,  $\pm$  SD). The pH of the zinc solutions was adjusted using HCl and NaOH and the initial concentration was  $200 \mu\text{mol/l}$ .

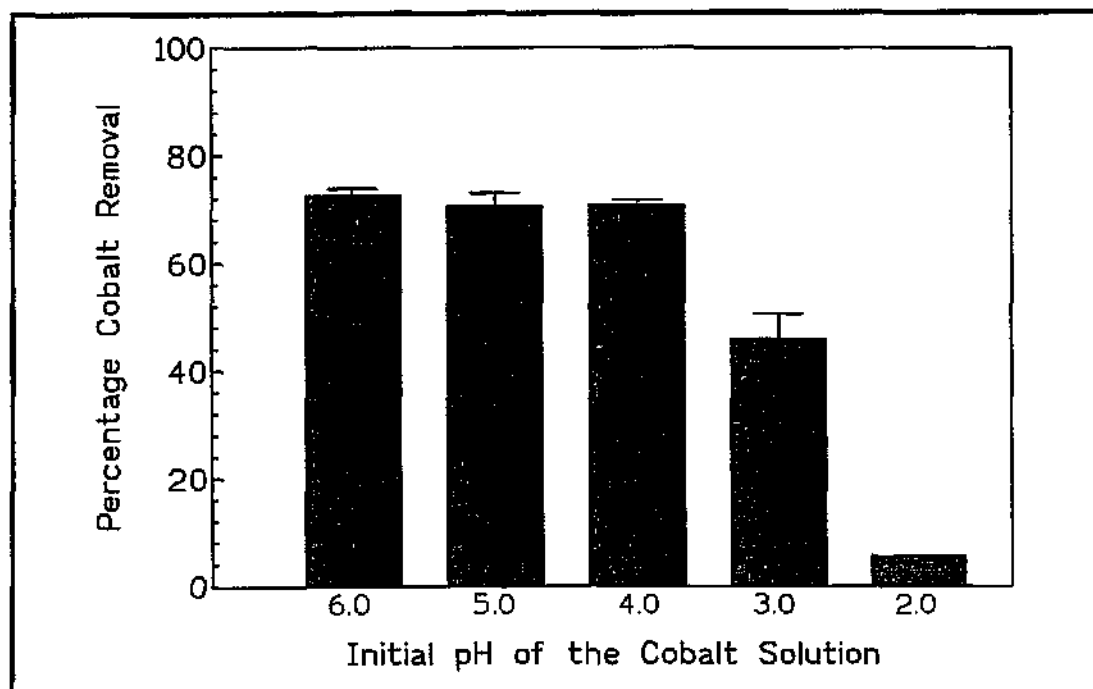


Figure 10.5 : Removal of cobalt from aqueous solutions over a pH range in batch reactors by immobilised *Saccharomyces cerevisiae* ( $n=5$ ,  $\pm$  SD). The pH of the cobalt solutions was adjusted using HCl and NaOH and the initial concentration was  $200 \mu\text{mol/l}$ .

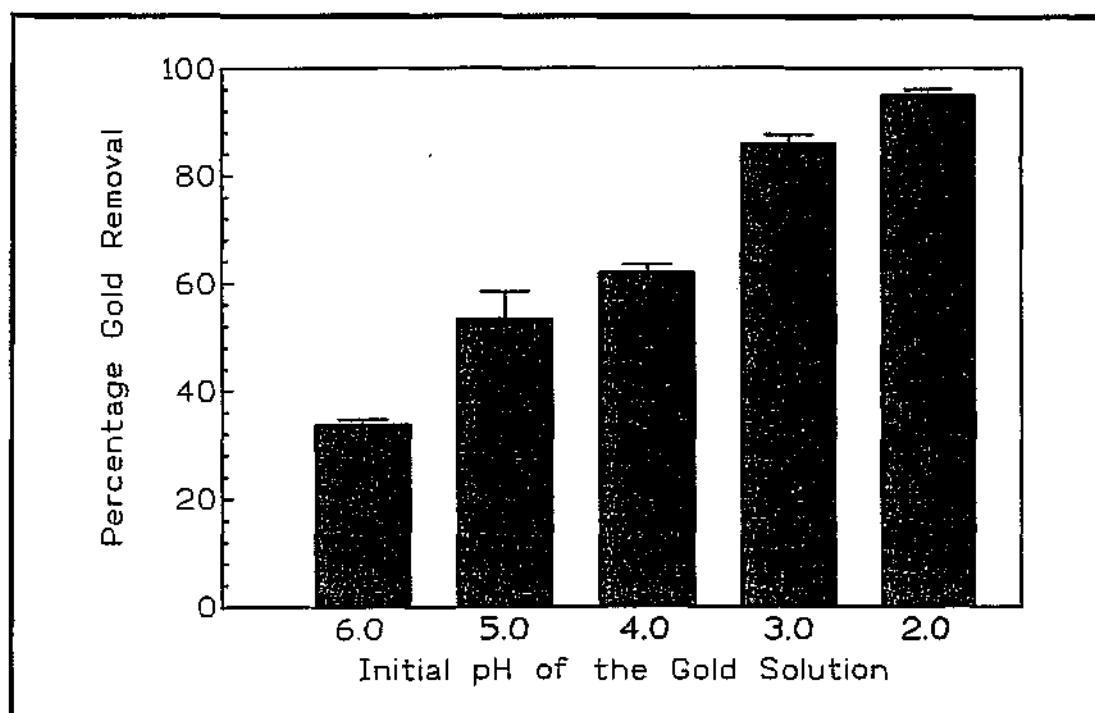


Figure 10.6 : Removal of gold from aqueous solutions over a pH range in batch reactors by immobilised *Saccharomyces cerevisiae* ( $n=5$ ,  $\pm$ SD). The pH of the gold solutions was adjusted using HCl and NaOH and the initial concentration was  $200 \mu\text{mol/l}$ .

## 10.4.3 Sorption isotherms

Equilibrium binding isotherms were generated over an initial metal concentration range of 100 to 2000  $\mu\text{mol/l}$ . The metal solutions were initially pH 5 with the exception of gold at a pH 2. Biosorption followed Michaelis-Menten kinetics. Adsorption capacities and dissociation constants of metal equilibrium were calculated by linear transformation of binding data using the Hanes-Woolf plot.  $K_d$  and  $B_{\text{max}}$  are given in table 10.1. Equilibrium biosorption isotherms of chromium, cadmium and gold are presented in Figure 10.7, Figure 10.8 and Figure 10.9 respectively.

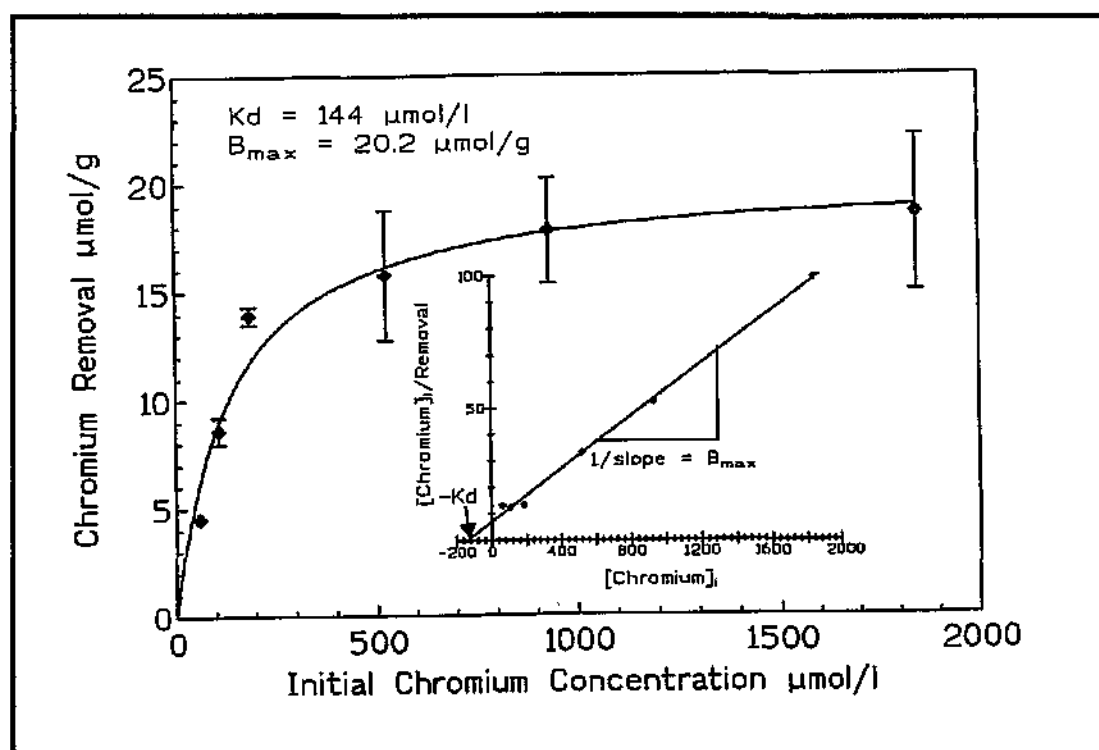


Figure 10.7 : Removal of chromium from an aqueous solution by immobilised *Saccharomyces cerevisiae* in batch reactors ( $n=5$ ,  $\pm\text{SD}$ ).  $K_d$  and  $B_{\text{max}}$  were calculated as  $144 \mu\text{mol/l}$  and  $20.2 \mu\text{mol/g}$  respectively.

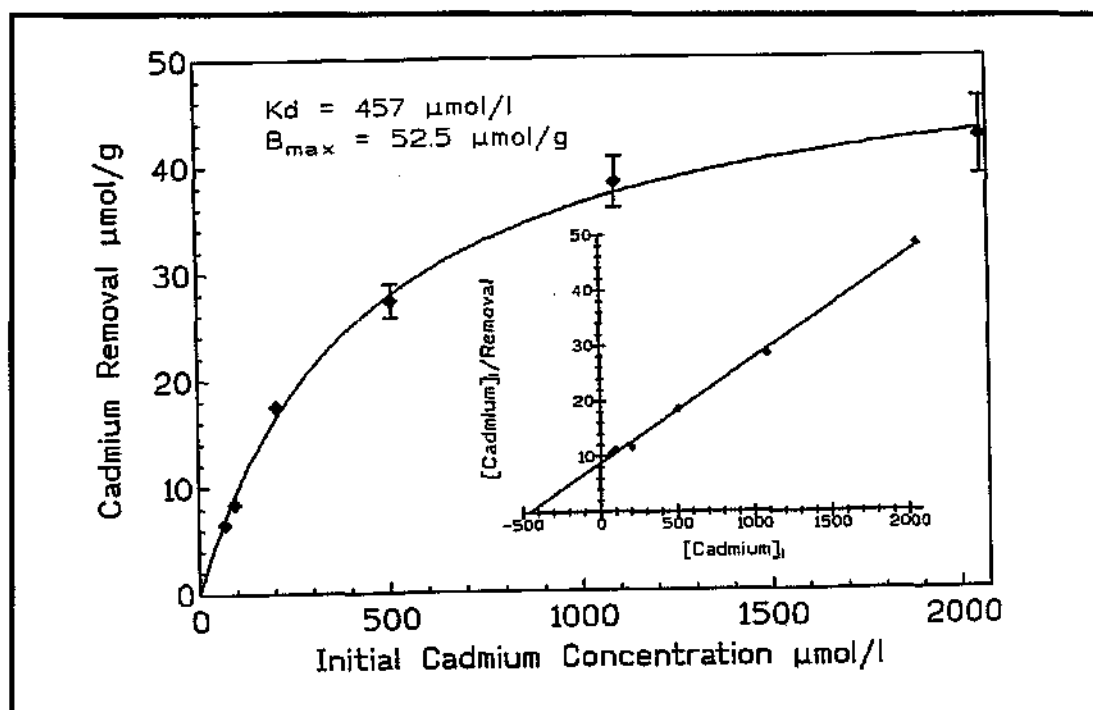


Figure 10.8 : Removal of cadmium from aqueous solutions by immobilised *Saccharomyces cerevisiae* in batch reactors ( $n=5$ ,  $\pm\text{SD}$ ).  $K_d$  and  $B_{\text{max}}$  were calculated as  $457 \mu\text{mol/l}$  and  $52.5 \mu\text{mol/g}$  respectively.

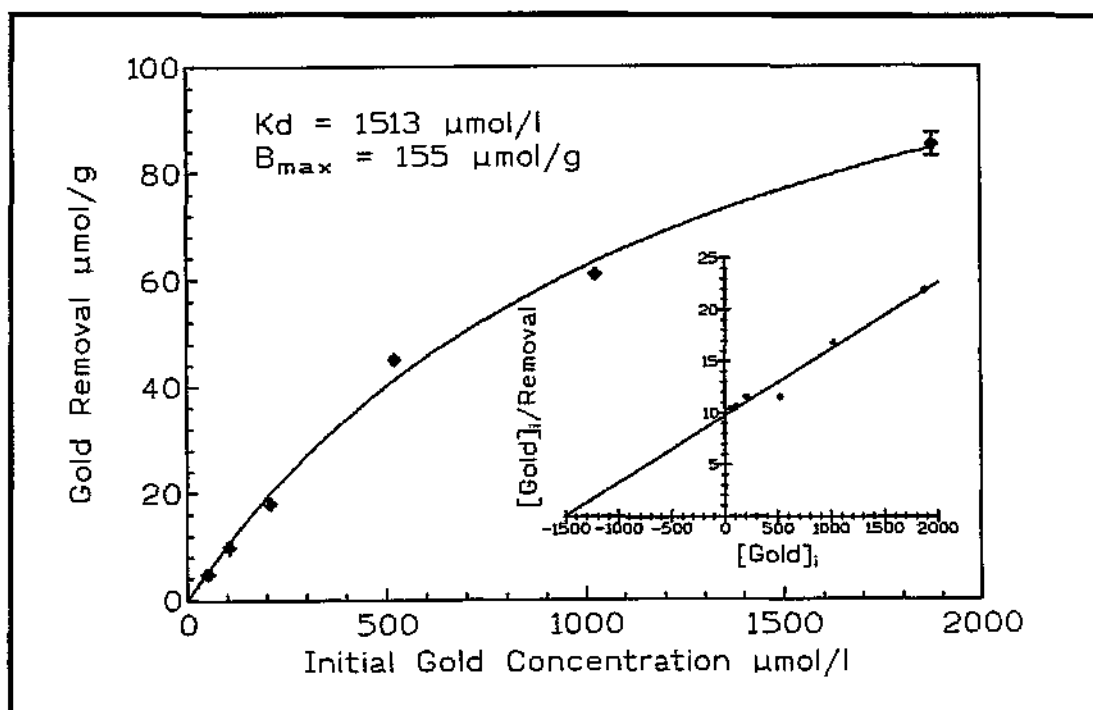


Figure 10.9 : Removal of gold from an aqueous solution by immobilised *Saccharomyces cerevisiae* in batch reactors ( $n=5$ ,  $\pm\text{SD}$ ).  $K_d$  and  $B_{\text{max}}$  were calculated as  $1513 \mu\text{mol/l}$  and  $155 \mu\text{mol/g}$  respectively.

**Table 10.1:** Biosorption capacities of metals by *S. cerevisiae* as generated from Hanes-Woolf transformation plots.

METAL	Kd ( $\mu\text{mol/l}$ )	B <sub>max</sub> ( $\mu\text{mol/g}$ )
Copper	413	24.1
Zinc	757	30.1
Nickel	151	19.5
Cadmium	457	52.5
Cobalt	500	49.6
Gold	1513	155
Chromium	144	20.2

## 10.5 DISCUSSION

Metal uptake was rapid. Gold and cobalt reached an equilibrium within 5 minutes of contact. The binding of  $\text{Cu}^{2+}$ ,  $\text{Zn}^{2+}$  and  $\text{Ni}^{2+}$  progressively increased up to 20 minutes reaching an equilibrium of 60 to 70 %. Cadmium removal, although high (88 %), was slower reaching an equilibrium in 30 minutes. Rapid binding is most likely associated to metabolism-independent adsorption to the cell wall. Wehrheim and Wettern (51) reported more than 90 % of the total bound metals to *Chlorella fusca* were surface bound within the first minute of contact with an initial concentration range of 5 to 100  $\mu\text{mol/l}$ .

Removal of and  $\text{Cu}^{2+}$ ,  $\text{Zn}^{2+}$ ,  $\text{Cr}^{3+}$ ,  $\text{Cd}^{2+}$ ,  $\text{Co}^{2+}$  and  $\text{Ni}^{2+}$  was enhanced at pH 4 and 5 and substantially reduced at pH 2. The decrease in metal removal at low pH is most likely a result of  $\text{H}^+$  ion competition for binding sites (224). The decreased binding of metal cations at lower pH indicates a possible recovery protocol for these metals. Binding of gold was highest at lower pH values. These results were consistent with those described by several authors (225, 226). Ramelow *et al* (227) found the bioremediation of  $\text{Cu}^{2+}$ ,  $\text{Zn}^{2+}$ ,  $\text{Pb}^{2+}$ ,  $\text{Cd}^{2+}$  and  $\text{Ni}^{2+}$  was strongly pH dependant with a minimum binding at pH 2, but increased rapidly with pH and reached a maximum at pH 5-6. Gold and silver were only slightly effected by pH and in an opposite manner to the other metals. Maximum chromium(iv) adsorption rates by *S. cerevisiae* were at pH 1.0-2.0 at 100 mg/ml concentrations, indicating the importance of the metal speciation in solution (228). The reverse pH optimum of gold recovery may serve as a selective removal strategy for gold solutions contaminated

with metal cations by pH adjustment. Nui *et al* (229) demonstrated a selectivity for lead by *Penicillium chrysogenum* at an optimum pH 4.5 over other metals investigated.

The binding isotherms followed Michaelis-Menten kinetics. Metal accumulated by immobilised *S. cerevisiae* was by an equilibrated and saturatable mechanism with the metal accumulation increasing with increasing metal concentrations until saturated. Gold maximum uptake capacity was the highest at 155  $\mu\text{mol/g}$ . Cadmium and cobalt removal was relatively high at 52.5 and 49.6  $\mu\text{mol/g}$ . The maximum binding capacity ( $B_{\text{max}}$ ) is an important factor in determining the biosorbent's potential removal capabilities at high metal concentrations. The dissociation constant is the metal concentration corresponding to half-saturation of the biosorbent, a low  $K_d$  value indicating high affinity ( $K_a=1/K_d$ ) (183). This affinity related constant may be a useful consideration in bioreactor design. For example, a biosorbent with a low  $K_d$  for a particular metal may be applicable to a reactor which has low contact times such as a biosorption column. These constants may only be of value when comparing different metals or biosorbents if all other parameters remain consistent and should be considered in tandem.

Studies by Garnham *et al* (223) of cobalt and zinc by *Chorella salina* found uptake to be biphasic. Metal accumulation in the second phase followed Michaelis-Menten kinetics. Cellular compartmentation analysis showed metal bound to intracellular components and the cell wall. Higher concentrations of metal were detected in the vacuole than in the cytosol, accounting for the multi-phasic uptake. In the present investigation only one uptake phase was evident, with the possible exception of zinc. The predominant metal removal mechanism was most likely adsorption to the cell wall. This removal mechanism should allow for rapid desorption and high concentration factors of accumulated metal.

The maximum uptake capacities of the biosorbent in this study are relatively low if compared to the literature. The highest removal rate being for gold of 155  $\mu\text{mol/g}$  and a low of only 19.5  $\mu\text{mol/g}$  for nickel. The reasons for this being that the data is reported for a wet weight and the concentration range chosen for the investigation, although considerably above excepted drinking water criteria, is relatively low and therefore the metal removed per gram of biomass is decreased. The design of the study was to facilitate rapid removal and metal recovery, and biosorbent regeneration and reuse which is facilitated by surface binding. The criteria for a successful biosorbent is it's ability to remove metal from solution, decreasing the concentration to an acceptable level at a competitive cost.

The immobilised *S. cerevisiae* was able to remove the metals and provide water of potable quality.

Polyacrylamide gel controls, with no *S. cerevisiae*, removed minimal amounts of metal from solution.

## 10.6 CONCLUSION

Immobilised *S. cerevisiae* removed the metals investigated from aqueous solutions. The removal was relatively rapid with adsorption equilibriums being reached for all metals within 30 minutes of incubation. The process was pH dependant with the removal of cations being most effective at solution pH's above 3. Gold removal by the biosorbent was both high and rapid at pH 2. The isotherms followed typical Michaelis-Menten binding kinetics. The metal removal capabilities of *S. cerevisiae* in this study indicated a biosorbent suitable for remediation of relatively low metal concentration, high volume effluents.



## 11 RECOVERY OF METAL ACCUMULATED BY IMMOBILISED *SACCHAROMYCES CEREVISIAE*

### 11.1 INTRODUCTION

The recovery of bioaccumulated metals has both environmental and economic implications. Biologically bound metals, although removed from an aqueous solution, remain a potential treat to the environment. Unlike organic contaminants which can be metabolised to relatively innocuous compounds, bound metals are concentrated in localised areas and need to be recovered (230). Recovered metals are of economic value and can be recycled and returned to industrial processes thus subsidising their remediation. The successful recovery of bound metals from different microorganisms using a range of eluting agents has been reported by several researchers (231, 232). The potential of a bioremediation operation would be substantially enhanced if the biomass could be regenerated and used for repeated adsorption-desorption applications (233). The metal elution protocol should allow complete metal recovery and damage to the biosorbent should be minimal. This study investigated the ability of potential metal eluting agents to recover copper bound to immobilised *S. cerevisiae* biomass in batch reactors. The uptake capacity of the biosorbent and bound metal recoveries over repeated cycles were monitored to determine the reusability of the biosorbent. Electron microscopy studies allowed observation of any morphological changes or damage to the cell during repeated use.

### 11.2 MATERIALS

Commercial preparations of *S. cerevisiae* were obtained from Anchor Yeast Inc (production strain, 90 % cell viability).  $\text{CuCl}_2 \cdot 2\text{H}_2\text{O}$ ,  $\text{CaCl}_2 \cdot 2\text{H}_2\text{O}$ ,  $\text{Ca}_2\text{CO}_3$  and  $\text{CaHCO}_3$  were purchased from Merck. KOH, NaOH, KCl,  $\text{H}_2\text{SO}_4$ ,  $\text{HNO}_3$  and HCl were supplied by Saarchem. Ultra-pure deionised water was used in all experiments and was purified by a Milli-Q water system.

### 11.3 METHOD

#### 11.3.1 *S. cerevisiae* immobilisation

Yeast was immobilised as described previously in 10.3.1.

#### 11.3.2 Metal adsorption-desorption profiles

### 11.3.2 Metal adsorption-desorption profiles

Immobilised biosorbent (1g) was weighed into conical flasks. A 10 ml copper chloride solution of  $200\mu\text{mol/l}$  was added. The reaction mixture was incubated over 30 minutes with shaking at ambient temperature and then centrifuged for 5 minutes at 500 g. A 1 ml sample of the supernatant was removed for determination of metal accumulation. The post contact reaction mixtures were treated with potential eluting solutions. The acids  $\text{HNO}_3$ ,  $\text{HCl}$  and  $\text{H}_2\text{SO}_4$  (0.01-0.1 M) sequentially decreased the pH and desorption profiles were generated. The volumes and concentrations of acid used were recorded.  $\text{Ca}_2\text{CO}_3$ ,  $\text{CaHCO}_3$ ,  $\text{CaCl}_2 \cdot 2\text{H}_2\text{O}$ ,  $\text{KCl}$ ,  $\text{KOH}$  and  $\text{NaOH}$  solutions (1 M) were added to the reaction mixtures in aliquots of 0.1 ml, 0.5 ml and 1.0 ml.

### 11.3.3 Repeated use of the biosorbent

Eight adsorption-desorption cycles were investigated in batch reactors. Refer to Figure 11.1 for the batch reactor reusability protocol.

### 11.3.4 Metal Analysis

A GBC 909 atomic absorption spectrophotometer was used for copper analysis.

### 11.3.5 Transmission electron microscopy

Yeast cells were investigated by TEM to observe potential morphological changes of cells and to gain insight into binding mechanisms during adsorption-

desorption of metals. Free suspension yeast cells conditioned as described in section 10.3.1 served as controls. Cells exposed to  $200\mu\text{mol/l}$  copper and cells exposed to copper and acid desorption cycles were prepared for TEM. *S. cerevisiae* cells were prepared for TEM using standard techniques (240). The sections were examined under a JEOL 100 CX transmission electron microscope.

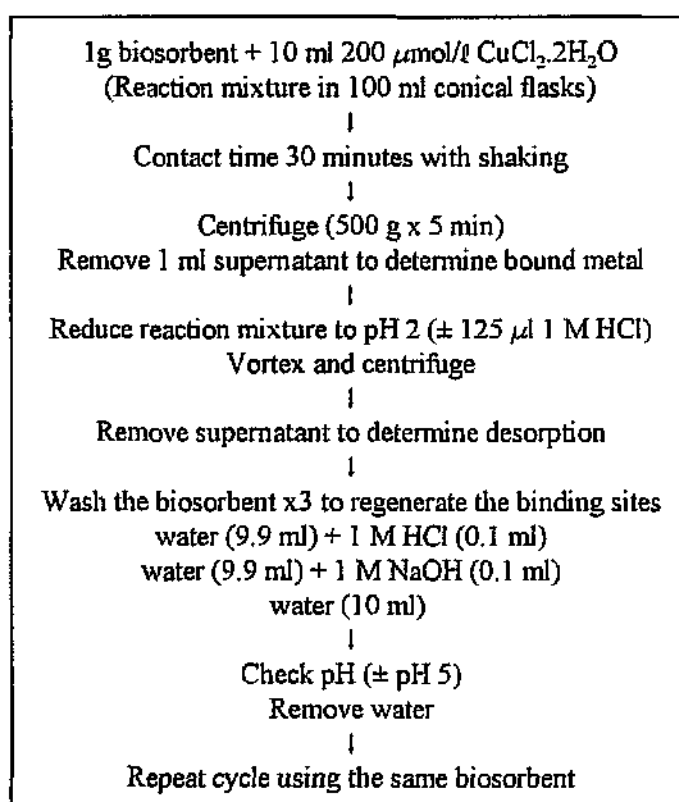


Figure 11.1 : A flow-diagram of the batch reactor adsorption-desorption protocol.

## 11.4 RESULTS

### 11.4.1 Copper recovery from the biosorbent

Copper recovery was most efficient using the mineral acids. By decreasing the pH a copper recovery of  $\geq 80\%$  was achieved at pH 2 (Figure 11.2). HCl,  $\text{H}_2\text{SO}_4$  and  $\text{HNO}_3$  effectively desorbed bound copper by addition of small volumes of 1.0 M solutions (0.13, 0.2 and 0.25 respectively) to the remaining 9 ml reaction mixtures (Table 11.1).  $\text{CaHCO}_3$ ,  $\text{CaCl}_2 \cdot 2\text{H}_2\text{O}$ ,  $\text{Ca}_2\text{CO}_3$  and KCl were relatively ineffective at recovering copper and desorbed 32.1 %, 24.9 %, 14.3 % and 9.3 % respectively (Table 11.1). NaOH and KOH increased copper removal from solution.

**Table 11.1 :** Percentage desorption of copper from immobilised *S. cerevisiae* in batch reactors.

Eluting solution (1 M)	Volume (ml)	Desorption %	$\pm$ SD
$\text{H}_2\text{SO}_4$	0.20	85.0	4.3
HCl	0.13	80.4	5.5
$\text{HNO}_3$	0.25	89.5	4.3
$\text{CaHCO}_3$	1.0	32.1	6.1
$\text{Ca}_2\text{CO}_3$	1.0	14.3	2.6
KCl	1.0	9.3	1.8
$\text{CaCl}_2 \cdot \text{H}_2\text{O}$	1.0	24.9	4.2
Water control	0.5	1.2	0.8

### 11.4.2 Adsorption-desorption cycles

Adsorption-desorption was investigated over 8 cycles to assess the reusability of the immobilised *S. cerevisiae*. Copper removal from solution in batch reactors increased from an initial 65 % to between 70-85 % efficiency in the latter cycles. (Figure 11.3). Desorption was achieved by reducing the pH using HCl. Recovery of metal was high with an average recovery of  $\geq 85\%$  over the repeated cycles. No apparent damage was done to the biosorbent and no adverse effect on uptake or recovery of the metal was observed. The immobilised biomass was easily recovered and regenerated for reuse. Adsorption-desorption studies using free cell suspensions were unsuccessful due to the significant loss of cells between each cycle.

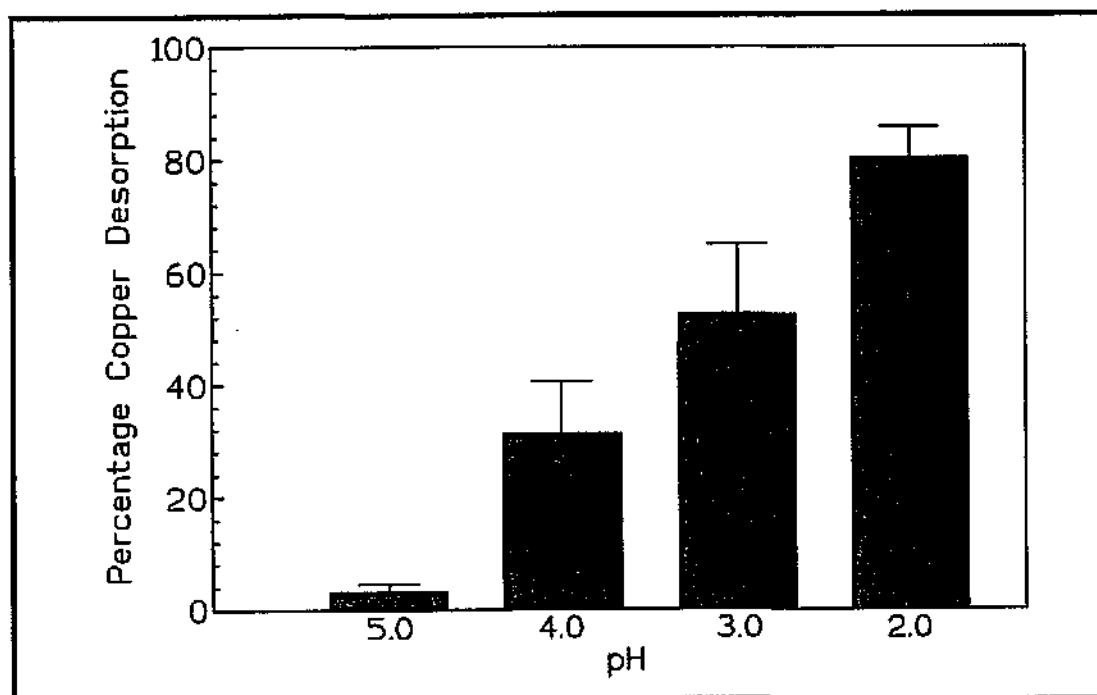


Figure 11.2 : Desorption of copper accumulated to immobilised *Saccharomyces cerevisiae* ( $n=4$ ,  $\pm$ SD). The desorption profile was generated by sequential reduction of the pH using dilute HCl.

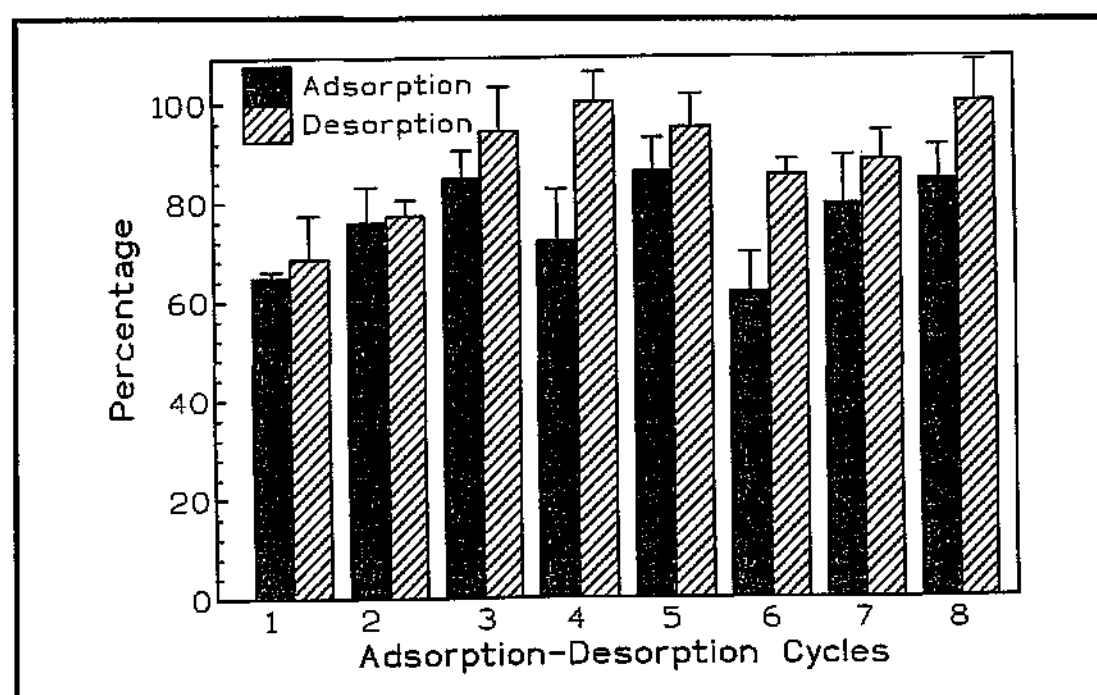


Figure 11.3 : Eight repeated adsorption-desorption cycles in batch reactors determined the reusability of the immobilised *Saccharomyces cerevisiae* biosorbent ( $n=5$ ,  $\pm$ SD). The initial copper concentration was  $200 \mu\text{mol/l}$  and desorption was achieved using HCl.

#### 11.4.3 Transmission electron microscopy of *S. cerevisiae*

Cells exposed to copper and dilute acid treatment were observed under TEM to determine the extent of any structural damage to the cell integrity, morphological changes and to assess the type of bioaccumulation. Untreated cells were used as controls and compared to copper and acid treated specimens (Refer to figure 11.4). From the randomly selected micrographs no damage to the metal exposed cells was detected. Characteristic of the cells exposed to copper were dark electron dense walls (Refer to Figure 11.5). Cells exposed to adsorption-desorption cycles were more spherical in appearance and did not have as electron dense cell walls (Refer to Figure 11.6).

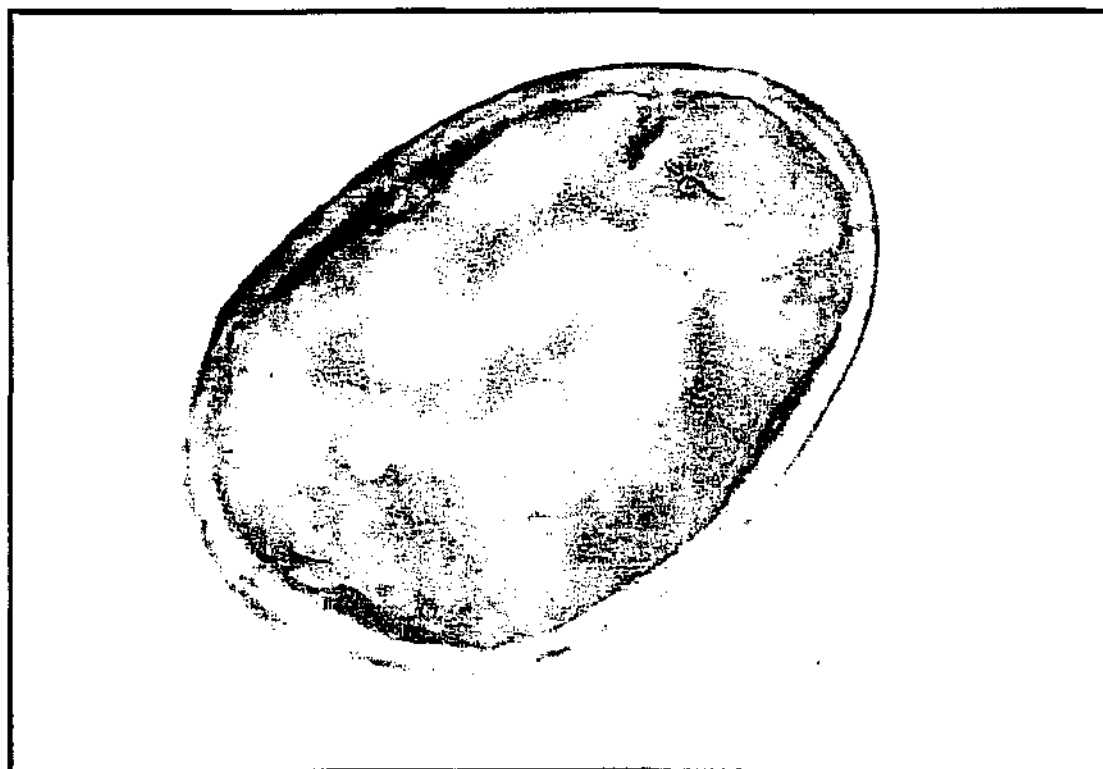
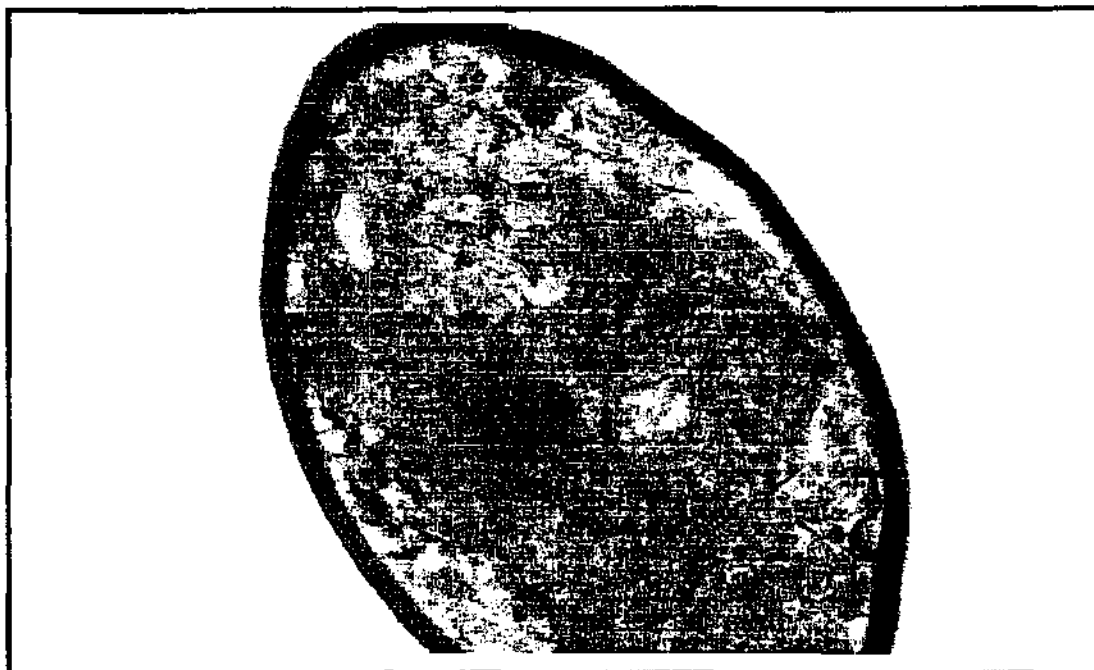
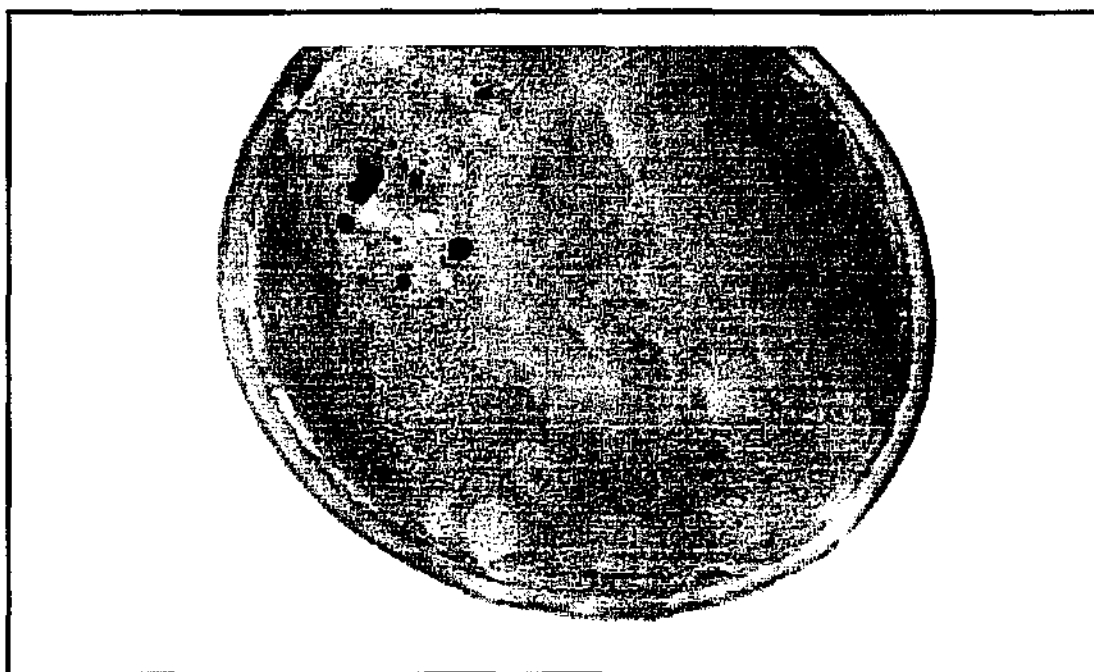


Figure 11.4 : A transmission electron micrograph of a yeast cell. *Saccharomyces cerevisiae* cells were washed in d.d. water and prepared as controls. A single cell is shown at a magnification of 14 000.



**Figure 11.5 :** A transmission electron micrograph showing a cross-sectional view of a *Saccharomyces cerevisiae* cell (magnification 14 000). The cells were prepared for TEM after 30 minutes exposure to copper chloride.



**Figure 11.6 :** A transmission electron micrograph of cross-sectional view of a *Saccharomyces cerevisiae* cell. The yeast cells were prepared for TEM after a 30 minute exposure to copper chloride and acid treatment to release bound metal. A single cell is shown at a magnification of 19 000.

## 11.5 DISCUSSION

Metal recovery was most efficient using the mineral acids. By sequentially decreasing the reaction mixture pH with nominal volumes of HCl, H<sub>2</sub>SO<sub>4</sub> and HNO<sub>3</sub> a copper recovery of  $\geq 80\%$  was achieved. Similar results were obtained in the desorption of copper from *Streptomyces noursei* by mineral and organic acids (234). The advantage of dilute acid elution is the low chemical stress to the cells. The high metal recovery supports the proposed metal removal mechanism of adsorption to the cell wall of the yeast cells. The calcium carbonates, calcium chloride and potassium chloride were ineffective as eluting solutions. NaOH and KOH increased adsorption. NaOH was used for biosorbent regeneration post acid desorption. It neutralised the biosorbent pH and had the beneficial side-effect of enhancing metal removal efficiency.

Adsorption-desorption of copper was investigated over 8 cycles in batch studies with no apparent adverse effect on uptake capacity or recovery. The ability to recycle the yeast enhances its potential for continuous and scale-up bioremediation operation. The ability for repeated use of a biosorbent was reported by Harris and Ramelow (235). Copper was desorbed from *C. vulgaris* and *S. quadricauda* using 0.05 M sodium acetate at pH 2. Up to eight cycles of copper adsorption-desorption cycles were run. All the copper was recovered from *S. quadricauda* with two sodium acetate washes per cycle and recovery from *C. vulgaris* was 63 %. Purified cell walls of *Bacillus subtilis* exposed to repeated copper-HNO<sub>3</sub> adsorption-desorption increased copper uptake over 5 cycles due to enhanced exposure of binding sites (233). The major implication of a reusable biosorbent is that it substantially improves the economics of the bioremediation system.

Transmission electron microscopy was used to determine the effect of continuous metal and acid exposure to the cell structure. Cells exposed to copper showed no apparent damage to cell integrity or any morphological changes when compared to the untreated controls. The micrographs of cells exposed to copper were characterised by dark, electron dense cell walls, which may indicate copper binding. One of the limitations of TEM is the inability to positively identify the metals which appear as these dark electron dense areas. Beveridge and Murray (45) reported that metals with atomic numbers greater than 11 could be detected by electron microscopy on the cell walls of *Bacillus subtilis*. Their findings were supported by x-ray diffraction. Golab (236) presented electron micrographs of *Streptomyces sp* showing lead bound to the cell surface. The binding of

metal to the cell wall would be expected as it comprises many potential negative sites for cationic deposition.

The micrographs of cells exposed to both copper and acid treatment were spherical in appearance and did not have cell walls that were as electron dense. The micrographs suggest a metabolism independant surface binding which would allow rapid adsorption and recovery of bound metal and thus repeated use of the biosorbent.

## 11.6 CONCLUSION

Copper accumulation by immobilised *S. cerevisiae* biomass was reversible and was most successfully recovered using HCl, H<sub>2</sub>SO<sub>4</sub> and HNO<sub>3</sub>. Removal and recovery efficiencies of the immobilised biosorbent improved with up to 8 repeated adsorption-desorption cycles in batch reactors. Electron micrographs showed no damage to the cells and supported the mechanism of metal binding to the cell surface. The biosorbent showed the potential for reuse in continuous bioremediation systems.



## 12 METAL REMOVAL AND RECOVERY FROM *SACCHAROMYCES CEREVISIAE* BIOSORPTION COLUMNS

### 12.1 INTRODUCTION

Immobilised biomass in packed-bed bioreactors have shown realistic potential for industrial application of metal removal and recovery. Tsezos *et al* (237) demonstrated the reusability of an immobilised *R. arrhizus* biosorbent in continuous packed-bed columns for up to 12 cycles with no apparent indication of failure. The main advantages of a fixed-bed reactor is ease of liquid/solid separation and biosorbent regeneration. The biosorbent should have a high affinity for the target metal and be tolerant to continuous application of metal effluent and the eluting solution. The behaviour of the biosorption column should allow for high flux rates and swelling of the biomass must be minimal to prevent clogging.

The objectives of this study was to investigate the binding of the metals copper, cobalt, zinc, cadmium, nickel, chromium and gold to immobilised *S. cerevisiae* in packed-bed semi-continuous flow columns, to determine recovery and concentration potential and to assess the reusability of the biomass. Two flow columns in series were used to demonstrate the potential for selective binding from mixed metal solutions. The metals were eluted from the columns using dilute acid.

### 12.2 MATERIALS

As described previously in 10.2.

### 12.3 METHOD

#### 12.3.1 *S. cerevisiae* immobilisation

Yeast immobilisation as described previously in 10.3.1.

#### 12.3.2 Biosorption columns preparation

LKB chromatography columns were packed with 20 ml of the immobilised yeast slurry and conditioned by passing 20 ml 0.1 M HCl, 20 ml NaOH and 40 ml water through the column. Single metal applications of 200  $\mu\text{mol/l}$  and a volume of 500 ml were passed through the columns at a flow

### *Biosorption columns*

rate of 1 ml per minute. Metal chloride solutions investigated were  $\text{Cu}^{2+}$ ,  $\text{Zn}^{2+}$ ,  $\text{Co}^{2+}$ ,  $\text{Cd}^{2+}$ ,  $\text{Ni}^{2+}$ ,  $\text{Cr}^{3+}$  at pH 5. Gold was investigated at pH 2. The eluent was collected in 10 ml fractions. The metals were then eluted from the columns with 50 ml 0.1 M HCl and collected in 2 ml fractions. The columns were reconditioned by washing with 20 ml 0.05 M NaOH and 20 ml water. The metal solutions were then reapplied and the process repeated.

#### 12.3.3 Selective recovery of metals from a mixed metal solution

Mixed metal solutions were passed through two columns set in series. The columns were monitored for metal saturation. At saturation the columns were disconnected and the metals eluted.

#### 12.3.4 Reusability of the biosorbent columns

Eight adsorption-desorption cycles were investigated for a biosorption column for a 200  $\mu\text{mol/l}$  copper solution.

## 12.4 RESULTS

### 12.4.1 Metal uptake on immobilised *S. cerevisiae* biosorption columns

Typical bioaccumulation profiles are shown in Figures 12.1-12.4. The biosorbent removed the metals until reaching a saturation threshold, following which the uptake declined rapidly. The metals were desorbed and recovered with 0.1 M HCl elution. Removal of metals are reported as  $\mu\text{mol/g}$  of *S. cerevisiae* and recovery of bound metals as a percentage in table 4.1. Above 90 % of the copper, zinc and cobalt recovered was concentrated in a 10 ml acid elution volume. Cadmium and nickel were recovered in approximately 15 ml acid eluant. The columns were reconditioned and the metals reapplied to assess reusability (table 12.1). Chromium and gold were not desorbed using 0.1 M HCl. Increasing the acid concentration to 1.0 M yielded a 34 % chromium recovery. Gold was recovered from the biosorption columns using 0.1 M  $\text{CaCl}_2$  in 3 M HCl.

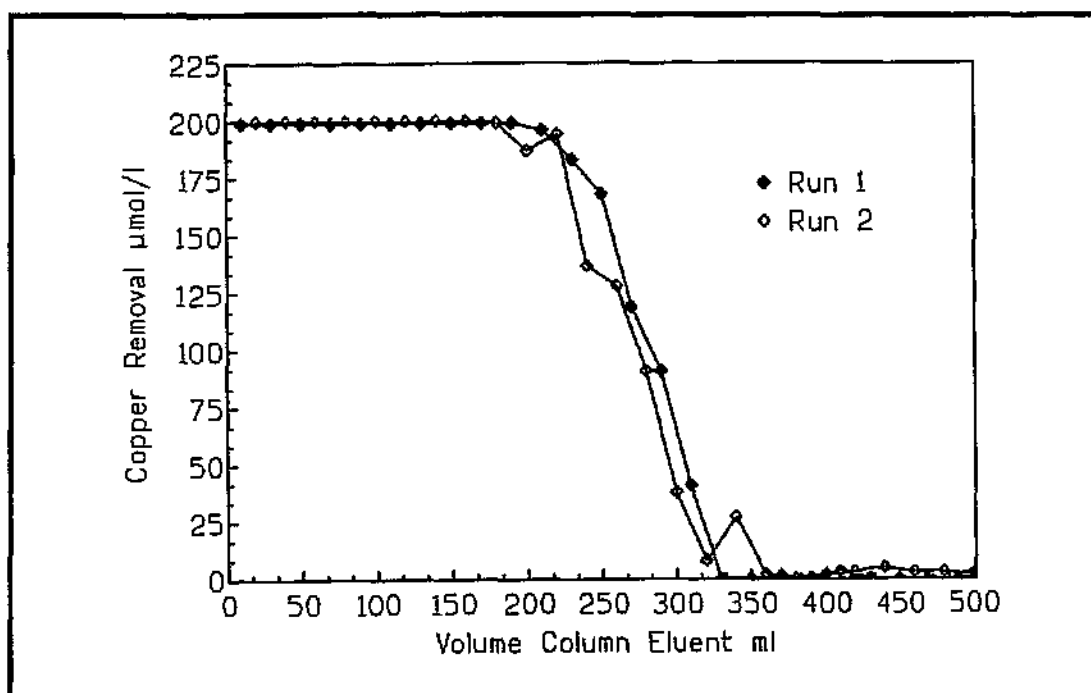


Figure 12.1 : Bioaccumulation of copper on a 20 ml immobilised *Saccharomyces cerevisiae* column. The copper was desorbed using 0.1 M HCl, the column was recondition and the copper reapplied to determine reusability of the biosorbent.

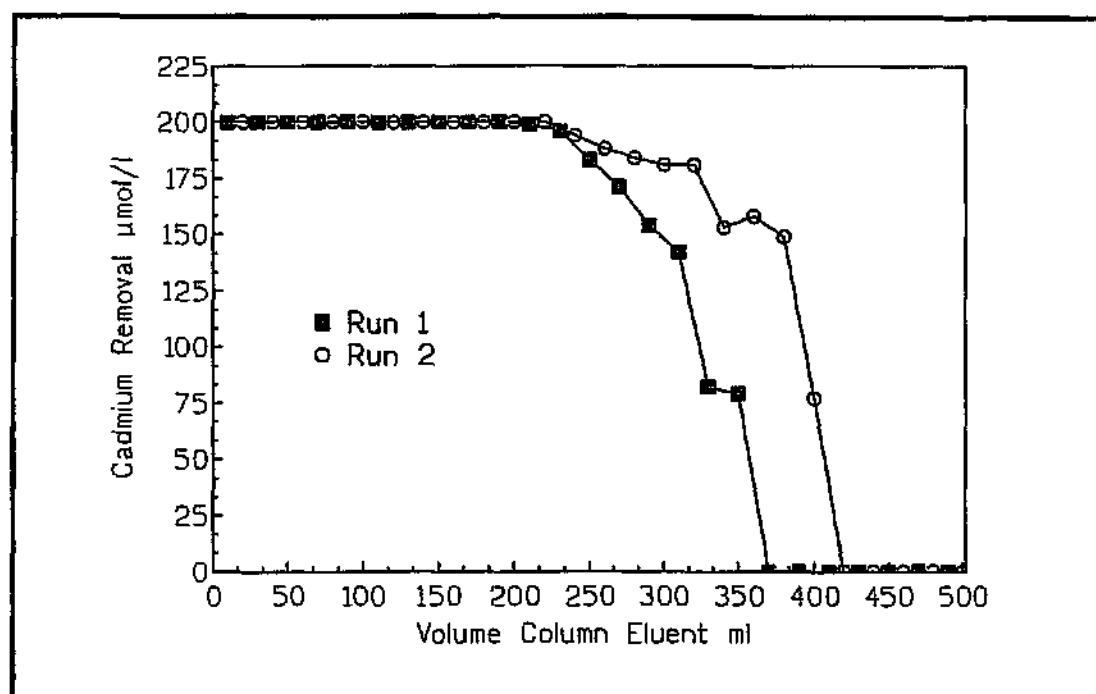


Figure 12.2 : Bioaccumulation of cadmium on a 20 ml immobilised *Saccharomyces cerevisiae* column. The cadmium was desorbed using 0.1 M HCl, the column was recondition and the cadmium reapplied to determine reusability of the biosorbent.

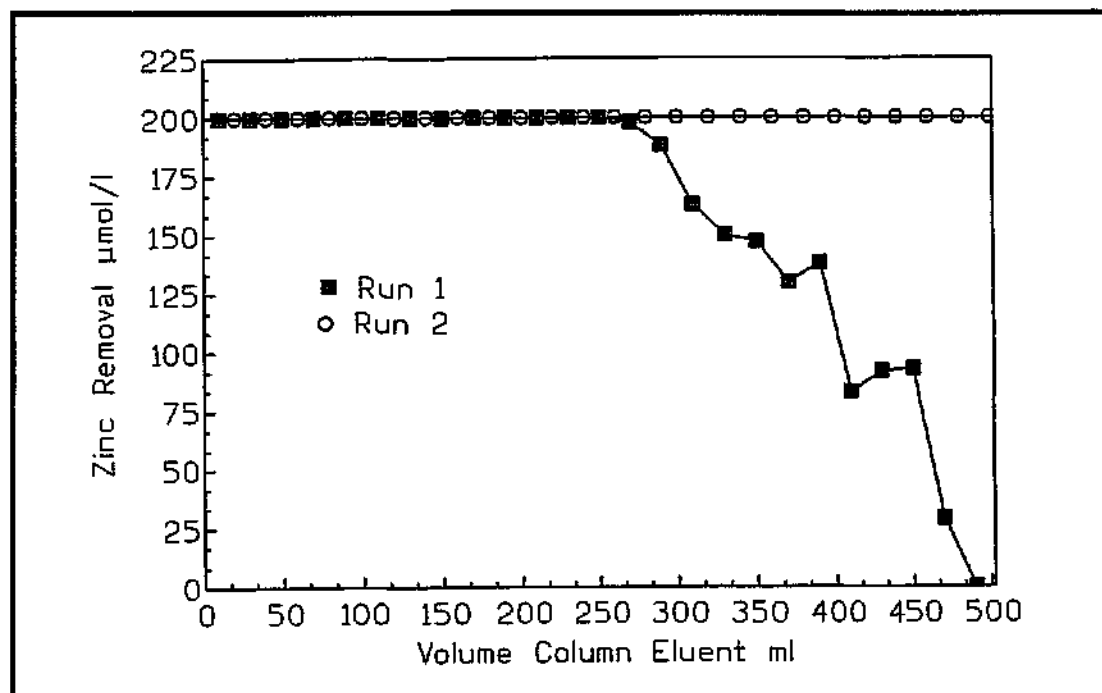


Figure 12.3 : Bioaccumulation of zinc on a 20 ml immobilised *Saccharomyces cerevisiae* column. The zinc was desorbed using 0.1 M HCl, the column was recondition and the zinc reapplied to determine reusability of the biosorbent.

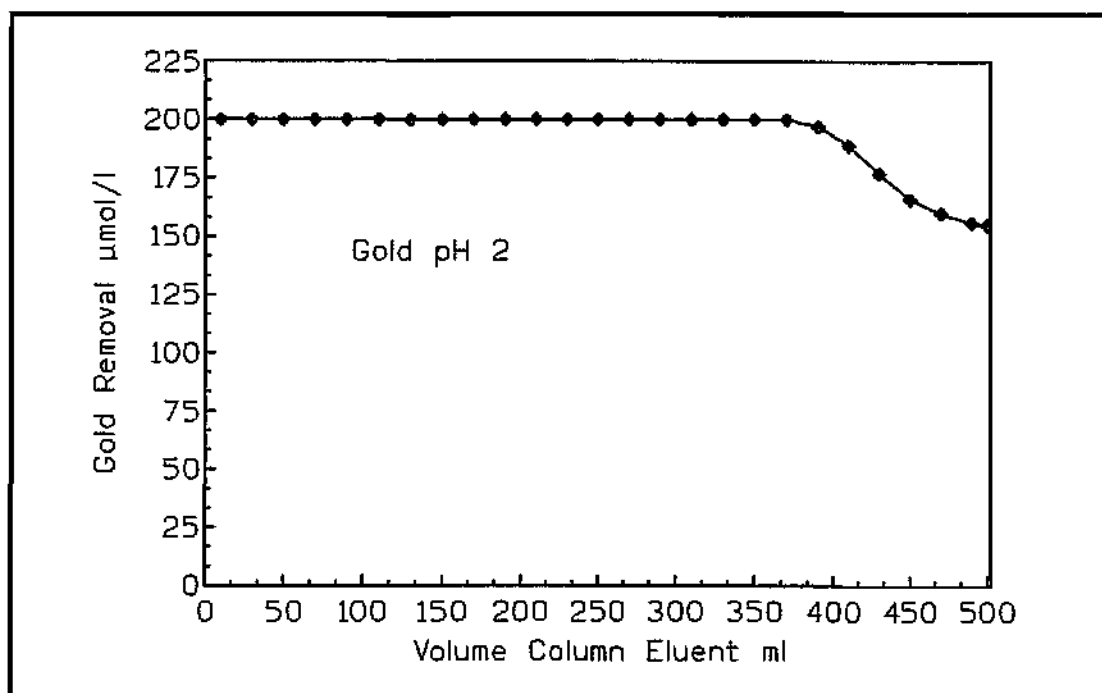


Figure 12.4 : Bioaccumulation of gold on a 20 ml immobilised *Saccharomyces cerevisiae* column.

**Table 12.1** : Metal uptake on a *S. cerevisiae* column and metal recovery

METAL	Removal* $\mu\text{mol/g}^{**}$		Recovery* percentage	
	Run 1	Run 2	Run 1	Run 2
Copper	27.9	27	100	91
Cobalt	49.7	50	100	99
Cadmium	31.6	37.3	100	100
Nickel	33.7	38.7	100	91
Zinc	40.7	49.9	89	61
Chromium	28.6	—	34***	—
Gold	42.2	—	67****	—

\* Typical results reported

\*\* Bioaccumulation results expressed as  $\mu\text{moles/g}$  wet weight *S. cerevisiae*

\*\*\* Chromium recovered with 1 M HCl.

\*\*\*\* Gold recovered with 0.1 M  $\text{CaCl}_2$  in 3 M HCl

#### 12.4.2 Selective recovery of metals from mixed metal solutions

Mixed metal solutions of two metal species were passed through two columns run in series. The two columns were separated and washed individually with 0.1 M HCl and the metal accumulated on each column recovered. Copper bioaccumulation and recovery from the first of the columns in series was the most efficient of the metals investigated. Copper displaced other metals to the second column. Zinc was displaced by copper at a binding ratio of 6:1. Cadmium was displaced by copper, however substantial mixing occurred and selective recovery was not achieved. Copper bound preferentially to cadmium at a ratio of 2:1. Copper bound preferentially to cobalt at a binding ratio of 4:1. Desorption profiles of the 2 columns are presented in Figure 12.5 and 12.6. The metal recovered and concentrated from the first column was  $\geq 75\%$  copper. The second of the two column series bound predominantly cobalt (99 %).

#### 12.4.3 Repeated adsorption-desorption cycles of a biosorption column

Copper chloride was applied repeatedly for eight success cycles to a single immobilised *S. cerevisiae* biosorption column. Copper bioaccumulation initially declined (cycles 2 and 3), but increased in the latter cycles (Table 12.2).

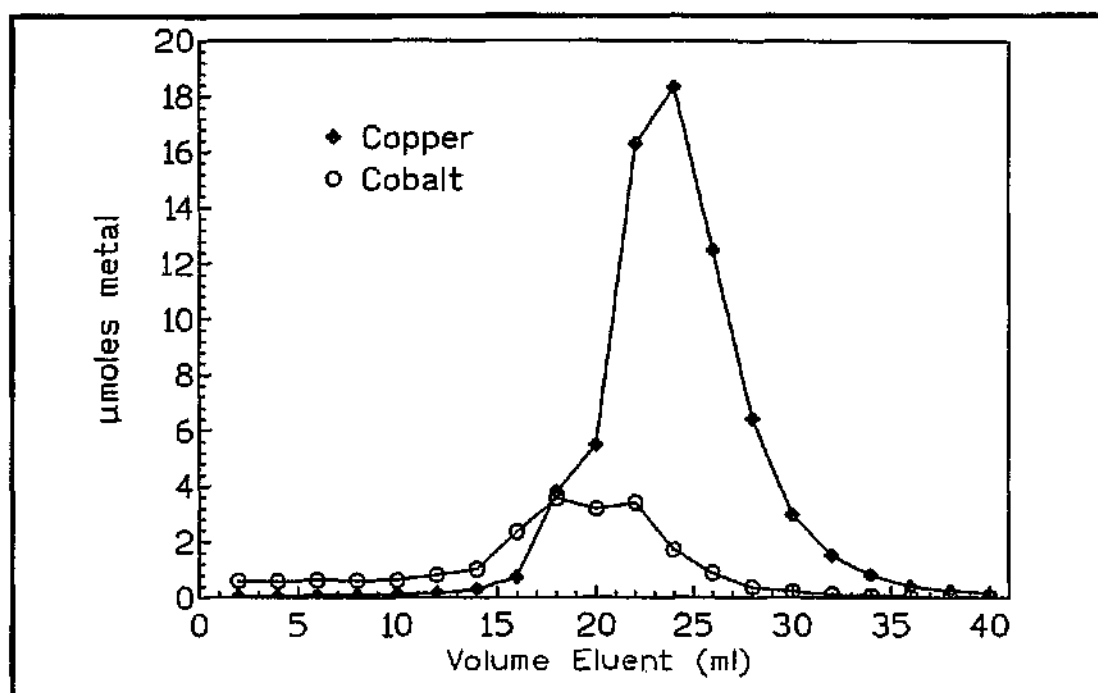


Figure 12.5 : Desorption of copper and cobalt from a 20 ml immobilised *Saccharomyces cerevisiae* column (column 1 of 2 in series). Desorption was achieved using 0.1 M HCl. The results are expressed as  $\mu\text{moles}$  metal recovered per 2 ml eluent. The predominant metal eluted from this first column was copper.

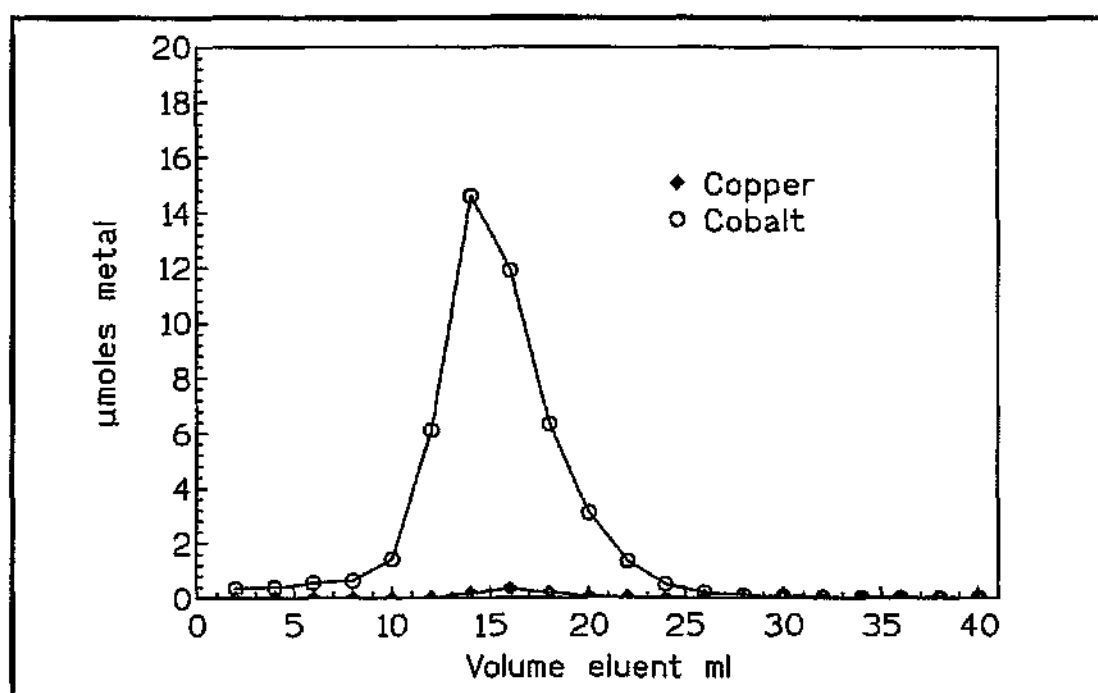


Figure 12.6 : Desorption of copper and cobalt from a 20 ml immobilised *Saccharomyces cerevisiae* column (column 2 of 2 in series). Desorption was achieved using 0.1 M HCl. The results are expressed as  $\mu\text{moles}$  metal recovered per 2 ml eluent. The predominant metal eluted from this second column was cobalt.

**Table 12.2** : Adsorption-desorption reusability investigation. Adsorption of copper to an immobilised *S. cerevisiae* biosorption column over 8 cycles.

Run Number	Copper Adsorption $\mu\text{mol/g}$	Percentage Recovery
1	31.3	85
2	26.8	96
3	24.3	100
4	28.1	96
5	32.0	100
6	37.7	81
7	47.8	100
8	44.4	100

## 12.5 DISCUSSION

The metal ions were effectively removed from solution by the immobilised yeast in the fixed-bed biosorption column reactors. The biosorbent removed the metals until reaching a saturation threshold, following which the uptake declined rapidly. The metals were desorbed and recovered from the biosorbent by eluting the column with 0.1 M HCl. The initial recovery of accumulated copper, cobalt and cadmium was 100 %. The high recovery of metal by mild acid elution concurs with passive binding to the cell walls of the *S. cerevisiae*. The recovered metals were concentrated in small volumes. Copper, zinc, cadmium, nickel and cobalt were detected in 10-15 ml acid eluant, representing up to a 40 fold reduction from the initial volume. From a practical perspective, a high concentration factor reduces the volume of metal bearing solution making an effluent more manageable. High recovery of bound metal is also necessary for biosorbent reuse.

Chromium was not desorbed using 0.1 M HCl and increasing the acid concentration to 1.0 M yielded a 34 % recovery. The inability to recover chromium by mild acid treatment could lead to selective desorption between the chromium and the other cations examined. Gold was recovered (67%) from the biosorption column using an acidic  $\text{CaCl}_2$  eluant.

The columns were reconditioned and the metals reapplied to assess reusability. Bioaccumulation with the second metal application remained constant or was increased with certain metals. Cadmium, nickel and zinc exhibited substantial increases in adsorption. Cadmium was initially

### *Biosorption columns*

accumulated at a rate of 31.6  $\mu\text{mole/g}$  and 37.3  $\mu\text{mole/g}$  on the second application. All adsorbed cadmium was recovered by 0.1 M HCl elution, a 33% fold volume reduction was observed for both applications. Cobalt was accumulated the most successfully, with an initial 99.9% and then a 100 % removal from the applied 500 ml solutions. Zinc recovery from the biosorbent by acid elution was reduced after the second application, possibly a result of internalisation.

The beneficial consequence of the adsorption-desorption cycles demonstrate the ability for continuous utilisation of the biosorption columns. Reconditioning of the biosorbent with NaOH may benefit the uptake capacity by exposing of additional binding sites.

Mixed metal solutions of two metal species were passed through two columns set in series to determine the extent of selective uptake of the cations due to different affinities for sorption binding sites on the biomass. Post metal bioaccumulation the two columns were separated and washed individually with 0.1 M HCl and the metal accumulated on each column recovered. Copper bioaccumulation and recovery from the first of the columns in series was the most efficient of the metals investigated, displacing other metals to the second column. Zinc was displaced by copper at a binding ratio of 6:1. Cadmium was displaced by copper, however substantial mixing occurred and selective recovery was not achieved. Copper bound preferentially to cadmium at a ratio of 2:1. Selectively binding was clearly demonstrated between the metals copper and cobalt. Copper bound preferentially to the first column (binding ratio of 4:1) and cobalt was displaced by the copper ions onto the second column. The metal recovered and concentrated from the first column was  $\geq 75\%$  copper. The second of the two column series bound predominantly cobalt and a 99 % pure cobalt concentrate was obtained.

Nakajima *et al* (238) demonstrated the ability of *Chlorella regularis* to accumulate metals selectively. The amount of metal cations taken up in batch reactors decreased in the order  $\text{Cu} \gg \text{Zn} \geq \text{Co} \geq \text{Cd} \geq \text{Ni}$ . They concluded that the selectivity of *C. regularis* is due to the strength of coupling between the metals and the cell components, particularly proteins. The influence of competing ions is a factor which requires consideration when developing a bioremediation operation for an industrial effluent. Knowledge of the different affinities of the metals for a biosorbent can be used to maximise the efficiency of the remediation process allowing selective removal of target metals.



A single column was used for eight consecutive adsorption-desorption cycles. The copper uptake declined from 31.3  $\mu\text{mol/g}$  to 24.2  $\mu\text{mol/g}$  over 3 cycles, thereafter uptake progressively increased after each cycle to 47.8  $\mu\text{mol/g}$  at cycle 7. The quantity of copper accumulated corresponded to the quantity eluted indicating complete elution. As was observed in the batch studies, metal accumulation increased with repeated application and metal recovery remained high.

## 12.6 CONCLUSION

The immobilised *S. cerevisiae* packed-bed biosorption columns removed metals from aqueous solutions. The bioaccumulated metals were recovered by 0.1 M HCl elution. The desorption protocol utilised a minimum quantity of dilute acid and yielded a concentrated, low volume metal eluant. The ease of metal elution and recovery from the columns implied passive binding to the cell wall. The biomass was reusable. The adsorption-desorption process did not adversely affect the uptake capacity of the biosorbent and the uptake of certain metals was enhanced with continuous use. A copper solution was run on a single column through 8 cycles with no apparent decrease in biosorbent performance. The potential for selective recovery by the biosorbent and elution protocol was demonstrated. The success of selective binding and recovery of metals from mixed metal solutions was dependant on affinity of the metals and their initial concentration in solution. The reusability of the biosorbent and the selective recovery of target metals could lead to the development of a viable, cost effective metal bioremediation technology.

## **13 THE REMOVAL OF METALS FROM MINING EFFLUENT BY IMMOBILISED *SACCHAROMYCES CEREVISIAE***

### **13.1 INTRODUCTION**

Present metal removal methods from industrial waste waters include chemical precipitation, chemical oxidation or reduction, filtration and evaporation are often ineffectual and expensive particularly when dealing with large volumes at relatively low metal concentrations ( $\leq 100$  ppm) (192). Bioremediation technology can potentially provide an efficient, inexpensive alternative to these traditionally used methods. Bioremoval of metals could also be utilised to complement an established remediation operation. Transfer of the technology from the laboratory to scaled-up operations presents a major challenge due to the unpredictable nature of different effluents and uncontrollable environmental factors. The performance of bioremediation is site specific and each effluent requires individual investigation to determine the effectiveness of the proposed process (222).

In this study bioremediation of a effluent supplied from a copper, zinc and lead mine was investigated on a fundamental level to assess the feasibility of using the immobilised *Saccharomyces cerevisiae* biosorbent. The target metals in the effluent were copper, iron, zinc and lead. The pH was low and it contained a range of co-contaminating waste compounds. The mine's main concern being metal removal and the supply of metal free water for reuse in their extraction operations.

### **13.2 MATERIALS**

#### **13.2.1 Mine effluent**

Mining effluent was supplied from Goldfields of South Africa Ltd. The effluent was obtained from Plaatjiesvlei, a wastewater catchment zone.

### **13.3 METHOD**

#### **13.3.1 pH profile**

The pH of the mine effluent was sequential adjusted with NaOH and the metal content analysed over a pH range of 2 to 6.

### 13.3.2 Batch remediation

As described in section 10.3.3.

## 13.4 RESULTS

### 13.4.1 Effluent composition and pH profile

The composition of the mine effluent is represented in Table 13.1.

**Table 13.1 :** Composition of the mine effluent.

Analysis	Result	Units
pH	2	
COD	148	mg/l
Calcium	22 207	$\mu\text{mol/l}$
Magnesium	4 978	$\mu\text{mol/l}$
Copper	21.3	$\mu\text{mol/l}$
Lead	7.3	$\mu\text{mol/l}$
Zinc	39.2	$\mu\text{mol/l}$
Iron	1 078	$\mu\text{mol/l}$
Chlorine	17 453	$\mu\text{mol/l}$
Sulphate	37 683	$\mu\text{mol/l}$

The pH of the mine effluent was increased using NaOH. Iron, copper, lead and zinc levels in solution were all influenced by the increase in pH. The iron concentration was reduced from 1078  $\mu\text{mol/l}$  at pH 2 to 187  $\mu\text{mol/l}$  at pH 6. Lead was reduced from 7.3  $\mu\text{mol/l}$  to 0.82  $\mu\text{mol/l}$ , copper from 21.3  $\mu\text{mol/l}$  to 0.6  $\mu\text{mol/l}$  and zinc from 39.2  $\mu\text{mol/l}$  to 19.3  $\mu\text{mol/l}$ .

### 13.4.2 Bioremediation of heavy metals iron, lead, copper and zinc by immobilised *S. cerevisiae*

The bioremediation process was dependant on the effluent pH. Removal of metals from the effluent using bioremediation at sequentially increased pH are shown in Figures 13.1-13.4. At pH 2 metal removal was negligible (lead 24%, iron 7%, copper and zinc 0%). At pH 4 iron was

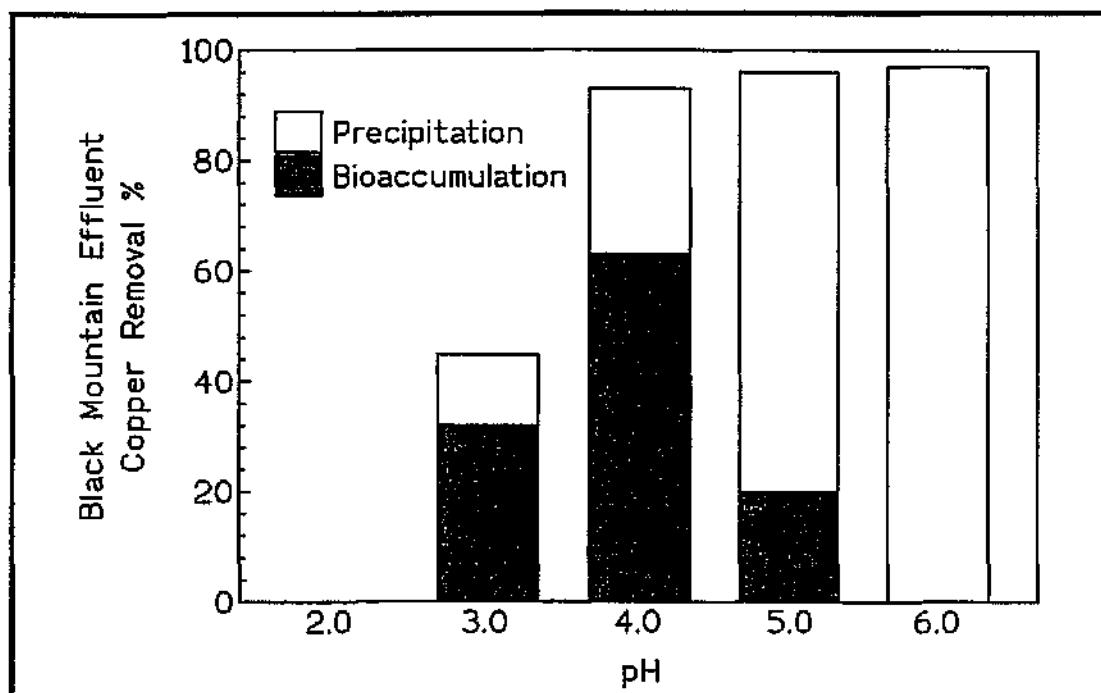


Figure 13.1 : Removal of copper from the Black Mountain mine effluent by immobilised *Saccharomyces cerevisiae* in batch reactors. The initial copper concentration was  $21.3 \mu\text{mol/l}$ . By increasing the effluent pH using NaOH the copper was removed from solution by  $\square$  precipitation  $\blacksquare$  bioaccumulation.

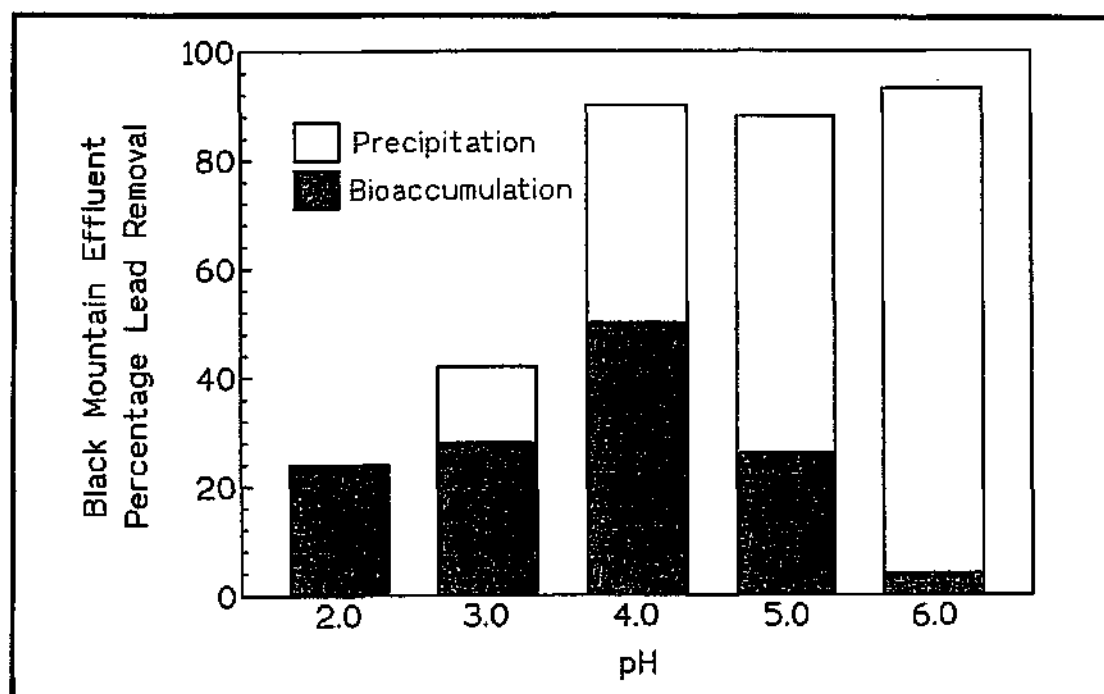
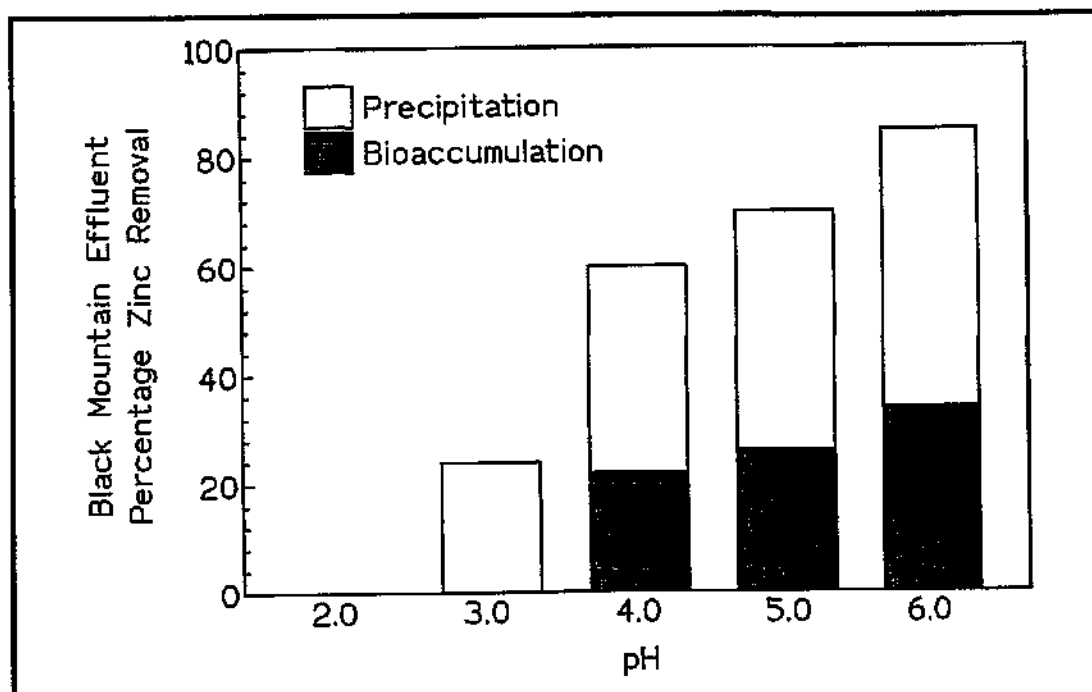
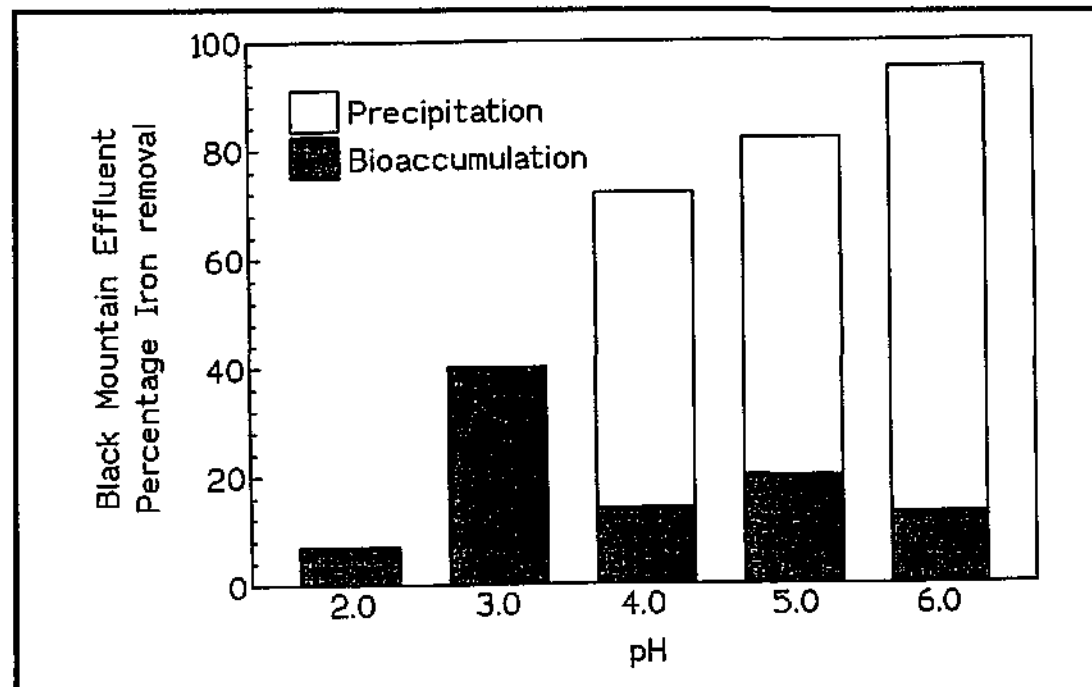


Figure 13.2 : Removal of lead from the Black Mountain mine effluent by immobilised *Saccharomyces cerevisiae* in batch reactors. The initial lead concentration was  $6.2 \mu\text{mol/l}$ . By increasing the effluent pH using NaOH the lead was removed from solution by  $\square$  precipitation  $\blacksquare$  bioaccumulation.



**Figure 13.3 :** Removal of zinc from the Black Mountain mine effluent by immobilised *Saccharomyces cerevisiae* in batch reactors. The initial zinc concentration was  $39.2 \mu\text{mol/l}$ . By increasing the effluent pH using NaOH the zinc was removed from solution by  precipitation  bioaccumulation.



**Figure 13.4 :** Removal of iron from the Black Mountain mine effluent by immobilised *Saccharomyces cerevisiae* in batch reactors. The initial iron concentration was  $1078 \mu\text{mol/l}$ . By increasing the effluent pH using NaOH the iron was removed from solution by  precipitation  bioaccumulation.

decreased by 72 %, copper by 93 %, lead by 90 % and zinc by 60 %. The percentage metal removal was by a combination of precipitation as a result of the pH change and of bioremediation as shown.

### 13.5 DISCUSSION

The mine effluent contains a multitude of contaminants which affect metal removal. The degree of heavy metal removal from waste water depends on the multimetal competitive interactions in solution with the sorbent material (239). The Plaatjiesvlei effluent is further complicated by the low pH which is not appropriate for cation bioremoval. At pH 4 the biosorbent's metal uptake capacity was improved and a large percentage of the iron precipitated from solution. Because of its geological abundance iron is commonly found in mine waste waters. High iron concentrations have the affect of inhibiting the uptake of coexisting metals. The ease of iron removal by precipitation support a combination strategy of pH adjustment and bioremediation. Copper and lead were the target metals most successfully removed by bioremediation. The high sulphate content of the effluent is a contaminant not dealt with in this investigation, however it could provide an alternative treatment strategy. Metals can be precipitated as insoluble sulphides which can be biologically generated by sulphate reducing bacteria from the sulphate in the effluent as demonstrated by Hammack and Edenborn (128).

### 13.6 CONCLUSION

The combined use of chemical precipitation and bioremediation was used to remediate a metal-laden mine effluent. The complexity of the effluent and its interaction with the biomaterial requires substantial fundamental and applied research before its full potential can be attained. At present, the immobilised *Saccharomyces cerevisiae* biomass has limited application to the effluent investigated but may be used to complement a chemical remediation operation.

## 14. THE USE OF *SPIRULINA SP* FOR THE TREATMENT OF A MINE EFFLUENT

### 14.1 Introduction

Three major problem areas have been identified which currently prevent the recycling of the water used in the extraction of metals at the Black Mountain Mine. These are the acid pH of the effluent, the high sulphate content and the heavy metals which remain in solution. In view of this we have set about developing a system which can address these three areas. The system essentially consists of three units, the first an algal based ponding system designed to precipitate the majority of the heavy metals and raise the pH, the second a sulphate reducing step utilising bacterial sulphate reduction and finally a polishing step.

Alkaline precipitation of heavy metals from acidic effluents is a widely practised treatment method. The process usually involves the addition of lime ( $\text{CaCO}_3$ ) to the effluent. The alkaline material usually has to be added continuously or at regular intervals to obtain sufficient metal removal. The idea behind the algal system is to develop a system which is able to be self-regulating, maintaining the pH at a level high enough to sustain sufficient precipitation without necessitating further addition of chemicals.

The enzyme carbonic anhydrase (CA) is central to the ability of the algae to increase the pH of its surrounding medium. As algae are autotrophs they are dependent on the import of inorganic carbon into the cells to be used in the photosynthetic pathway. In plants, which are constantly exposed to the air carbon is obtained from atmospheric carbon dioxide ( $\text{CO}_2$ ). Submerged plants, such as algae, are dependent on dissolved  $\text{CO}_2$  to fulfil this need. In the presence of low levels of dissolved  $\text{CO}_2$  the algae are able to induce an inorganic carbon ( $\text{C}_i$ ) accumulating mechanism. The induction of this mechanism is primarily dependent on a reduction in levels of  $\text{C}_i$  and light.

Carbonic anhydrase catalyses the interconversion of dissolved  $\text{CO}_2$  and carbonic acid ( $\text{H}_2\text{CO}_3$ ) to bicarbonate ions ( $\text{HCO}_3^-$ ) via enhanced rates of hydration/dehydration. The reactions involved in the accumulation of dissolved inorganic carbon are as follows:

1.  $\text{CO}_2 + \text{H}_2\text{O} \rightarrow \text{H}_2\text{CO}_3$
2.  $\text{H}_2\text{CO}_3 \rightarrow \text{HCO}_3^- + \text{H}^+$
3.  $\text{HCO}_3^- \rightarrow \text{CO}_2 \text{ (inside cell)} + \text{OH}^- \text{ (outside cell)}$

The  $\text{HCO}_3^-$  is converted to  $\text{CO}_2$ , which is internalised and incorporated into the photosynthetic pathway, and  $\text{OH}^-$  ions which remain in solution. The  $\text{H}^+$  ions generated by the ionisation of the carbonic acid are removed from the solution by the cell. The result is a net increase of hydroxyl ions in the medium, which leads to the alkalisation.

Due to the filamentous nature of the *Spirulina* used in these experiments a novel method of determining the strength of the culture was required. Cell counts or photometric methods are not possible because the number of cells in the filaments varies. As a result a method was developed in which the dry mass of the algae can be estimated from the chlorophyll *a* concentration of 5ml of algal suspension. Figure 14.1 shows the standard curve from which these estimations were made.

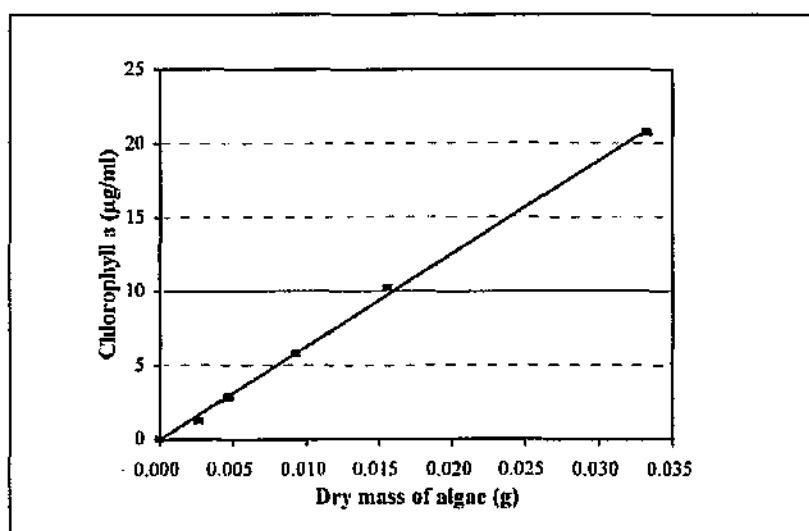


**Figure 14.1:** Standard curve for the estimation of algal dry mass from chlorophyll *a* concentrations.



## 14.2 Materials and Methods

All the algal based precipitation experiments were performed in duplicate, using effluent from the Plaatjiesvlei storage pond. In all cases the *Spirulina* was cultivated using Zarrouk's medium, a defined medium ideally suited for growing halophilic algae. The initial experiment was performed in a so-called "open" system, where evaporation could take place. The experiment was performed using 2l flasks, divided into four experimental (groups 1-4) and one control group. All groups were inoculated with 300ml of a *Spirulina* culture on day 0. On day 1 and every second day after that a 5ml sample was removed for chlorophyll extraction and the pH and salinity values were measured in each flask. The control group was given an additional 50ml of growth medium and the four experimental flasks 50ml of a effluent/growth media mix. Effluent/growth media ratios were as follows: group 1 (20:80), group 2 (40:60), group 3 (60:40) and group 4 (100:0). The pH and salinity values were measured after the additions. It was decided to delay the additions that were to have been made on day 19 to day 20 to see if the extra period between additions had any effect. A further three flasks were set up as volume controls to measure the effect of evaporation. Their volumes were measured prior to each addition. On day 2 and every second day subsequently a 5ml sample was removed, filtered and the iron, lead, copper and zinc concentrations determined using an atomic absorption (AA) spectrophotometer. The flasks were agitated for the duration of the experiment. A set of controls, using 50% volumes, containing no algae initially (ie 150ml growth medium) were set up and subjected to the same treatment as the experimental flasks.

### 14.3 Results

The results for pH, salinity and algal concentration for the duration of the experiment are shown in Figures 14.2-14.4.

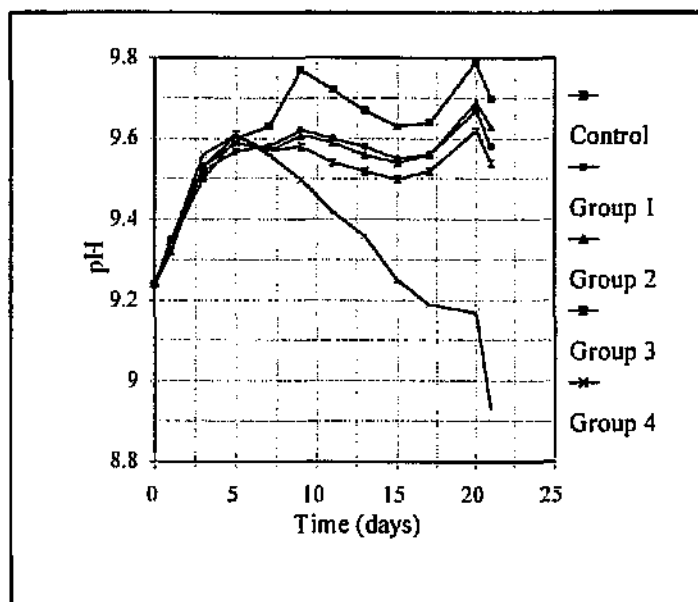


Figure 14.2: Graph of pH vs time.

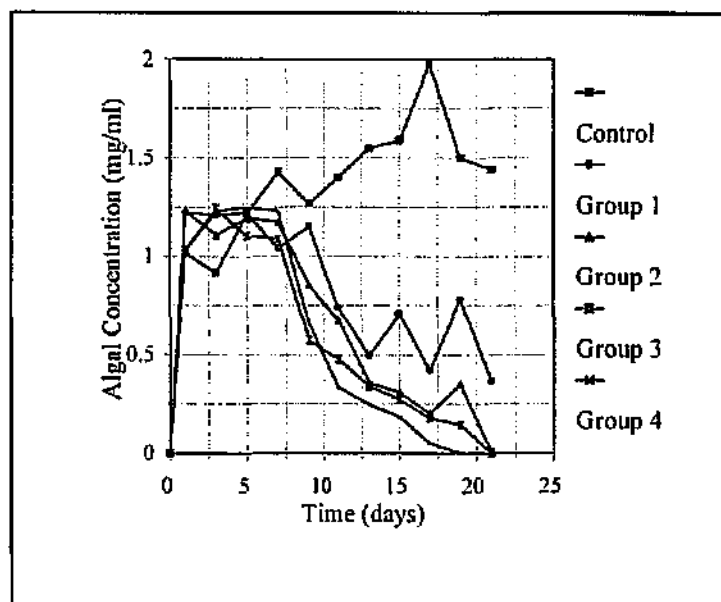
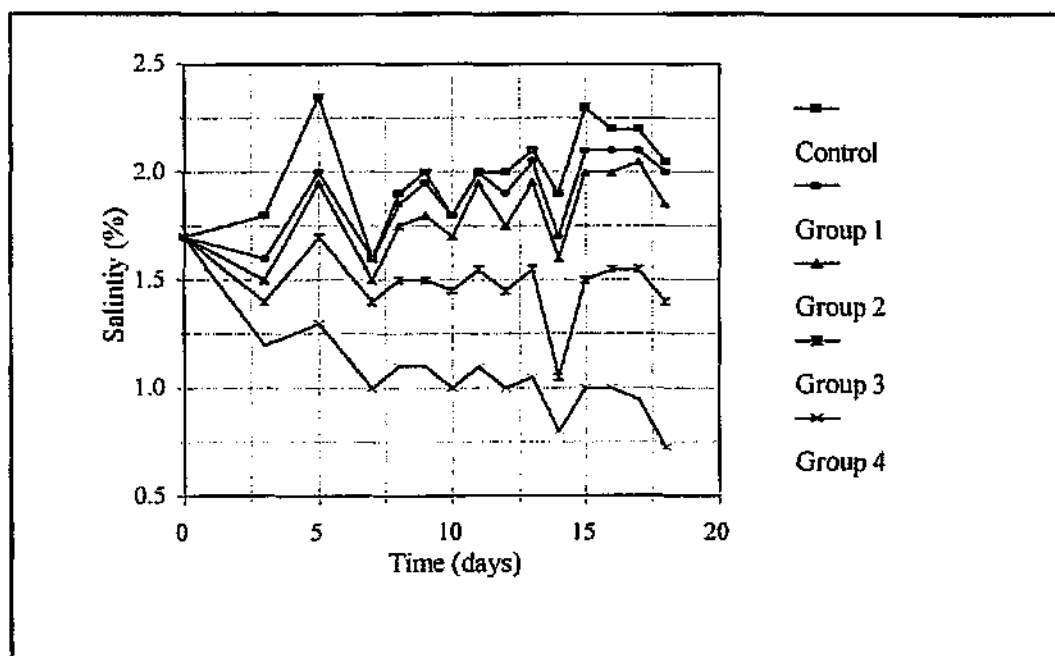


Figure 14.3: Graph of algal concentration vs time. Algal concentration (mg dry mass/ml).

From the above results it can be seen that for the first week of the experiment all five groups exhibited essentially similar behaviour. There was a steady increase in pH up to approximately 9.6, while the concentration of algae in the flasks remained at between 1.2 and 1.25 mg/ml. After the first week there was a rapid decline in the strength of the algal culture, especially in groups 2, 3 and 4. The decline was slower in group 1, while the control group, which received no effluent increased by almost 50%. By the 19th day of the experiment, all the algae in group 4 were dead and groups 2 and 3 were at between 10 and 20% of their original concentrations. Group 1 was the least affected, due to the lower amount of effluent added to it. Considering the pH data in the context of the culture strengths one would expect the graphs to look more similar. However, the relatively high salinity of the growth medium means that it has a relatively high buffering capacity. This explains why only group 4 showed a really significant decline in pH corresponding with the decrease in culture strength. It is particularly interesting to notice the effect of the delayed addition of effluent on day 20. It can clearly be seen that the pH of all the groups with the exception of group 4 increased in relation to the

results from day 17. The increase was in the region of 0.1 pH unit. However, in group 4, where all the algae had died, there was in fact a slight decrease in pH. These results clearly implicate the algae in maintaining the high pH. The salinity data (Figure 14.4) was self explanatory and showed that as the relative proportion of effluent increased the salinity of the culture decreased, simply due to the dilution of the saline medium with less saline effluent. The relatively low salinity observed in group 4 would reduce the buffering capacity of the medium and contribute towards the decreased pH.



**Figure 14.4:** Graph of salinity vs time. NaCl salinity determined using a salinity refractometer.

The data obtained for the various metals indicates that for all the metals studied, except copper, the removal of the metal from precipitation was not dependant on the amount added and was therefore most likely due to precipitation rather than adsorption to the surface of the cells. Figure 14.5 shows the amount of copper, in the form of effluent, added to the various groups and Figure 14.6 the amount of copper remaining in solution.

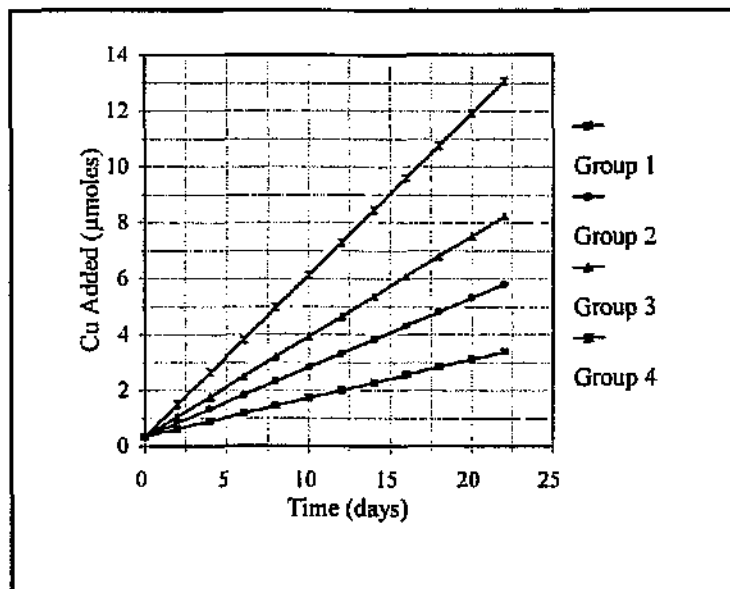


**Figure 14.5:** Cumulative copper addition ( $\mu\text{moles}$ ) vs time for experimental groups.

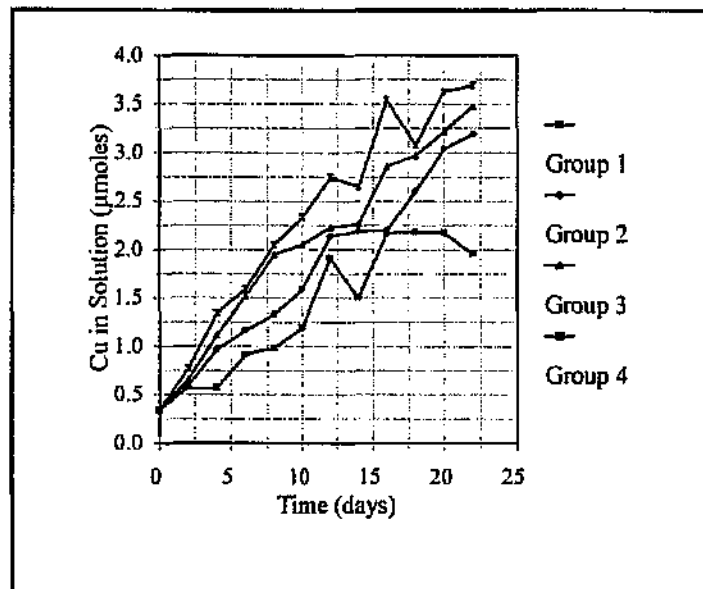


**Figure 14.6:** Amount of copper ( $\mu\text{moles}$ ) remaining in solution.

The above results showed that the amount of copper remaining in solution was dependent on the amount added, although the relationship was not proportional. These results differ from those obtained for the other metals, where the amount of metal in solution was not at all dependent on the amount added. An example of this, for iron, can be seen in Figure 14.8. The fact that the amount of metal in solution was not directly proportional to the amount added suggests that the majority of metal removal was still by precipitation and not an equilibrium dependent reaction such as adsorption to the cell surface. The results obtained for lead, zinc and iron suggest that at the pH's occurring in the flasks these metals precipitate out leaving a residual amount in solution. The results for percentage removal (Figures 14.9-14.12) seem to confirm this with copper having the lowest cumulative percentage removal. The results indicate that as more metal is added the percentage removal increases which is consistent with a precipitation mechanism.

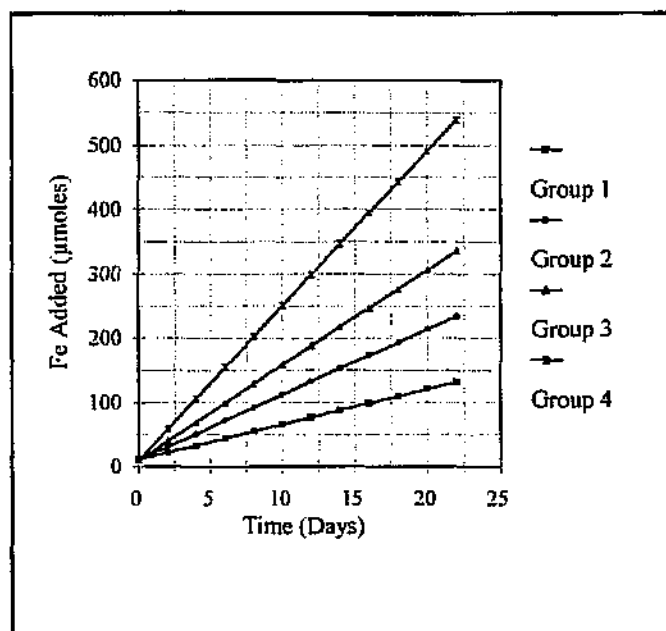


**Figure 14.7:** Cumulative iron addition ( $\mu\text{moles}$ ) vs time in experimental groups.

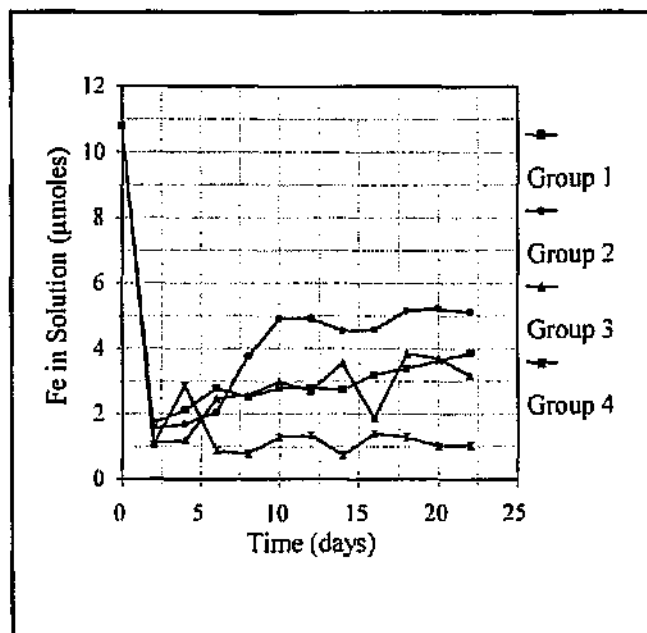


**Figure 14.8:** Amount of iron ( $\mu\text{moles}$ ) remaining in solution.

From these results it can be seen that the majority of the iron added to the system had been removed. In comparison to the copper data there seemed to be no correlation between the amount of metal added to the system and the amount of metal which remained. The data for the percentage removal showed that of the four metals tested for the iron was removed with by far the greatest efficiency. For lead (Figure 14.11) and zinc (Figure 14.12) the metal removal was relatively efficient, ranging from 60-90% depending on the amount of metal added. There appears to be precipitation down to a baseline level. This explains the fact that the graphs for the different groups run almost in parallel. The percentage removal for copper was lower suggesting that precipitation may not be the only factor involved.

The results for the control flasks were essentially very similar to the experimental ones, both in terms of pH and metal removed from solution. It was however, found that the controls became contaminated with a variety of organisms, including diatoms and bacteria, after approximately a week. The effect of these contaminating organisms on the pH and hence the metal removal could not be assessed.

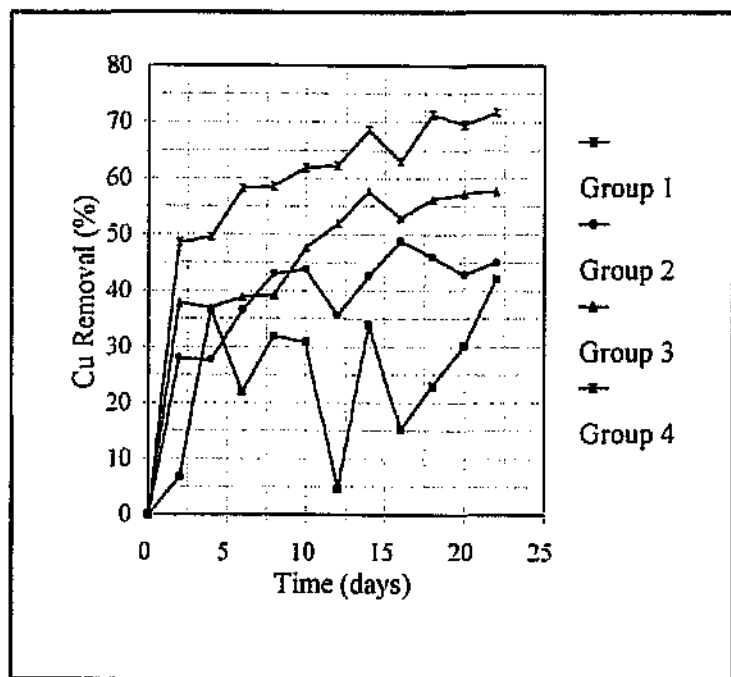


**Figure 14.9:** Efficiency (cumulative %) of algal system at removing copper from added effluent.

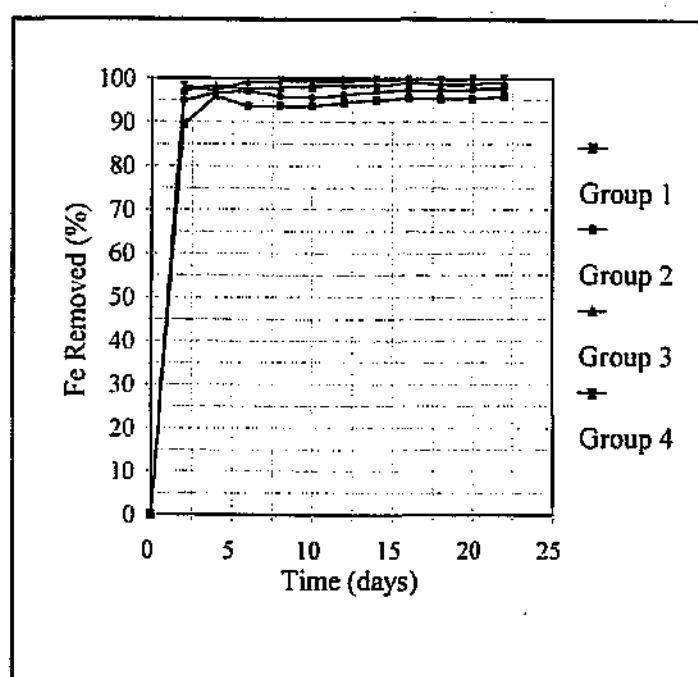


**Figure 14.10:** Efficiency (cumulative %) of algal system at removing iron from added effluent.

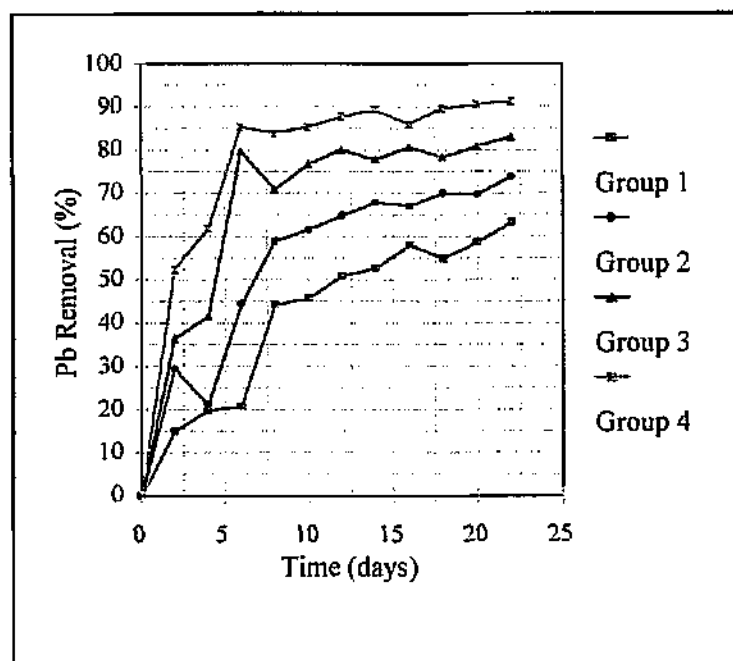


**Figure 14.11:** Efficiency (cumulative %) of algal system at removing lead from added effluent.

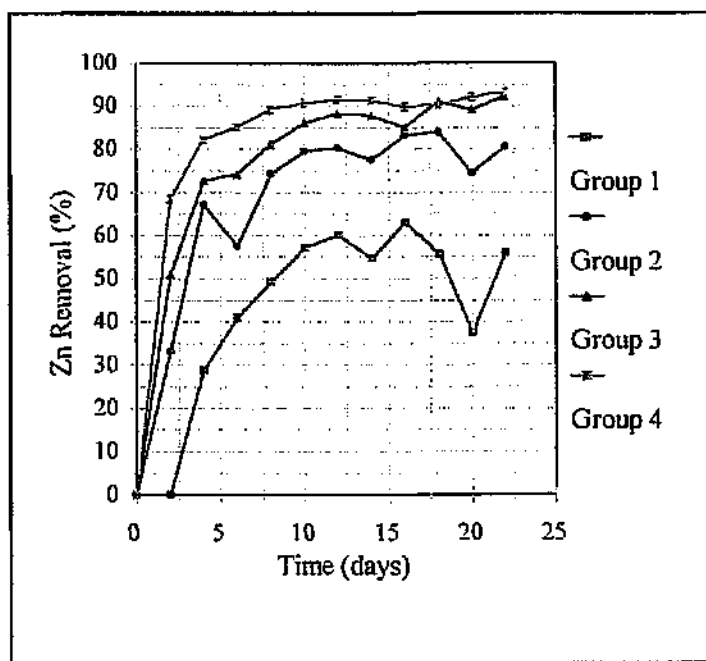


**Figure 14.12:** Efficiency (cumulative %) of algal system at removing zinc from added effluent.

### 14.3.1 Effluent Treatment in a Volume Controlled System

Following the completion of the first set of experiments some alterations to the system were made. The evaporation rate occurring under the constant environment conditions was considered to be unnaturally high, at over 40% of the total volume. As a result the flasks used in the second set of experiments were capped with foil to prevent evaporation. In addition, to make the system resemble a more "continuous type" process it was decided to maintain the volume at 400ml by removing the excess every second day. The idea is that the removed volume would be passed into the next stage of the process. Finally, no extra growth medium was added with the effluent. The experimental procedure followed was essentially the same as in the first set of experiments, with the following changes:

- a) the initial volume of algal suspension was 400ml
- b) only effluent was added (ie 10, 20, 30 and 50 mls to groups 1-4)
- c) no additional growth medium was added to the control group
- d) evaporation was restricted
- e) volume was maintained at 400ml
- f) experiments were conducted for 44 days

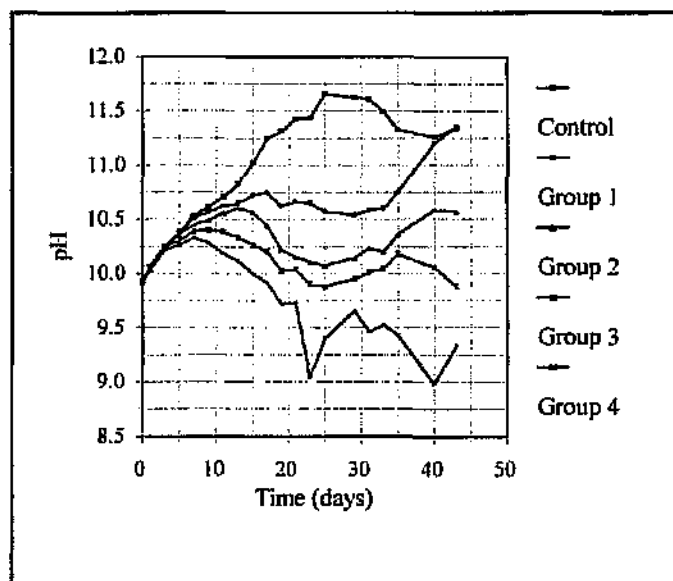


Figure 14.13: Change in pH over time for flasks in volume controlled system.

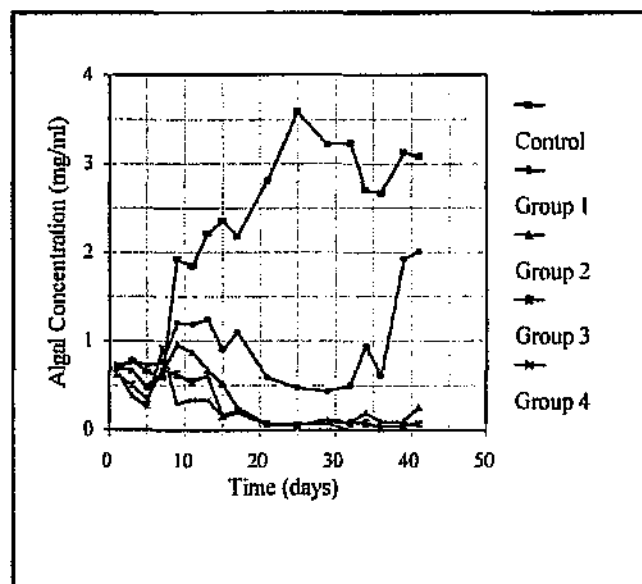


Figure 14.14: Change in algal concentration over time. Algal concentration as mg dry mass per ml.

The results demonstrate a similar trend as in the open system, with there being little difference in the pH or algal concentrations between the groups for the first week. After an initial increase in pH, while all the cultures are still healthy there is a steady decrease in pH in groups 2-4. The pH of group 1 remained relatively constant, while the pH of the control flasks increases (Figure 14.13) in conjunction with the increased algal concentration (Figure 14.14). The rate at which the pH decreased in the experimental groups appeared proportional to the amount of effluent added and the strength of the algal culture.

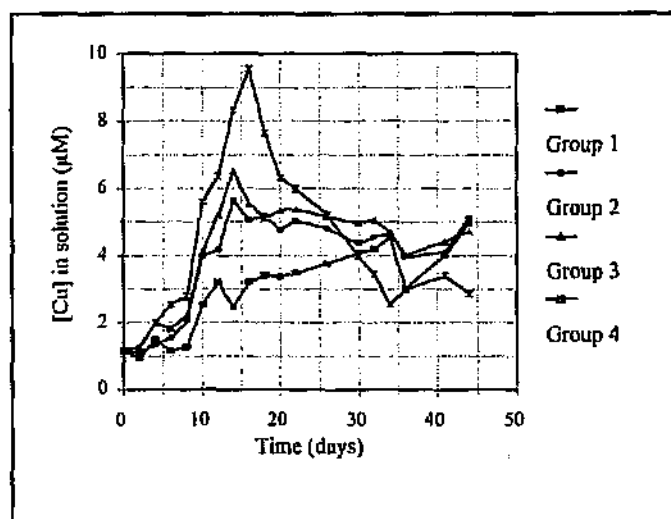
As the conditions in the flasks become less favourable for the growth of *Spirulina* as succession of other organisms began to develop. Initially these consisted of a number of species of diatoms, but after about a month the culture contains a species of *Oscillatoria*, a filamentous algae and even paramecia. The *Oscillatoria* is thought to exist at very low concentrations in the original *Spirulina* culture and flourishes as the conditions become more favourable. The diatoms, in turn, originate from the actual raw effluent as they appeared in the non-algal controls as well.

The effect of the *Oscillatoria* was clearly evident in the control and group 1 and 2 flasks from approximately day 35. There was a marked increase in the amount of algae in the flasks. Light microscopy confirmed a mixed culture of the two algal species, with the uncoiled *Oscillatoria* dominating (Figure 14.15). The effect on pH was also significant in groups 1 and 2.

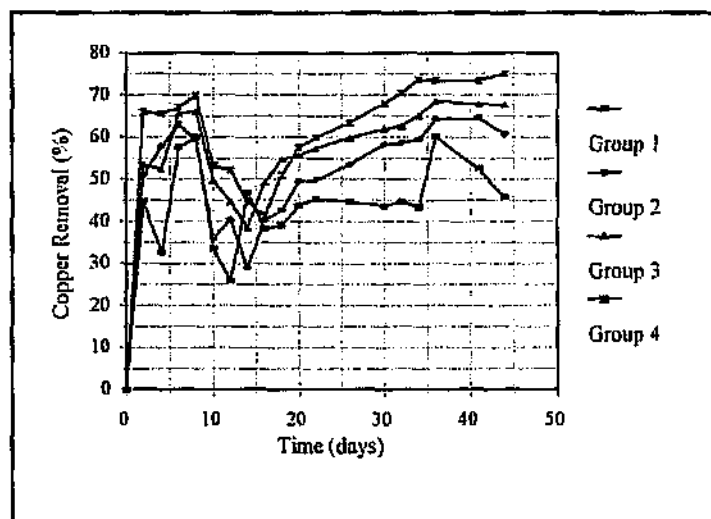


Figure 14.15: Light micrograph showing the presence of a mixed culture of *Spirulina*, *Oscillatoria* and diatoms - day 37. (Magnification x 40).





**Figure 14.16:** Copper concentration ( $\mu\text{M}$ ) in solution over time in volume controlled (400ml) algal system.



**Figure 14.17:** Copper removal (cumulative %) from solution in a volume controlled algal system.

The results for copper remaining in solution (Figure 14.16) were initially very similar to those observed in the open system. There was a steady increase in the amount of copper in solution. This increase was generally proportional to the amount of copper added. After two weeks, however this trend was completely reversed and the copper concentration in group 4 became the lowest and remains as such for the duration of the experiment. This change coincided with the change of the culture from a monoculture of *Spirulina* to a more complex consortium of organisms. The percentage removal data was similar to that in the open system, over the corresponding time period, but for the last 14 days of the experiment the graph resembled those for lead or zinc (Figures 14.18 and 14.19).

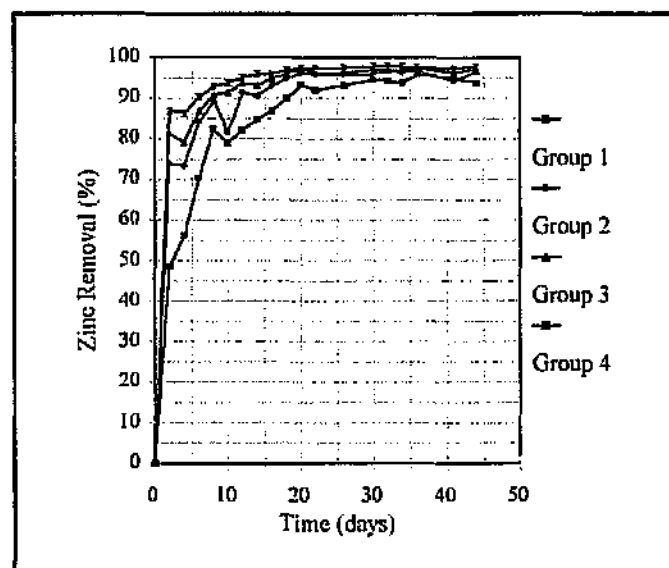
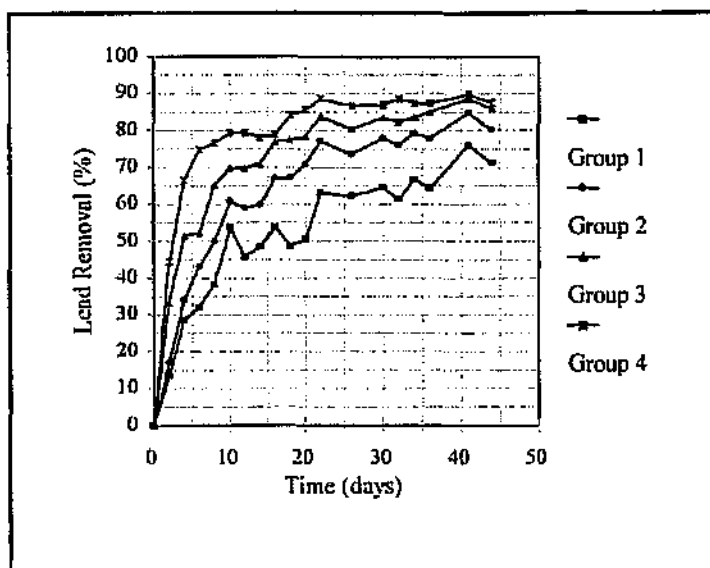


**Figure 14.18:** Lead removal (cumulative %) vs time.

**Figure 14.19:** Zinc removal (cumulative %) vs time.

The system was again most efficient at the precipitation of iron, as seen in Figure 14.20. Over 99% of the iron was removed from solution in all the groups.

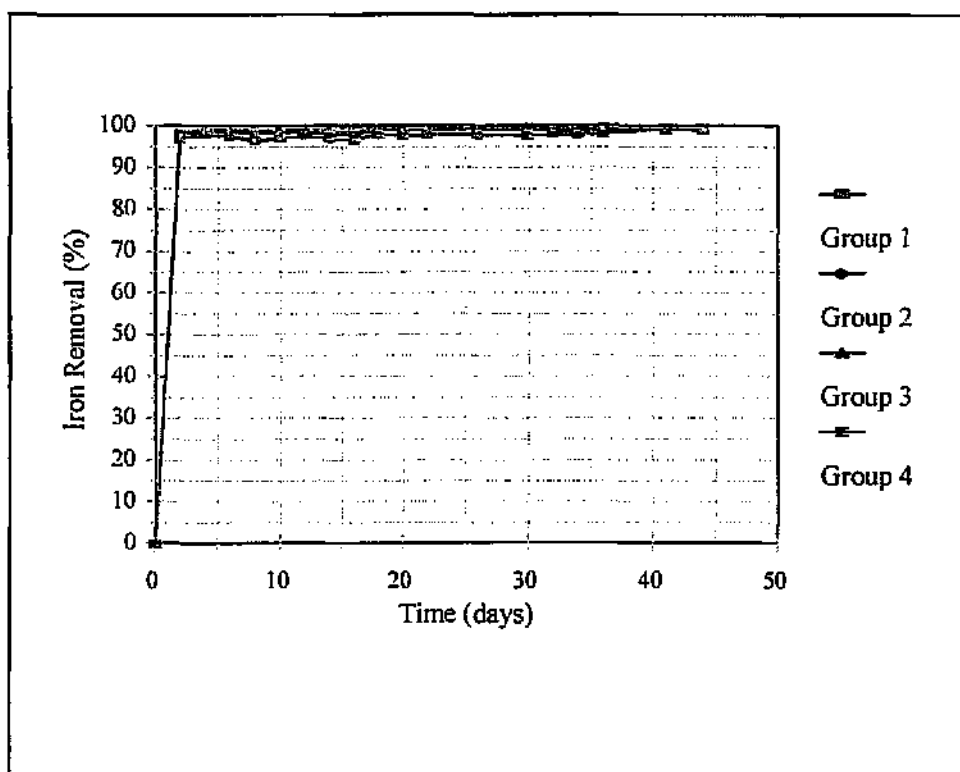


**Figure 14.20:** Iron removal (cumulative %) vs time.

A clearer understanding of the percentage removal graphs can be obtained by considering them in the context of an effluent pH profile (Figure 14.21). The profile was obtained by sequentially increasing the pH of the raw effluent, using sodium hydroxide (NaOH), and determining the percentage of the metal which remained in solution.

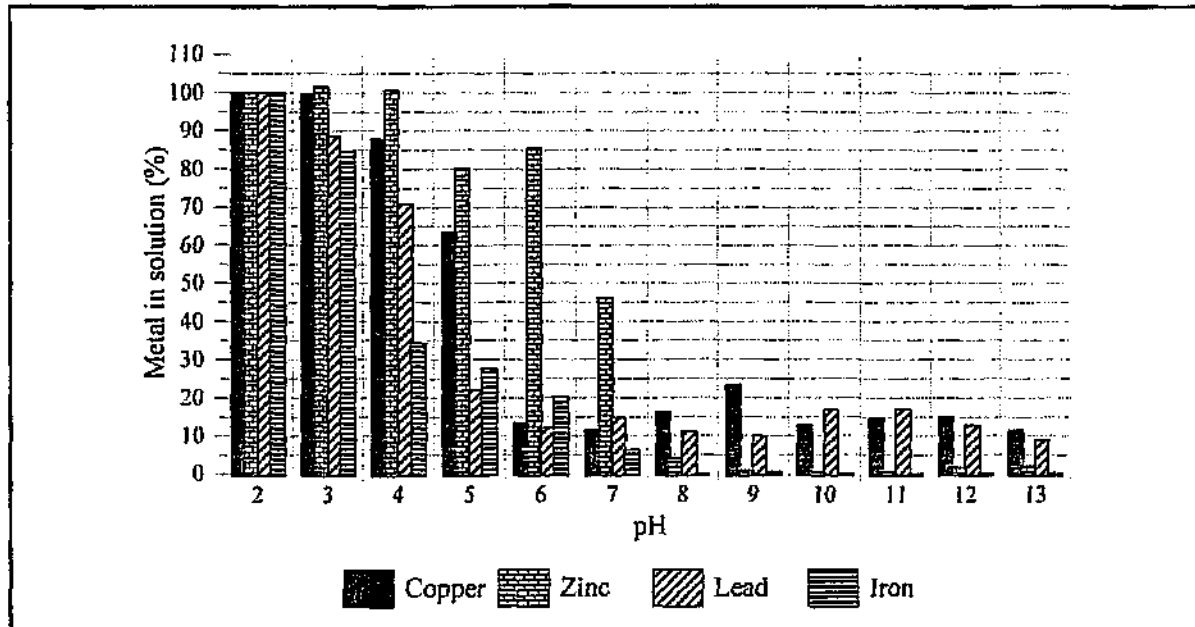


**Figure 14.21:** pH profile of Plaatjiesvlei effluent.

The pH profile shows that at the pH's at which the experiments were conducted (8.5 - 10) zinc and iron were almost completely precipitated. This explains the shape of the percentage removal graphs for these two metals. The removal climbed very steeply to over 90% and remained there for the duration of the experiment. For copper and lead it can be seen that the precipitation was not complete. This explains the slightly lower percentage removal obtained for these metals and also why the slope of the lines for these metals increased more slowly.

The control flasks again became contaminated, as in the open system experiments with similar effects. To prevent this it was decided to repeat the control experiments autoclaving both the growth medium and the effluent to ensure all possible contaminating organisms were killed.

### 14.3.2 Autoclaved Control Experiment (Volume Controlled)

The experiment was conducted in a laminar flow hood to prevent airborne organisms from contaminating the flasks. The duration of the experiment was 44 days, allowing the results obtained to be compared to those of the volume controlled system. Figure 14.22 shows the pH graph obtained for the control experiment.

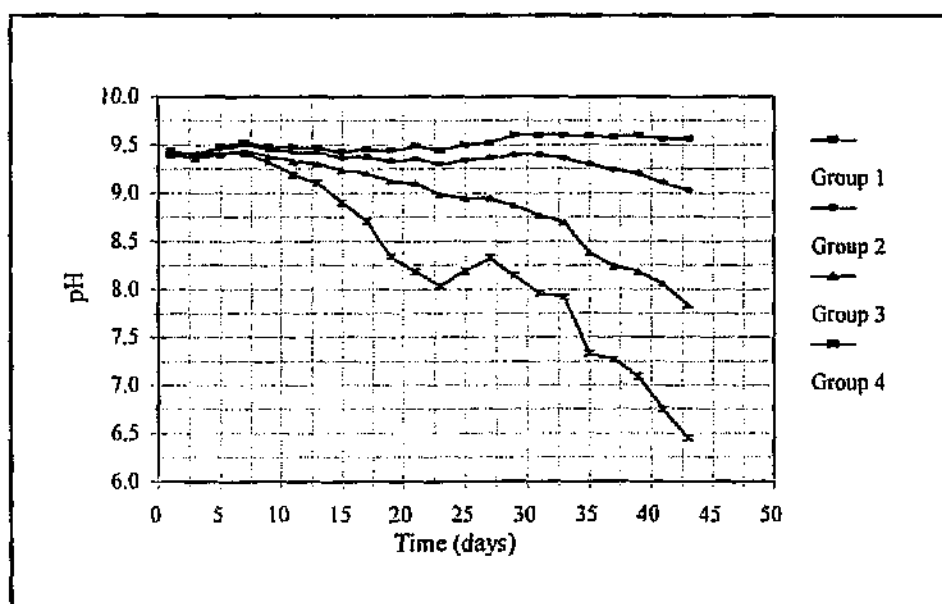
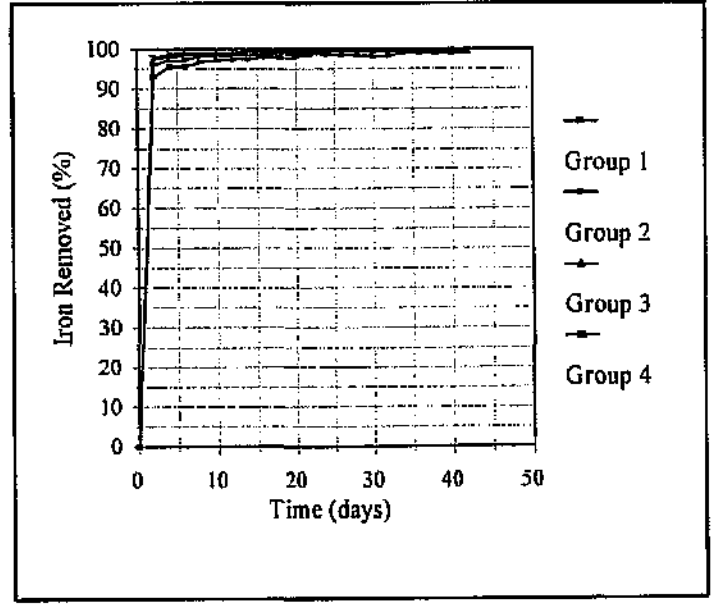
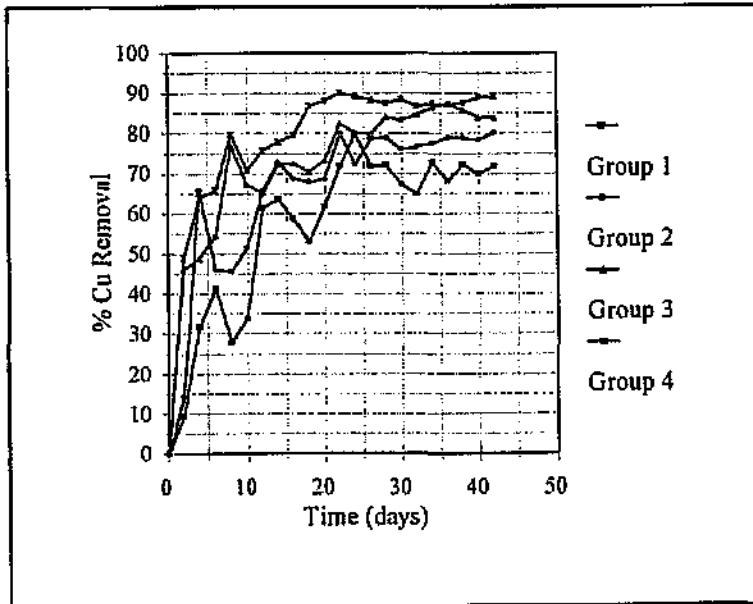


Figure 14.22: Graph of pH vs time for autoclaved control experiment.

The pH data indicated the high buffering capacity of the Zarrouk's medium. This was most likely due to the high bicarbonate content ( $16.8\text{ g NaHCO}_3\text{ l}^{-1}$ ). Despite the high buffering capacity of the growth medium the effect of the algae can clearly be seen when the above data is compared to that of the volume controlled algal system. The pH of group 4 dropped to below 6.5 on day 43 in the control experiment. In comparison the lowest pH value attained in the flasks containing algae was approximately 9.0. In addition there is no significant increase in pH observed in any of the groups over the first week, as is noted in the presence of algae.

When the pH is considered in the context of the effluent pH profile it would be expected that the precipitation of all the metals, with the exception of zinc, would be almost complete and this is the case (Figures 14.23-14.25). The percentage removal results are comparable to those of the open and volume controlled experiments.



**Figure 14.23:** Cumulative removal (%) of copper added to Zarrouks's medium.

**Figure 14.24:** Cumulative removal (%) of iron added to Zarrouk's medium.

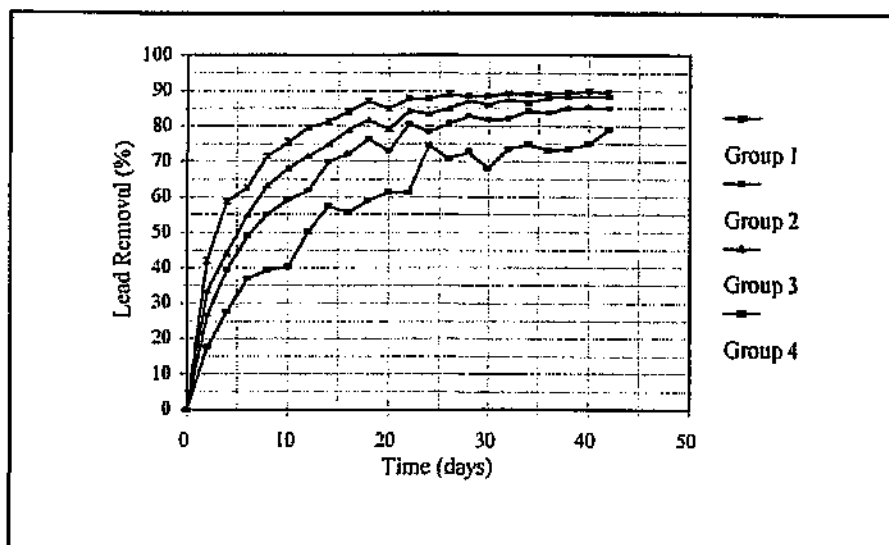


**Figure 14.25:** Cumulative removal (%) of lead added to Zarrouk's medium.

The results for zinc removal were particularly interesting. The pH profile results indicated that at a pH between 6 and 7, between 45 and 85% of the zinc should remain in solution. The control experiment results for zinc (Figure 14.26) confirmed this. As the pH dropped to approximately 7, on day 37, the percentage removal began to decrease. The results for daily percentage removal while the pH was below 7 (Table 14.1) indicated that the zinc in the effluent added does not precipitate. In addition the results indicate that zinc which had been added previously and precipitated was beginning to come out of solution.

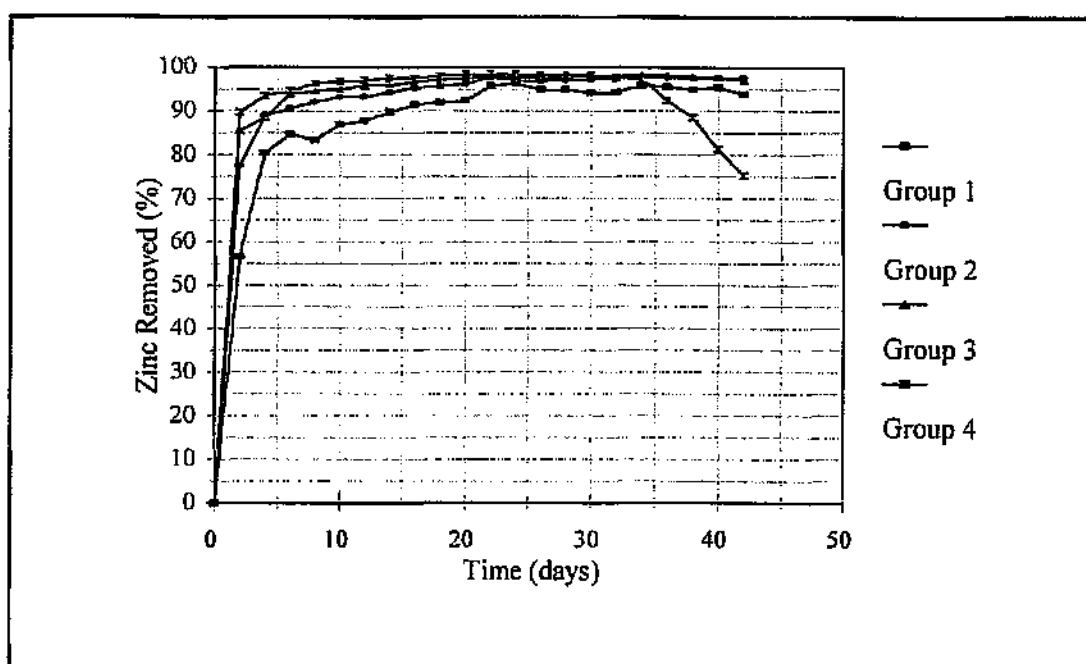


**Figure 14.26:** Cumulative removal (%) of zinc added to Zarrouk's medium.

**Table 14.1 :** Results from day 34 to 42 showing zinc removal per day in group 4 of the control experiment. Zinc added and removed values expressed as  $\mu\text{moles}$ .

Day	Zn conc ( $\mu\text{moles/l}$ )	Zn added (cumulative)	Zn removed (cumulative)	% removal/day
34	1.189	17.625	17.162	78.62
36	5.274	18.653	17.214	6.27
38	8.386	19.681	17.443	9.68
40	14.679	20.710	16.841	-22.29
42	19.792	21.738	16.352	-12.34

The negative percentage removal results for days 40 and 42 indicated that precipitated zinc is going back into solution.

### 14.3.3 Distilled Water Control

This experiment was set up in a similar fashion to the other control experiments, except that instead of Zarrouk's medium the initial 150ml consisted of distilled water, adjusted to a pH of 9 with sodium hydroxide (NaOH). The experiment was performed to confirm that the results obtained in the autoclaved control experiment were as a result of the buffering capacity of the medium and not the high initial pH. Table 14.2 shows the progression of pH in flasks over the duration.

**Table 14.2:** Progression of pH over time for duration of distilled water control

Group 1			Group 2		Group 3		Group 4	
Day	Effluent	pH	Effluent	pH	Effluent	pH	Effluent	pH
0	0ml	9.00	0ml	9.00	0ml	9.00	0ml	9.00
2	5ml	3.90	10ml	3.22	15ml	3.08	25ml	2.94
4	10ml	3.36	20ml	3.03	30ml	2.92	50ml	2.79
6	15ml	3.19	30ml	2.89	45ml	2.77	75ml	2.67
8	20ml	3.02	40ml	2.75	60ml	2.65	100ml	2.53
10	25ml	2.87	50ml	2.62	75ml	2.53	125ml	2.43

The effluent pH profile data would suggest that very little precipitation would occur under the above pH conditions and this holds true. The metal removal was not significant, less than 10%, for all metals in all groups. This confirms that it was the capacity of the growth medium to buffer against changes in pH, induced by the addition of acidic effluent, that allowed the growth medium to act as a good precipitator of metals. This result also has considerable implications for any further system. Either the system must be able to rapidly increase the pH by a significant degree immediately after effluent addition or have a relatively good buffering capacity. Ideally the system would combine both these properties.

#### 14.4 Discussion

From the results it is clear that there is potential for the development of a viable, biologically based system for the treatment of the effluent at the Black Mountain Mine. A pH mediated precipitation of the majority of the metals has been achieved using an algal based system. Micro algae have been very successfully cultivated on a large scale in pond systems and the climatic conditions prevalent in the area surrounding the mine are ideal for the large scale cultivation of algae in ponds. The one potential problem with a *Spirulina* based system is the lack of availability of a large volume of high saline medium. Using a defined medium such as Zarrouk's medium on a large scale will most likely be prohibitively expensive.

Further studies will be aimed at screening a wider range of organisms, including those which do not require a highly saline medium, for potential bioremediation properties. These will focus particularly on those with carbonic anhydrase activity, their nutrient requirements and resistance to heavy metal toxicity. The *Spirulina* will be further studied to quantify the carbonic anhydrase activity, determine which metals are toxic to the organisms and to characterise its growth on a more dilute growth medium.



## 15. GENERAL DISCUSSION AND CONCLUSIONS

The use of *S. cerevisiae* for heavy metal removal from solutions and effluents was found to be an effective and efficient system for bioremediation of metal containing wastewater. Mechanisms of metal biosorption and uptake were elucidated and polymers involved in such metal binding were identified. A relatively low cost method of yeast biomass immobilisation was developed for use in stirred tank or upflow type bioreactors. Such bioreactors were used for heavy metal removal from electroplating effluent. Both volume and biomass concentration were found to have a significant effect on the efficiency of metal removal. After optimisation, 5-10 l bioreactor tanks were able to remove 80-100% of the Cu, Cr, Ni, Zn and Cd from an electroplating effluent and use of a system of 2 stirred tanks in series facilitated a bioremediation process which could treat relatively large volumes of effluent in a continuous process. The potential for scale-up of this process was identified.

Further studies with the *S. cerevisiae* biomass to treat a Zn, Cr and Ni containing electroplating effluent led to a novel immobilisation procedure which was low cost and exhibited good mechanical strength and rigidity in a continuous flow operation. Almost complete removal and subsequent recovery of the Zn and Ni was achieved while Cr in the form of  $\text{Cr}^{6+}$  was less efficiently removed but reduction to  $\text{Cr}^{3+}$  afforded a complete removal. Recovery of the Cr required reduction of all of the Cr to  $\text{Cr}^{3+}$  prior to recovery.

Investigations of the kinetics of metal removal by yeast biomass showed that metal adsorption followed typical Michaelis-Menten kinetics and that the process was pH dependant. The data indicated a biosorbent suitable for relatively low metal concentration, high volume effluents. A number of desorbents were found to be successful for metal recovery from the biomass. Use of the biomass in column bioreactors enabled the development of a protocol for repeated adsorption-desorption cycles in which very little efficiency was lost with repeated cycles. The potential for reuse of the biomass in a continuous bioremediation system was demonstrated as was a protocol for selective recovery of the metals.

The *S. cerevisiae* biomass was applied to the treatment of a gold and copper-zinc mine effluent. Gold removal was both high and rapid but required an operating pH of 2. In the case of the copper-zinc mine effluent, metal removal was only achieved when the natural effluent pH (2.0) was elevated to pH 4-5. It was concluded that this system of yeast biomass has limited application to mine effluent

bioremediation due to the large volumes of effluent to be treated and at best may be used to complement a chemical remediation operation.

A final study involved the use of the algae, *Spirulina*, in the treatment of a zinc-copper mine effluent. This system utilised a property of algae to elevate effluent pH and to bind metals. Metal removal was effectively achieved through a pH mediated precipitation by the algal system as well as a bio-remediation process. This system may prove very useful for the treatment of large volumes of metal containing effluents provided a high saline medium is available at the site of the operation.

Future studies will focus on the development of pilot scale bioreactor systems to demonstrate the scale-up potential of this technology. This will primarily focus on the algal based system. In addition, the use of algal exopolysaccharides produced under stress conditions, will be investigated as metal biosorbents. A further biomass which will be studied particularly with a view to its use in treatment of low volume, high concentration effluents is the water fern, *Azolla*. This biomass is a very effective metal biosorbent, has good mechanical properties for use in continuous bioreactors and is very inexpensive.

## 16. REFERENCES

1. Woods, D.; Rawlings, D.E. (1989) Bacterial leaching and biomining. In: *A Revolution in Biomining*, Marx, J.L. (Ed), Cambridge University Press, Cambridge, 82-93.
2. Baker, A.; Brooks, R.; Reeves, R. (1988) Graing for gold and copper and zinc. *New Scientist*. ??, 44-48.
3. Norris, P.R.; Kelly, D.P. (1977), Accumulation of cadmium and cobalt by *Saccharomyces cerevisiae*. *J. Gen. Microbiol.* 99, 317-324.
4. Norris, P.R.; Kelly, D.P. (1977) Accumulation of metals by bacteria and yeasts. *Dev. Industrial Microbiology*. 20, 299-308.
5. Failla, M.L.; Benedict, C.D.; Weinberg, E.D. (1976) Accumulation and storage of  $Zn^{2+}$  by *Candida utilis*. *J. Gen. Microbiol.* 94, 23-36.
6. Tsezos, M.; Volesky, B. (1981) Biosorption of uranium and thorium. *Biotechnol. Bioeng.* 23, 583-604.
7. Tsezos, M.; Volesky, B. (1981) The mechanism of uranium biosorption by *Rhizopus arrhizus*. *Biotechnol. & Bioeng.* 24, 385-401.
8. Tsezos, M.; Volesky, B. (1982) The mechanism of thorium biosorption by *Rhizopus arrhizus*. *Biotechnol. & Bioeng.* 24, 955-969.
9. Kelly, D.P.; Norris, P.R. (1979) Microbiological methods for the extraction and recovery of metals. *Soc. Gen. Microbiol.* 29, 263-308.
10. Shumate II, S.E.; Stranoberg, G.W. (1985) Accumulation of metals by microbial cells. In: *Comprehensive Biotechnology*, Moo-Young, M. (Ed), Vol. 4; Ch. 13, 235-247.
11. Kotyk, A. (1989) Kinetic studies of transport in yeast. *Methods in Enzymology*. 174, 567-591.
12. Jones, R.P.; Gadd, G.M. (1990) Ionic nutrition of yeast-physiological mechanisms involved and implications for biotechnology. *Enzyme Microbiol. Technol.* 12, 402-418.
13. Borst-Pauwels, G.W.F.H. (1981) Ion transport in yeasts. *Biochimica et Biophysica Acta*. 650, 88-127.
14. Willsky, S.R. (1979) Characterization of the plasma membrane  $Mg^{2+}$  - ATPase from the yeast *Saccharomyces cerevisiae*. *J. Biol. Chem.* 254, 3326-3332.
15. Bertz, A.; Gradmann, D.; Slayman, C.L. (1992) Calcium and voltage-dependent ion channels in *Saccharomyces cerevisiae*. *Phil. Trans. R. Soc. London. B.* 338, 63-72.
16. Borst-Pauwels, G.W.F.H. (1993) Mutual interaction of ion uptake and membrane potential. *Biochim. Biophys. Acta*. 1145, 15-24.

17. Skulachev, V.P. (1978) Membrane-linked energy buffering as the biological function of  $\text{Na}^+/\text{K}^+$  gradient. *FEBS-letters*. **87**, 171-179.
18. Manon, S.; Guerin, M. (1992)  $\text{K}^+/\text{H}^+$  exchange in yeast mitochondria: sensitivity to inhibitors, solubilization and reconstitution of the activity in proteolysosomes. *Biochim. et Biophys. Acta*. **1108**, 169-176.
19. Okorokov, L.A.; Andreeva, N.A.; Lichko, L.P.; Valiakhmetov, A.Y. (1983) Transmembrane gradient of  $\text{K}^+$  ions as an energy source in the yeast *Saccharomyces carlsbergensis*. *Biochem. Inter.* **6**, 463-472.
20. Pena, A.; Ramirez, J. (1991) An energy dependent efflux for potassium ions in yeast. *Biochim. et Biophys. Acta*. **1068**, 237-244.
21. Pena, A. (1975) Studies on the mechanism of  $\text{K}^+$  transport in yeast. *Arch. Biochem. Biophys.* **167**, 397-409.
22. Fuhrmann, G.F.; Rothstein, A. (1968) The transport of  $\text{Zn}^{2+}$ ;  $\text{Co}^{2+}$  and  $\text{Ni}^{2+}$  into yeast cells. *Biochim. Biophys.* **163**, 325-330.
23. Borst-Pauwels, G.W.F.H. (1989) Ion transport in yeast including lysophilic ions. *Methods in Enzymology*. **174**, 603-616.
24. Eraso, P.; Portillo, F. (1994) molecular mechanism of regulation of yeast plasma membrane  $\text{H}^+$ -ATPase by glucose. *J. Biol. Chem.* **269**, 10393-10399.
25. Kotyk, A.; Georgiou, G. (1994) Both glucose-type monosaccharides and one of their metabolites are required for activation of yeast plasma membrane. *Cell Biology International*. **18**, 813-817.
26. Borbolla, M.; Pena, A. (1980) Some characteristics of  $\text{Ca}^{2+}$  uptake by yeast cells. *J. Membrane Biol.* **54**, 149-156.
27. Eilam, Y.; Othman, M.; Halachmi, D. (1990) Transient increase in  $\text{Ca}^{2+}$  influx in *Saccharomyces cerevisiae* in response to glucose: effects of intracellular acidification and cAMP levels. *J. Gen. Microb.* **136**, 2537-2543.
28. Conway, E.J.; Beary, M.E. (1958) Active transport of magnesium across the yeast cell membrane. *Biochem. J.* **69**, 215-280.
29. Armstrong, W.McD.; Rothstein, A. (1964) Discrimination between alkali metal cations by yeast: 1. Effect of pH on uptake. *J. Gen. Physiol.* **48**, 61-71.
30. Borst-Pauwels, G.W.F.H.; Theuvenet, A.P.R. (1984) Apparent saturation kinetics of divalent cation uptake in yeast caused by a reduction in the surface potential. *Biochim. et Biophys. Acta*. **771**, 171-176.
31. Lesuisse, E.; Raguzzi, F.; Crichton, R.R. (1987) Iron uptake by the yeast *Saccharomyces cerevisiae*: Involvement of a reduction step. *J. of Gen. Microbiol.* **133**, 3229-3236.

32. Joho, M.; Imai, M.; Murayama, T. (1985) Different distribution of  $\text{Cd}^{2+}$  between Cd-sensitive and Cd resistant strains of *Saccharomyces cerevisiae*. **131**, 53-56.
33. Kessels, B.G.F.; Belde, P.J.M.; Borst-Pauwels, G.W.F.H. (1985) Protection of *Saccharomyces cerevisiae* against  $\text{Cd}^{2+}$  toxicity by  $\text{Ca}^{2+}$ . *J. of Gen. Microbiol.* **131**, 2533-2537.
34. Belde, P.J.M.; Kessels, B.G.F.; Moelans, I.M.; Borst-Pauwels, G.W.F.H. (1988)  $\text{Cd}^{2+}$  uptake,  $\text{Cd}^{2+}$ -binding and loss of cell  $\text{K}^+$  by a  $\text{Cd}^{2+}$  sensitive and a  $\text{Cd}^{2+}$  resistant strain of *Saccharomyces cerevisiae*. *FEMS Microbiol. Lett.* **49**, 493-498.
35. Okorokov, L.A.; Lichko, P.; Kadomtseva, V.M.; Kholodenko, V.P.; Titovsky, V.T.; Kulaen, I.S. (1977) Energy dependant transport of magnesium into yeast cells and distribution of accumulated ions. *Eur. J. Biochem.* **75**, 373-377.
36. Ohsumi, Y.; Kitamoto, K.; Anraku, Y. (1988) Changes induced in the permeability barrier of the yeast plasma membrane by cupric ion. *J. Bacteriol.* **170**, 26796-2682.
37. Rothstein, A.; Hayes, A.D. (1956) The relationship of the cell surface to metabolism, XIII. The cation-binding proportion of the yeast cell surface. *Arch Biochim. Biophys.* **63**, 87-99.
38. Davidova, E.G.; Kasparova, S.G. (1993) Sorption of heavy metals by yeast cell walls. *Microbiology.* **61**, 582-585.
39. Davidova, E.G.; Kasparova, S.G. (1992) Adsorption of metals by yeast cell walls. *Microbiology.* **61**, 716-719.
40. Brady, D.; Duncan, J.R. (1994) Binding of heavy metals by the cell walls of *Saccharomyces cerevisiae*. *Enzyme Microb. Technol.* **16**, 633-638.
41. Lyons, T.P.; Hough, J.S. (1970) Cation-binding by the yeast cell walls. *Biochem. J.* **119**, 10.
42. Doyle, R.J.; Matthews, T.H.; Streips, U.N. (1980) Chemical basis for selectivity of metal ions by the *Bacillus subtilis* cell wall. *J. Bacteriol.* **143**, 471-480.
43. Beveridge, T.J. (1986) The immobilization of soluble metals by bacterial walls. *Biotechnol. Bioeng.* **16**, 127-139.
44. Beveridge, T.J.; Koval, S.F. (1981) Binding of metals to cell envelopes of *E.coli* K-12. *Appl. Environ. Microbiol.* **42**, 325-335.
45. Beveridge, T.J.; Murray, R.G.E. (1976) Uptake and retention of metals by cell walls of *Bacillus subtilis*. *J. Bacteriol.* **127**, 1502-1518.
46. Beveridge, T.J.; Murray, R.G.E. (1980) Sites of metal deposition in the cell wall of *Bacillus subtilis*. *J. Bacteriol.* **141**, 876-887.
47. Crist, R.H.; Oberholser, K.; Shank, N.; Nguyen, M. (1981) Nature of binding between metallic ions and algal cell walls. *Environ. Sci. Technol.* **15**, 1212-1217.

48. Wehrhein, B.; Wetter, M. (1994) Biosorption of cadmium, copper and lead by isolated mother cell walls and whole cells of *Chlaella fusca*. *Appl. Microbiol. Biotechnol.* **41**, 725-728.
49. Blundell, T.L.; Jenkins, J.A. (1977) The binding of heavy metals to proteins. *Chem. Soc. Reviews.* **6**, 139-171.
50. Phaff, H.J. (1971) Structure and biosynthesis of the yeast cell envelope. In: *The Yeasts*, Rose, A.H.; Harrison, J.S. (Eds), Academic Press, London, Vol. 2, 135-184.
51. Klis, F.M. (1994) Review: Cell wall assembly in yeast. *Yeast.* **10**, 851-869.
52. Cabib, E.; Roberts, R.; Bowers, B. (1982) Synthesis of the yeast cell wall and its regulation. *Ann. Rev. Biochem.* **51**, 763-793.
53. Bartnicki-Garcia, S.; McMurrough, M. (1971) Biochemistry of morphogenesis in yeasts. In: *The Yeasts*, Rose, A.M.; Harrison, J.S. (Eds), Academic Press, New York, 2nd edit, 441-455.
54. Northcote, D.H.; Horne, R.W. (1952) The chemical composition and structure of the yeast cell wall. *Biochem. J.* **51**, 232-236.
55. Korn, E.D.; Northcote, D.H. (1960) Physical and chemical properties of polysaccharides and glycoproteins of the yeast cell wall. *Biochem. J.* **75**, 12-17.
56. Bartnicki-Garcia, S.; Nickerson, W.J. (1962) Isolation, composition and structure of cell walls of filaments and yeast-like forms of *Mucor rouxii*. *Biochimica et Biophysica, acta.* **58**, 102-119.
57. Bacon, J.S.D.; Farmer, V.C.; Jones, D.; Taylor, I.F. (1969) The glucon components of the cell wall of baker's yeast (*Saccharomyces cerevisiae*) considered in relation to its ultrastructure. *Biochem. J.* **114**, 557-567.
58. Phaff, H.J. (1963) Cell wall of yeasts. *Ann. Rev. Microbiol.* **17**, 15-30.
59. Muzzarelli, R.A.A. (1977) *Chitin*. Pergamon Press, New York.
60. Muzzarelli, R.A.A.; Tanfani, F.; Emanuelli, M.; Gentile, S. (1980) The chelation of cupric ions by chitosan membranes. *J. Appl. Biochem.* **2**, 350-389.
61. Uraki, Y.; Fujii, T.; Matsuoka, T.; Miura, Y.; Tokura, S. (1993) Site specific binding of calcium ions to anionic chitin derivatives. *Carbohydrate Polymers.* **20**, 139-143.
62. Oda, Y.; Ichida, S.; Aonuma, S.; Shibahara, T. (1988) Interactions of cadmium with yeast mannans. *Chem. Pharm. Bull.* **36**, 2695-2698.
63. Nieboer, E.; Richardson, D.H.S. (1980) The replacement of the nondescript term "heavy metals" by a biologically and chemically significant classification of metal ions. *Envir. Pollut. Ser.* **1**, 3-26.

64. Brady, D.; Stoll, A.D.; Starke, L.; Duncan, J.R. (1994) Chemical and enzymatic extraction of heavy metal binding polymers from isolated cell walls of *Saccharomyces cerevisiae*. *Biotechnol. Bioeng.* **44**, 297-302.
65. Wada, Y.; Ohsumi, Y.; Tanifuji, M.; Kasai, M.; Anraku, Y. (1987) Vacuolar ion channel of the yeast *Saccharomyces cerevisiae*. *J. Biol. Chem.* **262**, 17260-17263.
66. Ohsumi, Y.; Anraku, Y. (1981) active transport of basic amino acids driven by a proton motive force in vacuolar membrane vesicles of *Saccharomyces cerevisiae*. *J. Biol. Chem.* **256**, 2079-2082.
67. Sato, T.; Ohsumi, Y.; Anraku, Y. (1984) An arginine/histidine exchange transport system in vacuolar membrane vesicles of *Saccharomyces cerevisiae*. *J. Biol. Chem.* **259**, 11509-11511.
68. Kitamoto, K.; Yoshizawa, K.; Ohsumi, Y.; Anraku, Y. (1988) Dynamic aspects of vacuolar and cytosolic amine acid pools of *Saccharomyces cerevisiae*. *J. Bacteriol.* **170**, 2683-2686.
69. Nicolay, K.; Scheffers, W.A.; Bruinenberg, P.M.; Kaptein, R. (1982) Phosphorus-31 nuclear magnetic resonance studies of intracellular pH, phosphate compartmentation and phosphate transport in yeasts. *Arch. Microbiol.* **133**, 83-89.
70. Klionsky, D.J.; Herman, P.K.; Emr, S.D. (1990) The fungal vacuole: Composition, function and biogenesis. *Microbiol. Rev.* **54**, 266-292.
71. Cornelius, G.; Nakashima, H. (1987) Vacuole play a decisive role in calcium homeostasis in *Neurospora crassa*. *J. Gen. Microbiol.* **133**, 2341-2347.
72. Kitamoto, K.; Yoshizawa, K.; Ohsumi, Y.; Anraku, Y. (1988) Mutants of *Saccharomyces cerevisiae* with defective vacuolar function. *J. Bact.* **170**, 2687-2691.
73. Lichko, L.P.; Okorokov, L.A.; Kulaev, I.S. (1982) Participation of vacuoles in regulation of  $K^+$ ,  $Mg^{2+}$  and orthophosphate ions in cytoplasm of the yeast *Saccharomyces cerevisiae*. *Arch. Microbiol.* **132**, 289-293.
74. Okorokov, L.A.; Lichko, L.P.; Kulaev, I.S. (1980) Vacuoles: Main compartments of potassium, magnesium and phosphate ions in *Saccharomyces cerevisiae* cells. *J. Bact.* **144**, 661-665.
75. Eide, D.J.; Bridgham, J.T.; Zhao, Z.; Mattoon, J.R. (1993) The vacuolar  $H^+$ -ATPase of *Saccharomyces cerevisiae* is required for efficient copper detoxification, mitochondrial function and iron metabolism. *Mol. Gen. Genet.* **241**, 447-456.
76. Lichko, L.P.; Okorokov, L.A.; Kulaev, I.S. (1980) Role of vacuolar ion pool in *Saccharomyces cerevisiae*: potassium efflux from vacuoles is coupled with manganese or magnesium influx. *J. Bact.* **144**, 666-671.
77. Miller, J.J. (1984) In vitro experiments concerning the state of polyphosphate in the yeast vacuole. *Can. J. Microbiol.* **30**, 236-246.

78. Raguzzi, F.; Lesuisse, E.; Crichton, R.R. (1988) Iron storage in *Saccharomyces cerevisiae*. *FEBS letters*. **231**, 253-258.
79. Yazgon, A.; Özcengiz, G. (1994) Subcellular distribution of accumulated heavy metals in *Saccharomyces cerevisiae* and *K. marxianus*. *Icheme-Adv. Biochem. Eng.* ??, 151-153.
80. Okorokov, L.A.; Kulakovskaya, T.V.; Lichko, L.P.; Polorotova, E.V. (1985) H<sup>+</sup>/ion antipart as the principle mechanism of transport systems in the vacuolar membrane of the yeast *Saccharomyces carlsbergensis*. *FEBS letters*. **192**, 303-306.
81. Ohsumi, Y.; Anraku, Y. (1983) Calcium transport driven by a proton motive force in vacuolar membrane vesicles of *Saccharomyces cerevisiae*. *J. Biol. Chem.* **258**, 5614-5617.
82. Kane, P.M.; Stevens, T.H. (1992) Submit composition, biosynthesis, and assembly of the yeast vacuolar proton-translocating ATPase . *J. Bioenergetics and Biomembranes*. **24**, 383-393.
83. White, C.; Gadd, G.M. (1987) The uptake and cellular distribution of zinc in *Saccharomyces cerevisiae*. *J. Gen. Microbiol.* **133**, 727-737.
84. Uribe, S.; Sanchez, N.; Pena, A. (1991) Effects of K<sup>+</sup> and other monovalent cations on yeast mitochondria. *Biochem. Inter.* **24**, 615-624.
85. Uribe, S.; Rangel, P.; Pardo, J.P.; Pereira-Da-Silva, L. (1993) Interactions of calcium and magnesium with the mitochondrial inorganic pyrophosphatase from *Saccharomyces cerevisiae*. *Eur. J. Biochem.* **217**, 657-660.
86. Jenkins, W.T. (1994) Yeast mitochondrial F1-ATPase - effects of metal ions. *Arch. Biochem. Biophysics*. **313**, 89-95.
87. Pieterse, M.J. (1989) Drinking water quality criteria with special reference to the South African experience. *Water SA*. **15**, 169-178.
88. Kempster, P.L.; Hattingh, W.H.J.; Van Vliet, H.R. (1980) *Summarized water quality criteria*. Dept. Environmental Affairs, R.S.A., Report No. TR108.
89. Leland, H.V.; Luoma, S.N.; Elder, J.F.; Wilkes, D.J. (1978) Heavy metals and related trace elements. *Journal WPCF*. **50**, 1469-1514.
90. Gadd, G.M.; Griffiths, A.J. (1978) Microorganisms and heavy metal toxicity. *Microbial Ecology*. **4**, 303-317.
91. Trevors, J.T.; Stratton, G.W.; Gadd, G.M. (1986) Cadmium transport, resistance, and toxicity in bacteria, algae, and fungi. *Can. J. Micro.* **32**, 447-464.
92. Schubauer-Berigan, M.K.; Amato, J.R.; Ankley, G.T.; Baker, S.E.; Burkhard, L.P.; Dierkes, J.R.; Jenson, J.J.; Lukase-Wycz, M.T.; Norberg-King, T.J. (1993) The behaviour and identification of toxic metals in complex mixtures: Examples from effluent and sediment pore water toxicity identification evaluations. *Arch. Environ. Contam. Toxicol.* **24**, 298-306.



93. Guan, L.; Petersen, J.N.; Johnstone, D.L.; Yonge, D.R.; Brouns, T.M. (1993) Equilibrium sorption of  $\text{Cr}^{6+}$  by a consortia of denitrifying bacteria. *Biotech. Letters*. 15, 727-732.
94. Babich, H.; Stotzky, G. (1983) Influence of chemical speciation on the toxicity of heavy metals in the microbiota. In: *Aquatic toxicology*, Nriagu, J.O. (Ed), John Wiley & Sons Inc., New York, 1-46.
95. Matis, K.A.; Zaubeculis, A.I.; Hancock, I.C. (1994) Biosorption and flotation for metal effluent treatment. *Icheme-Environ. Biotech.* ??, 86-88.
96. Hutchins, S.R.; Davidson, M.S.; Brierley, J.A.; Billerley, J.A. (1986) Microorganisms in reclamation of metals. *Ann. Rev. Microbiol.* 40, 311-336.
97. Wilson, M.W.; Edyvean, R.G. (1994) Biosorption for the removal of heavy metals from industrial wastewaters. *Icheme-Environ. Biotech.* ??, 89-91.
98. Gadd, G.M.; White, C. (1993) Microbial treatment of metal pollution - a working biotechnology. *TIBTECH.* 11, 353-359.
99. Garnham, G.W.; Codd, G.A.; Gadd, G.M. (1992) Uptake of technetium by freshwater green algae. *Appl. Microbiol. Biotechnol.* 37, 679-684.
100. Garnham, G.W.; Codd, G.A.; Gadd, G.M. (1993) Accumulation of zirconium by microalgae and cyanobacteria. *Appl. Microbiol. Biotechnol.* 39, 666-672.
101. Appanna, V.D.; Huang, J. (1992) Bioaccumulation of yttrium in *Pseudomonas fluorescens*. *Bul. Env. Can.* 49, 620-625.
102. White, C.; Gadd, G.M. (1990) Biosorption of radionuclides by fungal biomass. *J. Chem. Biotechnol.* 46, 331-343.
103. McCabe, A. (1986) The potential significance of microbial activity in radioactive waste disposal - Review. *Experientia.* 46, 779-787.
104. Ehrlich, H.L. (1986) What types of microorganisms are effective in bioleaching, bioaccumulation of metals, ore beneficiation, and desulfurization of fossil fuels. *Biotech. Bioeng. Symp.* 16, 227-238.
105. Norris, P.R.; Kelly, D.P. (1979) Accumulation of metals by bacteria and yeasts. *Dev. Ind. Microbiol.* 20, 299-308.
106. Francis, A.J. (1990) Microbial dissolution and stabilization of toxic metals and radionuclides in mixed wastes. *Experientia.* 46, 840-851.
107. Volesky, B. (1992) Removal of heavy metals by biosorption. *Amer. Chem. Soc. J.* 1054, 462-466.
108. Nakajima, A.; Sakaguchi, T. (1986) Selective accumulation of heavy metals by microorganisms. *Appl. Microbiol. Biotechnol.* 24, 59-64.

109. Ting, Y.P.; Lawson, F.; Prince, I.G. (1989) Uptake of cadmium and Zinc by the algae *Chlaella vulgaris*: Part 1. Individual ion species. *Biotechnol. Bioeng.* **34**, 990-999.
110. de Carvalho, R.P.; Chong, K.H.; Volesky, B. (1995) Evaluation of the Cd, Cu, and Zn biosorption in two-metal systems using an algal biosorbent. *Biotechnol. Prog.* **11**, 39-44.
111. Holan, Z.R.; Volesky, B. (1994) Biosorption of lead and nickel by biomass of marine algae. *Biotechnol. Bioeng.* **43**, 1001-1009.
112. McHardy, B.M.; George, J.J. (1990) Bioaccumulation and toxicity of zinc in the green algae, *Cladophora glomerata*. *Environ. Pollut.* **66**, 55-66.
113. Huisman, J.; Ten Hoopen, H.J.G.; Fuchs, A. (1980) The effect of temperature upon the toxicity of mercuric chloride to *Scenedesmus acutus*. *Environ. Pollut.* **22**, 133-148.
114. Wong, P.K.; Chang, L. (1992) Effects of bi- and trimetallic combinations of heavy metal ions on inorganic nitrogen and phosphorus uptake in *Chloella*. *Microbios.* **71**, 65-74.
115. Vymazal, J. (1987) Zinc uptake by *Clodophora glomerata*. *Hydrobiologia.* **148**, 97-101.
116. Vymazal, J. (1984) Short-term uptake of heavy metals by periphyton algae. *Hydrobiologia.* **119**, 171-179.
117. Reiniger, P. (1977) Concentrations of cadmium in aquatic plants and algal mass in flooded rice cultures. *Environ. Poll.* **14**, 297-301.
118. Brady, D.; Letebele, B.; Duncan, J.R.; Rose, P.D. (1994) Bioaccumulation of metals by *Scenedesmus*, *Scenastrum* and *Chloella* algae. *Water SA* **20**, 213-218.
119. Prahalad, A.K.; Seenayya, G. (1988) Bioavailability of zinc and cadmium and their effect on microbial growth and metal uptake. *Bull. Environ. Contam. Toxicol.* **41**, 921-927.
120. Slawson, R.M.; Trevors, J.T.; Lee, H. (1992) Silver accumulation and resistance in *Pseudomonas stutzeri*. *Arch. Microbiol.* **158**, 398-404.
121. Tornabene, T.G.; Edwards, H.W. (1972) Microbial uptake of lead. *Science.* **176**, 1334-1335.
122. Chmielowski, J.; Klapcinska, B. (1986) Bioaccumulation of Germanium by *Pseudomonas putida* in the presence of two selected substrates. *Appl. Environ. Microbiol.* **51**, 1099-1103.
123. Friis, N.; Myers-Keith, P. (1986) Biosorption of uranium and lead by *Streptomyces longwoodensis*. *Biotechnol. Bioeng.* **28**, 21-28.
124. Cabral, J.P.S. (1992) Selective binding of metal ions to *Pseudomonas syringae* cells. *Microbiol.* **71**, 47-53.
125. Yoshida, N.; Morinaga, T.; Murooka, Y. (1993) Characterization and identification of bacterial strains isolated from corroded concrete in the accumulated stratum and their resistance levels to heavy metals. *J. Fermentat. Bioeng.* **76**, 400-402.

126. Bosecker, K. (1986) Bacterial metal recovery and detoxification of industrial waste. *Biotechnol. Bioeng. Symp.* **16**, 105-120.
127. Yoshida, N.; Murooka, Y. (1994) Absorption of bacterial cells to crystal particles of heavy metals: Role of electrostatic interaction. *J. Ferm. Bioeng.* **77**, 636-641.
128. Hammack, R.W.; Edenborn, H.M. (1992) The removal of nickel from mine waters using bacterial sulfate reduction. *Appl. Microbiol. Biotech.* **37**, 674-678.
129. Wong, P.K.; So, C.M. (1993) Copper accumulation by a strain of *Pseudomonas putida*. *Microbios.* **13**, 113-121.
130. Townsley, C.C.; Atkins, A.S. (1986) Comparative coal fines desulphurization using the iron-oxidising bacterium *Thiobacillus ferrooxidans* and the yeast *Saccharomyces cerevisiae* during simulated froth flotation. *Proc. Biochem.* **21**, 188-191.
131. Tyagi, R.D.; Couillard, D.; Grenier, Y. (1991) Effects of medium composition on the bacterial leaching of metals from digested sludge. *Environ. Pollut.* **71**, 57-67.
132. Thompson, G.A.; Watling, R.J. (1987) Bioaccumulation potential of heterotrophic bacteria for lead, selenium and arsenic. *Bull. Environ. Contam. Toxicol.* **38**, 1049-1054.
133. Kruckeberg, A.L.; Wu, L. (1992) Copper tolerance and copper accumulation of herbaceous plants colonizing inactive California mines. *Eco. Env. Saf.* **23**, 307-319.
134. Scott, C.D. (1992) Removal of dissolved metals by plant tissue. *Biotech. Bioeng.* **39**, 1064-1068.
135. Gadd, G.H. (1986) Fungal responses towards heavy metals. In: *Microbes in extreme environments*, Herbet, R.A.; Codd, G.A. (Eds), Academic Press Inc., Ltd., London, 84-110.
136. Tobin, J.M.; Cooper, D.G.; Neufeld, R.J. (1984) Uptake of metal ions by *Rhizopus orrhizus* biomass. *J. Appl. Environ. Microbiol.* **47**, 821-824.
137. Nrigu, J.O.; Pacyna, J.M. (1988) Quantitative assessment of worldwide contamination of air, water and soils by trace minerals. *Nature.* **333**, 134-139.
138. Volesky, B.; Holan, Z.R. (1995) Biosorption of heavy metals. *Biotechnol. Prog.* **11**, 235-250.
139. Brady, D.; Stoll, A.D.; Duncan, J.R. (1994) Biosorption of heavy metal cations by non-viable yeast biomass. *Environ. Tech.* **15**, 429-438.
140. Brierley, C.L.; Brierley, J.A. (1993) Immobilization of biomass for industrial application of biosorption. In: *Proc. Intl. Biohydrometallurgy Symp. Vol.II: Biohydrometallurgical technologies*, Torma, A.E.; Apel, M.L.; Brierley, C.L. (Eds), 35-44.
141. Cotoras, D.; Viedma, P.; Pimentel, J. (1993) Biosorption of metal ions by attached bacterial cells in a packed-bed reactor. In: *Proc. Intl. Biohydrometallurgy Symp. Vol.II: Biohydrometallurgical technologies*, Torma, A.E.; Apel, M.L.; Brierley, C.L. (Eds), 103-110.

142. Brierley, J.A. (1987) Microbial removal of metals from industrial wastewaters. *Waste and Wastewater Int.* 2, 31-34, 54.
143. Jeffers, T.H.; Corwin, R.R. (1993) Waste water remediation using immobilized biological extractants. In: *Proc. Intl. Biohydrometallurgy Symp. Vol.II: Biohydrometallurgical technologies*, Torma, A.E.; Apel, M.L.; Brierley, C.L. (Eds), 1-13.
144. Jeffers, T.H.; Ferguson, C.R.; Bennett, P.G. (1991) Biosorption of metal contaminants using immobilized biomass - A laboratory study. In: *Report of Investigations/1991. RI 9340*, Bureau of mines, 1-9.
145. Jones, R.P.; Greenfield, P.F. (1984) A review of yeast ionic nutrition. Part 1. Growth and fermentation requirements. *Proc. Biochem.* 19, 48-60.
146. Fourest, E.; Serre, A.; Roux, J.C. (1995) Biosorption of heavy metals from water purification: contribution of carboxyl groups to binding sites in fungal walls. *7th Europ. Cong. Biotech.*
147. Catley, B.J. (1988) Isolation and analysis of cell walls. In: *Yeast: A practical approach*, Campbell, I.; Dulfus, J.H. (Eds), IRL Press Ltd., London, 163-183.
148. Marrack, J.; Campbell Smith, F. (1932) Quantitative aspects of immunity reactions: The combination of antibodies with simple haptens. *Brit. J. Exp. Path.* 13, 394-402.
149. Tsezos, M. (1983) The role of chitin in uranium adsorption by *R. arrhizus*. *Biotech. Bioeng.* 25, 2025-2040.
150. Kuyucak, N.; Volesky, B. (1988) Biosorbents for recovery of metals from industrial solutions. *Biotechnol. Lett.* 10, 137-142.
151. Shumate II, S.E.; Strandberg, G.W. (1985) Accumulation of metals by microbial cells. In: *Comprehensive Biotechnology*, Moo-Yang, A. (Ed), Vol. 4, Ch. 13, 235-247.
152. Boller, T.; Wiemken, A. (1986) Dynamics of vacuolar compartmentation. *Ann. Rev. Plant Physiol.* 37, 137-164.
153. Okorokov, L.A. (1985) Main mechanisms of ion transport and regulation of ion concentration in the yeast cytoplasm. In: *FEMS Symposium 23, Environmental regulation of microbial metabolism*, Kulacv, ??; Daves, ??; Tempost,??. (Eds), Academic Press, London, 339-349.
154. Sato, T.; Ohsumi, Y.; Anraku, Y. (1984) Substrate specification of active transport systems for amino acids in vacuolar-membrane vesicles of *Saccharomyces cerevisiae*. *J. Biol. Chem.* 259, 11505-11508.
155. Kakinuma, Y.; Ohsumi, Y.; Anraku, Y. (1981) Properties of H<sup>+</sup> translocating adenosine triphosphatase in vacuolar membranes of *Saccharomyces cerevisiae*. *J. Biol. Chem.* 256, 10859-10863.
156. Rose, A.H.; Veazey, F.J. (1988) Membranes and lipids of yeast. In: *Yeast: A practical approach*, Campbell, I.; Dulfus, J.H. (Eds), IRL Press Ltd., London, 255-275.

157. Wienken, A. (1975) Isolation of vacuoles from yeasts. In: *Methods in cell biology*, vol. 12, Prescott, D.M. (Ed), Academic Press Inc., New York, 99-109.
158. Indge, K.J. (1968) Yeast protoplasts by osmotic shock; metabolic lysis of yeast protoplast; the isolation and properties of the yeast cell vacuole; polyphosphates of the yeast cell vacuole. *J. Gen. Microbiol.* **51**, 425-455.
159. Peterson, C.A. (1979) Selective vital staining of companion cells of potato tuber and parsnip root with neutral red. *Stain Tech.* **54**, 135-139.
160. Matile, P. (1978) Biochemistry and function of vacuoles. *Ann. Rev. Plant Physiol.* **29**, 193-213.
161. Wada, Y.; Ohsumi, Y.; Anraku, Y. (1992) Chloride transport of yeast vacuolar membrane vesicles: A study of in vitro vacuolar acidification. *Biochem. Biophys. Acta.* **1101**, 296-303.
162. Okorokov, L.A.; Lichko, L.P. (1983) The identification of a proton pump on vacuoles of the yeast *Saccharomyces carlsbergensis*. *FEBS Lett.* **155**, 102-106.
163. Gadd, G.M. (1990) Metal tolerance. In: *Microbiology of extreme environments*, Edwards, C. (Ed), Open University Press, Ch. 7, 178-209.
164. Wood, J.M.; Wong, H.K. (1983) Microbial resistance to heavy metals. *Environ. Sci. Technol.* **17**, 582-590.
165. Brady, D.; Glaum, D.; Duncan, J.R. (1994) Copper tolerance in *Saccharomyces cerevisiae*. *Lett. Appl. Microbiol.* **18**, 245-250.
166. Reddy, G.N.; Prasad, H.N.V. (1992) Cadmium induced potassium efflux from *Scenedesmus quadricauda*. *Bull. Environ. Contam. Toxicol.* **49**, 600-605.
167. White, C.; Gadd, G.M. (1986) Uptake and cellular distribution of copper, cobalt and cadmium in strains of *Saccharomyces cerevisiae* cultured on elevated concentrations of these metals. *FEMS Microbiol. Ecol.* **38**, 277-283.
168. Butt, T.R.; Ecker, D.J. (1987) Yeast metallothionein and applications in biotechnology. *Microbiol. Rev.* **51**, 351-364.
169. Macara, I.G. (1978) Accommodation of yeasts to toxic levels of cadmium ions. *J. Gen. Microbiol.* **104**, 321-324.
170. Meisch, H.U.; Beckmann, I.; Schmidt, J.A. (1983) A new cadmium-binding phosphoglycoprotein, cadmium-mycophosphatin from the mushroom *Agaricus macrosporus*. *Biochim. Biophys. Acta.* **745**, 259-266.
171. Ross, I.S. (1977) Effect of glucose in copper uptake and toxicity in *Saccharomyces cerevisiae*. *Trans. Br. Mycol.* **69**, 77-81.
172. Slavik, J. (1982) Intracellular pH of yeast cells measured with fluorescent probes. *FEBS Lett.* **140**, 22-26.

173. Volesky, B.; May, H.; Holan, Z.R. (1993) Cadmium biosorption by *Saccharomyces cerevisiae*. *Biotechnol. Bioeng.* **41**, 826-829.
174. Scott, J.A.; Palmer, S.J. (1990) Sites of cadmium uptake in bacteria used for biosorption. *Appl. Microbiol. Biotechnol.* **33**, 221-225.
175. Brady, D.; Duncan, J.R. (1994) Cation loss during accumulation of heavy metal cations by *Saccharomyces cerevisiae*. *Biotechnol. Lett.* **16**, 543-548.
176. De Rome, L.; Gadd, G.M. (1987) Measurement of copper uptake in *Saccharomyces cerevisiae* using a  $\text{Cu}^{2+}$  selective electrode. *FEMS Microbiol. Lett.* **43**, 283-287.
177. Cabral, J.P.S. (1990) Cupric ions induce both an efflux of potassium and low molecular mass in *Pseudomonas syringae*. *FEMS Microbiol. Lett.* **72**, 109-112.
178. Gadd, G.M.; Mowll, J.L. (1983) The relationship between cadmium uptake,  $\text{K}^+$  release and viability in *Saccharomyces cerevisiae*. *FEMS Microbiol. Lett.* **16**, 45-48.
179. Theuvsenet, A.P.R.; Kessels, B.G.F.; Blankenstein, W.M.; Borst-Pauwels, G.W.F.H. (1987) A comparative study of  $\text{K}^+$  loss from a cadmium-sensitive and a cadmium-resistance strain of *Saccharomyces cerevisiae*. *FEMS Microbiol. Lett.* **47**, 147-153.
180. Belde, P.J.M.; Vossen, J.H.; Borst-Pauwels, G.W.F.H.; Theuvsenet, A.P.R. (1993) Inositol 1,4,5-triphosphate releases  $\text{Ca}^{2+}$  from vacuolar membrane vesicles of *Saccharomyces cerevisiae*. *FEBS Lett.* **323**, 113-118.
181. Brady, D.; Duncan, J.R. (1994) Bioaccumulation of metal cations by *Saccharomyces cerevisiae*. *Appl. Microbiol. Biotechnol.* **41**, 149-154.
182. Volesky, B.; May-Phillips, H.A. (1995) Biosorption of heavy metals by *Saccharomyces cerevisiae*. *Appl. Microbiol. Biotechnol.* **42**, 797-806.
183. Fourest, E.; Roux, J.C. (1992) Heavy metal biosorption by fungal mycelial by-products: mechanisms and influence of pH. *Appl. Microbiol. Biotechnol.* **37**, 399-403.
184. Hsu, T.; Lee, L.W.; Chang, T.H. (1992) Influence of temperature and nutrient strength on the susceptibility of *Saccharomyces cerevisiae* to heavy metals. *Bul. Env. Can.* **49**, 444-448.
185. Ting, Y.P.; Lawson, F.; Prince, I.G. (1991) Uptake of cadmium and zinc by the alga *Chlorella vulgaris*: II. Multi-ion situation. *Biotechnol. Bioeng.* **37**, 445-455.
186. Brown, T.A.; Smith, D.G. (1977) Cytochemical localization of mercury in *Cryptococcus albiclus* grown in the presence of mercuric chloride. *J. Gen. Microbiol.* **99**, 435-439.
187. Tsezos, M. (1984) Recovery of uranium from biological adsorbents - Desorption equilibrium. *Biotechnol. Bioeng.* **26**, 973-981.
188. Okorokov, L.A.; Kadomtseva, V.M.; Titovskii, B.I. (1979) Transport of manganese into *Saccharomyces cerevisiae*. *Folia Microbiol.* **24**, 240-246.

189. Mowll, J.L.; Gadd, G.M. (1984) Cadmium uptake by *Aurobasidium pullulans*. *J. Gen. Microbiol.* **130**, 279-284.
190. Boutry, M.; Foury, F.; Goffeau, A. (1977) Energy dependent uptake of calcium by the yeast *Schizosacchremyces pombe*. *Biochim. Biophys. Acta.* **464**, 602-612.
191. Peberdy, J.F. (1979) Fungal protoplasts. *Ann. Rev. Microbiol.* **33**, 30-31.
192. Volesky, B. (1987) Biosorbents for metal recovery. *Tibtech.* **5**, 96-101.
193. Tsezos, M. (1985) The selective extraction of metals from solution by microorganisms: A brief overview. *Can. Metallurgical Quart.* **24**, 141-144.
194. Sharma, D.C.; Forster, C.F. (1995) Continuous adsorption and desorption of chromium ions by sphagnum moss peat. *Proc. Biochem.* **30**, 293-298.
195. Strandberg, G.W.; Shumate II, S.E.; Parrott Jr., J.R. (1981) Microbial cells as biosorbents for heavy metals: Accumulation of uranium by *Saccharomyces cerevisiae*. *Appl. Environ. Microbiol.* **41**, 237-245.
196. Kratochvil, D.; Fourest, E.; Volesky, B. (1995) Biosorption of copper by *Sorgassum fluitans* biomass in fixed bed column. *Biotechnol. Lett.* **17**, 777-782.
197. de Rome, L.; Gadd, G.M. (1991) Use of pelleted and immobilized yeast and fungal biomass for heavy metal and radio-nuclide recovery. *J. Ind. Microbiol.* **7**, 97-104.
198. Wu, K.A.; Wisecarver, K.D. (1992) Cell immobilization using PVA crosslinked with boric acid. *Biotechnol. Bioeng.* **39**, 447-449.
199. Chen, K.C.; Lin, Y.F. (1994) Immobilization of microorganisms with phosphorylated polyvinyl alcohol (PVA) gel. *Enzyme Microb. Technol.* **16**, 79-83.
200. Shindo, S.; Kamimura, M. (1990) Immobilization of yeast with hollow PVA gel beads. *J. Fermentat. Bioeng.* **70**, 232-234.
201. Caplan, J.A. (1993) The world-wide bioremediation industry - prospects for profit. *Tibtech.* **11**, 320-323.
202. Apel, M.L.; Torma, A.E. (1993) Diffusion kinetics of metal recovery biosorption processes. In: *Proc. Intl. Biohydrometallurgy Symp. Vol.II: Biohydrometallurgical technologies*, Torma, A.E.; Apel, M.L.; Brierley, C.L. (Eds), 25-33.
203. Schoeman, J.J.; Steyn, A. (1995) Researches evaluate membrane technology for the treatment of electroplating effluents. *SA Water Bull.* **21**, 12-15.
204. McDonough, W.P.; Steward, F.A. (1971) The use of the integrated waste treatment approach in the large electroplating shop. *Chem. Eng. Prog. Symp. Series.* **67**, 428-431.
205. Hill Jr., C.J. (1977) Basic concepts in reactor design and ideal reactor models. In: *An introduction into chemical engineering kinetics and reactor design*, Wiley & Sons, New York, Ch. 8, 245-305.

206. Hill Jr., C.J. (1977) Reactor design for heterogenous catalytic reactions. In: *An introduction into chemical engineering kinetics and reactor design*, Wiley & Sons, New York, Ch. 12, 425-437.
207. Wong, Y.W.; Niedzwiecki, J.L. (1982) A simplified model for multi-component fixed bed adsorption. *AIChE Symp. Series*. 219, 120-127.
208. Harwell, J.H.; Liapis, A.I.; Litchfield, R.; Hanson, D.T. (1980) A non-equilibrium model for fixed bed multi-component adiabatic adsorption. *Chem. Eng. Scie.* 35, 2287-2296.
209. Weber, W.J.; Liu, J.R.; Liu, K.T. (1980) Determination of mass transport parameters for fixed-bed adsorbers. *Chem. Eng. Commun.* 6, 49-60.
210. Trujillo, E.M.; Jeffers, T.H.; Ferguson, C.; Stevenson, H.Q. (1991) Mathematically modelling the removal of heavy metals from a waste water using immobilized biomass. *Environ. Scie. Tech.* 25, 1559-1565.
211. McKay, G.; Bino, M.J. (1990) Fixed bed adsorption for the removal of pollutants from water. *Envir. Pollut.* 66, 33-53.
212. Tsezos, M.; Deutschmann, A.A. (1990) An investigation of engineering parameters for the use of immobilized biomass particles in biosorption. *J. Chem. Tech. Biotechnol.* 48, 29-39.
213. Duncan, J.R., Dean, B. and Rose, P.D. (1995) The use of immobilized yeast cells for heavy metal removal. *Mineral Bioprocessing II*, edn. D.S.Holmes & R.W.Smith, The Mineral, Metals & Materials Society, USA.
214. Blackwell, K.J., Singleton, I. and Tobin, J.M. (1995) Metal cation uptake by yeast: a review. *Appl. Microbiol. Biotechnol.* 43, 579-584.
215. Schiewer, S., Fourest, E., Chong, K.H. and Volesky B. (1995) Ion exchange biosorption by dried seaweed: experiments and model predictions. *Biohydrometallurgical Processing*, edn. Jerez *et al.*, University of Chile.
216. Anon (1985) Standard Methods for the Examination of Water and Wastewater, 16th edn., APHA, AWWA, WPCF, Washington, DC, USA.
217. Martin, R.J. and Ng, W.J. (1987) The repeated exhaustion and chemical regeneration of activated carbon. *Water Res.* 20, 21-26.
218. Sharma, D.C. and Forster, C.F. (1996) A comparison of the sorptive characteristics of leaf mould and activated carbon columns for the removal of hexavalent chromium. *Process Biochem.* 31, 213-218.
219. Tan, W.T., Ooi, S.T. and Lee, C.K. (1993) The removal of chromium(VI) from dilute solutions by coconut husk and palm-pressed fibres. *Env. Technol.* 11, 673-697.
220. Sengupta, A.K. and Clifford, D. (1986) Chromate ion exchange mechanism for cooling water. *Ind. Eng. Chem. Fundam.* 25, 249-258.



221. Sharma, D.C. and Forster, C.F. (1993) Removal of hexavalent chromium using sphagnum moss peat. *Water Res.* **27**, 1201-1208.
222. Blackburn J.W. and Hafker W.R. (1993) The impact of biochemistry, bioavailability and bioactivity on the selection of bioremediation techniques. *TIBTECH* **11**, 328-333.
223. Garnham G.W., Codd G.A. and Gadd G.M. (1992b) Kinetics of uptake and intracellular location of cobalt, manganese and zinc in the estuarine green alga *Chlorella salina*. *Appl. Microbiol. Biotechnol.* **37**, 270-276.
224. Huang C.P., Westman D., Quirk K. and Huang J.P. (1988) The removal of cadmium (II) from dilute aqueous solutions by fungal adsorbent. *Wat. Sci. Tech.* **20**, 369-376.
225. Sağ Y., Özer D. and Kutsal T. (1995) A comparative study of the biosorption of lead II ions to *Z. ramigera* and *R. arrhizus*. *Process Biochem.* **30**, 169-174.
226. Hao Y., Roach A.L. and Ramelow G.J. (1993) Uptake of metals by non-living biomass derived from *Sphagnum* moss and water hyacinth roots. *A28*, 2333-2343.
227. Ramelow G.J., Fralick D. and Zhao Y. (1992) Factors affecting the uptake of metal ions by dried seaweed biomass. *Microbios.* **72**, 81-93.
228. Nourbakhsh M., Sağ Y., Özer D., Aksu Z., Kutsal T. and Çağlar. (1994) A comparative study of various biosorbents for removal of chromium (VI) ions from industrial waste waters. *Process Biochem.* **29**, 1-5.
229. Nui H., Xu X.S., Wang J.H. and Volesky B. (1993) Removal of lead from aqueous solutions by *Penicillium* biomass. *Biotech. Bioeng.* **42**, 785-787.
230. Summers A.O. (1992) The hard stuff: metals in bioremediation. *Current Opinion in Biotechnol.* **3**, 271-276.
231. Galun M., Keller P., Feldstein H., Galun E., Siegel S. and Siegel B. (1983) Recovery of uranium (VI) from solution using fungi II. Release from uranium-loaded *Penicillium* biomass. *Water, Air, and Soil Pollution* **20**, 277-285.
232. Kuyucak N. and Volesky B. (1989a) The mechanism of cobalt biosorption. *Biotech. Bioeng.* **33**, 823-831.
233. McLean R.J.C., Campbell A.M., Khu P.T., Persaud A.T., Bickerton L.E. and Beauchemin D. (1992) *World J. Microbiol. Biotechnol.* **10**, 472-474.
234. Mattuschka B. and Straube G. (1993) Biosorption of metals by a waste biomass. *J. Chem. Tech. Biotechnol.* **58**, 57-63.
235. Harris P.O. and Ramelow G.J. (1990) Binding of metal ions by particulate biomass derived from *Chorella vulgaris* and *Scenedesmus quadricauda*. *Environ. Sci. Technol.* **24**, 220-228.
236. Golab Z., Orlowska and Smith R.W. (1991) Biosorption of lead and uranium by *Streptomyces* sp. *Water, Air, and Soil Pollution* **60**, 99-106.

237. Tsezos M., McCready R.G.L. and Bell J.P. (1989) The continuous recovery of uranium from biological leached solutions using immobilised biomass. *Biotechnol. Bioeng.* 34, 10-17.
238. Nakajima A., Horikoshi T. and Sakaguchi T. (1981) Studies on the accumulation of heavy metal elements in biological systems. *European J. Appl. Microbiol. Biotechnol.* 12, 76-83.
239. Chong K.H. and Volesky B. (1995) Description of two-metal biosorption equilibria by langmuir-type models. *Biotech. Bioeng.* 47, 451-460.
240. Cross R.M.H. (1989) *Micron and Microscopica Acta* 20, 1-7.